



Design of novel IL-4 antagonists employing site-specific chemical and biosynthetic glycosylation

Herstellung neuer IL-4 basierter Antagonisten durch zielgerichtete chemische und biosynthetische Glykosylierung

Doctoral thesis for a doctoral degree at the Graduate School of Life Sciences,
Julius-Maximilians-Universität Würzburg,
Biomedicine

submitted by
Sarah Katharina Thomas
from
Frankfurt am Main

Würzburg 2018



Submitted on:

.....

Office stamp

Members of the *Promotionskomitee*:

Chairperson: Prof. Dr. Georg Gasteiger

Primary Supervisor: Prof. Dr. Thomas D. Müller

2nd Supervisor: PD Dr. Heike Hermanns

3rd Supervisor: Prof. Dr. Manfred Lutz

Date of Public Defence:

Date of Receipt of Certificates:

.....

Table of contents

Table of contents	I
1. Introduction	1
1.1 Role of interleukin-4 and interleukin-13 in the adaptive immune system	1
1.1.1 IL-4 induces development of type 2 helper T-cells (Th2).....	1
1.1.2 Inflammatory effector functions of interleukin-4 and interleukin-13	3
1.2 IL-4 and IL-13 receptor assembly and signal transduction	6
1.2.1 IL-4 and IL-13 use overlapping receptor complexes.....	6
1.2.2 Ligand binding induces sequential receptor formation	8
1.2.3 Molecular structure of IL-4	10
1.3 IL-4 and IL-13 are key targets in treatment of atopic diseases	11
1.4 Targeting the shared IL-4R α receptor for simultaneous blockade of IL-4 and IL-13	13
1.5 Aim: Design of novel, more effective IL-4 antagonists	14
2. Results	16
2.1 Recombinant expression of IL-4 protein in Hek293 cells.....	16
2.1.1 Cloning and protein expression of IL-4 in Hek293 cells.....	17
2.1.2 Protein purification via immobilized metal-ion affinity chromatography.....	17
2.1.3 Hek293 cell-derived wildtype IL-4 carries a single N-glycan at Asn38, which is not important for biologic activity	18
2.2 Recombinant expression of IL-4 cysteine variants in <i>E. coli</i>	21
2.2.1 Cloning and protein expression	21
2.2.2 Extraction of IL-4 protein from inclusion bodies and oxidative refolding ...	22
2.2.3 1 st step of IL-4 protein purification: Cation exchange chromatography	24
2.2.4 2 nd step of IL-4 protein purification: Reverse Phase-High Performance Liquid Chromatography	24
2.3 Prokaryotic expression and purification of glutaredoxin-1	25

2.4	Generation of glycoengineered IL-4 receptor typeI/typeII antagonist.....	27
2.4.1	Engineered N-glycosylation site at position 121 is not used by Hek293 cells 28	
2.4.2	Chemical glycoengineering of <i>E. coli</i> -derived IL-4 variant F82D R121C ...	29
2.4.2.1	Enzymatic deglutathionylation of IL-4 F82D R121C-GSH using glutaredoxin.....	29
2.4.2.2	Coupling of amino-glycans via the crosslinker SMCC	31
2.4.2.3	Coupling of thiol-glycans using phenylselenylbromide activation	34
2.4.2.4	Chemical glycosylation via refolding in the presence of thiol-glycans .	37
2.4.3	Chemical glycosylation of Hek293 cell-derived IL-4 variant F82D R121C	40
2.4.3.1	Hek293 cell-derived IL-4 F82D R121C is conjugated to a cysteine	40
2.4.3.2	Hek293 cell-derived IL-4 F82D R121C can not be reduced by enzymatic means	41
2.4.3.3	Chemical glycosylation of Hek293 cell-derived IL-4 F82D R121C by refolding	41
2.4.4	Glycoengineered IL-4 F82D R121C analogues display increased binding for receptor IL-4R α	43
2.4.5	Glycosylated IL-4 F82D R121C analogues are highly effective IL-4 antagonists in cell-based assays	45
2.5	Synthesis of an IL-4 receptor type II specific antagonist.....	49
2.5.1	Chemical glycosylation of an unpaired cysteine residue at position 117	51
2.5.1.1	Glutathione moiety conjugated to Cys117 can not be released by enzymatic reaction.....	51
2.5.1.2	Chemical glycosylation of IL-4 F82D K117C variant using refolding .	52
2.5.2	Introduction of an N-glycan at position 117 using expression in Hek293 cells 54	
2.5.2.1	An engineered N-glycosylation site at position 117 is partially occupied 54	

2.5.2.2	Purification of glycosylated IL-4 F82D N38Q K117N using concanavalin A affinity chromatography	55
2.5.3	Interaction analysis of glycosylated IL-4 K117C/N variants with the IL-4R α receptor	56
2.5.4	Glycoengineered IL-4 F82D K117C/N variants display partially agonistic activity in a cell-based assay	57
2.6	Hyperglycosylated Hek293 cell-derived IL-4 variants display increased proteolytic stability	61
2.6.1	Synthesis of hyperglycosylated IL-4 variants in Hek293 cells	62
2.6.2	N-glycan at position 28 disrupts binding to IL-13 R α 1	63
2.6.3	Design of a hyperglycosylated IL-4 antagonistic variant by combining chemical and synthetic glycoengineering	65
2.6.4	Hyperglycosylated Hek293 cell-derived IL-4 shows increased proteolytic stability	67
3.	Discussion.....	71
3.1	Site-specific glycoengineering to establish blockage of receptor binding in IL-4	71
3.1.1	Site-specific introduction of complex N-glycans in IL-4 using Hek293 cells	73
3.1.2	Cysteine labelling for site-directed chemical introduction of glycans in IL-4	75
3.1.3	Chemical glycosylation of IL-4 cysteine variants – Refolding strategy has the potential for large-scale application	78
3.2	Glycoengineering yields effective IL-4 antagonists	80
3.2.1	Glycoengineering of position 121 generates potent type I and type II receptor antagonists more effective than Pitrakinra	80
3.2.2	Design of IL-4 receptor type II specific antagonists	81
3.2.2.1	Antagonistic effect of glycoengineered IL-4 F82D K117C depends on the architecture of the conjugated glycan	82

Table of contents

3.2.2.2	Introduction of a complex N-glycan at position 28 attenuates binding to IL-13R α 1	84
3.3	Combination of biosynthetic and chemical glycoengineering generates a highly effective IL-4/IL-13 antagonist with increased stability	86
3.4	Future perspective – Design of IL-4 antagonists with tailored glycosylation pattern	88
4.	Materials	91
4.1	Software	91
4.2	Laboratory Equipment	91
4.3	Consumables	92
4.4	Chromatography Columns	92
4.5	Reagents	92
4.6	Kits	93
4.7	Enzymes	93
4.8	Cell lines	94
4.8.1	Bacterial strains	94
4.8.2	Mammalian cell lines	94
4.9	Vectors	95
4.10	Mutagenesis oligonucleotides	95
5.	Methods	97
5.1	Molecular methods	97
5.1.1	Polymerase chain reaction	97
5.1.2	Restriction-digest and ligation	98
5.1.3	DNA agarose gel electrophoresis	99
5.1.4	Preparation of plasmid DNA	99
5.1.4.1	Generation of chemically competent <i>E. coli</i> cells	99
5.1.4.2	DNA transformation into chemically competent <i>E. coli</i> cells	100
5.1.4.3	Plasmid DNA preparation	100

5.1.4.4	Sequencing	100
5.1.5	Gene expression analysis using qPCR	100
5.1.5.1	RNA isolation and first strand cDNA synthesis.....	100
5.1.5.2	Quantitative Real-Time PCR	101
5.2	Protein analysis methods	103
5.2.1	Polyacrylamide gel analysis	103
5.2.1.1	SDS-PAGE.....	103
5.2.1.2	Coomassie staining.....	104
5.2.1.3	Silver staining.....	104
5.2.1.4	Periodic Acid Schiff (PAS) staining of glycosylated proteins.....	105
5.2.2	Western Blot.....	105
5.2.2.1	Electrophoretic blotting on membrane.....	105
5.2.2.2	Detection of proteins containing a polyhistidine tag.....	106
5.2.3	Deglycosylation of proteins using endoglycosidase.....	106
5.2.4	Spectrophotometric determination of protein concentration	107
5.2.5	Mass spectrometry	107
5.2.5.1	ESI-MS analysis of proteins.....	107
5.2.5.2	ESI-MS analysis of SMCC and SMCC-GlcN conjugate.....	107
5.3	Recombinant protein expression in <i>E. coli</i>	108
5.3.1	Protein extraction of soluble proteins containing a polyhistidine tag	108
5.3.2	Expression of aggregated protein in form of inclusion bodies.....	109
5.3.2.1	Protein extraction from inclusion bodies	109
5.3.2.2	Oxidative refolding employing a glutathione redox-couple	109
5.4	Expression in Hek293 cells	110
5.4.1	Culture conditions of Freestyle™ 293F/Expi293F™ cells.....	110
5.4.2	Transient protein expression in Hek293 cells.....	110
5.5	Chemical glycoengineering of IL-4 cysteine variants.....	111

Table of contents

5.5.1	Enzymatic deglutathionylation of engineered cysteine residues.....	111
5.5.2	Coupling to amine-containing glycan via the bifunctional crosslinker SMCC 112	
5.5.2.1	Preparation of SMCC-glucosamine intermediate	112
5.5.2.2	Conjugation of SMCC-glucosamine to IL-4.....	112
5.5.3	Coupling of thiol-carbohydrates using phenylselenenylbromide activation... 112	
5.5.4	Preparation of disulphide-linked IL-4 glycoconjugates via refolding	113
5.5.4.1	Refolding of <i>E. coli</i> -derived IL-4 cysteine variants in the presence of thiol-glycans	113
5.5.4.2	Refolding of Hek293 cell-derived IL-4 cysteine variants in the presence of thiol-glycans.....	113
5.6	Chromatographic methods for protein purification.....	114
5.6.1	Cation exchange chromatography	114
5.6.2	Immobilized metal ion affinity chromatography (IMAC)	114
5.6.3	Reversed-phase high-pressure liquid chromatography (RP-HPLC)	115
5.6.4	Size exclusion chromatography	116
5.6.5	Lectin affinity chromatography.....	116
5.6.6	Sulfhydryl immobilization	117
5.7	Methods for analysis of pharmacological parameters <i>in vitro</i>	117
5.7.1	Surface Plasmon Resonance (SPR).....	117
5.7.1.1	Biotinylation of ybbR-fusion protein.....	118
5.7.1.2	SPR experimental set-up.....	118
5.7.2	Proteolytic stability assay	119
5.7.3	Cellular experiments	119
5.7.3.1	HEK-Blue cell SEAP reporter gene assay	119
5.7.3.2	TF-1 cell proliferation assay	120
6.	Summary	122
7.	Zusammenfassung.....	124

8.	Literature	126
9.	Supplement	146
9.1	Generation of glycoengineered IL-4 analogues.....	146
9.2	Analytics of IL-4 glycoconjugates	148
9.2.1	Mass spectrometry analysis of glycoengineered IL-4 F82D R121C/K117C analogues	148
9.2.2	Biologic activity in cell-based assays.....	150
9.3	Gene Expression Analysis of IL-4 receptors IL-4R α , γ c (IL2RG) and IL-13R α 1 in TF-1 cells.....	154
9.4	Abbreviations	155
9.5	Acknowledgements	158
9.6	Curriculum Vitae	159
9.7	Affidavit	160

Figures

Figure 1.1:	Cytokine dependent priming of different helper CD4+T-cell lineages.	2
Figure 1.2:	Effector mechanism of Th2-specific cytokines in allergic reactions.....	5
Figure 1.3:	Structure of IL-4 receptor IL-4R α as a typical representative of the class I cytokine receptor family.....	6
Figure 1.4:	IL-4 and IL-13 mediated receptor assemblies.	7
Figure 1.5:	Sequential assembly of IL-4 and IL-13 receptors.....	9
Figure 1.6:	Four alpha-helix bundle topology of IL-4.....	10
Figure 2.1:	Purification of IL-4 from Hek293 cell culture supernatant using immobilized metal-ion affinity chromatography.....	18
Figure 2.2:	SDS-PAGE analysis of Hek293 cell-derived IL-4 F82D treated with Endo-H.	19
Figure 2.3:	IL-4 N-glycosylation pattern derived from expression in Hek293 cells.....	20
Figure 2.4:	SDS-PAGE analysis of recombinant protein expression of IL-4 in <i>E. coli</i>	22
Figure 2.5:	SDS-PAGE analysis of IL-4 inclusion bodies.	23
Figure 2.6:	Purification of IL-4 using cation exchange chromatography.....	24
Figure 2.7:	Purification of IL-4 using Reverse Phase HPLC.	25

Table of contents

Figure 2.8: Purification of <i>E. coli</i> -derived glutaredoxin-1 using immobilized metal-ion affinity chromatography.....	27
Figure 2.9: Location of residues Arg121 and Tyr124 in the IL-4 binding epitope for receptors γc and IL-13R $\alpha 1$	28
Figure 2.10: Transient expression of IL-4 F82D N38Q R121N K123S in Hek293 cells...	29
Figure 2.11: Selective reduction of engineered IL-4 cysteine residue using the glutaredoxin system.....	30
Figure 2.12: SDS-PAGE analysis of glutathionylated IL-4 variant F82D R121C after reaction with glutaredoxin-1.	30
Figure 2.13: Conjugation of glucosamine to IL-4 engineered cysteine residue via the bifunctional crosslinker SMCC.....	32
Figure 2.14: Purification of glucosamine-SMCC intermediate using Reverse Phase HPLC.	33
Figure 2.15: Purification of IL-4 F82D R121C conjugated to SMCC-glucosamine using Reverse Phase HPLC.	34
Figure 2.16: Conjugation of thiol-glycans to reduced IL-4 F82D R121C using phenylselenenylbromide activation.....	35
Figure 2.17: SDS-PAGE analysis of IL-4 F82D R121C after Glyco-SeS treatment.....	36
Figure 2.18: ESI-MS analysis of IL-4 F82D R121C-Glc derived from Glyco-SeS method.	37
Figure 2.19: Conjugation of thiol-glycans to IL-4 F82D R121C during refolding.....	38
Figure 2.20: SDS-PAGE analysis of IL-4 F82D (N38C) R121C derived from refolding with thio-glucose (tetraacetate).	38
Figure 2.21: ESI-MS analysis of IL-4 F82D N38C R121C-Glc derived from refolding with thiol-glucose (tetraacetate).	39
Figure 2.22: Analysis of Hek293 cell-derived IL-4 F82D R121C treated with Endo- H...	40
Figure 2.23: SDS-PAGE analysis of Hek293 cell-derived IL-4 F82D R121C-Cys treated with glutaredoxin.....	41
Figure 2.24: Analysis of Hek293 cell-derived IL-4 F82D R121C-Glc obtained from refolding with thiol-glucose.	42
Figure 2.25: <i>In vitro</i> SPR analysis of IL-4 F82D R121C glycoconjugates interaction with IL-4R α -ECD.....	44
Figure 2.26: Biologic activity of glycoengineered IL-4 F82D R121C variants in HEK-Blue and TF-1 cells.....	47

Figure 2.27: Dose-dependent competition of glycoengineered IL-4 F82D R121C variants in TF-1 cells.....	48
Figure 2.28: Position of residue Lys117 in the IL-4 binding epitope for receptors γc and IL-13R $\alpha 1$	50
Figure 2.29: Enzymatic removal of conjugated glutathione from IL-4 F82D K117C-GSH is not possible.....	52
Figure 2.30: SDS-PAGE of purified IL-4 F82D K117C-(4ac)glc under reducing conditions.	52
Figure 2.31: ESI-MS analysis of IL-4 F82D K117C variants derived from refolding with thiol-glucose (tetraacetate).	53
Figure 2.32: Immobilized metal ion affinity chromatography purification of IL-4 F82D N38Q K117N.....	54
Figure 2.33: Purification of N-glycosylated IL-4 variant F82D N38Q K117N using ConA affinity chromatography.	55
Figure 2.34: Biologic activity of glycosylated IL-4 F82D K117C/N variants in HEK-Blue and TF-1 cells.	58
Figure 2.35: Glutathione is two times longer than glucose.	59
Figure 2.36: Dose-dependent competition of glutathionylated/glycoengineered IL-4 K117C/N variants in cell-based experiments.	60
Figure 2.37: SDS-PAGE of purified IL-4 hyperglycosylated variants obtained from Hek293 cells.....	62
Figure 2.38: Position of residue Thr28 in the IL-4 binding epitope for receptors γc and IL-13R $\alpha 1$	63
Figure 2.39: Biologic activity of glycoengineered IL-4 F82D N38Q T28N variant in HEK-Blue cells.	65
Figure 2.40: Purification of N-glycosylated Hek293 cell-derived IL-4 F82D variant Q20NT28NK61N using ConA affinity chromatography.	66
Figure 2.41: Dose response curves of glycoengineered IL-4 variant F82D Q20N T28N K61N R121C-Glc in TF-1 cells.	67
Figure 2.42: Proteolytic “half-life” of IL-4 analogues treated with trypsin.	69
Figure 2.43: IL-4 glycoprotein derived from <i>E. coli</i> , yeast and Hek293 cells.	70
Figure 3.1: Species-specific variations of eukaryotic N-glycan patterns.	73
Figure 3.2: Wrench-like architecture of IL-13R $\alpha 1$ in the type II receptor complex.	86
Figure S9.1: IL-4 coding sequence.....	146

Table of contents

Figure S9.2: Mass spectrometry of IL-4 F82D R121C glycoconjugates.	149
Figure S9.3: Biologic activity of glutathionylated IL-4 F82D K117C variants in HEK-Blue cells.....	151
Figure S9.4: Biologic activity of Hek293 cell derived IL-4 analogues containing engineered N-glycosylation sites in TF1- cell assay.	152
Figure S9.5: Biologic activity of Hek293 cell derived IL-4 analogues containing engineered N-glycosylation sites in HEK-Blue cells.	153
Figure S9.6: Quantitative Real Time PCR of IL-4 receptor transcript levels in TF1 cells.	154

Tables

Table 2.1: Binding affinities of glycoengineered IL-4 F82D R121C variants to IL-4R α ECD measured by surface plasmon resonance analysis.....	45
Table 2.2: Inhibitory constants of the glycoengineered IL-4 F82D R121C variants <i>in vitro</i>	49
Table 2.3: Binding affinities of glycoengineered IL-4 F82D R121C variants to IL-4R α ECD measured by SPR.	56
Table 2.4: Inhibitory constants of the glycoengineered IL-4 F82D K117C/N variants <i>in vitro</i>	61
Table 2.5: Comparison of proteolytic stability of differentially glycosylated IL-4 variants derived from eukaryotic expression systems.	68
Table 5.1 Pipetting protocol for PCR reaction.....	97
Table 5.2: Thermocycler conditions.....	98
Table 5.3: Restriction digest.....	98
Table 5.4: Ligation of vector and insert.	99
Table 5.5: Pipetting protocol for qPCR.....	102
Table 5.6: Thermocycler conditions for qPCR.	102
Table 5.7: Preparation of SDS stacking and resolving gels.	103
Table 5.8: Protocol for silver staining.	104
Table 5.9: Enzymatic deglutathionylation of an IL-4 cysteine variant.	111
Table 5.10: Running protocol for reverse phase HPLC.	116
Table 5.11: CoA labelling of ybbR tag using SFP-synthase.....	118
Table 5.12: parameter setting employed for analysis by simple 1:1 Langmuir-type interaction model.....	119

Table S9.1: Chemical compounds/glycans used for modification of IL-4 cysteine analogues.
 147

Table S9.2: Theoretical and measured molecular weights of IL-4 F82D R121C/K117C
 glycoconjugates. 148

Table S9.3: Biologic activity of glycoengineered IL-4 variants in HEK-Blue and TF-1 cells.
 150

Table S9.4: Biologic activity of glycoengineered IL-4 variants in HEK-Blue cell-assay. 151

Table S9.5: Readily available qPCR primers for IL-4R α , IL-13R α 1, γ c and GAPDH were
 purchased from Sigma Aldrich..... 154

Table S9.6: Abbreviations 155

1. Introduction

1.1 Role of interleukin-4 and interleukin-13 in the adaptive immune system

1.1.1 IL-4 induces development of type 2 helper T-cells (Th2)

The adaptive immune system of higher vertebrates has evolved to recognize an almost infinite number of foreign molecules, so-called antigens (antibody generators) derived from invading pathogens and to respond highly specific to eradicate the threat. Major cellular components of the adaptive immune system are antigen presenting cells as well as B- and T-lymphocytes. Professional antigen presenting cells, which include dendritic cells, macrophages and also B-cells are crucial for the induction of the adaptive immune response, since only these cells express co-stimulatory molecules required to efficiently activate T-cells. Among these three types of antigen presenting cells dendritic cells are most potent in activating conventional CD4+T-lymphocytes, also known as T-helper (Th) cells. The latter play a key role in immunity as they orchestrate the adaptive and innate immune response to eliminate the infection most efficiently. Dendritic cells express cytoplasmic or membrane-bound receptors, so-called pattern recognition receptors, e.g. Toll-like receptors (TLR) or nucleotide-binding oligomerization domain (NOD)-like receptors (NLR) specialized in capturing different pathogenic antigens, like lipopolysaccharide derived from gram-negative bacteria or viral RNA. Antigens captured by dendritic cells are internalized, processed intracellularly and the resulting peptides are presented within class II major histocompatibility complexes (MHC class II) on the surface of the dendritic cell. Subsequently, the activated dendritic cell undergoes a maturation process and migrates to the lymph nodes, where it selects rare uncommitted, naïve antigen-specific CD4+T-lymphocytes (Th0). Upon receptor-mediated interaction, the dendritic cell transfers antigen-dependent signals to the T-helper cell, which induce its differentiation and proliferation (reviewed in: (Walsh and Mills 2013)).

T-helper cells can develop into various subtypes, which are specialized in driving the appropriate immune response against different types of infections. The best-understood lineages are type 1 helper T-cells (Th1-cells) and type 2 helper T-cells (Th2-cells). Th1-cells help to control infections with intracellular microbes, especially pathogens that replicate within macrophages, whereas Th2-cells are mainly involved in the elimination of

extracellular parasites, like helminths. One of the major factors, which determines helper T-cell polarization and proliferation is the local cytokine environment. Cytokines are a broad group of small proteins that function as intercellular mediators between immune and non-immune cells. The cytokine milieu in the secondary lymphoid organs, where T-cell priming takes place, is determined by other immune cells. For example, the cytokine interleukin 12 (IL-12) is secreted by macrophages upon their encounter with microbial antigens (Ladel et al. 1997; Vieira et al. 1994). Together with interferon gamma (IFN- γ), IL-12 is regarded as the key stimulus, that triggers the development of Th1-cells (Seder et al. 1993; Heufler et al. 1996). In contrast, IL-4 is the primary cytokine directing the differentiation of Th2-cells (Hsieh et al. 1992; Le Gros et al. 1990; Maggi et al. 1992; Swain et al. 1990) (figure 1.1).

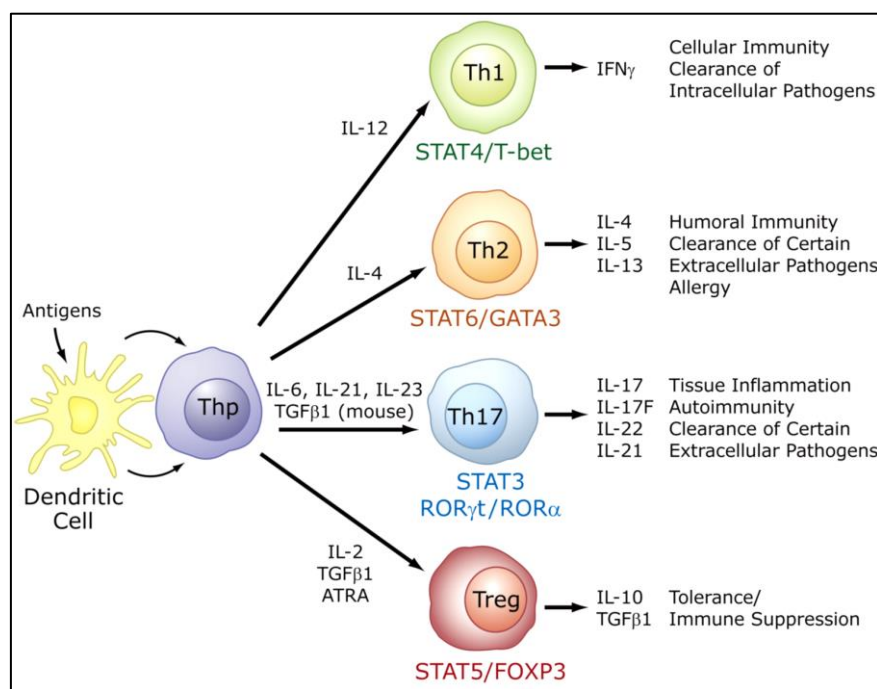


Figure 1.1: Cytokine dependent priming of different helper CD4+T-cell lineages.

Naïve conventional CD4+T-helper cells (Th0) can differentiate into four different subsets referred to as type 1 helper T-cells (Th1), type 2 helper T-cells (Th2), type 17 helper T-cells (Th17) and regulatory T-cells (Treg). The fate of Th0-cells is mainly determined by a combination and balance of lineage-specific cytokines, which stimulate distinct intracellular signalling pathways. Thus, development of Th1-cells is induced by a predominance of IFN- γ and IL-12, resulting in the activation of transcription factors STAT1 (Signal Transducer and Activator of Transcription 1) and STAT4. Elevated levels of IL-4 stimulate differentiation of Th2-cells by mediating STAT6-dependent activation of transcription factor GATA3. (Adapted with permission of Jetten AM (2009) Retinoid-related orphan receptors (RORs): critical roles in development, immunity, circadian rhythm, and cellular metabolism. Nucl Recept Signal. 7: e003. Copyright (2009)).

Upon activation helper T-cells also secrete a specific subset of cytokines, that promote their own proliferation in a positive feedback mechanism and at the same time down-regulate the development of other helper T-cell phenotypes. In the case of Th1-cells the signature

cytokine is IFN- γ , whereas production of IL-4, IL-5 and IL-13 is associated with the Th2-phenotype (reviewed in: (Abbas et al. 1996; Lappin and Campbell 2000)).

1.1.2 Inflammatory effector functions of interleukin-4 and interleukin-13

As aforementioned, a predominance of IL-4 during the early CD4+T-cell priming phase induces the development of type 2 helper T-cells. By further increasing the IL-4 concentration, Th2-cells suppress the polarization of Th1-phenotype and reinforce the signal for the differentiation of Th2-cells through a positive feedback mechanism (Parronchi et al. 1992; Nakamura et al. 1997). Moreover, by providing IL-4 together with IL-5 and IL-13, Th2-cells help to control infections with extracellular parasites, particularly helminths. As these parasites are much bigger and more complex than microbes, the immune system has evolved a specific defence mechanism. For instance, IL-5, which is known as a key regulator of eosinophilic granulocytes (short: eosinophils), promotes proliferation of eosinophils and their entry into the circulation (Sanderson 1992; Clutterbuck et al. 1989). Upon activation, eosinophils release cytotoxic molecules as well as immunomodulatory cytokines, chemokines, and lipid mediators, and thus are involved in the direct killing of the parasite (reviewed in: (Davoine and Lacy 2014)). The physiological effects of IL-4 and IL-13 partially coincide. For instance, both cytokines induce upregulation of vascular cell adhesion molecule-1 (VCAM1) on endothelial cells and thus facilitate leucocyte migration from the blood to the site of infection (Schleimer et al. 1992; Bochner et al. 1995).

While under normal conditions these Th2-effector functions are crucial for the clearance of parasites, in atopic individuals innocuous antigens not associated with infectious agents can trigger an aberrant Th2-immune response leading to severe allergic reactions. Pathophysiologically most significant is the ability of IL-4 and IL-13 to induce immunoglobulin class switching in B-cells to produce antibodies of the immunoglobulin E (IgE) class (reviewed in: (Worm and Henz 1997)). Class switching is a process during B-cell development, which induces B-cells to synthesize different types of antibodies. After primary antigen encounter within secondary lymphoid tissue, B-cells present antigenic peptides within MHC class II complexes on their cell-surfaces that can be recognized by activated helper T-cells specific for the same antigen. Receptor-mediated interaction between helper T-cells and B-cells together with cytokines, like IL-21 released by helper T-cells induce B-cell proliferation and survival (see review: (Parker 1993)) (Zotos et al. 2010). Some of these proliferating B-cells then differentiate into plasma-cells, whose main function is to secrete large amounts of antigen-specific antibodies. The primary antibody repertoire

1 Introduction

of naive B-cells is initially composed of IgM and (later) IgD isotype (see review: (Geisberger et al. 2006)), which provides some immediate protection. However, to eliminate an infection most effectively B-cells undergo further processes that include switching from IgM to other antibody classes, i.e. IgG, IgA and IgE. Immunoglobulin class switching involves irreversible DNA recombination within the constant-chain region of the antibody heavy-chain loci (see review: (Stavnezer and Schrader 2014)). This event is largely controlled by cytokines secreted by CD4⁺T-cells. For instance transforming growth factor beta (TGF- β) released by regulatory T-cells acts as a switch factor for the synthesis of IgG2b and IgA (Sonoda 1989; Coffman 1989; McIntyre 1993; Park et al. 2012; Wang et al. 2015), whereas IL-4 and IL-13 secreted by Th2-cells induce class switching to IgG4 and IgE isotype in B-cells (Coffman et al. 1986; Del Prete et al. 1988; Lundgren et al. 1989; Gascan et al. 1991; Punnonen et al. 1993; Defrance et al. 1994). The different immunoglobulin isotypes excite distinct effector functions (reviewed in: (Schroeder and Cavacini 2010)). Thus, pentameric IgM is mainly found in the blood stream, where it helps to control infections by activation of the complement system. Antibodies of the other classes are smaller and can also diffuse into the tissues. IgG for instance is widely distributed in tissue, where it helps phagocytes to take up pathogens by coating microbial surfaces, a process called opsonization. IgE antibodies are only present in low amounts in blood or extracellular fluids but trigger strong allergic reactions by mediating the release of powerful inflammatory molecules from mast cells and basophilic granulocytes (basophils). Mast cells and basophils primarily reside in tissue and blood circulation, respectively, where they act as first responders for invading parasites and antigens. Both cell types express IgE receptors on their cell surface, termed Fc-epsilon receptors I (Fc ϵ RI), which bind to the Fc-region of circulating IgE with high affinity (reviewed in: (Kinet 1999)). The recognition of a specific antigen/allergen through the IgE/Fc ϵ RI complex on mast cells and basophils stimulates cell degranulation and the release of potent inflammatory mediators from cytoplasmic granules, like the anticoagulant heparin and the vasodilator histamine, which promote transport of immune cells to the site of infection but also induce allergic symptoms like itching and tissue swelling associated with atopic diseases. In addition, prostaglandins, leukotrienes and proteases facilitate local inflammation by causing muscle constriction and tissue remodelling (reviewed in: (Stone et al. 2010)). By mediating the degranulation of mast cells and basophils, IgE antibodies therefore play a major role in the onset and progression of various atopic diseases, such as asthma, atopic dermatitis and allergic rhinitis (figure 1.2).

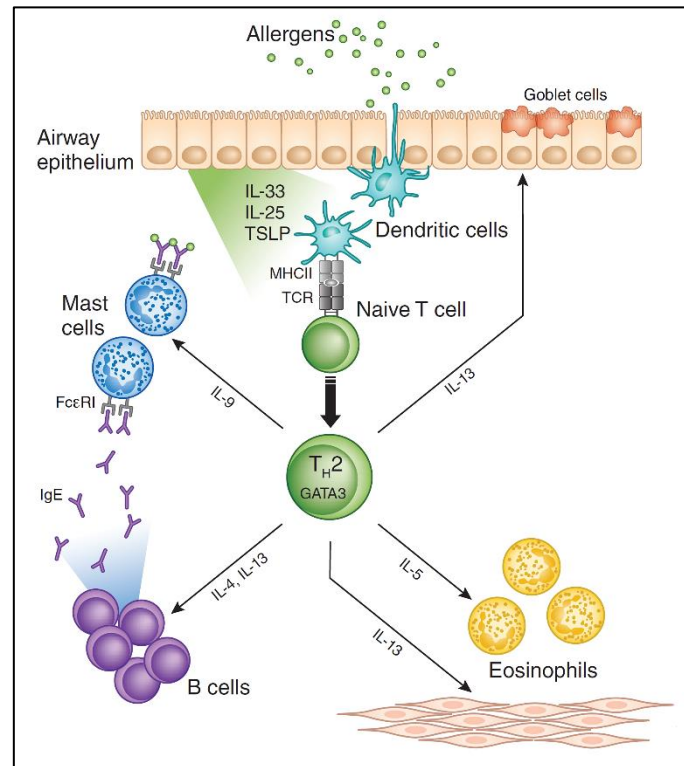


Figure 1.2: Effector mechanism of Th₂-specific cytokines in allergic reactions. In atopic individuals, allergens induce the development of Th₂-cells, which predominantly produce IL-4, IL-5 and IL-13. IL-4 and IL-13 induce B-cell immunoglobulin class switching to IgE production, which in turn facilitates degranulation of mast cells and basophils. Additionally, IL-5 mediates activation of eosinophils. Degranulation of mast cells, basophils and eosinophils leads to release of cytotoxic mediators, which can cause significant damage to the host tissue. Histamine and heparin promote blood flow, muscle constriction and vascular permeability, leading to airway swelling and potentially to anaphylactic shock. IL-13 is strongly involved in tissue remodelling by augmenting mucus production, causing goblet cell hyperplasia and inducing collagen production in fibroblasts. (Adapted by permission from Springer Nature: Nat Med; Brusselle GG, Maes T, Bracke KR (2013) Eosinophils in the spotlight: Eosinophilic airway inflammation in nonallergic asthma. (Copyright 2013)).

By upregulating the expression of FcεRI-receptors on mast cells (Xia et al. 1997; Kaur et al. 2006), IL-4 and IL-13 further promote IgE dependent responses.

However, there are also functional differences between IL-4 and IL-13. Thus, because human T-cells only express functional IL-4 receptors (termed IL-4 type I receptor; will be discussed in more detail below) which can only be activated by IL-4, IL-13 does not play a role in Th₂-cell polarization but rather seems to be important for the inflammatory effector phase (Zurawski et al. 1993; Waal Malefyt et al. 1995; Sornasse et al. 1996; Wang et al. 2004). In particular, IL-13 was shown to stimulate mucus production and to be strongly involved in tissue remodelling by causing fibrosis or goblet cell hyperplasia (Zhu et al. 1999; Hershey 2003; Chung et al. 2016).

1.2 IL-4 and IL-13 receptor assembly and signal transduction

1.2.1 IL-4 and IL-13 use overlapping receptor complexes

IL-4 and IL-13, with a size of 129 and 111 amino acids, respectively, both belong to the short-chain four-helix bundle-cytokine family (Smith et al. 1992; Walter et al. 1992; Eisenmesser et al. 2001; Moy et al. 2001)(reviewed in: (Sprang and Fernando Bazan 1993)). Even though they show little sequence homology members of this family, which besides IL-4 and IL-13 comprises cytokines, like IL-3, IL-9, IL-5 and GM-CSF (granulocyte-macrophage colony stimulating factor), share a common structural motif consisting of four antiparallel α -helices (Rozwarski et al. 1994) (reviewed in: (Mott and Campbell 1995)).

For cell signalling these cytokines use structurally related transmembrane receptors, which constitute the class I cytokine receptor family, also known as the hematopoietin receptors. A common feature of these receptors is the presence of an extracellular “cytokine binding homology region (CHR)”, which contains two joined fibronectin type III (FnIII) modules forming the classical elbow-shaped structure (Bazan 1990) (reviewed in: (Wang et al. 2009)). Each of these FnIII domains consists of a seven-stranded antiparallel β -sandwich. The N-terminal FnIII domain, designated D1, contains a pattern of conserved disulphide bonds, whereas the C-terminal FnIII domain, designated D2, contains a highly conserved 'Trp-Ser-X-Trp-Ser' motif (figure 1.3).

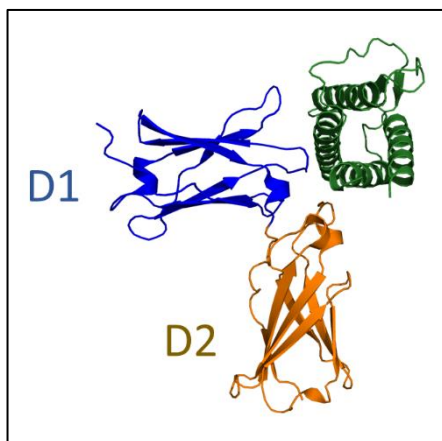


Figure 1.3: Structure of IL-4 receptor IL-4R α as a typical representative of the class I cytokine receptor family.

The extracellular domain of IL-4 receptor IL-4R α consists of two fibronectin type III modules (FnIII) characteristic for the class I cytokine receptor family. Shown is the crystal structure (cartoon representation) of human IL-4 complexed to the extracellular domain of IL-4R α receptor (Hage et al. 1999) (blue colour: IL-4R α FnIII module D1; orange colour: IL-4R α FnIII module D2; green colour: IL-4).

Most members of the four-helix bundle cytokine family bind to heterodimeric receptor complexes for cell signalling (reviewed in: (Wang et al. 2009)). Hematopoietin receptors have no intrinsic enzymatic activity, but their cytoplasmic domains are noncovalently associated with tyrosine kinases of the Janus kinase (JAK) family. Ligand binding induces receptor assembly, thereby bringing the kinases into close proximity, allowing them to

phosphorylate and activate each other. Distinct phosphorylated tyrosine residues in the receptor tails serve as binding sites for a family of transcription factors, termed STAT (signal transducer and activator of transcription). Binding of inactive STAT monomers to the phosphorylated tyrosine residues leads to their phosphorylation and subsequent dimerization. Activated STAT dimers can translocate into the nucleus, where they induce the transcription and expression of genes encoding T-helper cell lineage-specific cytokines, transcription factors, etc.

For signal transduction, IL-4 and IL-13 share a highly overlapping set of heterodimeric receptors of the hematopoietin family (reviewed in: (McCormick and Heller 2015)). IL-4 thereby can form two types of receptor assemblies, termed interleukin-4 type I and type II receptor. The type I receptor is formed by assembly of IL-4 receptor α (IL-4R α) (CD124) and the common γ chain (short: γ c; CD132), the type II receptor consists of IL-4R α and IL-13 receptor IL-13R α 1 (CD213a1). The type II receptor is also the functional receptor of IL-13 (figure 1.4).

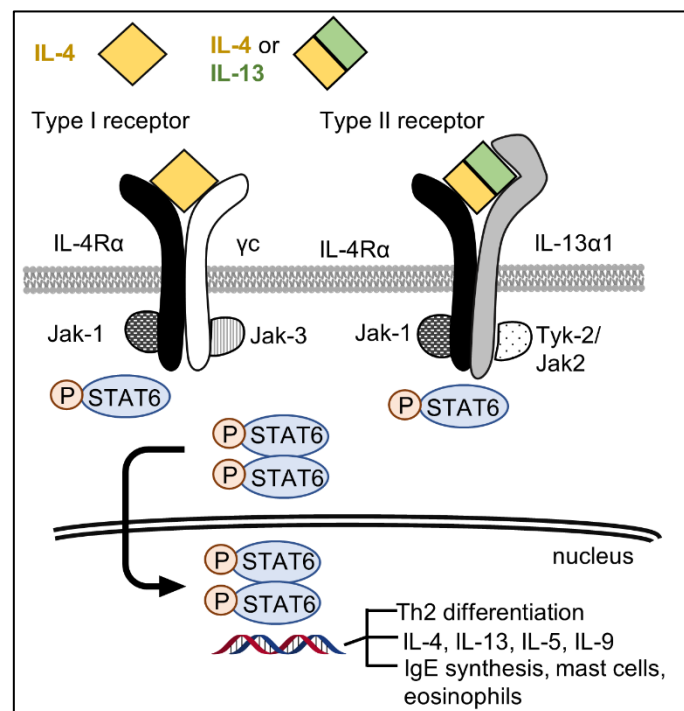


Figure 1.4: IL-4 and IL-13 mediated receptor assemblies. Binding of IL-4 to the type I receptor, consisting of IL-4R α and common γ chain (γ c), induces activation of cytoplasmic kinases JAK 1 and 3. The IL-4 receptor type II, consisting of IL-4R α and IL-13R α 1, is also the functional receptor of IL-13. Ligand binding results in activation of kinases JAK1 and JAK2 or TYK2. Activated kinases bind and phosphorylate tyrosine residues within the cytoplasmic receptor domain. These phospho-tyrosine residues serve as docking sites for signal proteins, which is primarily STAT6 or alternatively IRS (insulin receptor substrate)-2, STAT3 and other STATs. Phosphorylated STAT6 form homodimers, which facilitates its translocation to the nucleus and transcription of genes involved in Th2-cell differentiation, e.g. lineage-specific cytokines. (reviewed in: (McCormick and Heller 2015)).

1.2.2 Ligand binding induces sequential receptor formation

While IL-4 binds to IL-4R α with high affinity of about 100 pM (Kruse et al. 1992; Shen et al. 1996; Kraich et al. 2006; Andrews et al. 2006; Duppatla et al. 2012), no direct or only very weak (>100 μ M) interaction of IL-4 with IL-13R α 1 or γ c could be detected in cell-based experiments and *in vitro* interaction analysis (Caput et al. 1996; Miloux et al. 1997; Letzelter et al. 1998; Andrews et al. 2002; Kraich et al. 2006). However, binding affinities in low micromolar range could be observed for the interaction of IL-13R α 1 or γ c with the binary IL-4/IL-4R α assembly. Hence, a sequential binding mechanism has been proposed (figure 1.5), where IL-4 first binds to IL-4R α and then recruits the second receptor subunit, which is either the common γ chain (K_D of about 0.5 to 4 μ M) (Letzelter et al. 1998; Zhang et al. 2002; Kraich et al. 2006; Andrews et al. 2006; LaPorte et al. 2008) to form the IL-4 type-I receptor, or IL-13R α 1 (K_D of about 0.5 to 1 μ M) (Kraich et al. 2006; LaPorte et al. 2008) to form the IL-4 type-II receptor. The type I receptor is activated exclusively by IL-4, although the common γ chain itself is shared with other cytokine receptors, e.g. IL-2, IL-7, IL-9, IL-15 and IL-21 (reviewed in: (Leonard 2001)). The IL-4 type II receptor can also be activated by IL-13. Sharing of the IL-4R α /IL-13R α 1 receptor assembly is the molecular basis for the overlapping biological functions of IL-4 and IL-13. However, IL-13 induces receptor assembly in a reversed order, where IL-13 first binds to its high-affinity receptor IL-13R α 1 before engaging IL-4R α (Andrews et al. 2002; LaPorte et al. 2008; Kraich et al. 2006). Several studies demonstrated that IL-13 is not able to interact with IL-4R α alone (Caput et al. 1996; Miloux et al. 1997; Andrews et al. 2002; Andrews et al. 2006), but exhibits nanomolar affinity for IL-13R α 1 (between 4 – 40 nM) (Miloux et al. 1997; Andrews et al. 2002; LaPorte et al. 2008; Kraich et al. 2006). However, picomolar affinity was reported for binding of IL-13 to the binary IL-4R α /IL-13R α 1 receptor complex (K_D 20-600 pM) (Andrews et al. 2002; Miloux et al. 1997; Arima et al. 2005). A cooperative binding mechanism has been proposed to lead to an increase in affinity of IL-13 for the binary IL-4R α /IL-13R α 1 assembly, thereby stabilizing the ternary IL-13 type II receptor complex (see dissertation: (Kraich 2008)).

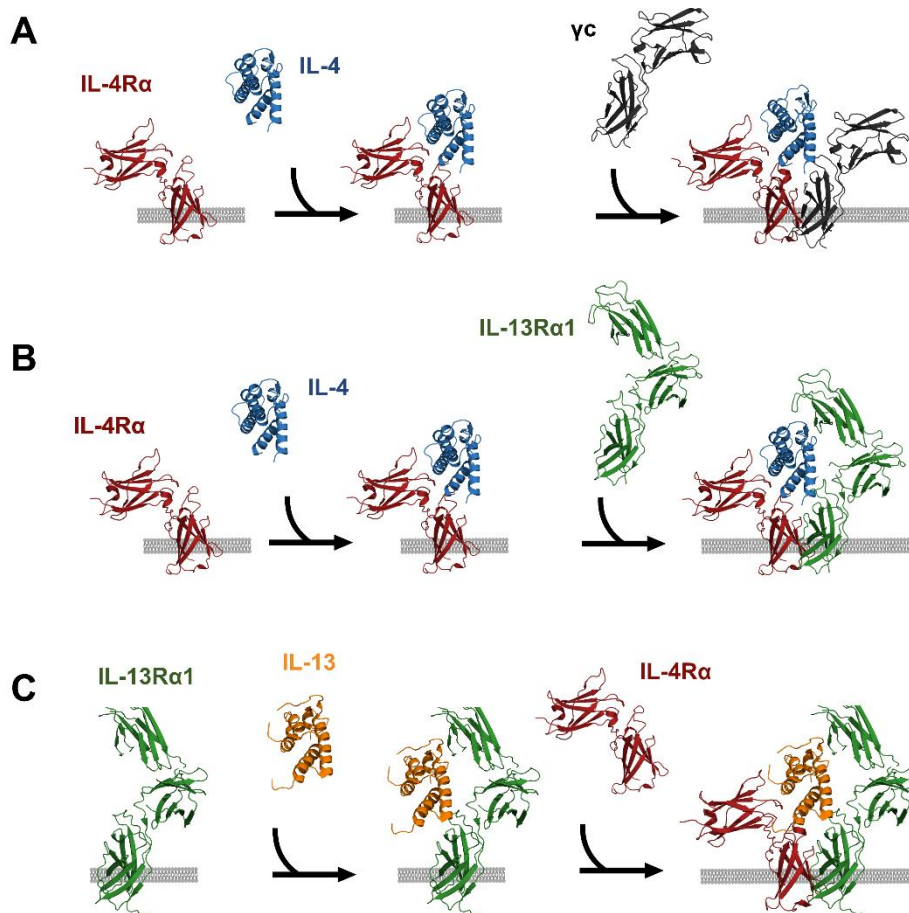


Figure 1.5: Sequential assembly of IL-4 and IL-13 receptors. A) IL-4 receptor type I: IL-4 first binds to its high-affinity receptor IL-4R α , followed by recruitment of γ B) IL-4 receptor type II: IL-4 first binds to its high-affinity receptor IL-4R α followed by recruitment of IL-13R α 1 C) IL-13 induced assembly of type II receptor: IL-13 first binds IL-13R α 1 followed by recruitment of IL-4R α . (colour code: red: IL-4R α , blue: IL-4, black: common γ chain, green: IL-13R α 1; orange: IL-13)

Besides IL-13R α 1, another receptor for IL-13 was identified, named IL-13 receptor α 2 (short: IL-13R α 2; CD213a2), which binds IL-13 with very high affinity, but does not interact with IL-4 (Caput et al. 1996). Initially, it was assumed, that IL-13R α 2 solely acts as a decoy receptor for IL-13, negatively regulating IL-13 concentration (Donaldson et al. 1998). However, recently it was found, that this receptor possibly mediates IL-13 effector functions distinct from heterodimeric IL-4R α /IL-13R α 1 receptor complex. It was demonstrated, that IL-13 signalling via IL-13R α 2 receptor stimulates TGF- β 1 synthesis in a murine macrophage cell line (Fichtner-Feigl et al. 2006). TGF- β 1 production is associated with pulmonary fibrosis. Additionally, IL-13R α 2 activity is implicated in cancer pathology (Fujisawa et al. 2012).

1.2.3 Molecular structure of IL-4

Like the other members of the small four-helix-bundle cytokine family, IL-4 consists of four α -helices, designated A, B, C and D. Helices A and B are antiparallel to helices C and D, adopting a so-called “up-up-down-down” topology (Smith et al. 1992; Walter et al. 1992; Wlodawer et al. 1992; Powers et al. 1992, 1993). The helices are connected by two long loops between helices A and B as well as C and D, which form an antiparallel β -sheet. Helices B and C are joined by a relatively short loop (figure 1.6). Conformational stability of IL-4 is strengthened by six cysteines that form three disulphide bridges. Disulphides between Cys3 and Cys127 join N- and C-terminus, Cys24-Cys65 restricts loop AB and loop BC and Cys46-Cys99 links helix B to loop CD (Carr et al. 1991; Kruse et al. 1991; Wlodawer et al. 1992).

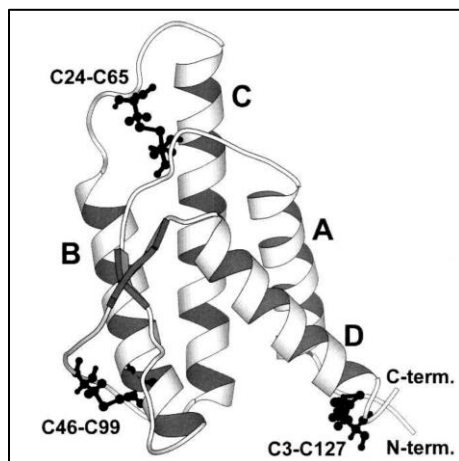


Figure 1.6: Four alpha-helix bundle topology of IL-4. Ribbon representation of human Interleukin-4 with the four helices labelled A to D; loops AB and CD are joined by a short antiparallel β -sheet (arrows); the three disulphide bonds C3–C127, C24–C65, and C46–C99 are indicated. (Adopted by permission from John Wiley and Sons: Protein Science; Vaz DC, Rodrigues JR, Sebald W, Dobson CM, Brito RM. (2006) Enthalpic and entropic contributions mediate the role of disulfide bonds in the conformational stability of Interleukin-4. (Copyright 2009).

The binding epitope for the high-affinity receptor IL-4R α , termed site I, is located on IL-4 helices A, B and C (Kruse et al. 1993; Shen et al. 1996). High-affinity binding of IL-4 to IL-4R α is based on electrostatic interactions between complementary charged interfaces, i.e. the IL-4-binding site on IL-4R α has an excess of negatively charged side chains complementary to the positive, basic residues in the AC binding epitope of the ligand IL-4 itself. Mutational analysis revealed the main binding determinants of IL-4 for IL-4R α to be residues glutamic acid 9 (Glu9) and arginine 88 (Arg88), which largely contribute to the overall binding affinity through hydrogen bonding and salt bridges (Wang et al. 1997)(reviewed in: (Mueller et al. 2002)). Moreover, it was found that mutation of threonine 13 (Thr13) or phenylalanine 82 (Phe82), both located in IL-4 site I, to aspartate stabilizes the IL-4/IL-4R α assembly, resulting in super-agonistic analogues with a threefold higher binding affinity for IL-4R α (Kraich et al. 2006).

Site II, which comprises the IL-4 binding interface for γ c and IL-13R α 1, largely overlaps and is centred around the hydrophobic residues isoleucine 11 (Ile11) on helix A and tyrosine 124 (Tyr124) on helix D. However, mutational studies revealed differences in the contribution of individual residues to the binding affinity of IL-4 for γ c and IL-13R α 1 (reviewed in: (Mueller et al. 2002)). While arginine 121 (Arg121) does not significantly contribute to the interaction with the common γ chain, mutating of Arg121 to glutamic acid or cysteine strongly disrupted binding to IL-13R α 1 (Shanafelt et al. 1998; Duppatla et al. 2014). The interaction of asparagine 15 (Asn15) with either receptor subunit is also of different strengths, being more important for binding to γ c than to IL-13R α 1 (Schnarr et al. 1997; Letzelter et al. 1998; Zhang et al. 2002).

Structural comparison between the interaction of IL-13 and IL-14 with the IL-4 receptor type II complex revealed a third binding site in IL-4 for IL-13R α 1, which is centred around asparagine 105 and threonine 108 in IL-4. In contrast to the common γ chain, which exhibits the classic tandem fibronectin type 3 (FNIII) domains-structure, the extracellular region of IL-13R α 1 is composed of three FNIII modules, D1, D2, and D3 that adopt a wrench-like architecture (LaPorte et al. 2008; Patino et al. 2011). The additional N-terminal fibronectin type III domain (D1) was reported to be only required for binding of IL-13R α 1 to IL-13, but not to IL-4 (Arima et al. 2005; LaPorte et al. 2008; Ito et al. 2009). It was proposed, that this particular structural feature of the IL-13/IL-13R α 1 interaction might allow the type II receptor to respond differentially to IL-4 and IL-13 (Ito et al. 2009), also explaining the different biological effects, which these cytokines exert via the type II receptor assembly.

1.3 IL-4 and IL-13 are key targets in treatment of atopic diseases

Because of the inflammatory reaction associated with the Th2 cytokine pattern, IL-4 and IL-13 have long been implicated with the pathophysiology of atopic diseases, like allergies, asthma, dermatitis or ulcerative colitis. As a consequence, these cytokines, as well as their signalling pathways, have been of great interest as key targets for novel therapeutic approaches.

Due to their overlapping receptor usage, IL-4 and IL-13 have some redundant functions. Pathophysiologically most relevant, IL-4 and IL-13 mediate the isotype class switching in B-cells to produce IgE antibodies. Studies of IL-4 and IL-13 knockout mice demonstrated that mice deficient in either IL-4 or IL-13 still produced antigen-specific IgE and only simultaneous disruption of IL-4 and IL-13 resulted in complete abrogation of IgE expression,

eosinophil infiltration and IL-5 production (McKenzie et al. 1999). Likewise, peritoneal mast cells from mice deficient in both IL-4 and IL-13 or IL-4R α were absent of surface-bound IgE and showed no detectable degranulation following treatment with anti-IgE *in vitro*. In contrast, peritoneal mast cells recovered from IL-4^{-/-} or IL-13^{-/-} mice only deficient in either one cytokine, had detectable IgE bound to the cell surface (Fish et al. 2005). These data clearly demonstrate that IL-4 and IL-13 are able to partially compensate each other and simultaneous blockage of both cytokines is required to adequately inhibit their biologic effects. This likely explains, why drugs directed against either IL-4 or IL-13 so far failed to show significant therapeutic efficacy in clinical trials for atopic diseases. For example, Altrakincept/Nuvance (Immunex), a soluble recombinant IL-4R α receptor directed against IL-4 initially showed some improvement in treating allergic asthma, e.g. improved FEV1 (forced expiratory volume in one second), but later failed to show efficacy in clinical phase III trials (Borish et al. 1999). Likewise, a humanized monoclonal antibody, capable of binding and neutralizing IL-4, Pascolizumab (GlaxoSmithKline)(Walter et al. 1992), did not demonstrate clinical efficacy in clinical phase II for treatment of asthma and was discontinued (reviewed in: (Cook and Bochner 2010)).

Among several therapeutics targeting IL-13, monoclonal antibodies Tralokinumab (MedImmune/AstraZeneca) and Lebrikizumab (Genentech/Roche) showed the most promising results and reached late-stage clinical development. These antibodies prevent IL-13 induced type II receptor assembly by binding to different epitopes in IL-13, Lebrikizumab preventing binding of IL-13 to IL-4R α and Tralokinumab blocking the interaction of IL-13 with IL-13R α 1 (Popovic et al. 2017; Ultsch et al. 2013). However, in phase III clinical trials for severe asthma Tralokinumab showed disappointing results, as it did not significantly reduce the annual exacerbation rate (Panettieri et al. 2018). Similarly, Roche discontinued any further development of Lebrikizumab for treatment of asthma after two inconclusive phase III trials (Korenblat et al. 2018). However, both antibodies are still under evaluation for the treatment of atopic dermatitis.

With these rather unimpressive treatment results of targeting IL-4 and IL-13 individually, dual cytokine inhibition by blocking the shared IL-4R α receptor represents a more promising strategy for treatment of atopic diseases associated with an aberrant Th2 response.

1.4 Targeting the shared IL-4R α receptor for simultaneous blockade of IL-4 and IL-13

Receptor sharing of IL-4 and IL-13 is a distinct feature that enables simultaneous inhibition of downstream signalling pathways of both IL-4 and IL-13 by specifically targeting the receptor IL-4R α . Therapeutics acting in this manner have been established. AMG 317 (Immunex/Amgen) is a monoclonal antibody directed against IL-4R α . It potently inhibited IL-4 and IL-13 dependent inflammatory effects *in vitro*, but later failed to show overall efficacy in a clinical phase 2 trial for asthma therapy (Corren et al. 2010). In contrast to AMG-317, Dupilumab (Regeneron/Sanofi), another fully humanized monoclonal antibody targeting the IL-4R α receptor, has demonstrated consistent clinical efficacy not only in asthma therapy, but also significantly improved atopic dermatitis and reduced nasal polyp burden in patients with chronic sinusitis and nasal polyposis (reviewed in: (Gandhi et al. 2017)). This has led to recent approval of Dupilumab for therapy of atopic dermatitis. Currently Dupilumab is being evaluated for the treatment of patients with moderate-to-severe asthma.

In the past, a second, not antibody-based strategy to inhibit IL-4 and IL-13 signalling has been implemented using a mechanistically highly similar approach as for Dupilumab. Already in the early 90s mutagenesis studies performed by Kruse and colleagues revealed three positions in IL-4, Arg121, Tyr124 and Ser125 located in IL-4 binding site II for γ c and IL-13R α 1, which upon amino acid replacement were shown to generate IL-4 variants with impaired binding to γ c and/or IL-13R α 1, but wildtype-like affinity for IL-4R α (Kruse et al. 1992; Kruse et al. 1993). A combination of Arg121 and Tyr124 both being replaced by aspartate was shown to be most effective resulting in a highly potent antagonist, incapable of activating either the type I or the type II receptor (Tony et al. 1994; Andrews et al. 2006; Schnarr et al. 1997). This IL-4 double variant, harbouring the mutations R121D and Y124D, was termed Pitrakinra.

Since human and rodent IL-4 act species-specific, meaning human IL-4 does not interact with the murine IL-4R α chain and vice versa, a murine Pitrakinra analogue was generated for analysis in preclinical trials. The murine version of Pitrakinra Q116D Y119D inhibited IL-4 and IL-13 dependent responses *in vitro*, e.g. downregulation of IL-4 induced STAT6 phosphorylation, and also acted as a potent antagonist for endogenous IL-4/IL-13 *in vivo*, e.g. it inhibited ovalbumin-specific IgE production (Grunewald et al. 1997; Grunewald et al. 1998). Based on these promising results Pitrakinra was tested for its therapeutic application

in asthma. It reached clinical phase 2, where it showed significant improvement for several asthma-related markers like a decrease in FEV1 and lower resting nitric oxide level (Wenzel et al. 2007). In addition to the above-described improvements, fewer asthma-related adverse events (wheezing, dyspnea, etc.) were observed in participants receiving Pitrakinra, thus requiring less rescue medication. However, the study also showed no differences between the Pitrakinra and placebo-group on airway hyperresponsiveness and also the number of sputum eosinophils and IgE level did not significantly differ between both participant groups. Thus, while several improvements were observed in the late-phase asthma response, the early-phase asthma response remained unaffected, which prompted some criticism about the potential clinical efficacy of Pitrakinra. Follow-up studies demonstrated, that Pitrakinra did considerably reduce asthma exacerbations in a subset of patients suffering from eosinophilic asthma and in individuals with specific IL-4R α genotypes (Slager et al. 2012), indicating that Pitrakinra might be effective in a defined subset of patients. Nevertheless, further developments of Pitrakinra were stopped after a clinical phase 2.

However, the recent success of Dupilumab, which mechanistically resembles the action of Pitrakinra, clearly illustrates that simultaneous blockage of IL4/IL13 signalling at the IL4 receptor IL4R α is an effective strategy for the treatment of atopic diseases. This encouraged us to design novel IL-4 based antagonists, which evade Pitrakinra's inherent disadvantages responsible for its poor performance in clinical trials.

1.5 Aim: Design of novel, more effective IL-4 antagonists

Structure analysis revealed that the antagonistic effect of Pitrakinra is not mediated through structural changes, but through introduction of an electrostatic mismatch in the binding interface for γ c and IL-13R α 1 (Müller et al. 1994). This was further supported by the fact, that negatively charged residues were most effective in creating an IL-4 antagonistic variant (Kruse et al. 1992) (reviewed in: (Mueller et al. 2002)).

We hypothesized that instead of an electrostatic mismatch as in Pitrakinra, implementing steric hindrance would yield a superior antagonist, because binding to either γ c or IL-13R α 1 is more effectively blocked. Duppatla and colleagues introduced cysteine residues in IL-4's binding epitope for γ c and IL-13R α 1 and used thiol-reactive, bulky compounds like N-ethylmaleimide or polyethylene glycol (PEG) polymers to induce steric hindrance (Duppatla et al. 2014). They found that in contrast to the previous double mutation approach R121D Y124D, site-specific modification of a single IL-4 residue, i.e. R121 is already sufficient to

effectively disrupt binding to γc and IL 13R α 1, thereby providing a potent IL-4/IL-13 antagonist.

Depending on the compound employed for modification, using a steric hindrance-based approach for the design of antagonistic IL-4 variants offers a novel strategy of implementing IL-4 antagonism while simultaneously improving the pharmacological parameters of the antagonist. However, modification with synthetic chemical compounds, as employed by Duppatla and colleagues always bears the risk to induce immunogenicity, thus lowering the drug's safety. For instance, a pharmacological disadvantage of polyethylene glycol (PEG), which is often employed to improve the pharmacokinetic profile of biologics, is the poor degradability of PEG leading to its accumulation in the liver. Also, in some, albeit rare cases anti-PEG antibodies have been detected limiting the efficacy of the therapeutic (Armstrong et al. 2007)(reviewed in: (Zhang et al. 2014)). Additionally, PEGylation, i.e. the conjugation of large polyethylene glycol (PEG) polymers, can also decrease the therapeutic efficacy by negatively affecting the drug's activity (Rodríguez-Martínez et al. 2009; Roberts and Harris 1998)(reviewed in: (Zalipsky 1995)). Substantial loss of conjugate activity was also observed for a pegylated version of Pitracinra. Thus, while the clearance rate of the Pitracinra-PEG conjugate was slowed down significantly (plasma half-life was extended from a few hours to 5 days) due to the size increase, the modification strongly impaired the efficacy of the IL-4 inhibitor, even though coupling of the PEG moiety was done site-specific (see patent: WO2011106779A1, (Tomkinson 2011)). Hence, PEGylation certainly is not an ideal modification.

For the development of novel IL-4 based antagonists we therefore wanted to employ compounds for introduction of steric hindrance, which simultaneously afford an optimization of IL-4's pharmacological parameters (e.g. molecular stability, clearance rate, absorption) but do not exhibit the inherent disadvantages of PEG (increased immunogenicity, poor degradability, loss of conjugate activity). Furthermore, a strategy should be developed that would allow introduction of the compound in a site-directed manner to not affect the efficacy of the antagonist.

2. Results

Glycosylation is a natural modification found in many secreted proteins, which positively affects pharmacology of proteins (reviewed in: (Solá and Griebenow 2010)). Thus, glycosylated proteins show increased serum half-life (Fernandes and Gregoriadis 1997; Egrie et al. 2003), metabolic stability (Fernandes and Gregoriadis 1996; Ueda et al. 2009), solubility (Runkel et al. 1998; Tams et al. 1999) and absorption compared to their non-glycosylated analogues (Egleton et al. 2000).

Since IL-4 itself is a glycoprotein, we decided to use a carbohydrate moiety to modify IL-4, thereby producing an IL-4 antagonist with improved pharmacokinetic parameters.

The main objectives of this work were firstly to find a method, which allows site-specific introduction of sterically demanding glycan molecules into central positions of IL-4's binding epitope for γc and IL-13R $\alpha 1$. Since chemical and biosynthetic glycoengineering approaches offer complementary qualities, strategies allowing for chemical glycan coupling to e.g. "naked" IL-4 protein derived from expression in bacteria, as well as biosynthetic glycosylation, exploiting the enzymatic glycosylation machinery of eukaryotic expression systems were thus assessed for site-directed introduction of glycans.

Secondly, the antagonistic efficacy of the glycoengineered IL-4 variants should be characterized using *in vitro* interaction analysis, employing surface plasmon resonance technology, as well as cell-based assays. To produce IL-4 antagonists with superior antagonistic efficacy to Pitrakinra and to compensate for potentially lower binding affinity due to abrogated interaction with the secondary receptor subunits, mutations increasing the affinity for IL-4R α should be additionally introduced and evaluated.

2.1 Recombinant expression of IL-4 protein in Hek293 cells

In contrast to prokaryotic expression systems, eukaryotic expression systems are capable of complex protein processing, such as proper disulphide formation and complex N-linked glycosylation. In this work, IL-4 variants were recombinantly expressed in human embryonic kidney 293 (Hek293) cells to obtain IL-4 glycoproteins containing complex N-linked glycans at selected positions. Therefore, IL-4 variants were designed to contain novel engineered N-glycosylation motifs at specific sites, which then were transiently expressed in Hek293 cells.

2.1.1 Cloning and protein expression of IL-4 in Hek293 cells

For recombinant protein expression of IL-4 in Hek293 cells the cDNA-sequence encoding the mature human IL-4 protein (UniProtKB/Swissprot P05112) without the N-terminal signal peptide of 24 amino acids was used as a template (Supplement figure S9.1). Novel N-glycosylation sites were introduced by two-step PCR using specific oligonucleotides containing the desired mutation (chapter 4.10/ 5.1.1). The final PCR product was cloned into the pHLsec(throm) vector using AgeI and KpnI endonucleases (chapter 5.1.2). The pHLsec(throm) vector is a derivative of the mammalian expression vector pLEXm, which carries an optimized secretion-signal and an N-terminal affinity hexahistidine tag (Aricescu et al. 2006). A six-residue recognition sequence (-VPR↓GS-) for the endopeptidase thrombin, which is located downstream of the N-terminal hexahistidine tag, allows for subsequent removal of the hexahistidine tag from the purified IL-4 protein.

Two Hek293 cell lines, Freestyle™ 293F and Expi293F™, were employed for recombinant expression of IL-4 protein. Prior to transfection, Freestyle™ 293F cells were seeded in growth medium at a density of 0.75×10^6 cells/mL, and Expi293F™ cells were seeded in growth medium at a density 2.5×10^6 cells/mL (chapter 5.4.2). The plasmid DNA was transiently transfected into cells using polyethylenimine (PEI) transfection reagent. For test expression 5 mL of cells were transfected with a mixture of 5 µg of plasmid DNA and 10 µg polyethylenimine. Five days after transfection, immunoblotting was used to examine the cell culture supernatant for the presence of IL-4 protein. For detection of hexahistidine tagged IL-4 protein, a horseradish peroxidase (HRP)-antibody conjugate, specific for the hexahistidine tag, was used (chapter 5.2.2).

For higher expression yield in milligram scale, a minimum of 200 mL of cells were transfected.

2.1.2 Protein purification via immobilized metal-ion affinity chromatography

The pHLsec(throm) derived IL-4 protein carries an N-terminal hexahistidine fusion tag, which allows affinity purification by immobilized metal-ion affinity chromatography (IMAC). After five days of expression, the cell culture supernatant was harvested by centrifugation and extensively dialysed against IMAC binding buffer containing 10 mM imidazole, to reduce non-specific binding (chapter 5.6.2). The clarified protein solution was loaded onto a 5 mL HisTrap™ excel column (GE Healthcare) and the protein was purified using isocratic elution with 100% elution buffer, which contained 500 mM imidazole (figure

2 Results

2.1A). Protein containing fractions (figure 2.1B) were pooled and dialysed against 1 mM HCl. For long-term storage, the protein was freeze-dried and stored at -80 °C.

Depending on the position and number of engineered N-glycosylation sites the protein yield varied. However, the average protein yield for Expi293FTM expression was generally higher than for expression in FreestyleTM 293F, e.g. expression of IL-4 variant F82D in Expi293FTM cells yielded about 0.9 mg per 100 mL of culture, whereas only 0.2 mg of this variant could be obtained from 100 mL of FreestyleTM 293F culture.

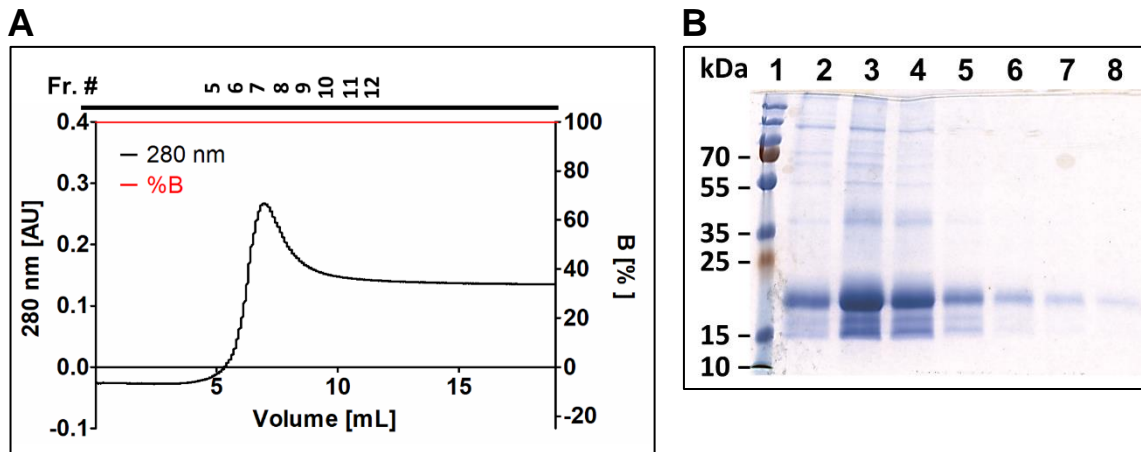


Figure 2.1: Purification of IL-4 from Hek293 cell culture supernatant using immobilized metal-ion affinity chromatography. A) Elution profile of IL-4 IMAC chromatography B) SDS-PAGE analysis of elution fractions: 1: size standard; 2: frac. 6; 3: frac. 7; 4: frac. 8; 5: frac. 9; 6: frac. 10; 7: frac. 11; 8: frac. 12. Protein containing fractions 6-9 were pooled.

2.1.3 Hek293 cell-derived wildtype IL-4 carries a single N-glycan at Asn38, which is not important for biologic activity

Since the N-glycosylation pattern of Hek293 cell-derived human IL-4 protein has yet to be determined, in-depth analysis employing mass spectrometry was performed. Characterization of glycoproteins by e.g. mass spectrometry is difficult since glycoproteins often consist of a heterogeneous mixture of glycoforms that differ in glycan content, as well as glycan composition and architecture. Endoglycosidases can reduce or fully remove oligosaccharides from glycoproteins, releasing structurally defined proteins, thereby facilitating protein analysis. Endoglycosidase-H (Endo-H) cleaves after the first N-acetylglucosamine (GlcNAc), thereby removing almost the entire N-glycan, leaving a single N-acetylglucosamine moiety attached to the asparagine residue in the N-X-T motif. Hence, mass spectrometry analysis of glycoproteins treated with endoglycosidase-H does not only

provide information about the peptide sequence, but the amount of identified N-acetylglucosamine molecules also indicates the prevalent glycoform the protein exists in. About 10 μg of Hek293 cell-derived IL-4 F82D were incubated with 150 U of Endo H_f (chapter 5.2.3; Endo-H digest was performed by Dr. Juliane Fiebig). Unfortunately, IL-4 F82D protein treated with endoglycosidase-H did not show a downward shift in SDS-PAGE, which would be expected after deglycosylation due to decrease in protein size. This suggests, that endoglycosidase-H is not able to cleave and remove N-linked glycans from Hek293 cell-derived IL-4 protein (figure 2.2A). The mannosidase inhibitor kifunensine affects N-glycan processing and allows the preparation of high-mannose glycoproteins, which show a higher susceptibility for endoglycosidase H (Endo-H) (Elbein et al. 1990; Chang et al. 2007). Therefore, expression of IL-4 in Hek293 cells was performed in the presence of 5 μM kifunensine (chapter 5.4.2.). After treatment with endoglycosidase-H, IL-4, derived from “kifunensine expression”, now clearly showed a strongly reduced apparent molecular weight in SDS-PAGE due to the removal of N-glycans (figure 2.2B).

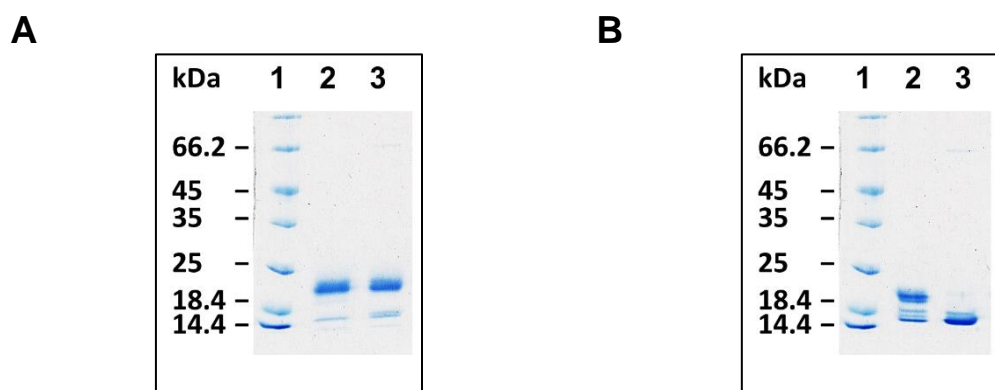


Figure 2.2: SDS-PAGE analysis of Hek293 cell-derived IL-4 F82D treated with Endo-H. SDS-PAGE was performed under non-reducing conditions. A) Endo-H digest of protein expressed without kifunensine. 1: size standard; 2: IL-4 protein (untreated); 3: IL-4 protein treated with Endo-H. B) Endo-H digest of protein expressed in the presence of kifunensine. 1: size standard; 2: IL-4 protein (untreated); 3: IL-4 protein treated with Endo-H.

For subsequent mass spectrometry analysis, the protein was purified by reverse-phase high performance liquid chromatography. Mass spectrometry detected one major protein species with a molecular weight of 16526 Da, which is consistent with the theoretical mass of IL-4 F82D carrying a single GlcNAc residue (figure 2.3A) (Supplement Table S9.2). Besides this monoglycosylated form, a non-glycosylated IL-4 protein species with a mass of 16322 Da was identified, that made up of about 10% of isolated protein and also minor amounts of multiglycosylated protein containing two (16729 Da) or three (16932 Da) N-acetylglucosamine molecules were detected. These data suggest that IL-4 protein obtained

2 Results

from expression in Hek293 cells predominantly consists of a monoglycosylated variant. This is consistent with the results from previous studies analysing glycosylation pattern of hIL-4 derived from various eukaryotic expression systems. Thus, human IL-4 protein was shown to contain two potential N-linked glycosylation sites, i.e. Asn-X-Ser/Thr motifs, at position 38 and 105, but only Asn38 has been found to carry an N-linked glycan and O-glycosylation has not been reported (Carr et al. 1991; Tsarbopoulos et al. 1995; Li et al. 2014). We also identified Asn38 as the prevalent N-glycosylation site used by Hek293 cells, as in SDS-PAGE a Hek293 cell-derived IL-4 variant with Asn38 mutated to glutamine showed a strongly reduced apparent molecular weight of about 16 kDa, which is consistent with the mass of non-glycosylated IL-4 protein (figure 2.3C).

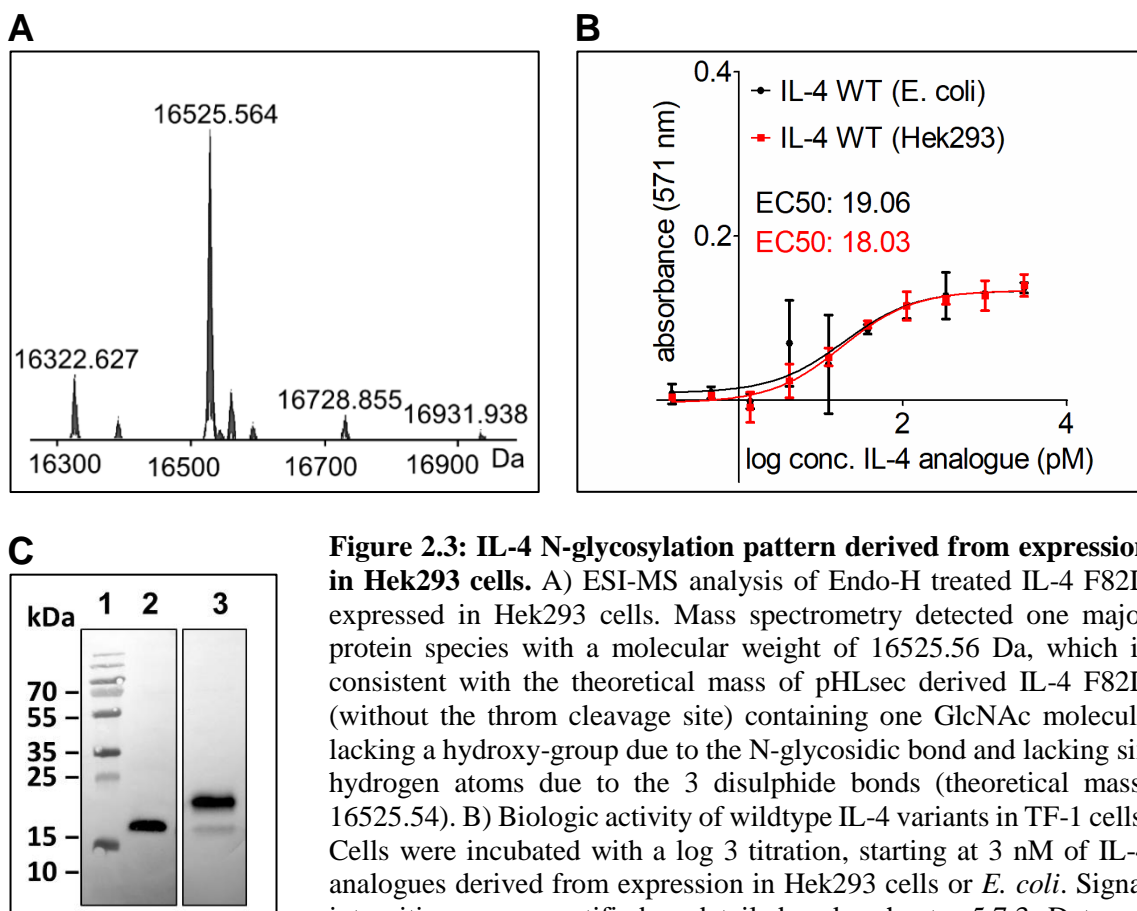


Figure 2.3: IL-4 N-glycosylation pattern derived from expression in Hek293 cells. A) ESI-MS analysis of Endo-H treated IL-4 F82D expressed in Hek293 cells. Mass spectrometry detected one major protein species with a molecular weight of 16525.56 Da, which is consistent with the theoretical mass of pHLsec derived IL-4 F82D (without the throm cleavage site) containing one GlcNAc molecule lacking a hydroxy-group due to the N-glycosidic bond and lacking six hydrogen atoms due to the 3 disulphide bonds (theoretical mass: 16525.54). B) Biologic activity of wildtype IL-4 variants in TF-1 cells. Cells were incubated with a log 3 titration, starting at 3 nM of IL-4 analogues derived from expression in Hek293 cells or *E. coli*. Signal intensities were quantified as detailed under chapter 5.7.3. Data are shown from a single experiment. C) Western Blot analysis of IL-4 F82D N38Q expressed in Hek293 cells. Cell supernatants were submitted to SDS-PAGE and Western Blot analysis. The IL-4 variants carrying a polyhistidine-tag were detected using an anti-His6 tag antibody conjugated to HRP. 1: size standard; 2: IL-4 F82D N38Q; 3: IL-4 WT.

To determine, whether glycosylation influences the biologic activity of IL-4, N-glycosylated Hek293 cell-derived IL-4 protein and non-glycosylated (“naked”) IL-4 protein obtained

from expression in *E. coli* were analysed in a TF-1 cell proliferation assay (analysis was performed by Dr. Juliane Fiebig). TF-1 cells are human hematopoietic cells, which proliferate in response to IL-4, thereby serving as a reporter system for IL-4 signalling. Identical EC50 values of about 20 pM could be obtained for both IL-4 variants (figure 2.3B), EC50 thereby referring to the half maximal effective concentration of the tested variant. This clearly indicates, that N-glycosylation is not required for IL-4 signal transduction *in vitro*. This is consistent with previous findings, that glycosylation is not important for IL-4's biologic function (Le et al. 1988).

2.2 Recombinant expression of IL-4 cysteine variants in *E. coli*

Recombinant protein expression in bacteria offers many advantages over eukaryotic expression systems, like fast growth rate, simple genetic manipulation, and low-cost media. However, in contrast to eukaryotic expression systems, *E. coli* only performs limited post-translational modifications, e.g. *E. coli* is not capable of protein N-glycosylation. Hence, *E. coli*-derived proteins can only be glycosylated by synthetical means. For chemical coupling of carbohydrate molecules, we decided to introduce cysteine residues in IL-4 for several reasons. Firstly, IL-4 has three disulphide bonds but does not contain an unpaired cysteine residue. Thus, introduction of an additional cysteine residue provides great specificity. Additionally, cysteine labelling has the advantage that most coupling procedures take place under near physiological conditions and proceed rapidly due to the strong nucleophilic character of the cysteine thiol. Various thiol-reactive compounds are available, such as maleimides or haloalkyl reagents, which usually do not show non-specific reactions with other polar groups present in a protein.

2.2.1 Cloning and protein expression

For recombinant protein expression of IL-4 in *E. coli*, the cDNA-sequence encoding the mature human IL-4 protein (UniProtKB/Swissprot P05112) without the N-terminal signal peptide of 24 amino acids was used as a template (Supplement figure S9.1). An N-terminal ATG-sequence (methionine) was added to serve as a start codon. Cysteine residues were introduced in a two-step PCR, employing specific oligonucleotides containing the desired mutation (chapter 4.2; 5.1.1). Previous studies in our laboratory have shown that introducing the mutation F82D, i.e. exchanging Phe82 in the third helix of IL-4 by aspartate, greatly increases the refolding yield of recombinant IL-4 protein. Additionally, the mutation F82D enhances the binding affinity of IL-4 to its high-affinity receptor IL-4R α about threefold and

thus is also beneficial for the designed antagonists (Kraich et al. 2006), as these will more effectively compete against endogenous IL-4. Therefore, all engineered IL-4 antagonists in this study additionally contain the F82D mutation.

The modified IL-4 DNA was cloned into the pQE-80L-derived expression vector, termed pQKA, which carries the IL-4 gene under the control of an IPTG inducible T5/lac promoter, using the endonucleases XhoI and BamHI (chapter 5.1.2). For recombinant protein expression, the plasmid DNA was transformed into chemically competent *E. coli* BLR(DE3) cells (chapter 5.1.4.2). Transformed *E. coli* cells were cultivated in LB-medium and protein expression of IL-4 was induced by addition of 1 mM IPTG, when cells reached the exponential growth phase (chapter 5.3). Protein overexpression proceeded for four hours before cells were harvested by centrifugation. SDS-PAGE analysis of the cell lysate prepared four hours after IPTG addition revealed a prominent protein band with an apparent molecular weight of about 15 kDa consistent with the expected size of IL-4 (figure 2.4). One litre of expression culture yielded about 2.4 g of *E. coli* cell biomass.

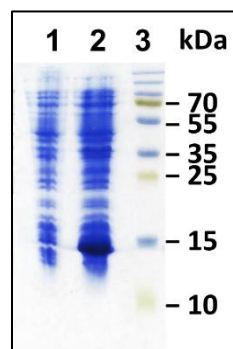


Figure 2.4: SDS-PAGE analysis of recombinant protein expression of IL-4 in *E. coli*. Cell lysates were prepared prior (1) and 4 hours after (2) addition of IPTG to *E. coli* culture; (3) size standard. IL-4 protein with an apparent molecular weight of about 15 kDa is clearly visible after 4 hours of protein expression.

2.2.2 Extraction of IL-4 protein from inclusion bodies and oxidative refolding

Recombinant expression of proteins that contain structurally important disulphide bonds, such as IL-4, is difficult in *E. coli*, due to the reducing environment in the cytoplasm, which impedes proper disulphide bond formation (reviewed in: (Singh and Panda 2005)). Hence, overexpression of IL-4 in *E. coli* leads to the formation of insoluble aggregates of misfolded IL-4 protein, so-called inclusion bodies (IB), which make proper protein refolding necessary. For the extraction and purification of the IL-4 containing inclusion bodies, 5 g of frozen, pelleted cells were taken up in STE-buffer containing 1 mM DTT, subjected to sonication and centrifuged (chapter 5.3.2.1). The pelleted cells were again solubilized in STE buffer

and sonicated once more, followed by two washing steps. SDS-PAGE analysis of samples taken during extraction of the inclusion bodies (figure 2.5A) demonstrates that cell debris are removed with the supernatant, whereas the IL-4 protein remains in the sediment fraction. One gram of *E. coli* cell-pellet yielded about 0.3 g of IB (wet weight).

To determine the amount of IL-4 protein contained in the inclusion bodies, purified inclusion bodies were taken up in TRIS-buffer and samples were prepared. For protein quantification via SDS-PAGE, defined amounts of IL-4 protein were loaded onto the SDS-gel together with serial dilutions of the unknown inclusion bodies sample (figure 2.5B). A subsequent analysis employing Biorads ImageLab software allowed absolute quantification of IL-4 protein contained in the loaded samples based on band intensities. Using the absolute quantity tool, it could be estimated, that one gram of inclusion bodies contained about 38 mg of IL-4 protein.

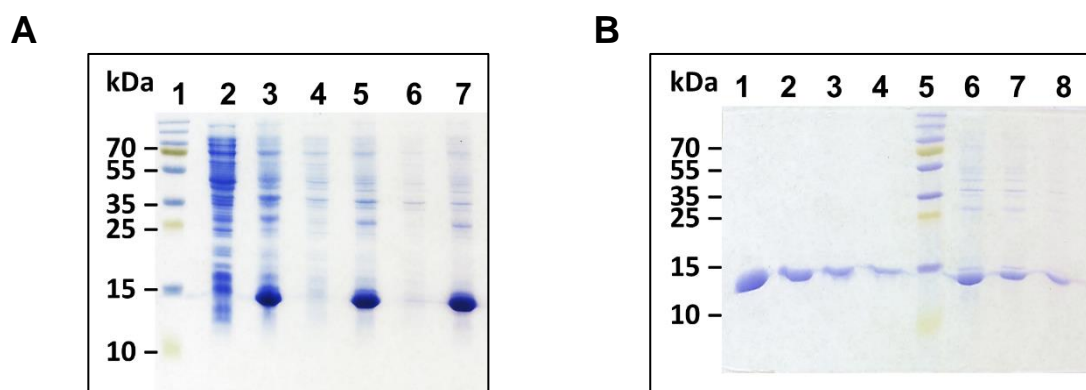


Figure 2.5: SDS-PAGE analysis of IL-4 inclusion bodies. A) Purification of IL-4 inclusion bodies. During IB extraction samples were taken at different steps and submitted to SDS-PAGE. 1: size standard; 2: supernatant after 1st sonication/centrifugation step; 3: solubilized pellet after 1st sonication/centrifugation step; 4: supernatant after 2nd sonication/centrifugation step; 5: solubilized pellet after 2nd sonication/centrifugation step; 6: supernatant after 3rd centrifugation step; 7: solubilized pellet after 3rd centrifugation step. SDS-PAGE was performed under reducing conditions. B) Quantification of IL-4 contained in purified inclusion bodies. Defined amounts of IL-4 R121C were submitted to SDS-PAGE in order to determine the IL-4 concentration in the IB. SDS-PAGE was performed under reducing conditions 1: 10 µg IL-4 R121C; 2: 5 µg IL-4 R121C; 3: 2.5 µg IL-4 R121C; 4: 1.25 µg IL-4 R121C; 5: size standard; 6: 1:10 dilution of solubilized IB; 7: 1:20 dilution of solubilized IB; 8: 1:40 dilution of solubilized IB.

To completely solubilize the aggregated IL-4 protein, hydrophobic interactions were disrupted by mixing the inclusion bodies suspension with a buffer containing 8 M guanidine hydrochloride. Additionally, the solution was supplemented with 1 mM DTT to reduce IL-4's disulphide bonds and achieve complete protein denaturation. The suspension was kept at 21 °C for 2 h under mild stirring. For subsequent refolding of IL-4 protein, the clarified light brown solution was added dropwise to ice-cold refolding buffer containing 1 M

2 Results

arginine and a glutathione redox couple (5 mM oxidized GSSG, 2 mM reduced GSH) to give a protein concentration of about 50 $\mu\text{g/mL}$ (chapter 5.3.2.2). The refolding solution was incubated for three days at 4 $^{\circ}\text{C}$.

2.2.3 1st step of IL-4 protein purification: Cation exchange chromatography

The IL-4 protein has a theoretical isoelectric point of about 9, which makes purification by cation exchange chromatography possible. For cation exchange chromatography an ammonium acetate buffer was used with a pH of 5.0, at which the IL-4 protein is in its protonated state (chapter 5.6.1). Buffer exchange of the refolding solution was achieved by extensive dialysis against 25 mM ammonium acetate pH 5.0, which only was accompanied by minor protein precipitation. The clarified protein solution was loaded onto a 5 mL HiTrapTM CM FF column (GE Healthcare) and for protein elution, a linear salt gradient from 0 to 1.5 M NaCl was applied. IL-4 protein eluted between 0.5 and 0.7 M NaCl (figure 2.6A) and the protein containing fractions (figure 2.6B) were pooled.

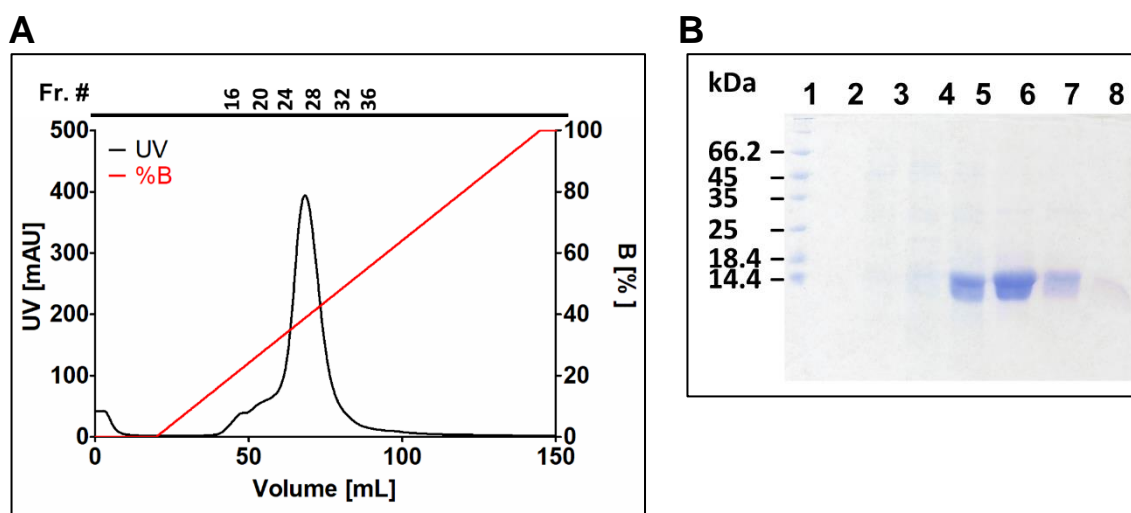


Figure 2.6: Purification of IL-4 using cation exchange chromatography. A) Elution profile of IL-4 cation exchange chromatography B) SDS-PAGE analysis of elution fractions: 1: size standard; 2: frac. 15; 3: frac. 18; 4: frac. 21; 5: frac. 24; 6: frac. 27; 7: frac. 30; 8: frac. 33. Protein containing fractions 23–30 were collected.

2.2.4 2nd step of IL-4 protein purification: Reverse Phase-High Performance Liquid Chromatography

Following cation exchange chromatography, IL-4 protein was further purified using a reverse phase-high performance liquid chromatography (RP-HPLC) (chapter 5.6.3). After cation exchange chromatography the clarified protein solution was applied to a C4 column (Phenomenex), and for protein elution, a linear gradient from 0 to 100% acetonitrile was

applied (figure 2.7A). IL-4 protein eluted at 65% acetonitrile and IL-4 protein containing fractions were pooled, freeze-dried and stored at $-80\text{ }^{\circ}\text{C}$ (figure 2.7B).

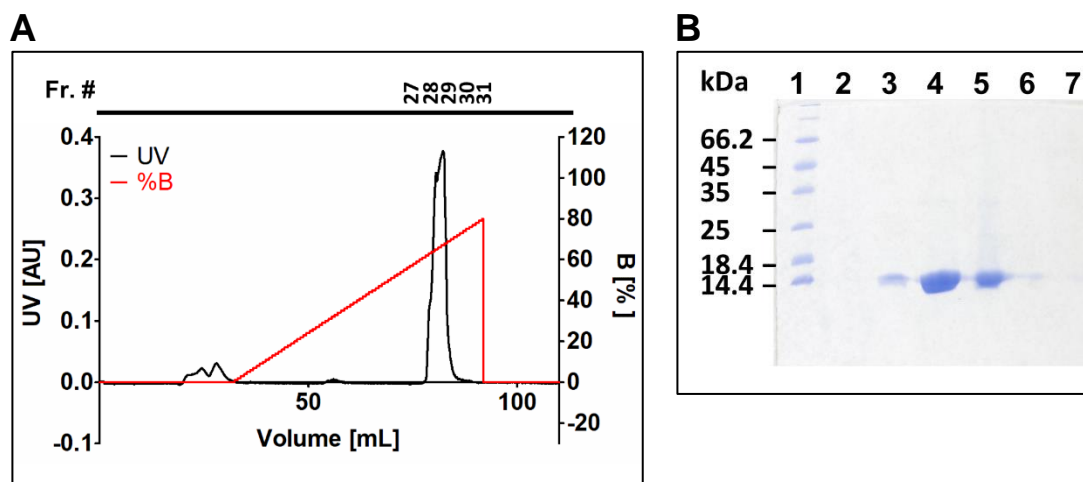


Figure 2.7: Purification of IL-4 using Reverse Phase HPLC. A) Elution profile of IL-4 RP-HPLC chromatography. IL-4 protein eluted between 64 and 68% acetonitrile. B) SDS-PAGE analysis of elution fractions: 1: size standard; 2: frac. 26; 3: frac. 27; 4: frac. 28; 5: frac. 29; 6: frac. 30; 7: frac. 31. Protein containing fractions 27-29 were pooled.

One gram wet weight of *E. coli* cell biomass yielded about 10 mg of purified IL-4 protein, which is about three times higher compared to the protein yield reported by Duppatla and colleagues (Duppatla et al. 2012). The higher IL-4 protein yield is probably the result of a change in protocol during the cation exchange chromatography step. Thus, the protocol used by Duppatla and colleagues employed a PBS buffer with pH 7.4 for dialysis of the IL-4 refolding solution. For subsequent cation exchange chromatography, the pH of the dialyzed protein solution had to be adjusted to 5.0, which was achieved by dropwise addition of highly concentrated ammonium acetate solution (4 M ammonium acetate pH 5.0). This harsh acidification resulted in a considerable protein loss due to precipitation. In contrast, direct dialysis of the refolding solution against 10 volumes of 25 mM ammonium acetate pH 5.0 employed in this work, was shown to be much milder, as only minor protein precipitation was observed.

2.3 Prokaryotic expression and purification of glutaredoxin-1

For oxidative refolding of IL-4 cysteine variants, a glutathione redox-couple was employed which was shown to facilitate native disulphide bond formation. Under these conditions, the engineered cysteine residue forms a mixed disulphide with a glutathione molecule (Duppatla et al. 2012). While this is beneficial, as it prevents the unpaired cysteine from non-specific reactions, it also requires an additional step for the removal of the glutathione moiety before

2 Results

glycan coupling can be performed. Initial attempts to remove the glutathione residue by chemical reduction, e.g. by employing DTT resulted in a complete reduction of the proteins disulphide bonds and irreversible protein precipitation. In contrast, an enzymatic approach developed by Duppatla and colleagues allowed specific cleavage of the mixed disulphide using the *E. coli* enzyme glutaredoxin-1 (grxA) molecule (Duppatla et al. 2012).

For synthesis of glutaredoxin-1 in *E. coli*, the cDNA-sequence encoding the mature GRXA protein (UniProtKB - P68688) was cloned into the expression vector Pet28b using BamHI and XhoI endonucleases (chapter 5.1.2). For protein expression, the plasmid DNA was transformed into chemically competent *E. coli* BLR(DE3) cells (chapter 5.1.4.2). Like described in chapter 5.3 transformed *E. coli* cells were cultivated in LB-medium and expression of IL-4 protein was induced by addition of 1 mM IPTG, when cells reached the exponential growth phase. Protein overexpression proceeded for four hours before cells were harvested by centrifugation

The N-terminal polyhistidine fusion tag allowed affinity purification of *E. coli*-derived glutaredoxin-1 by immobilized metal-ion affinity chromatography (IMAC). Pelleted cells were solubilized in IMAC binding buffer containing 10 mM imidazole to reduce non-specific binding, subjected to sonication and centrifuged. The clarified protein containing supernatant was loaded onto a 5 mL HisTrap™ excel column (GE Healthcare) and bound protein was eluted by direct application of 100% elution buffer, which contained 500 mM imidazole (figure 2.8A). SDS-PAGE analysis of the IMAC elution fractions revealed a protein species with an apparent molecular weight below 14.4. kDa, which is consistent with the theoretical mass of glutaredoxin-1 of 11.7 kDa (figure 2.8B). Fractions 26-34 were pooled and extensively dialysed to remove the imidazole. After dialysis precipitate was removed by centrifugation and glutaredoxin-1 could be recovered in high purity (figure 2.8B, lane 9/10). The protein was freeze-dried and stored at -80 °C. From one gram wet weight *E. coli* cell biomass about 19 mg glutaredoxin-1 could be obtained.

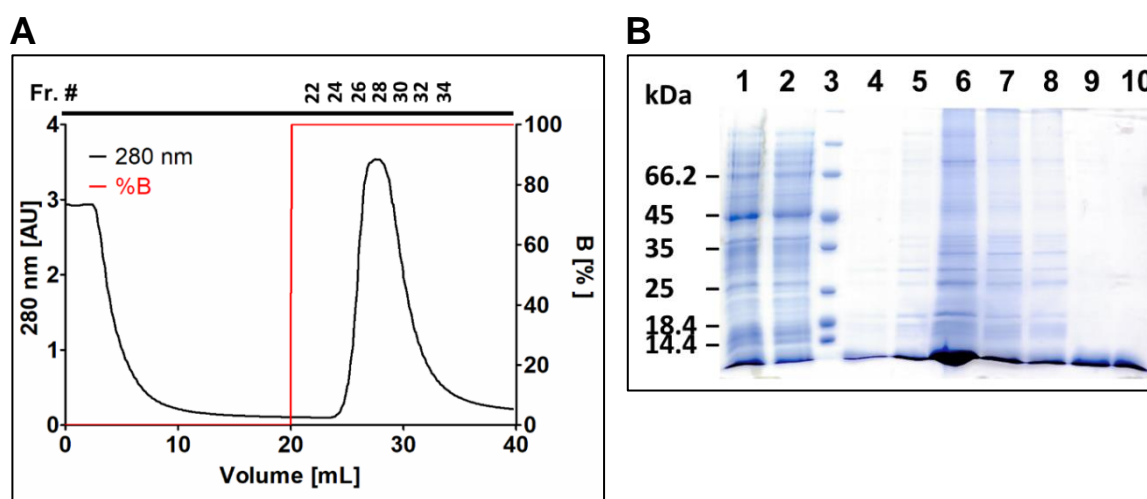


Figure 2.8: Purification of *E. coli*-derived glutaredoxin-1 using immobilized metal-ion affinity chromatography. A) Elution profile of glutaredoxin-1 purification via IMAC. B) SDS-PAGE analysis of elution fractions: 1: sample before purification; 2: IMAC flow-through; 3: size standard; 4: frac. 6; 5: frac. 24; 6: frac. 26; 7: frac. 28; 8: frac. 32; 9: protein after dialysis (non-reducing conditions); 10: protein after dialysis (reducing conditions). SDS-PAGE was performed under reducing conditions. Protein containing fractions 26-34 were pooled.

2.4 Generation of glycoengineered IL-4 receptor typeI/typeII antagonist

The IL-4 binding epitope for the low-affinity receptors γc and IL-13R $\alpha 1$ partially overlaps and is centred around IL-4 residues Arg121 and Tyr124 at the C-terminus of IL-4 helix D (reviewed in: (Mueller et al. 2002)) (figure 2.9). Although mutagenesis studies revealed, that Arg121 and Tyr124 are both major binding determinants for IL-4's interaction with γc and IL-13R $\alpha 1$, differences in the contribution of these residues for type I and type II receptor formation have been observed (Shanafelt et al. 1998; Duppatla et al. 2014; Kruse et al. 1992; Kruse et al. 1993; Schnarr et al. 1997). Substituting Arg121 or Tyr124 against aspartate introduced an electrostatic mismatch in the binding epitope for the receptors γc and IL-13R $\alpha 1$, yielding mutants with partially antagonistic behaviour. However, mutation Y124D was much more effective and resulted in a nearly complete loss of biologic activity, whereas IL-4 variant R121D still exhibited considerable agonistic activity (Kruse et al. 1993).

Instead of introducing an electrostatic mismatch, Duppatla and colleagues used site-specific chemical modification to generate IL-4 mutants with disrupted binding for receptor γc and IL-13R $\alpha 1$ (Duppatla et al. 2014). Thereby, site-specific introduction of the tripeptide glutathione at positions 121 and 124 equally reduced *in vitro* binding of IL-4 for γc and IL-13R $\alpha 1$ about background level. However, only the IL-4 variants modified at position 121 showed strongly reduced biologic activity and were potent antagonists inhibiting IL-4 and IL-13 dependent responses in cellular assays, whereas modification of 124 still permitted considerable agonistic activity (Duppatla et al. 2014).

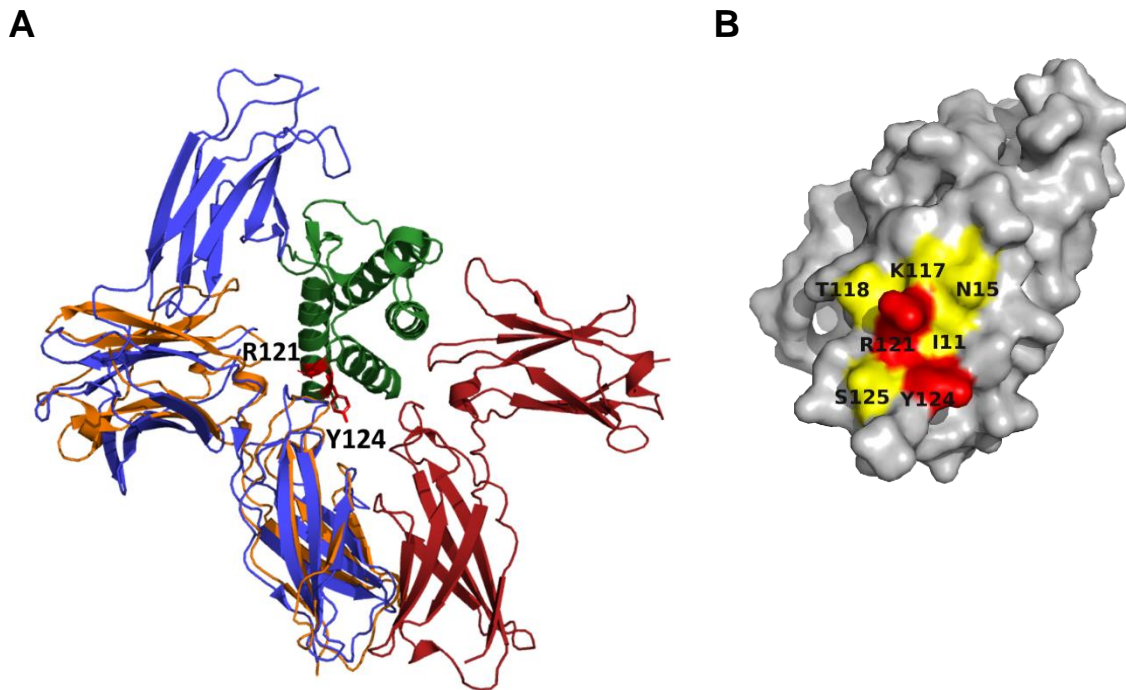


Figure 2.9: Location of residues Arg121 and Tyr124 in the IL-4 binding epitope for receptors γ c and IL-13R α 1. A) Cartoon representation showing the alignment of ternary type I and type II receptor complexes with IL-4 residues Arg121 and Tyr124 shown as sticks and coloured in red (IL-4: green colour; IL-4R α : red colour; γ c: orange colour; IL-13R α 1: blue colour). B) Surface representation of IL-4 protein. Residues Arg121 and Tyr124 are shown in red. Surrounding residues, which were shown to participate in interaction with receptors γ c and/or IL-13R α 1 are shown in yellow.

This suggests that a molecule introduced at position 124 is able to move out of the contact interface during receptor formation, permitting signal transduction. We hence reasoned that targeting position 121 by introduction of a glycan moiety should be most effective for disrupting IL-4's interaction with receptors γ c and IL-13R α 1.

2.4.1 Engineered N-glycosylation site at position 121 is not used by Hek293 cells

We first tried to introduce an N-glycan at IL-4 position 121 by biosynthetic means. Enzymatic N-linked glycosylation of secretory proteins takes place in the endoplasmic reticulum. Glycosyltransferases thereby transfer a preassembled glycan chain to an asparagine residue of the nascent polypeptide, which is part of an Asn-X-Thr/Ser motif, with X not being proline (see review: (Aebi 2013)). Using mutagenesis-PCR, two amino acid substitutions R121N and K123S were introduced into IL-4 to provide the potential N-glycosylation site Asn121 Glu122 Ser123. To facilitate the detection of an N-glycan at the new site, the native N-glycosylation site at position 38 was silenced by mutating Asn38 to glutamine. Unfortunately, transient expression of this IL-4 variant in Hek293 cells, however,

revealed that the engineered N-glycosylation site was not occupied, as IL-4 F82D N38Q R121N K123S showed the same apparent molecular weight as non-glycosylated IL-4 N38Q in Western Blot analysis (figure 2.10).

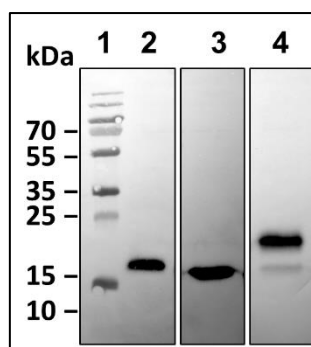


Figure 2.10: Transient expression of IL-4 F82D N38Q R121N K123S in Hek293 cells. Cell culture supernatants were submitted to SDS-PAGE and Western Blot analysis. The IL-4 variants, which contained a polyhistidine-tag were detected using an anti-His tag antibody conjugated to HRP. 1: size standard; 2: IL-4 variant F82D N38Q; 3: IL-4 variant F82D N38Q R121N K123S; 4: IL-4 WT.

This suggests that this engineered N-glycosylation site is not recognized by glycosyltransferases in the endoplasmic reticulum, which might be due to structural constraints (amino residues 121 to 123 are part of helix D). We hence reasoned that a glycan molecule at position 121 can only be introduced by chemical means.

2.4.2 Chemical glycoengineering of *E. coli*-derived IL-4 variant F82D R121C

2.4.2.1 Enzymatic deglutathionylation of IL-4 F82D R121C-GSH using glutaredoxin

For chemical introduction of a glycan moiety at position 121, IL-4 variant F82D with Arg121 being mutated to cysteine was recombinantly expressed in *E. coli* and purified in form of a mixed disulphide, i.e. Cys121 being conjugated to a glutathione moiety (chapter 2.1).

Duppatla and colleagues developed an enzymatic procedure to release the glutathione moiety from the mixed protein-glutathione conjugates using the *E. coli* enzyme glutaredoxin-1 (Duppatla et al. 2012). In the presence of low amounts of reduced glutathione (GSH), glutaredoxin preferably catalyses the cleavage of GSH-mixed disulphides. Glutathione which becomes oxidized in this reaction is again reduced in a catalytic cycle by glutathione reductase and NADPH (figure 2.11) (reviewed in: (Fernandes and Holmgren 2004)).

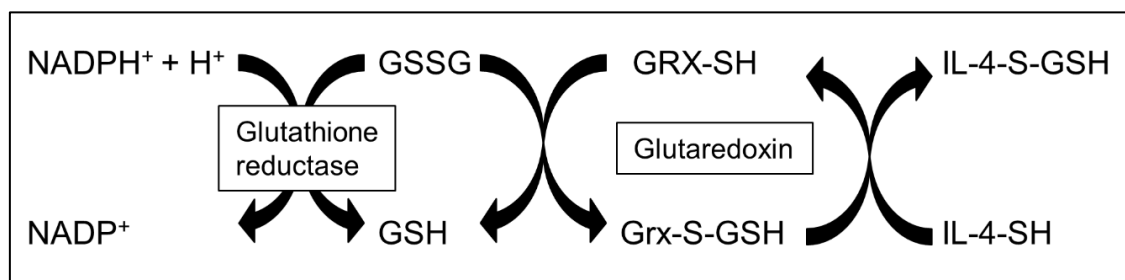


Figure 2.11: Selective reduction of engineered IL-4 cysteine residue using the glutaredoxin system. Glutaredoxin (Grx) catalyses the reduction of the protein cysteine-glutathione mixed disulphide; glutaredoxin, in turn, is reduced through the oxidation of glutathione (GSH); the glutathione reductase regenerates the GSH-pool through reduction of oxidised glutathione (GSSG) using NADPH.

At 50 μ M, glutathionylated IL-4 F82D R121C (from now on referred to as IL-4 F82D R121C-GSH) was incubated with 0.2 mM NADPH, 0.5 mM reduced glutathione and 6 μ g/mL glutathione reductase. The reaction was started by adding 0.33 μ g/mL glutaredoxin-1 to the solution (chapter 5.5.1). Samples were taken at different time points and treated with maleimide-conjugated polyethylene glycol (MA-PEG). Since maleimides specifically react with thiol-groups, incubation with maleimide-PEG allowed to monitor the enzymatic removal of glutathione from IL-4 cysteine variants in SDS-PAGE, as conjugation with maleimide-PEG resulted in a significant increase in protein size (figure 2.12).

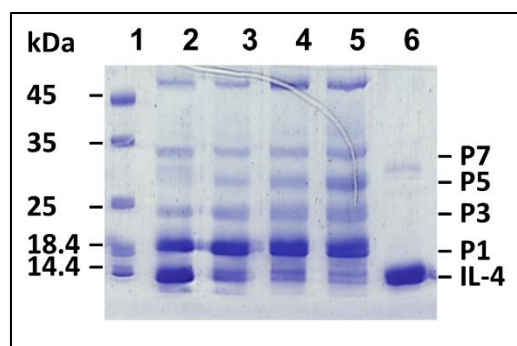


Figure 2.12: SDS-PAGE analysis of glutathionylated IL-4 variant F82D R121C after reaction with glutaredoxin-1. During incubation of IL-4 F82D R121C-GSH with glutaredoxin-1, samples were taken at different time points and incubated with 5 mM MA-PEG 1: size standard; 2: 0.5; 3: 2.5; 4: 5.0; 5 :15.0; 6: untreated control (not incubated with glutaredoxin-1) [min]. Electrophoretic mobility of monopegylated species is indicated by P1, multipegylated IL-4 species are marked P3, P5, and P7.

The low concentration of GSH allows to mainly reduce the glutathione mixed disulphide bond, but as longer incubation leads to a reduction of also the native disulphide bonds of IL-4, reaction times need to be optimized. In the case of IL-4 F82D R121C-GSH, an incubation time of 2.5 min was sufficient to achieve a nearly complete reduction of the engineered cysteine residue, which is clearly indicated by the primary presence of monopegylated IL-4

at 18.4 kDa (lane 3, figure 2.10). At later time points faint protein bands, representing multipegylated species, could be observed, which indicates cleavage of also the native disulphide bonds. To minimize non-specific reduction, the reaction was stopped after 2.5 min by adjusting the sample to 0.1% TFA. The protein was purified by reverse-phase high performance liquid chromatography with about 50-60% protein yield. In mass spectrometry, only non-conjugated IL-4 variant F82D R121C-SH with a free thiol-group could be detected with the native disulphide bonds being intact, showing that residual GSH-conjugated protein could be removed during RP-HPLC (Supplement figure S9.2A).

2.4.2.2 Coupling of amino-glycans via the crosslinker SMCC

Especially for drug design it is important to consider, that glycans play a critical role in the immune system, most importantly in the “self/non-self” discrimination process. We therefore wanted to use conjugation strategies, that would also allow the coupling of non-immunogenic complex human-like glycans isolated from natural glycoproteins.

This might be accomplished by enzymatic hydrolysis, e.g. by treatment with endoglycosidase PNGase-F, which does not require harsh chemical treatment, thereby minimizing the risk to chemically alter the glycan molecule. PNGase F cleaves the N-glycosidic bond between the first N-acetyl glucosamine (GlcNAc) residue of the glycan chain and the asparagine residue in the N-X-T/S protein sequence, releasing a glycan with a single amino group at the C1-atom. For coupling of the amino glycan to the engineered IL-4 cysteine residue we chose a heterobifunctional crosslinker, i.e. succinimidyl 4-(N-maleimidomethyl) cyclohexane-1-carboxylate (SMCC), containing an amine reactive N-hydroxysuccinimide (NHS) ester and a sulfhydryl-specific maleimide group for several reasons. Both coupling reactions occur under near-physiological conditions and result in an irreversible and stable bond formation. Secondly, SMCC is non-cleavable and thus the conjugate will be stable under *in vivo* conditions. Thirdly, the cyclohexane bridge of SMCC provides the maleimide group with an increased hydrolytic stability, making SMCC superior to pure aliphatic linkers. This being especially important, because the conjugation procedure must be performed stepwise (figure 2.13).

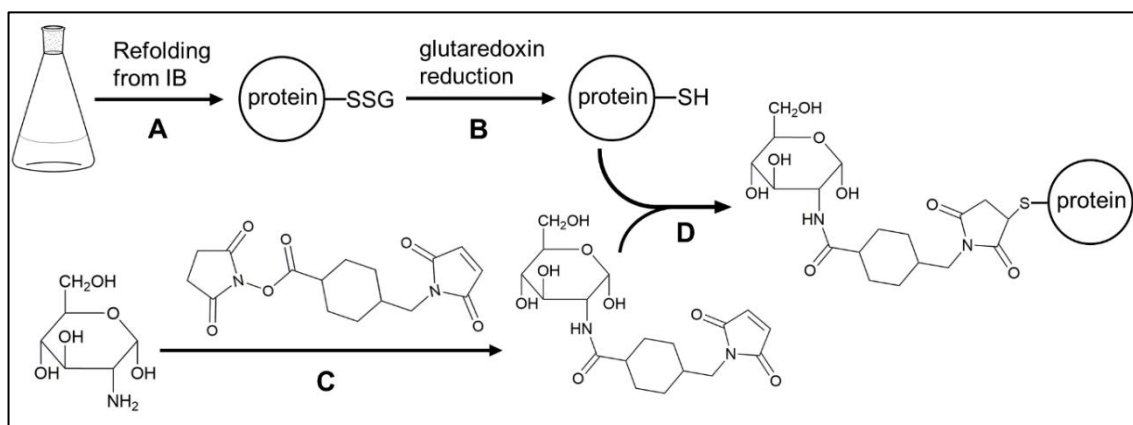


Figure 2.13: Conjugation of glucosamine to IL-4 engineered cysteine residue via the bifunctional crosslinker SMCC. A) Recombinant expression of IL-4 cysteine variants in *E. coli* and subsequent oxidative refolding in the presence of a glutathione redox couple B) To provide IL-4's engineered cysteine residue with a free thiol-group, glutaredoxin-1 is employed to remove the conjugated glutathione moiety C) Reaction of the bifunctional crosslinker SMCC with glucosamine D) Site-directed coupling of the purified SMCC-glucosamine to the free thiol-group of IL-4's engineered cysteine residue.

The feasibility of the approach was tested with the commercially available monosaccharide 2-glucosamine, which carries the amino function at C2-atom next to the anomeric C-atom. We first prepared the glucosamine-SMCC conjugate to prevent unwanted random labelling of IL-4's primary amino residues by non-specific reaction with the SMCC N-hydroxysuccinimide ester. A 1:1 solvent/buffer mixture was used, since the hydrophobic SMCC-linker was shown to precipitate at lower acetonitrile concentrations. Unfortunately, mass spectrometry analysis of the coupling product indicated a rather low conversion rate. This made purification of the SMCC-glucosamine adduct essential to avoid the presence of amino-reactive, non-modified SMCC in the subsequent coupling reaction with the IL-4 cysteine variant.

For purification of the glucosamine-SMCC conjugate, a reversed-phase chromatography was chosen, as the SMCC moiety exhibits rather high hydrophobicity, which is decreased when coupled to the hydrophilic glucosamine molecule. A μ RPC C2/C18 ST 4.6/100 column was used to separate the coupling product from non-reacted educts. As shown by subsequent analysis of the elution fractions by ultra performance liquid chromatography-tandem mass spectrometry (UPLC-MS-MS) (chapter 5.2.5.2), the SMCC-glucosamine conjugate was eluted at 55% acetonitrile concentration, whereas the non-reacted SMCC required 90% acetonitrile to be released from the reversed-phase resin (figure 2.14). The overall yield for the SMCC-glucosamine conjugate was estimated to about 5% only (based on SMCC as educt).

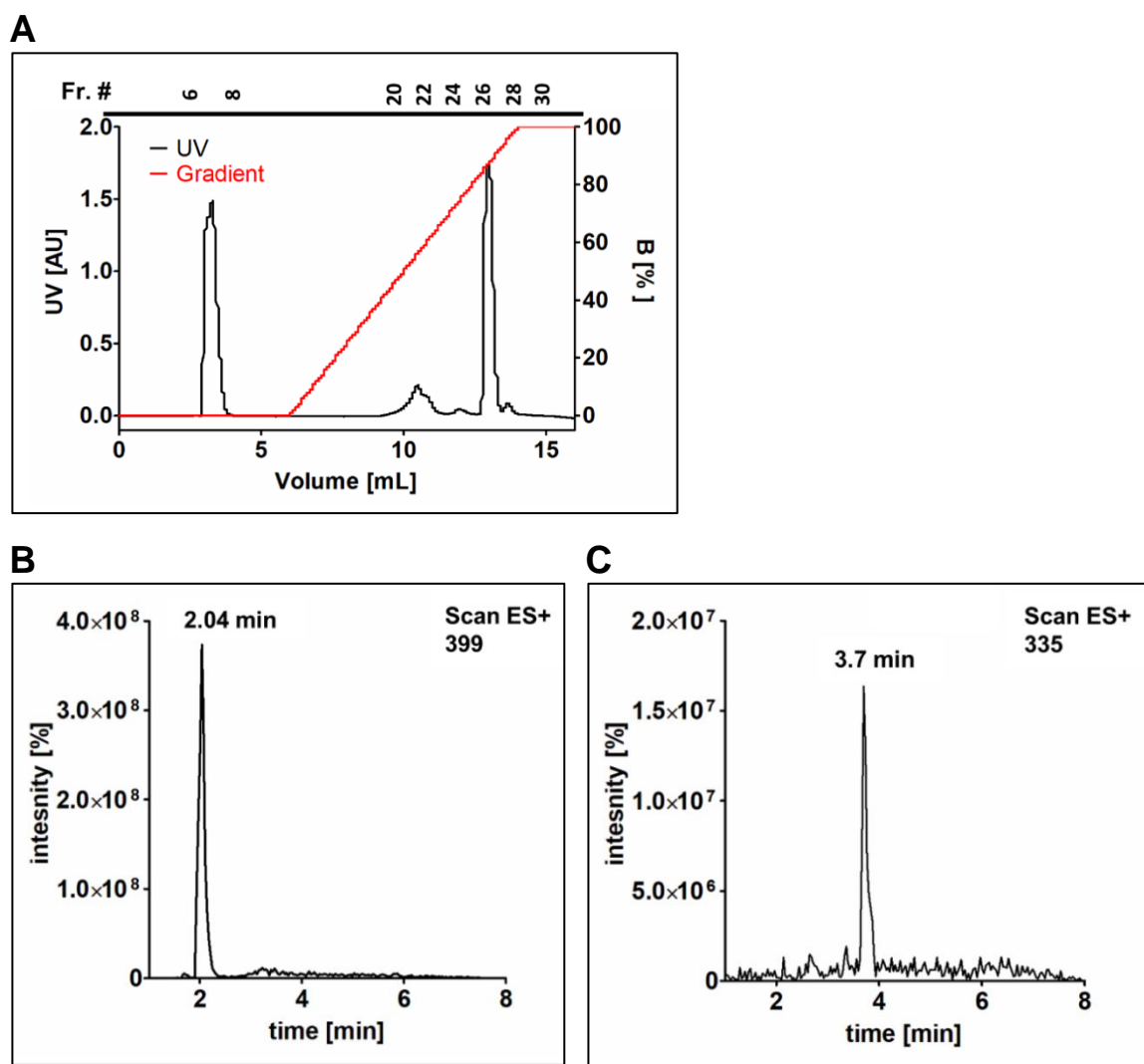
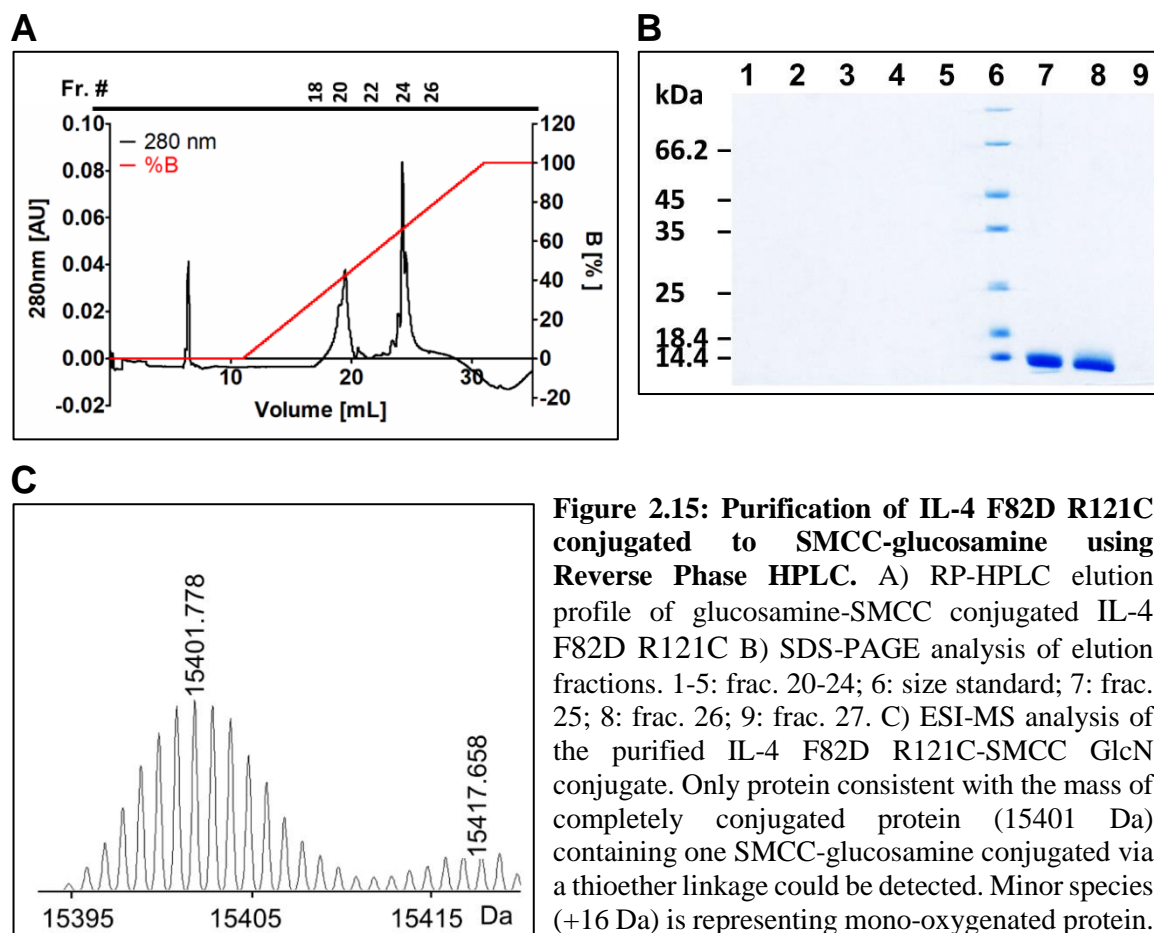


Figure 2.14: Purification of glucosamine-SMCC intermediate using Reverse Phase HPLC. A) RP-HPLC chromatography elution profile of glucosamine-SMCC. B) UPLC-MS detection of SMCC-glucosamine conjugate by selected reaction monitoring (SRM). SRM of elution frac. 24: selection of a m/z value of 399 corresponding to the theoretical mass of the SMCC-glucosamine conjugate yielded a single peak at a retention time of 2.04 min C) UPLC-MS detection of unmodified SMCC by selected reaction monitoring (SRM). SRM of elution frac. 29: selection of a m/z value of 335 corresponding to the theoretical mass of unconjugated SMCC yielded a single peak with a retention time of 3.7 min.

The conjugate was then reacted in a molar ratio of 100:1 in an aqueous buffer system for 2 h at room temperature with enzymatic activated IL-4 F82D R121C. In reverse-phase high performance liquid chromatography, the protein-SMCC-glycoconjugate, from now on referred to as IL-4 F82D R121C-SMCC-GlcN, eluted at 66% acetonitrile and was recovered at about 50% yield (figure 2.15A/B). Mass spectrometry confirmed that the IL-4 SMCC-glycoconjugate can be indeed prepared and coupling to the protein occurred specifically to the activated thiol-group, as only a single protein species with a mass of 15402 Da was

2 Results

detected corresponding to the theoretical mass of IL-4 F82D R121C conjugated to a single SMCC-glucosamine molecule via a thioether linkage (figure 2.15C).



Although the reaction was successful, we found the SMCC-glucosamine approach not ideal for several reasons. A major drawback is the inefficient SMCC-glucosamine conversion rate of about 5%. To compound the problem, the conjugate yield is further decreased by the required purification of the SMCC-glycoconjugate, which questions the feasibility of this procedure. This applies in particular when complex glycans will be used for coupling that have been obtained by enzymatic release from glycoprotein sources or come from expensive chemical synthesis.

Therefore, no optimization of the conditions was attempted and instead we were looking for an alternative method, which would permit linker-free glycan attachment.

2.4.2.3 Coupling of thiol-glycans using phenylselenenylbromide activation

To avoid the limitations of the crosslinker chemistry, we now were looking for an approach, which would allow direct conjugation of a glycan moiety to the engineered cysteine residue Cys121. A glycoengineering strategy, established by Gamblin and colleagues that is termed

Glyco-SeS, implements thiol functionalized carbohydrates for site-directed and linker-free conjugation to cysteine residues. Reaction with a phenylselenenylating reagent converts the free sulfhydryl group of an engineered cysteine residue into the corresponding phenylselenenylsulphide (Bernardes et al. 2006; Gamblin et al. 2004; van Kasteren et al. 2007). Because of the resulting electrophilic nature of the sulphur atom in the S-Se bond, it readily reacts with a thiol-containing carbohydrate to form a disulphide-linked protein-glycan conjugate (figure 2.16). This strategy can also be employed in the opposite direction, where the thiol-carbohydrate is first activated with phenylselenenylbromide, which can then be coupled to a protein cysteine residue. This approach was shown to be applicable to glycans isolated from natural sources, although the glycan first has to be thiol-functionalized, e.g. through reaction with Lawesson's reagent (Bernardes et al. 2006).

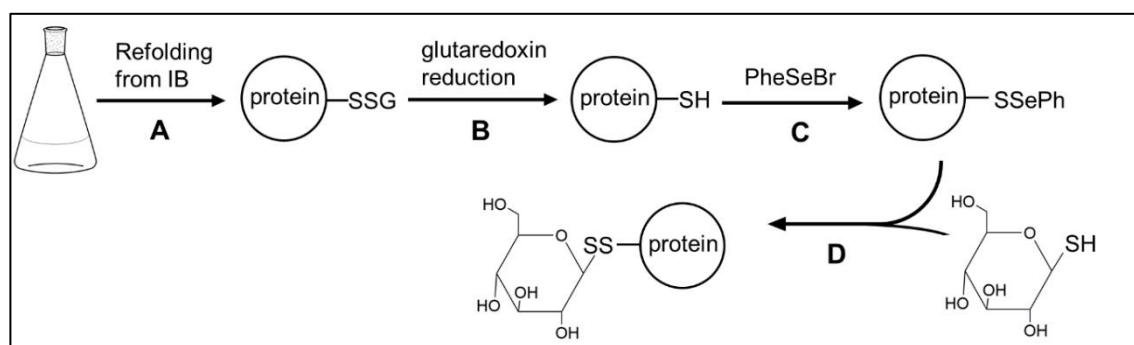


Figure 2.16: Conjugation of thiol-glycans to reduced IL-4 F82D R121C using phenylselenenylbromide activation. A) Recombinant expression of IL-4 cysteine variants in *E. coli* and subsequent oxidative refolding in the presence of a glutathione redox couple B) To provide IL-4's engineered cysteine residue with a free thiol-group, glutaredoxin-1 is employed to remove the conjugated glutathione moiety C) Activation of the free thiol-group of the engineered cysteine residue with phenylselenenylbromide to give the corresponding phenylselenenylsulphide D) Conjugation of the thiol-glycan yielding the disulphide-linked protein-glycan conjugate.

To demonstrate the feasibility of this approach for IL-4 F82D R121C, the commercially available thiol-carbohydrates 1-thio- β -D-glucose and its bigger acetylated derivative 1-thio- β -D-glucose tetraacetate were used (Supplement table S9.1). Enzymatically activated IL-4 F82D R121C protein was treated with 40-fold molar excess of phenylselenenyl bromide for 1 h at room temperature to give the selenenylsulphide intermediate (Figure 3). After a desalting step, the purified protein was then reacted with an 80-fold molar excess of the respective thiol-glycan for 40 min at room temperature. Using reverse-phase high performance liquid chromatography, the modified protein could be recovered with a 60% yield, which in SDS-PAGE showed a single protein band consistent with the size of monomeric IL-4 (figure 2.17).

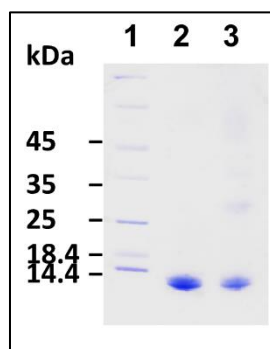


Figure 2.17: SDS-PAGE analysis of IL-4 F82D R121C after Glyco-SeS treatment. SDS-PAGE was performed under non-reducing conditions. 1: size standard; 2:IL-4 F82D R121C-4acGlc; 3: IL-4 F82D R121C-Glc.

Mass spectrometry identified one major protein species corresponding to the molecular weight of IL-4 F82D R121C with all three native disulphide bonds being present and conjugated to a single glucose or glucose tetraacetate (figure 2.18). Unfortunately, glycan-conjugation was incomplete, as mass spectrometry also revealed a minor protein peak consistent with the molecular weight of unmodified IL-4 F82D R121C containing a free thiol group (15004). Since non-conjugated IL-4 F82D R121C with a free thiol-group was reported to exhibit almost IL-4 wildtype-like activity in Jurkat cells (Duppatla et al. 2014), which is an IL-4 responsive T-cell line, the unmodified protein had to be removed to generate a potent full antagonist. SulfoLinkTM resin consists of iodoacetyl activated agarose beads, which covalently bind proteins with non-conjugated, free thiol-groups (chapter 5.6.6). About 1 mg of the partially glycosylated IL-4 F82D R121C protein was dissolved in 50 mM TRIS, 5 mM EDTA, pH 8.5 and mixed with about 1 mL of SulfoLink resin. After incubation for about 45 min at room temperature, the resin flow-through was collected. Subsequent mass spectrometry analysis verified, that non-conjugated IL-4 protein could be efficiently removed by treatment with SulfoLinkTM resin, yielding only glycosylated IL-4 F82D R121C (figure 2.18B).

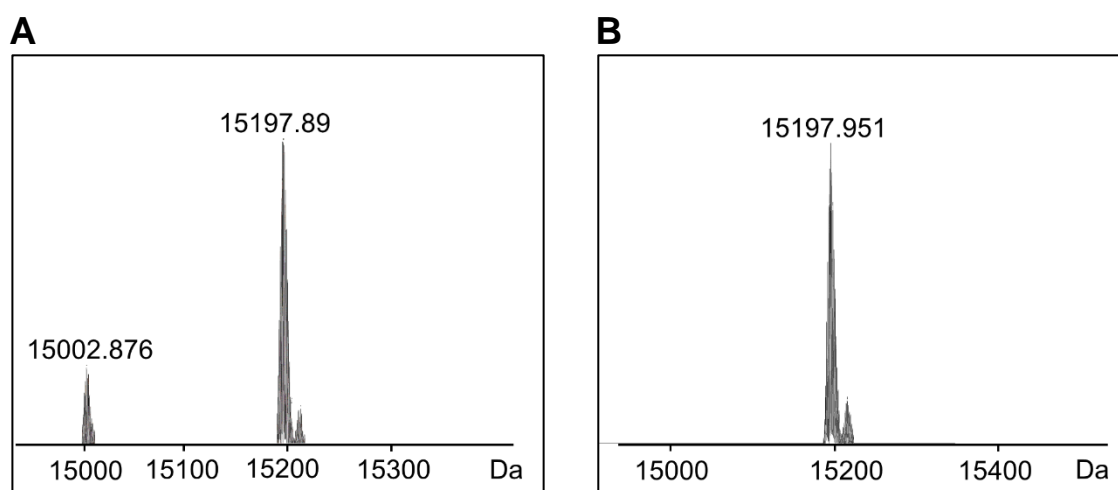


Figure 2.18: ESI-MS analysis of IL-4 F82D R121C-Glc derived from Glyco-SeS method.

A) Protein prior SulfoLink™ purification. Unconjugated species (15002 Da) with an additional hydrogen atom makes up about 10% of total protein. B) Protein after SulfoLink™ purification. Only protein consistent with the mass of glycosylated IL-4 F82D R121C (15197 Da) containing one glucose molecule and lacking one hydrogen atom was detected.

2.4.2.4 Chemical glycosylation via refolding in the presence of thiol-glycans

The oxidative refolding protocol used in this work for renaturation of IL-4 cysteine variants from inclusion bodies employs a glutathione GSH/GSSG redox couple, which promotes the formation of native disulphide bonds. Reduced glutathione (GSH) thereby non-specifically cleaves disulphide bonds whereas oxidized glutathione (GSSG) induces the formation of new disulphide bonds. Thus, a slow disulphide reshuffling occurs that facilitates native disulphide bond formation and thereby allows a protein to adopt its proper architecture.

The Glyco-SeS method allowed the preparation of disulphide-linked IL-4 glycoprotein. However, even though a large excess of thiol glycan was employed, no complete glycoconjugation could be achieved. This made subsequent removal of the unmodified protein necessary. Additionally, this approach still required the enzymatic deprotection step of the engineered cysteine residue, which makes it not feasible for large-scale production. We wondered if a disulphide-linked IL-4 glycoconjugate could be generated in a similar way as the glutathionylated IL-4 variants by adding a thiol-glycan instead of glutathione to the refolding buffer. This would make the time consuming enzymatic activation step unnecessary (figure 2.19). After expression in *E. coli*, misfolded IL-4 F82D R121C was extracted from inclusion bodies using guanidine hydrochloride and DTT (chapter 5.3.2.1). After mild stirring for 2 h at room temperature, the clarified protein solution was added dropwise to 25 volumes of ice-cold refolding buffer to give a protein concentration of about 50 µg/mL (chapter 5.5.4.1). Like in the original protocol, the refolding buffer contained 1 M arginine, which was shown to reduce protein aggregation and thus facilitate proper protein

2 Results

folding. However, instead of the glutathione redox couple (5 mM oxidized glutathione, 2 mM reduced glutathione), 1 mM of 1- β thio-glucose (tetraacetate) was added.

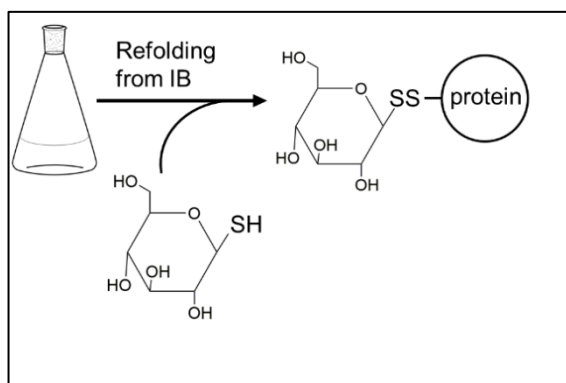


Figure 2.19: Conjugation of thiol-glycans to IL-4 F82D R121C during refolding. Recombinant expression of IL-4 cysteine variants in *E. coli* and subsequent oxidative refolding in the presence of thiol-glycans.

Surprisingly, even though no oxidizing redox-partner, such as oxidized glutathione was present, the protein yield, when using 1 mM thio-glucose (tetraacetate) was identical to the one obtained by refolding in the presence of the glutathione redox-couple (about 10 mg protein per gram *E. coli* cell biomass). Thereby, no difference in yield was observed between thio-glucose and thio-glucose tetraacetate. SDS-PAGE analysis showed that the two glycoconjugated IL-4 F82D R121C variants, from now on referred to as IL-4 F82D R121C-Glc and -4acGlc, could be afforded in high purity (figure 2.20).

Mass spectrometry only detected glycoconjugated IL-4 protein with Cys121 being disulphide bonded to glucose (tetraacetate). Non-conjugated protein was not present (Supplement figure S9.2B/D).

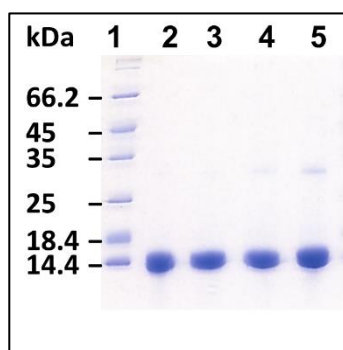


Figure 2.20: SDS-PAGE analysis of IL-4 F82D (N38C) R121C derived from refolding with thio-glucose (tetraacetate). SDS-PAGE of purified IL-4 F82D R121C-(4ac)glc and double cysteine variant IL-4 F82D N38C R121C-(4ac)glc under reducing conditions. 1: size standard; 2: IL-4 F82D R121C-Glc; 3: IL-4 F82D R121C -4acGlc; 4: IL-4 F82D N38C R121C-Glc; 5: IL-4 F82D N38C R121C-4acGlc.

Next, we wanted to see if chemical glycosylation of IL-4 by refolding was restricted to single-site glycoconjugation only or whether it might also be applicable for glycosylation of IL-4 variants carrying multiple unpaired cysteine residues. As a proof of principle, an IL-4 variant F82D R121C N38C was designed that contained an additional unpaired cysteine residue at position 38, which is the natural glycosylation site of IL-4. Refolding of IL-4 F82D R121C N38C was performed as outlined above delivering the same protein yield as for IL-4 F82D R121C. Mass spectrometry identified a protein species corresponding to the molecular weight of IL-4 F82D R121C N38C containing all three native disulphide bonds and the two engineered cysteine residues being conjugated to glucose (tetraacetate) (figure 2.21). Besides, also non- or mono-glycosylated IL-4 F82D R121C N38C could be detected, which was more prominent in the tetraacetate glucose conjugate (about 60 %) than in the glucose sample (about 10 %). This indicates that simultaneous conjugation of thio-glycans to several sites likely requires adaptation of the coupling conditions to achieve full conversion. This hypothesis is corroborated by the finding that the bulkier tetraacetate glucose showed a lower coupling rate than the smaller glucose.

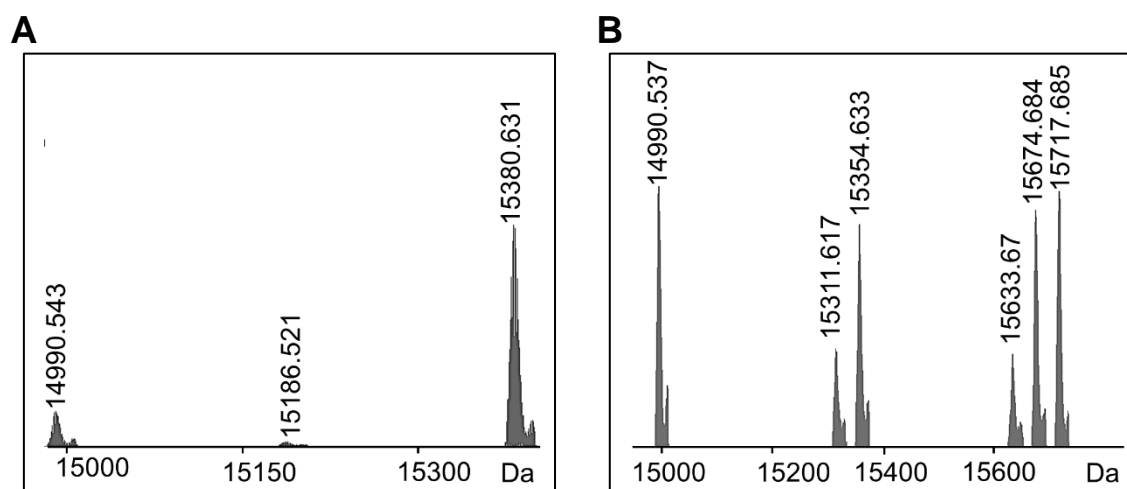


Figure 2.21: ESI-MS analysis of IL-4 F82D N38C R121C-Glc derived from refolding with thiol-glucose (tetraacetate). A) MS-spectra of IL-4 F82D N38C R121C-Glc. Protein species with a mass of 15381 Da represents diglycosylated IL-4 F82D N38C R121C containing two glucose molecules and lacking 8 hydrogen atoms. The species with a mass of 15186 represents monoglycosylated IL-4 F82D N38C R121C containing one glucose molecule and lacking 7 hydrogen atoms. Approximately 10% of total protein consists of non-glycosylated IL-4 F82D N38C R121C containing an additional disulphide bond, lacking 8 hydrogen atoms (14990 Da). B) MS-spectra of IL-4 F82D N38C R121C-4acGlc. Protein species with a mass of 15718 Da represents diglycosylated IL-4 F82D N38C R121C containing two disulphide-linked glucose tetraacetate molecules, lacking 8 hydrogen atoms. Side-peaks (-42 Da) are derived from the loss of acetate groups. About 30% of total protein consists of monoglycosylated protein with a mass of 15355 corresponding with the theoretical mass of IL-4 F82D N38C R121C containing one glucose tetraacetate molecule and lacking 7 hydrogen atoms. About 30% of total protein consist of non-glycosylated IL-4 F82D N38C R121C containing an additional disulphide bond, lacking 8 hydrogen atoms (14990 Da).

2.4.3 Chemical glycosylation of Hek293 cell-derived IL-4 variant F82D R121C

Since the introduction of a glycan moiety at position 121 cannot be achieved by biosynthetic means, we sought to determine if the thiol-specific glycosylation strategies we used for chemically coupling of glycans to Cys121 were restricted to *E. coli*-derived protein or if it could also be applied to IL-4 F82D R121C expressed in Hek293 cells. This would offer the possibility to combine chemical and biosynthetic glycosylation, as Hek293 cell-derived IL-4 carries a native N-glycan at Asn38.

2.4.3.1 Hek293 cell-derived IL-4 F82D R121C is conjugated to a cysteine

To facilitate mass spectrometry analysis, expression of IL-4 F82D R121C was performed in the presence of kifunensine, which allowed subsequent enzymatic deglycosylation employing endoglycosidase H (Endo-H), like described before (SDS-PAGE analysis in figure 2.22A). Mass spectrometry identified one major protein species with a mass of 16592 Da, which corresponds to the molecular weight of IL-4 F82D R121C containing an additional cysteine moiety and an N-acetylglucosamine molecule, i.e. it carries a single complex N-glycan (figure 2.22B). This suggests that the unpaired cysteine residue of IL-4 F82D R121C expressed in Hek293 cell forms a mixed disulphide with an isolated cysteine, which is very likely originating from the amino acids present in the growth medium.

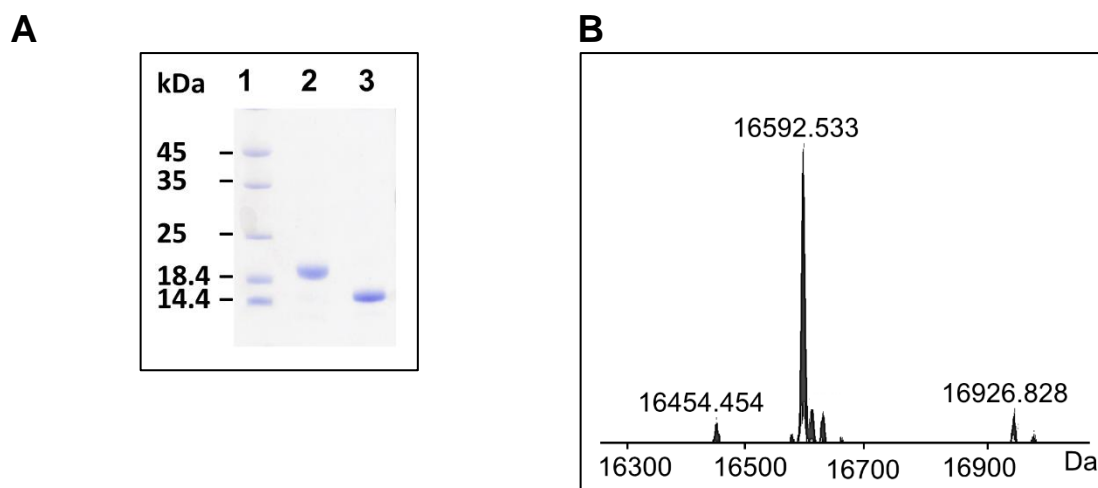


Figure 2.22: Analysis of Hek293 cell-derived IL-4 F82D R121C treated with Endo-H. A) SDS-PAGE analysis of Endo-H treated IL-4 F82D R121C, which was expressed in the presence of kifunensine. SDS-PAGE was performed under non-reducing conditions 1: size standard; 2: IL-4 F82D R121C (untreated); 3:IL-4 F82D R121C treated with Endo-H. B) Mass spectrometry analysis of Hek293 cell-derived IL-4 F82D R121C after deglycosylation with Endo-H. Mass spectrometry detected one major protein species of 16592.5 Da which is consistent with the theoretical molecular weight of pHlsec-derived IL-4 F82D R121C containing an additional cysteine and an N-acetyl glucosamine molecule lacking 8 hydrogen atoms and a hydroxy-group (due to the N-glycosidic linkage).

2.4.3.2 Hek293 cell-derived IL-4 F82D R121C can not be reduced by enzymatic means

To provide the engineered cysteine of IL-4 variant F82D R121C obtained from Hek293 cell expression in its reduced state with a free thiol-group, we first tried to remove the disulphide conjugated cysteine by treatment with glutaredoxin-1, following the same procedure as described for the *E. coli*-derived protein (chapter 5.5.1). Samples were taken during the reaction and incubated with maleimide-PEG to monitor reaction kinetics in SDS-PAGE. After 2.5 min a protein band consistent with the molecular weight of monopegylated IL-4 F82D R121C could be observed in SDS-PAGE but estimated from the band intensity this species represented only about 25% of total protein (figure 2.23). Unfortunately, no further increase of the monopegylated species could be observed. Instead, reduction of native disulphide bonds in IL-4 occurred at later time points, as bands representing multipegylated protein appeared, which acquired similar intensities as the monopegylated protein at 30 min. This suggests that glutaredoxin reaction could not discriminate between the engineered cysteine and the native disulphide bonds.

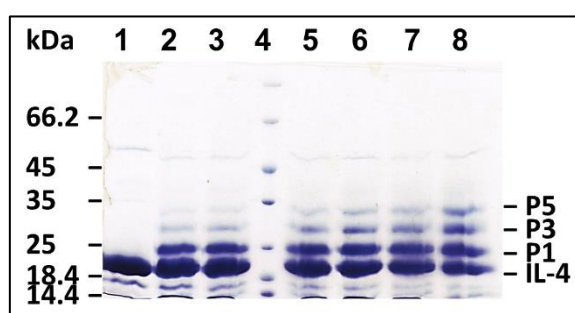


Figure 2.23: SDS-PAGE analysis of Hek293 cell-derived IL-4 F82D R121C-Cys treated with glutaredoxin. During incubation of Hek293 cell-derived IL-4 variant F82D R121C-Cys with glutaredoxin samples were taken at different time points and incubated with 5 mM MA-PEG [min] 1: untreated control (not incubated with glutaredoxin-1); 2: 2.5; 3: 5.0; 4: size standard; 5 :10; 6:15; 7:20; 8:30; Electrophoretic mobility of monopegylated species is indicated by P1, multipegylated IL-4 species are marked P3 and P5.

Hence removal of the conjugated cysteine residue of Hek293 cell-derived IL-4 F82D R121C by enzymatic means seems highly inefficient.

2.4.3.3 Chemical glycosylation of Hek293 cell-derived IL-4 F82D R121C by refolding

Since an enzymatic deprotection of the engineered cysteine residue of Hek293 cell-derived IL-4 F82D R121C was not possible, chemical glycosylation strategies allowing glucosamine conjugation via the bifunctional crosslinker SMCC or coupling of thiol-glycans by Glyco-SeS reaction are not applicable to Hek293 cell-derived IL-4 F82D R121C. However, the

2 Results

“refolding” protocol does not require enzymatic deprotection of the engineered cysteine residue but rather works in a one-pot fashion via complete chemical reduction of IL-4’s disulphide bonds, followed by refolding in the presence of thiol-glycans.

The IL-4 variant F82D R121C was recombinantly expressed in Hek293 cells without kifunensine supplementation of the medium. Similar to the refolding procedure applied to IL-4 protein obtained from protein expression in *E. coli*, purified Hek293 cell-derived IL-4 F82D R121C was solubilized in 5 M GuHCl, 100 mM TRIS-HCl pH 8.0 supplemented with 1 mM DTT at a concentration of 1 mg/mL and incubated for 2 h at RT to achieve complete protein denaturation (chapter 5.5.4.2). The protein solution was then added to the refolding buffer (1 M arginine, 50 mM TRIS-HCl, 5 mM EDTA pH 8.0) supplemented with 1 mM thiol-glucose. The final protein concentration was about 50 µg/mL. After three days of incubation, the protein, from now on referred to as IL-4 F82D R121C-Glc (Hek293), was purified using immobilized metal-ion affinity chromatography (IMAC), which afforded a yield of about 30% at high purity (figure 2.24A).

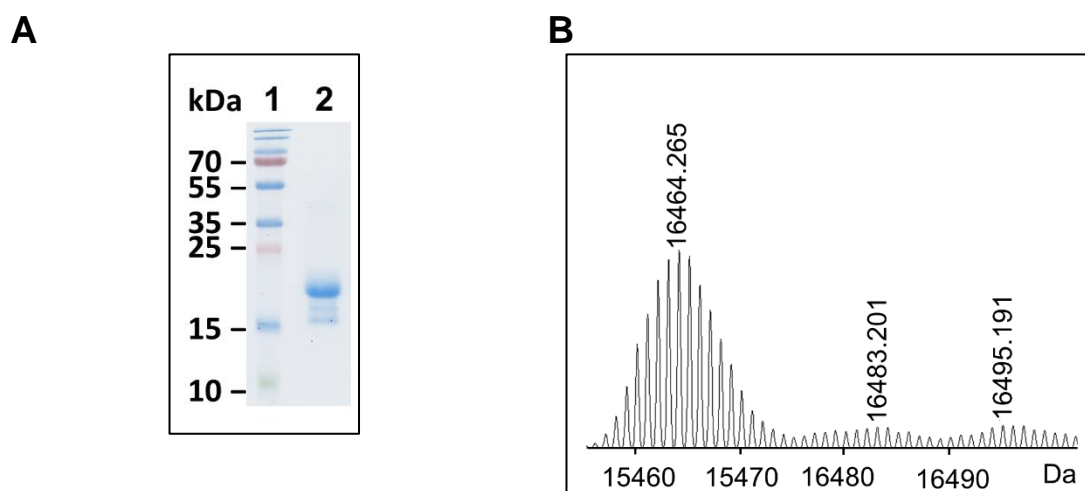


Figure 2.24: Analysis of Hek293 cell-derived IL-4 F82D R121C-Glc obtained from refolding with thiol-glucose. A) SDS-PAGE analysis of purified IL-4 F82D R121C-Glc. SDS-PAGE was performed under non-reducing conditions. 1: size standard; 2: purified IL-4 F82D R121C-Glc B) Mass spectrometry analysis of IL-4 F82D R121C-Glc after PNGase F treatment. For expression of IL-4 F82D R121C in Hek293 cells, a pHLsec vector was employed, which does not contain a thrombin cleavage site downstream of the histidine tag. Protein species with a mass of 16464 Da represents IL-4 F82D R121C containing one disulphide linked glucose molecule, lacking 7 hydrogen atoms and carrying aspartic acid instead of asparagine.

Since we employed IL-4 protein, which was expressed without kifunensine supplementation of the medium, deglycosylation with endoglycosidase H was not feasible. Endoglycosidase PNGase F, which has a broader substrate specificity than endoglycosidase H, is effective in cleaving almost all types of N-glycans. Thus, glycoproteins usually do not require

kifunensine treatment for deglycosylation with PNGase F. Briefly, about 200 μg of denatured protein were incubated with 80 U PNGase F at 37°C overnight. For subsequent mass spectrometry analysis, the protein was purified by reverse phase-high performance liquid chromatography. In mass spectrometry, a single protein species with a mass of 16464 Da could be detected (figure 2.24B). This is consistent with the theoretical mass of pHLsec-derived IL-4 F82C R121C containing a single disulphide-linked glucose moiety and an aspartic acid instead of an asparagine moiety; PNGase F removes the entire N-glycan chain by cleaving directly between the asparagine residue and GlcNAc molecule, thereby converting the asparagine into aspartic acid.

2.4.4 Glycoengineered IL-4 F82D R121C analogues display increased binding for receptor IL-4R α

To assess, whether binding of the glycosylated IL-4 F82D R121C variants to the IL-4 high-affinity receptor IL-4R α was affected, *in vitro* interaction analysis employing surface plasmon resonance (SPR) was performed to determine binding kinetics and affinities of the glycoengineered IL-4 F82D R121C analogues towards the IL-4R α receptor ectodomain (ECD). Expression of the IL-4R α receptor ectodomain with an N-terminal ybbR fusion tag enabled site-specific biotinylation of the ligand. This allowed for directed receptor immobilization onto a streptavidin-coated biosensor and thereby prevented a loss in ligand activity. For biotinylation the enzyme Sfp phosphopantetheinyl transferase was employed, which catalyses covalent attachment of a coenzyme A (CoA) conjugated-substrate, in this case, CoA-conjugated biotin to the 11-residue ybbR peptide tag (Yin et al. 2006, 2006; Yin et al. 2005). Briefly, the IL-4R α -ybbR protein with a size of 27.5 kDa (derived from recombinant protein expression in TriEx™ Sf9 insect cells and kindly provided by Dr. Juliane Fiebig) was incubated with CoA-biotin and SFP-synthase for 2 h at room temperature. Subsequently, the receptor was purified by ultrafiltration using HBST-300 buffer (10 mM HEPES, 300 mM NaCl, 3.4 mM EDTA, 0.005% Tween-20, pH 7.4). HBST-300 buffer was also employed for SPR measurements.

For activation, the biosensor surface was perfused with an EDC/sulfo-NHS mixture, followed by conjugation of streptavidin until a surface density corresponding to a signal intensity of 3000 RU was acquired (chapter 5.7.1.2). Residual non-conjugated carboxy moieties were quenched by perfusion with ethanolamine. Site-specifically biotinylated IL-4R α receptor ectodomain was immobilized on the biosensor surface at a density of 300 RU. For analysis of association and dissociation kinetics, the biosensor was perfused with

2 Results

IL-4 glycan-conjugates as analytes, employing six different concentrations (5.0, 2.5, 1.25, 0.625, 0.313 and 0.157 [nM] in HBST300). In this set-up the highest concentration of IL-4 ligand, i.e. 5.0 nM produced a response between 30 and 50 RU. Sensorgrams (exemplary sensorgrams: figure 2.25A/B) were generated by subtracting the signal obtained from a streptavidin-activated control lane, which had not been perfused with the IL-4R α receptor. Binding kinetics were determined by applying a simple 1:1 Langmuir-type interaction model.

Binding to the IL-4R α receptor ectodomain revealed an apparent K_D value of 183 ± 42 pM for wildtype IL-4 (*E. coli*), which is in good agreement with previous findings (Duppatla et al. 2014; Shen et al. 1996; Kraich et al. 2006). Glycoengineered IL-4 F82D R121C variants conjugated to different glycan moieties exhibited very high-affinity binding to IL-4R α , which exceeded that of wildtype IL-4 and PitraKinra by up to tenfold (Table 2.1). This is mainly attributable to reduced dissociation rates (k_{off}) due to the F82D mutation (Kraich et al. 2006). For disulphide-linked glucose and glucose tetraacetate modified IL-4 F82D R121C variants (*E. coli*) a K_D of about 17 pM and 35 ± 4 pM could be determined respectively.

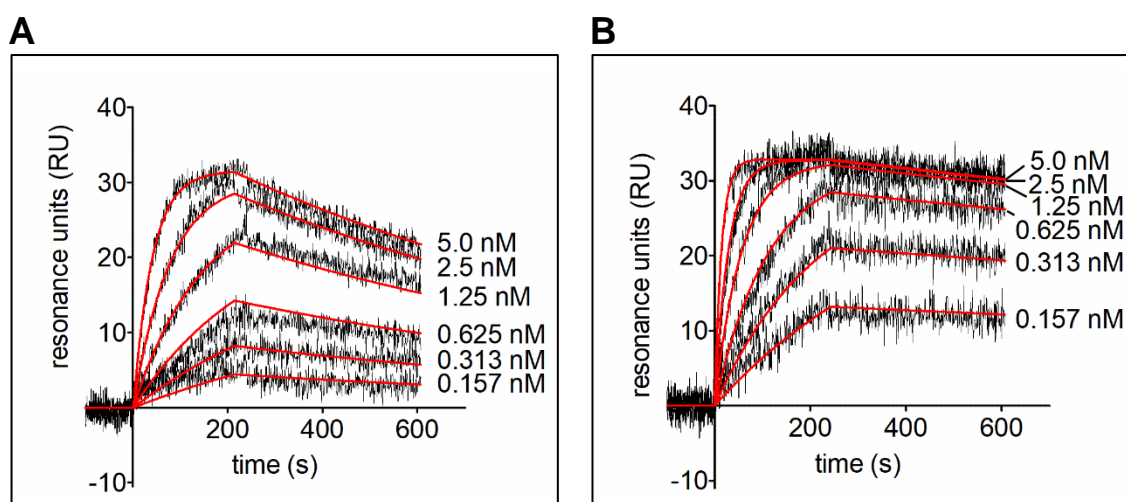


Figure 2.25: *In vitro* SPR analysis of IL-4 F82D R121C glycoconjugates interaction with IL-4R α -ECD. Glycan-conjugated IL-4 variants were perfused as analytes in six different concentrations over a ProteOnTM GLC biosensor chip, which was coated with IL-4R α -ECD. Employing a flow rate of 100 μ L/min, association of the IL-4 analytes with the receptor was measured for 240 sec and the analyte dissociation for 300 sec during perfusion with buffer-only. Exemplary: Sensorgrams for A) wildtype IL-4 (*E. coli*) B) IL-4 F82D R121C-Glc (*E. coli*).

Compared to the disulphide-linked glycoconjugates, the IL-4 variant F82D R121C coupled to glucosamine via the crosslinker SMCC exhibited a fourfold lower affinity of about 93 ± 26 pM for the IL-4R α receptor. This lower affinity may be due to the flexibility of the

SMCC-linker, which might negatively affect binding of the IL-4 protein to the IL-4R α receptor. However, this variant still bound to the IL-4R α receptor with a K_D twice as high as wildtype IL-4.

Table 2.1: Binding affinities of glycoengineered IL-4 F82D R121C variants to IL-4R α ECD measured by surface plasmon resonance analysis. Kinetic rate and equilibrium binding constants were derived from three independent experiments (n=3) using five different analyte concentrations. The binding parameters k_{on} , k_{off} , and K_D represent mean values and standard deviations.

IL-4 variant	k_{on} [$M^{-1}s^{-1}$] x 10^6	k_{off} [s^{-1}] x 10^{-4}	K_D [μM]
WT	5.34 \pm 1.49	9.37 \pm 0.25	183.33 \pm 41.68
F82D N38C-Glc	15.53 \pm 2.90	2.90 \pm 1.57	18.67 \pm 0.99
F82D R121C-GSH	5.76 \pm 0.24	2.30 \pm 0.83	39.67 \pm 13.00
F82D R121C-SMCC-GlcN	4.58 \pm 0.58	4.18 \pm 0.62	93.37 \pm 25.87
F82D R121C-4acGlc	7.28 \pm 0.82	2.57 \pm 0.39	35.23 \pm 3.72
F82D R121C-Glc	6.99 \pm 5.99	1.15 \pm 0.98	16.60 \pm 0.44
F82D R121C-Glc (Hek293)	1.43 \pm 0.17	1.71 \pm 0.30	120.00 \pm 24.27
R121D-Y124D	5.97 \pm 0.54	9.59 \pm 1.45	163.33 \pm 39.11

The Hek293 cell-derived IL-4 variant F82D R121C-Glc disulphide-linked to thiol-glucose exhibited a K_D of 120 \pm 24 μM , which is seven times lower compared to the K_D of *E. coli*-derived IL-4 F82D R121C-Glc analogue. The lower binding might result from the increased molecular weight caused by the complex eukaryotic N-linked glycosylation. Thus, Hek293 cell-derived IL-4, containing an N-linked glycan at position 38, exhibits a size of about 18 kDa, whereas *E. coli*-derived, non-glycosylated IL-4 only has a size of 15 kDa. The higher molecular weight of the Hek293 cell-derived IL-4 protein likely causes a decrease of the association rate, thereby lowering the binding affinity.

2.4.5 Glycosylated IL-4 F82D R121C analogues are highly effective IL-4 antagonists in cell-based assays

The biological activities of the glycan-conjugated IL-4 F82D R121C variants was assessed *in vitro* using two different cell-based experiments. HEK-BlueTM IL-4/IL-13 cells (Invivogen) are stable Hek293-cell transfectants that carry a secreted alkaline phosphatase (SEAP) as reporter gene coupled to an IL-4/IL-13 responsive promoter. This cell line expresses the IL-4R α and IL-13R α 1 subunit, thereby serving as a reporter system specifically for IL-4 receptor type II signalling. Briefly, HEK-Blue cells were seeded in a 96

well plate and incubated with IL-4 analogues for 24 h. For quantification of IL-4 bioactivity, the cell supernatant was incubated with p-nitrophenyl phosphate (PNPP) and the enzymatic hydrolysis of PNPP to p-nitrophenol, mediated by the secreted alkaline phosphatase, was quantified at 405/630 nm on a microplate reader (chapter 5.7.3.1).

TF-1 cells are a human erythroleukemic cell line, which requires medium supplementation with granulocyte-macrophage colony-stimulating factor (GM-CSF) for survival. In the absence of GM-CSF, this cell line shows IL-4- and/or IL-13- dependent proliferation (Lefort et al. 1995). As confirmed by qPCR analysis the TF-1 cells carry both, the γc and IL-13R $\alpha 1$ receptor in addition to IL-4R α and therefore can be used to simultaneously analyse IL-4 receptor type I and type II dependent signalling (Supplement figure S9.6). Briefly, TF-1 cells were seeded in a 96 well plate and incubated with IL-4 analogues for 72 h. Subsequently, the proliferation rate was assessed by NADPH/NADH-dependent conversion of resazurin into resofurin, which was quantified at 571 nm (chapter 5.7.3.2).

Both cell lines demonstrated high sensitivity for IL-4 with half-maximal effective concentrations (EC_{50}) of 4 pM for wildtype IL-4 (IL-4 WT) in HEK-Blue cells and 7 pM for wildtype IL-4 in TF-1 cells. These values are in agreement with published data (Duppatla et al. 2014; Tony et al. 1994). For measurement of biologic activities, cells were treated with glycan-conjugated IL-4 F82D R121C variants at a concentration of 50 pM, which is approximately tenfold higher than the half-maximal effective concentration (EC_{50}) of wildtype IL-4. At this concentration none of the glycoengineered IL-4 F82D R121C variants, independent whether the proteins were conjugated to SMCC-glucosamine or disulphide-linked to glucose or tetraacetate glucose, showed any activity (<1%) in either HEK-Blue or TF-1 cells, similar to Pitrakinra, which was used as reference (IL-4 R121D Y124D) (figure 2.26/Supplement table S8.3). The IL-4 variant R121E was virtually inactive in HEK-Blue cells, but still exhibited relatively high activity of $72.7 \pm 12.3\%$ in TF-1 cells, consistent with IL-4 R121E being reported as an IL-4 receptor type II-specific antagonist (Shanafelt et al. 1998). As a positive control we used an IL-4 variant with asparagine at position 38 mutated to cysteine. Asparagine 38 is the natural N-glycosylation site of IL-4 and site-specific modification of this position was therefore assumed to interfere least with receptor binding and inhibitory efficacy (Carr et al. 1991).

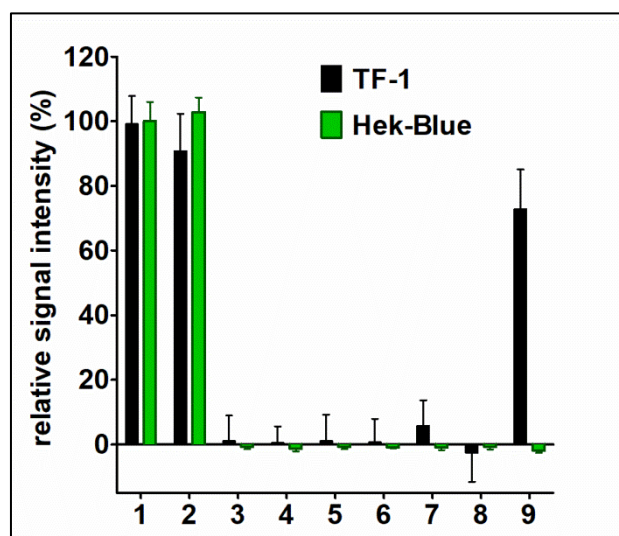


Figure 2.26: Biologic activity of glycoengineered IL-4 F82D R121C variants in HEK-Blue and TF-1 cells. Cells were incubated with 50 pM of each variant and signal intensity (quantified as detailed under chapter 5.7.3) was normalized to IL-4 WT. Data is shown from three independent experiments (n=3). 1: WT; 2: F82D N38C-Glc; 3: F82D R121C-SMCC-GlcN; 4: F82D R121C-Glc; 5: F82D R121C-4acGlc; 6: F82D R121C-Glc (Hek293); 7: F82D R121C-GSH; 8: R121D Y124D; 9: F82D R121E.

In our experiments, IL-4 F82D N38C-Glc derived from refolding with thiol-glucose exhibited biological activities identical to wildtype IL-4, thereby confirming that refolding with thiol-glycans affords a biological active IL-4 and that conjugation of thio-glycans occurs site-specific to the introduced cysteine residue.

To evaluate the antagonistic efficacy of glycoengineered IL-4 F82D R121C variants, we determined the half-maximal inhibitory concentration (IC₅₀) of each variant from competition against wildtype IL-4 in TF-1 and HEK-Blue cell-assays (figure 2.27). Together with the half-maximal effective concentration (EC₅₀) determined for wildtype IL-4, the obtained IC₅₀-values were used to calculate the inhibitory constant (K_i) for each glycoengineered IL-4 F82D R121C variant using the Cheng-Prusoff equation:

$$K_i = IC_{50} / (1 + [IL-4] / EC_{50}) \text{ (Cheng and Prusoff 1973).}$$

The inhibitory constant (K_i) is considered a measure of the binding affinity of an antagonist for its receptor, in this case, the glycoengineered IL-4 F82D R121C analogues for the IL-4R α receptor. All glycoengineered IL-4 F82D R121C variants were shown to be potent antagonists, able to completely abrogate IL-4 dependent responses similar to Pitakinra (figure 2.27).

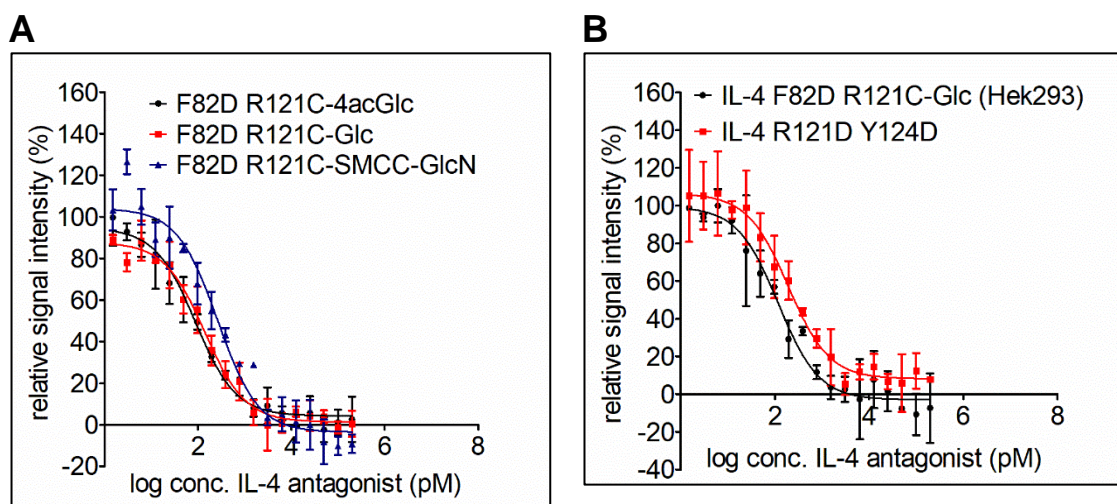


Figure 2.27: Dose-dependent competition of glycoengineered IL-4 F82D R121C variants in TF-1 cells. Cells were incubated with a log 2 titration of the indicated IL-4 variant in competition against 50 pM IL-4 WT. The signal intensity was normalized to IL-4 WT at 50 pM. Data is shown from three replicates. A) Dose-response curves for *E. coli*-derived IL-4 F82D R121C variants conjugated to SMCC-glucosamine or disulphide-linked to glucose (tetraacetate); B) Dose-response curves for *E. coli*-derived Pitracinra and Hek293 cell-derived IL-4 F82D R121C disulphide-linked to glucose.

The glucose (tetraacetate) conjugated variants exhibited K_i -values of about 20 pM in TF-1 (and HEK-Blue) cells, which is five times lower compared to the inhibitory efficacy of Pitracinra with a K_i -value of about 100 pM (table 2.2).

The Hek293 cell-derived IL-4 variant F82D R121C-Glc, obtained from refolding with thiol-glucose, also showed a K_i -value of about 24 pM in TF-1 cells. This is surprising, since in SPR-experiments this variant exhibited a binding affinity about seven times lower than the *E. coli*-derived IL-4 F82D R121C-Glc analogue. A possible reason for this could be that due to its complex eukaryotic N-glycosylation, the Hek293 cell-derived protein has a greater stability compared to the non-glycosylated *E. coli*-derived variant. Therefore, it might exhibit a longer half-life in the cell-assay medium, allowing the Hek293 cell-derived IL-4 antagonist to maintain a higher inhibitory activity over a longer period of time, which may compensate for its weaker affinity to the IL-4R α receptor.

The IL-4 F82D R121C variant conjugated to glucosamine via the SMCC-linker showed a slightly higher K_i -value of about 50 pM, supporting the assumption that the SMCC-linker negatively affects binding to the IL-4R α receptor.

Table 2.2: Inhibitory constants of the glycoengineered IL-4 F82D R121C variants *in vitro*. The K_i values were calculated using the IC_{50} values of the IL-4 F82D R121C variants and the EC_{50} value of IL-4 WT (TF-1: 6.7 ± 1.5 pM; HEK-Blue: 3.6 ± 1.0 pM) obtained from dose-response curves in TF-1 and HEK-Blue cell assays as detailed under experimental procedures. Data were used from three independent experiments (n=3).

IL-4 variant	Inhibitory constant (K_i) [pM]	
	TF-1	HEK-Blue
F82D R121C-SMCC-GlcN	51.2 ± 10.4	
F82D R121C-Glc	17.4 ± 6.4	13.1 ± 4.1
F82D R121C-4ac Glc	14.6 ± 6.3	
F82D R121C-Glc (Hek293)	24.1 ± 7.0	
R121D Y124D	98.3 ± 21.3	82.4 ± 20.7

The K_i -values obtained for the *E. coli*-derived IL-4 variants are in good agreement with the K_D -values determined by SPR-binding experiments, indicating that the glycoengineered IL-4 F82D R121C variants, especially the disulphide-linked glycan-conjugates, are indeed more effective than Pitrakinra.

2.5 Synthesis of an IL-4 receptor type II specific antagonist

While IL-4R α and IL-13R α 1 receptors are expressed on most cell types, the γ c receptor is primarily found on the cell surface of hematopoietic immune cells, which is why the type I receptor is considered to have a more immunoregulatory function. In contrast, signalling by the IL-4 type II receptor, which acts as the functional receptor of both IL-4 and IL-13, is strongly associated with inflammatory effector processes, e.g. airway hyperreactivity and increased mucus production (Ramalingam et al. 2008; Munitz et al. 2008). Thus, it might be useful to generate a selective antagonist, which is capable to specifically inhibit IL-4 receptor type II signalling without affecting γ c-dependent T-helper cell differentiation. We assumed that modifications of more peripheral positions of the interface II could yield IL-4 analogues that might possibly discriminate between γ c and IL-13R α 1 binding. Calculations of the buried surface area (BSA) performed by Duppatla and colleagues demonstrated that Lys117, which like Arg121 is located in helix D, is buried to a large extent (%BSA = 72%) upon complex formation with IL-13R α 1, but with the receptor subunit γ c Lys117 shares only little contact (%BSA = 3%) (figure 2.28) (Duppatla et al. 2014).

Hence, we regarded position 117 as a good candidate for the introduction of a glycan moiety and design of a selective IL-4 type II receptor antagonist.

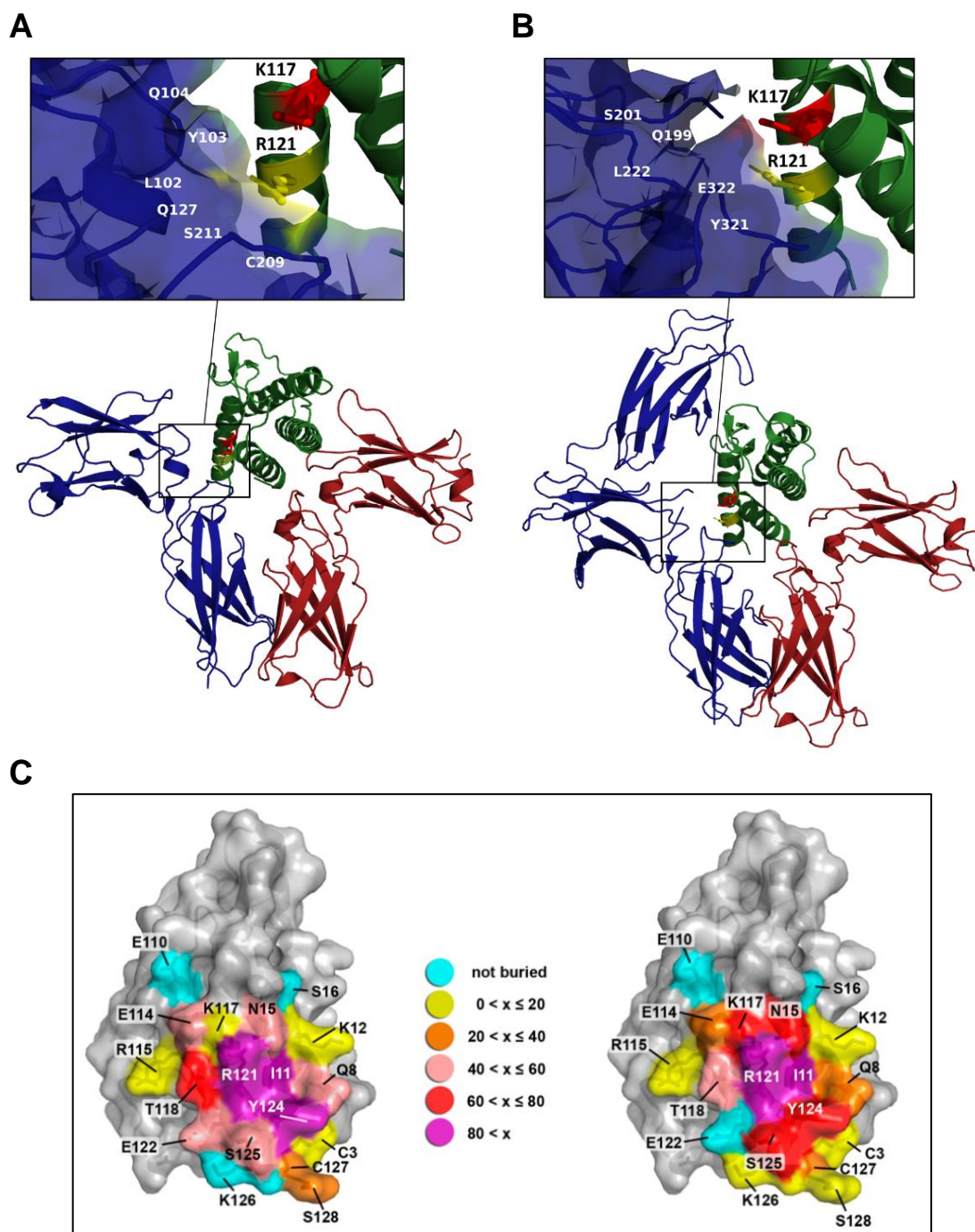


Figure 2.28: Position of residue Lys117 in the IL-4 binding epitope for receptors γc and IL-13R α 1. A) Cartoon representation of tertiary IL-4 type I receptor complex with IL-4 residues K117 and R121 shown as sticks (IL-4: green colour with K117 coloured in red and R121 coloured in yellow; γc : blue colour; IL-4R α : red colour). B) Cartoon representation of tertiary IL-4 type II receptor complex with IL-4 residues K117 and R121 shown as sticks (IL-4: green colour with K117 coloured in red and R121 coloured in yellow; IL-13R α 1: blue colour; IL-4R α : red colour). C) Surface representation of IL-4 with the surface colour-coded to highlight the residues buried upon complex formation of IL-4 with receptors γc (left panel) or IL-13R α 1 (right panel). The colour code is shown in the middle. (Adapted with permission of Duppatla et al. (2014) IL-4 analogues with site-specific chemical modification at position 121 inhibit IL-4 and IL-13 biological activities. *Bioconj. Chem.* 25, 52–62. Copyright (2018) American Chemical Society.)

2.5.1 Chemical glycosylation of an unpaired cysteine residue at position 117

2.5.1.1 Glutathione moiety conjugated to Cys117 can not be released by enzymatic reaction

For chemical coupling of a glycan moiety to position 117, the IL-4 variant F82D with Lys117 mutated to cysteine was recombinantly expressed in *E. coli* and purified in form of a mixed disulphide, with Cys117 being conjugated to a glutathione moiety (chapter 2.1). However, besides a glutathione conjugated species (from now on referred to as IL-4 F82D K117C-GSH), mass spectrometry also detected a small amount of protein (approximately 10% of total protein) representing non-modified IL-4 protein, with Cys117 lacking the glutathione moiety and containing a free thiol-group (figure 2.29A).

Employing the same procedure used for enzymatic liberation of the glutathionylated IL-4 Cys121 variants (chapter 2.4.2.1), purified IL-4 F82D K117C-GSH protein was treated with glutaredoxin to completely remove the glutathione protection group and provide Cys117 with a free thiol-group. During incubation with glutaredoxin, samples were taken at different time points and treated with maleimide-PEG to monitor the reaction progress in SDS-PAGE (figure 2.28B). Monopegylated IL-4 protein could already be observed in the untreated sample taken at time point 0 min, which had not been incubated with glutaredoxin (lane 1; figure 2.29B). This was due to PEGylation of the non-conjugated IL-4 protein species (containing a free thiol-group) in the starting material, which had been detected in mass spectrometry. However, no further accumulation of the monopegylated species could be observed, illustrating that enzymatic liberation of glutathionylated Cys117 did not occur (at a detectable level). Rather, the appearance of multipegylated protein species at later time points indicated non-specific cleavage of the native disulphide bonds. This suggests, that glutaredoxin did not or only to a very low extent remove the glutathione moiety from Cys117, possibly due to poor accessibility of Cys117 derived from electrostatic repulsion by the proximate charged residues Glu114 and Arg121 (figure 2.28C).

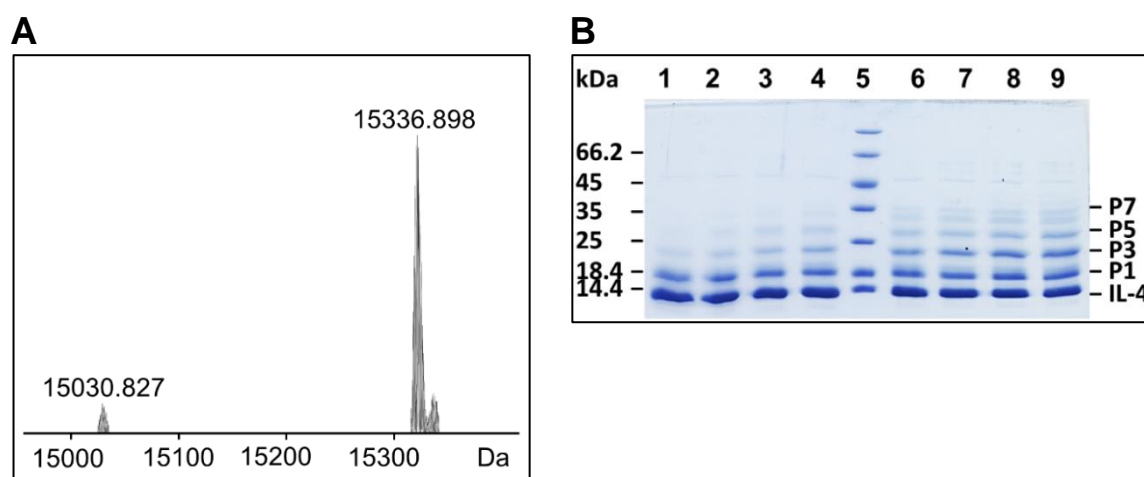


Figure 2.29: Enzymatic removal of conjugated glutathione from IL-4 F82D K117C-GSH is not possible. A) Mass spectrometry analysis of IL-4 F82D K117C-GSH. Unconjugated species (15031 Da) lacking a glutathione molecule and with an additional hydrogen atom makes up about 5% of total protein. B) SDS-PAGE of glutaredoxin-mediated deglutathionylation of IL-4 F82D K117C-GSH monitored by reaction with maleimide-PEG. SDS-PAGE was performed under reducing conditions. Samples were taken at different time points and mixed with 5 mM MA-PEG [min] 1: 0; 2: 0.5; 3: 1.0; 4: 2.5; 5: size standard; 6: 5.0; 7: 10; 8: 15; 9: 20. Electrophoretic mobility of monopegylated species is indicated by P1, multipegylated IL-4 species are marked P3, P5, and P7.

2.5.1.2 Chemical glycosylation of IL-4 F82D K117C variant using refolding

Chemical glycosylation strategies employing conjugation of glucosamine via the SMCC-linker or Glyco-SeS reaction were not applicable to IL-4 variant F82D K117C, since in both methods the engineered cysteine is required to be in a non-modified state, containing a free thiol-group. However, since oxidative refolding of *E. coli*-derived IL-4 variant F82D K117C with a glutathione redox couple allowed preparation of the glutathionylated protein in good yield, we assumed that refolding with thiol-glycans might be similar effective. Refolding in the presence of thiol-glycans and subsequent chromatographic purification was performed as described before (chapter 2.4.2.4) affording the protein in high purity (figure 2.30).

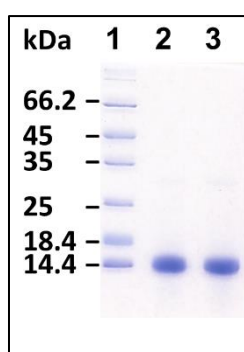


Figure 2.30: SDS-PAGE of purified IL-4 F82D K117C-(4ac)glc under reducing conditions. 1: size standard; 2: IL-4 F82D K117C-4ac Glc; 3: IL-4 F82D K117C-Glc.

Mass spectrometry of IL-4 F82D K117C obtained from refolding with thio-glucose (from now on referred to as IL-4 F82D K117C-Glc) showed one major protein species corresponding to the respective molecular weight of glycosylated protein (figure 2.31A). Also, a small amount (5%) of non-conjugated protein could be detected corresponding to IL-4 F82D K117C with a free thiol-group.

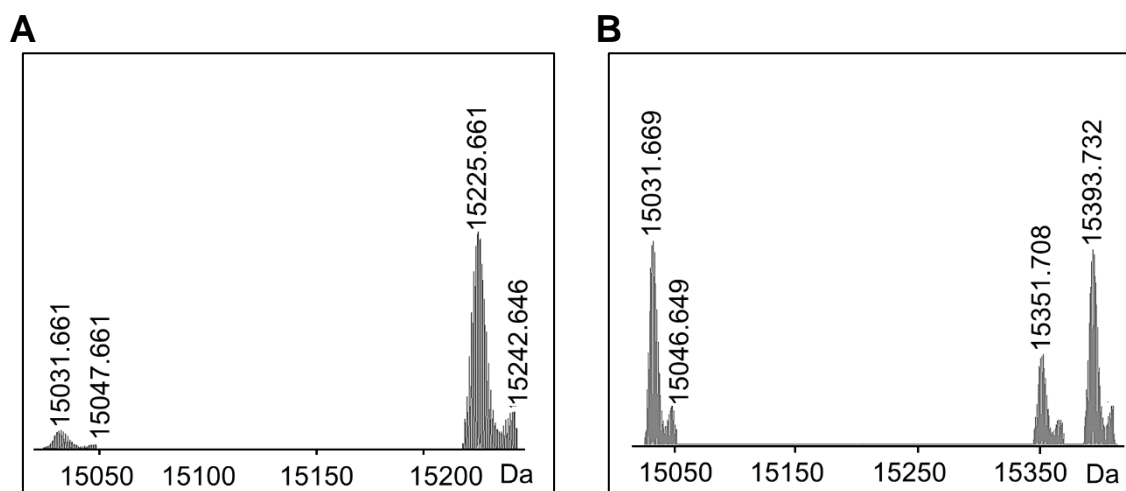


Figure 2.31: ESI-MS analysis of IL-4 F82D K117C variants derived from refolding with thiol-glucose (tetraacetate). A) Mass spectrometry analysis of IL-4 F82D K117C-Glc. The major protein species with a mass of 15225 Da represents IL-4 F82D K117C containing one disulphide-linked glucose molecule and lacking 7 hydrogen atoms. The species with a mass of 15031 Da represents non-glycosylated IL-4 F82D K117C with a free thiol-group lacking 6 hydrogen atoms. B) Mass spectrometry analysis of IL-4 F82D K117C-4acGlc. Protein species with a mass of 15393 Da represents IL-4 F82D R121C containing one disulphide-linked glucose tetraacetate molecule, lacking 7 hydrogen atoms. Side-peaks (-42 Da) are derived from the loss of acetate groups. About 50 % of total protein consists of non-glycosylated protein (15031 Da).

Glycosylated protein could also be detected for IL-4 F82D K117C derived from refolding with thio-glucose tetraacetate (from now on referred to as IL-4 F82D K117C-4acGlc), but approximately 50% of total protein consisted of a non-conjugated species containing a free thiol-group (figure 2.31B).

Since contamination with non-modified protein was not only observed for IL-4 F82D K117C derived from refolding with thiol-glycans but refolding with glutathione also yielded only partially modified protein, this suggests that chemical coupling of Cys117 might be hindered, possibly due to structural constraints as pointed out earlier. This assumption is supported by the finding that the bulkier glucose tetraacetate compound indeed showed a lower coupling yield than the smaller glucose.

To afford homogeneously glycosylated protein, the non-modified protein, which contained a free thiol-group, was removed by purification using iodoacetyl-activated agarose (chapter 2.4.2.3) (Supplement figure S9.2E/F).

2.5.2 Introduction of an N-glycan at position 117 using expression in Hek293 cells

2.5.2.1 An engineered N-glycosylation site at position 117 is partially occupied

For introduction of a eukaryotic complex N-glycan at IL-4 position 117 three amino acid substitutions K117N, T118A and I119T were created to provide an N-X-S/T motif. Additionally, IL-4's native N-glycosylation site was silenced by mutating Asn38 to glutamine. This facilitated the detection of an N-glycan at the engineered glycosylation site using SDS-PAGE analysis, since an additional N-glycan results in a protein mass increase of about 2 kDa, causing a visible decrease in electrophoretic mobility. This IL-4 variant, from now on referred to as F82D N38Q K117N, was transiently expressed in Hek293 cells and subsequently purified employing immobilized metal ion affinity chromatography, which was performed as described before (chapter 2.2). In SDS-PAGE purified IL-4 variant F82D N38Q K117N appeared as two protein species, which suggests that N-glycosylation at the new site occurred only partially (the protein is obtained as a mixture of glycosylated and non-glycosylated species) (figure 2.32).

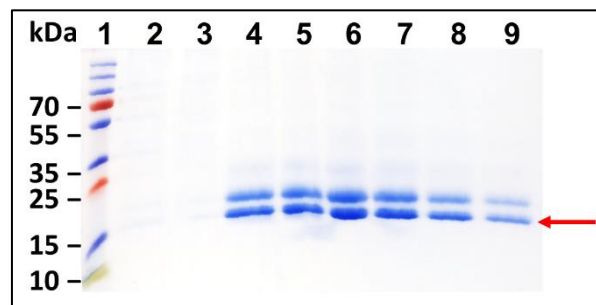


Figure 2.32: Immobilized metal ion affinity chromatography purification of IL-4 F82D N38Q K117N. In SDS-PAGE the protein containing fractions obtained from IMAC show two protein species, suggesting only partial glycosylation of the engineered N-glycosylation site N117 A118 I119T (arrow indicates the non-glycosylated species). 1: size standard; 2: sample before purification; 3: IMAC flow-through; 4-9: IMAC elution fractions.

2.5.2.2 Purification of glycosylated IL-4 F82D N38Q K117N using concanavalin A affinity chromatography

Since non-glycosylated IL-4 variant F82D N38Q K117N was shown to act as an agonist, stringent removal of the non-glycosylated protein was required. The plant lectin concanavalin A (ConA) binds N-glycans containing α -mannose and α -glucose and is routinely used for isolation of glycoproteins. IL-4 F82D N38Q K117N was adjusted to concanavalin A binding buffer and applied to a HiTrap Con A 4B column (GE Healthcare) (chapter 5.6.5). The protein was eluted by direct application of 100% (v/v) elution buffer, which contained 500 mM methyl-D-glucoside (figure 2.33A). Elution fractions containing protein with an apparent molecular weight of 18 kDa, representing glycosylated protein (figure 2.33B) were pooled and freeze-dried. As demonstrated by SDS-PAGE analysis of the purified IL-4 variant F82D N38Q K117N, non-glycosylated protein could be efficiently removed by concanavalin A affinity chromatography (figure 2.33C). Since the concanavalin A lectin does not bind all types of mammalian-derived N-glycans, i.e. it has a high specificity for oligomannose-type N-glycans but fails to bind more highly branched complex-type N-glycans (reviewed in (Varki et al. 2009)), concanavalin A purification was accompanied by a considerable loss of IL-4 F82D N38Q K117N glycoprotein that did not bind to the column (figure 2.33B, frac. 4) and which resulted in an overall low yield of only 10%.

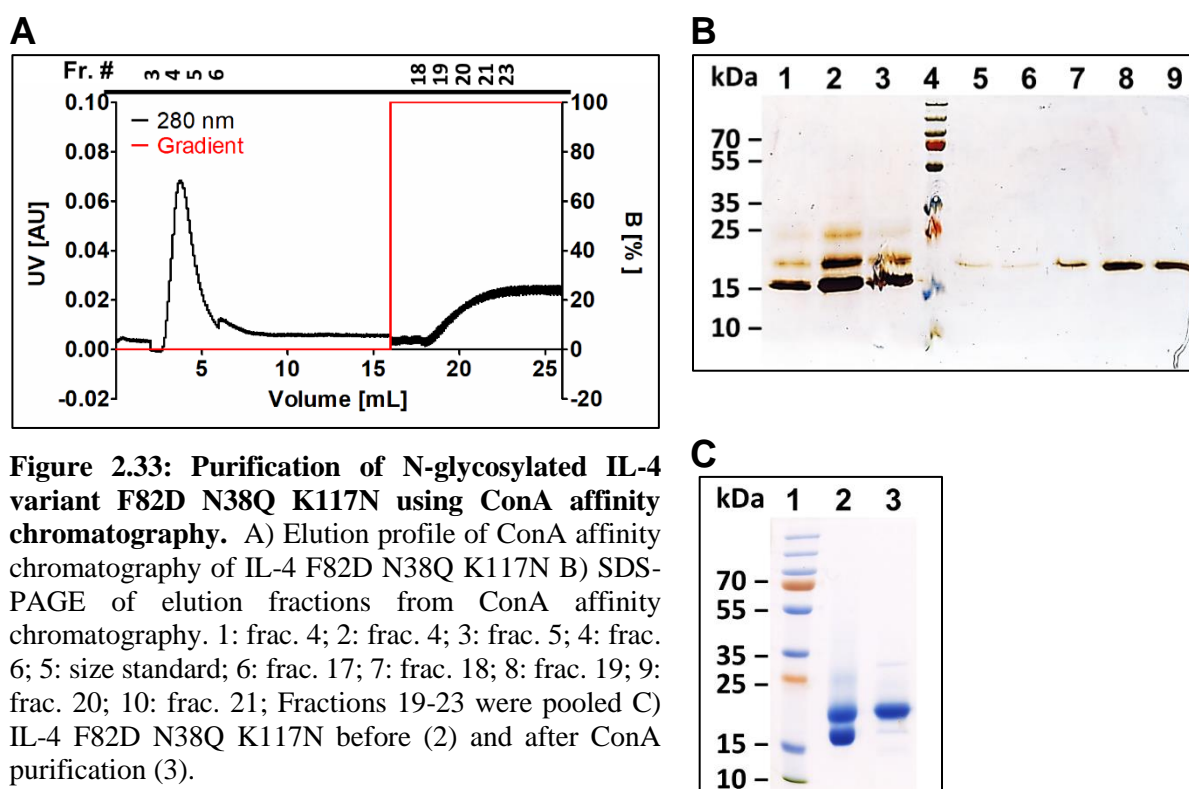


Figure 2.33: Purification of N-glycosylated IL-4 variant F82D N38Q K117N using ConA affinity chromatography. A) Elution profile of ConA affinity chromatography of IL-4 F82D N38Q K117N B) SDS-PAGE of elution fractions from ConA affinity chromatography. 1: frac. 4; 2: frac. 4; 3: frac. 5; 4: frac. 6; 5: size standard; 6: frac. 17; 7: frac. 18; 8: frac. 19; 9: frac. 20; 10: frac. 21; Fractions 19-23 were pooled C) IL-4 F82D N38Q K117N before (2) and after ConA purification (3).

2.5.3 Interaction analysis of glycosylated IL-4 K117C/N variants with the IL-4R α receptor

In vitro binding affinities of glycoengineered IL-4 F82D variants containing either a disulphide-linked thiol-glycan or a complex N-glycan at position 117 were measured employing surface plasmon resonance using the same experimental set-up as described for IL-4 F82D R121C variants (chapter 2.4.4). Disulphide-linked glucose and glucose tetraacetate modified IL-4 F82D K117C variants (purified via SulfoLink resin) showed a two- to threefold higher binding affinity for the IL-4R α receptor ectodomain compared to Pitracinra with K_D -values of about 55 ± 13 pM and 86 ± 12 pM, respectively (table 2.3). The glutathionylated IL-4 variant F82D K117C-GSH, which was analysed in parallel (purified via SulfoLink resin) also exhibited a lower K_D value of 30 pM. As pointed out earlier, the higher binding affinity is mainly attributable to reduced dissociation rates (k_{off}) due to the F82D mutation. For the Hek293 cell-derived IL-4 variant F82D N38Q K117N (purified by concanavalin A lectin chromatography) a K_D of 149 ± 40 pM could be determined, which is in the same range as Pitracinra (163 ± 39 pM) and wildtype IL-4 (183 ± 42 pM). The three times lower affinity compared to the *E. coli*-derived IL-4 F82D K117C-Glc glycoconjugate is due to the increased molecular size caused by the complex eukaryotic N-glycosylation. Thus, Hek293 cell-derived IL-4, containing an N-linked glycan at position 117, exhibits a size of about 18 kDa, whereas *E. coli*-derived, non-glycosylated IL-4 only has a size of 15 kDa. The higher molecular weight of the Hek293 cell-derived IL-4 protein likely causes a decrease in association rate, thereby lowering the binding affinity.

Table 2.3: Binding affinities of glycoengineered IL-4 F82D R121C variants to IL-4R α ECD measured by SPR. Kinetic rate and equilibrium binding constants were derived from three independent experiments (n=3) using five different analyte concentrations. The binding parameters k_{on} , k_{off} , and K_D represent mean values and standard deviations.

IL-4 variant	k_{on} [$M^{-1}s^{-1}$] x 10^6	k_{off} [s^{-1}] x 10^{-4}	K_D [pM]
WT	5.34 ± 1.49	9.37 ± 0.25	183.33 ± 41.68
F82D K117C-GSH	7.19 ± 0.22	2.12 ± 0.11	29.57 ± 0.21
F82D K117C-Glc	3.05 ± 0.19	1.70 ± 0.44	55.43 ± 12.92
F82D K117C-4acGlc	2.68 ± 0.13	2.31 ± 0.42	85.70 ± 11.90
F82D N38Q-K117N (Hek293)	1.64 ± 0.18	2.40 ± 0.39	149.33 ± 40.07
R121D-Y124D	5.97 ± 0.54	9.59 ± 1.45	163.34 ± 39.11

2.5.4 Glycoengineered IL-4 F82D K117C/N variants display partially agonistic activity in a cell-based assay

As initially outlined, by introducing a glycan moiety at IL-4 position 117, which is located at the periphery of the IL-4 binding epitope for receptors γc and IL-13R $\alpha 1$, we anticipated to generate an IL-4 receptor type II specific antagonist with impaired binding for IL-13R $\alpha 1$, while maintaining type I receptor-dependent activity. IL-4 F82D analogues containing a glycan attached to position 117 either derived from expression in *E. coli* or Hek293 cells were analysed in HEK-Blue and TF-1 cell experiments to evaluate their ability to activate IL-4 receptor type I or type II. HEK-Blue cells are engineered Hek293 cells, which express the SEAP (secreted alkaline phosphatase) gene under the control of an IL-4/IL-13 inducible promoter. Since they only express the receptors IL-4R α and IL-13R $\alpha 1$, they serve as a reporter system specific for IL-4 receptor type II signalling. TF-1 cells are human erythroleukemic cells, which carry both IL-4 receptors type I and II. This cell-line proliferates in response to IL-4 and IL-13, which can be photometrically quantified using resazurin staining.

At a concentration of 50 pM, glutathionylated IL-4 variant F82D K117C-GSH (purified by SulfoLink resin) was almost completely inactive in HEK-Blue cells (3% activity), whereas this variant still exhibited about 50% activity in TF-1 cells compared to wildtype IL-4. Hence, when coupled to a glutathione moiety IL-4 variant F82D K117C shows a similar activity to the IL-4 variant R121E, which is a reported type II specific antagonist (figure 2.34/Supplement table S8.3) (Shanafelt et al. 1998). This indicates that conjugation of a glutathione moiety to position 117 specifically disrupts interaction with IL-13R $\alpha 1$, while binding for γc is maintained. These findings are in contrast to the observations made by Duppatla and colleagues, who reported residual activity for IL-4 variant K117C-GSH of about 64% in HEK-Blue cells at a concentration of 1 nM (Duppatla et al. 2014). We therefore also tested higher concentrations of glutathionylated IL-4 F82D K117C (purified by SulfoLink resin) in HEK-Blue cells, but no considerable increase in biologic activity could be observed even at a concentration of 10 nM (figure 2.36D). As described in chapter 2.5.1.1, refolding of IL-4 F82D K117C with glutathione only yielded partially modified protein. Since non-modified IL-4 F82D K117C-SH with a free thiol-group seems to exhibit (full) activity in HEK-Blue cells (Supplement table S9.4/figure S9.3), the higher activity of IL-4 K117C-GSH reported by Duppatla and colleagues could be caused by contamination with

non-conjugated K117C-SH protein. This, however, can only be assumed as the authors did not show mass spectrometry data for this variant.

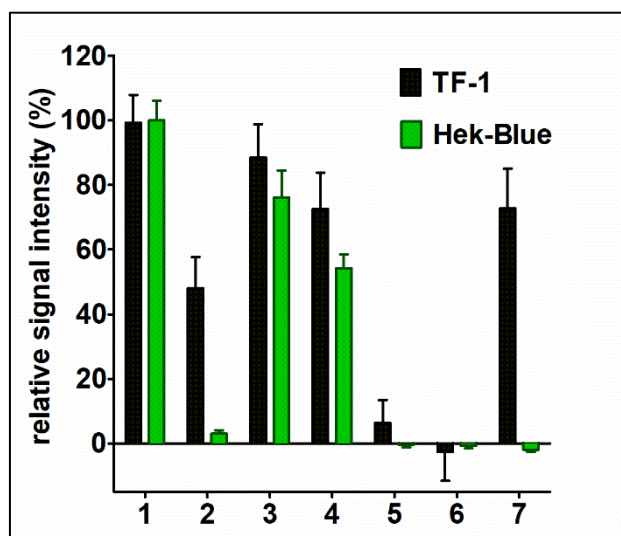


Figure 2.34: Biologic activity of glycosylated IL-4 F82D K117C/N variants in HEK-Blue and TF-1 cells. Cells were incubated with 50 pM of each variant and signal intensity (quantified as detailed under chapter 5.7.3) was normalized to wildtype IL-4. 1: WT; 2: F82D K117C-GSH; 3: F82D K117C-Glc; 4: F82D K117C-4acGlc; 5: F82D N38Q K117N (Hek293); 6: R121D Y124D; 7: F82D R121E.

In contrast to the glutathionylated variant, chemically glycosylated IL-4 F82D K117C analogues disulphide-linked to glucose and glucose tetraacetate (purified with iodoacetyl activated agarose) showed only slightly reduced biologic activity in TF-1 and HEK-Blue cells compared to wildtype IL-4 (figure 2.34/Supplement table S8.3). Thereby, conjugation of the bulkier glucose-tetraacetate moiety resulted in a stronger reduction in activity, with the respective variant exhibiting 54% activity in HEK-Blue and 73% activity in TF-1 cells. Thus, a monosaccharide, i.e. a glucose molecule is too small to induce steric hindrance at position 117 and effectively disrupt binding to IL-13R α 1. This, however, might be achieved by introduction of a bulkier di- or trisaccharide. This hypothesis was corroborated by the observation that introduction of a glutathione moiety at position 117 was much more effective in abrogating type II receptor activity. The tripeptide glutathione is a linear, but branched molecule with a length of about 12.5 Å, being two times longer in diameter than the pyranose ring structure of the glucose molecule, which though having a similar molecular weight as glutathione, has only a molecular diameter of 6.2 Å (figure 2.35).

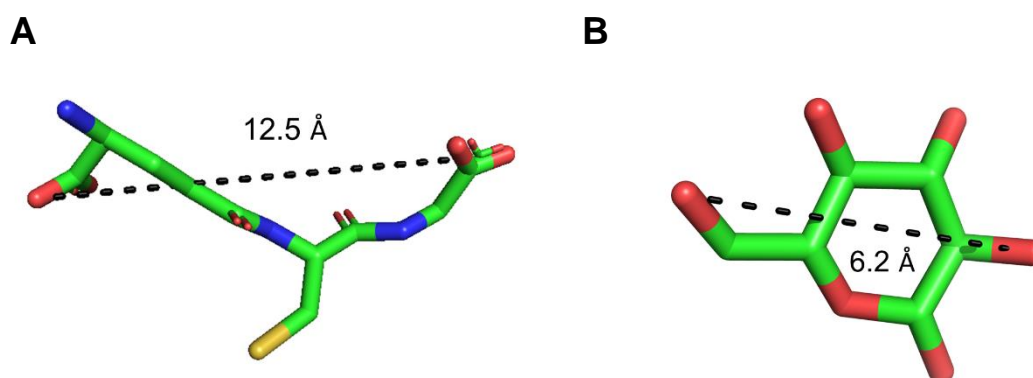


Figure 2.35: Glutathione is two times longer than glucose. A) Stick representation of glutathione. The molecular diameter between the two carboxyl ends measures about 12.5 Å. B) stick representation of glucose. The molecular diameter between the hydroxy groups of the C2- and C6- atom measures about 6.2 Å.

Surprisingly, the Hek293 cell-derived IL-4 F82D N38Q K117N variant (purified by concanavalin A lectin chromatography), which contains a complex biosynthetic N-glycan at position 117 was inactive in both cell-lines at a concentration of 50 pM, similar to Pitrakinra (IL-4 R121D Y124D). This concludes that introduction of a bigger molecule, like a complex N-glycan with a size of about 2-3 kDa at position 117 is able to impair interaction with both receptors γc and IL-13R $\alpha 1$.

Since only the glutathione conjugated IL-4 variant F82D K117C-GSH and the glycoengineered protein IL-4 F82D N38Q K117N expressed in Hek293 cells showed strongly reduced biologic activity, only these IL-4 variants were further analysed for their inhibitory efficacy in cell-based assays. The half maximal effective concentration (EC₅₀) for wildtype IL-4 and half maximal inhibitory concentrations (IC₅₀) for glycoengineered IL-4 K117C/N variants were determined from dose-response curves (exemplary figure 2.36), which were then employed to calculate the inhibitory constant (K_i) for each variant using the Cheng-Prusoff equation ($K_i = IC_{50}/(1 + [IL-4]/EC_{50})$).

In HEK-Blue cells, at 200 nM, the glutathionylated IL-4 variant F82D K117C-GSH (purified with iodoacetyl activated agarose) attenuated the activity of wildtype IL-4 at 50 pM to almost background level (figure 2.36A). A K_i-value of about 16 pM could be determined for IL-4 F82D K117C-GSH, which is five times lower compared to the K_i-value of Pitrakinra (82 ± 21 pM) (table 2.4).

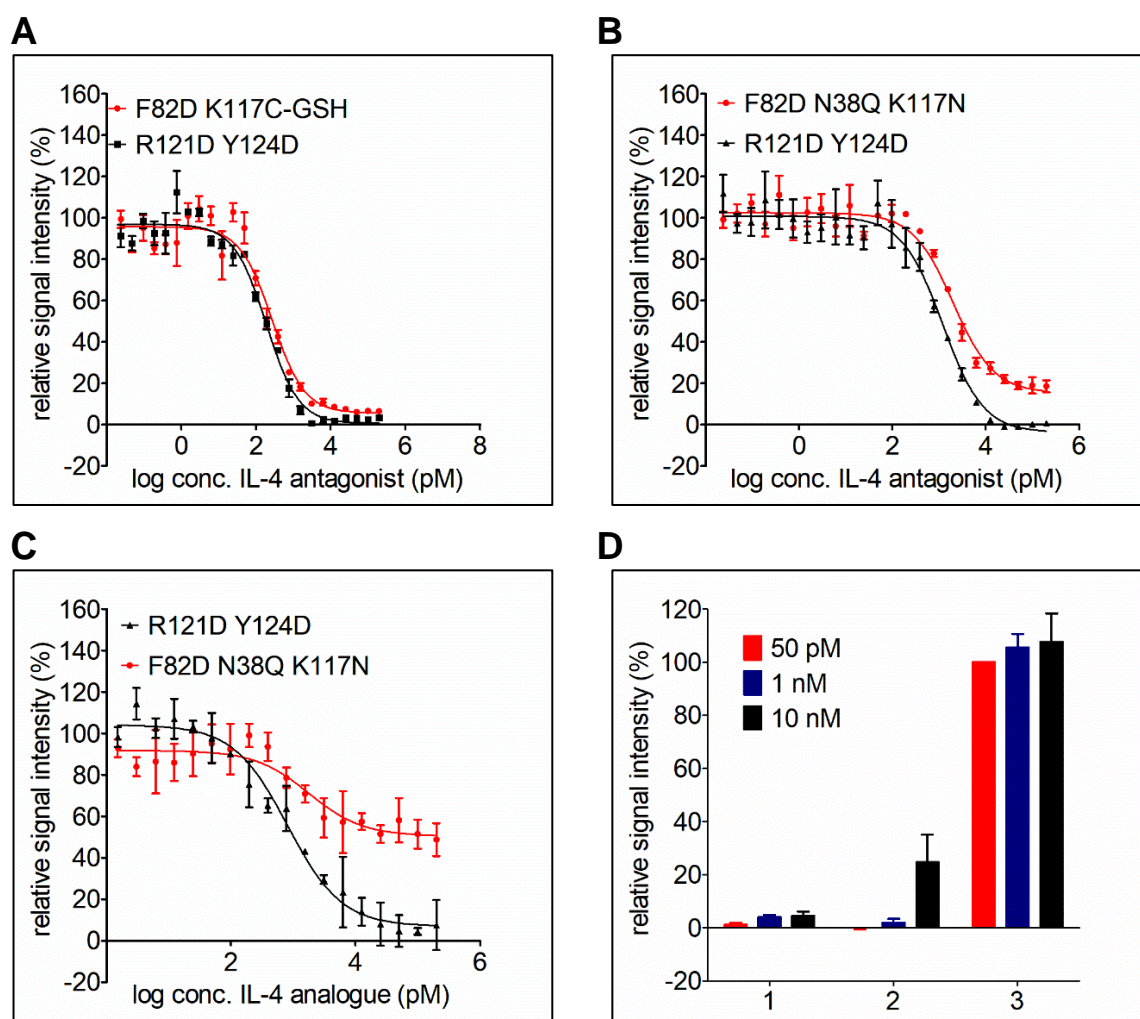


Figure 2.36: Dose-dependent competition of glutathionylated/glycoengineered IL-4 K117C/N variants in cell-based experiments. HEK-Blue or TF-1 cells were incubated with a log 2 titration of the indicated IL-4 variant in competition against 50 pM IL-4 WT. The signal intensity (quantified as detailed under chapter 5.7.3) was normalized to IL-4 WT at a concentration of 50 pM. Data is shown from three replicates. A) IL-4 F82D K117C-GSH in HEK-Blue cells B) IL-4 F82D N38Q K117N (purified by ConA) in HEK-Blue cells C) IL-4 F82D N38Q K117N (purified by ConA) in TF-1 cells. D) Biologic activity of glycoengineered IL-4 K117C/N analogues. HEK-Blue cells were incubated with 50 pM, 1 nM or 10 nM IL-4 variants (1: IL-4 F82D K117C-GSH (purified by SulfoLink); 2: IL-4 F82D N38Q K117N (purified by ConA); 3 IL-4 WT) and signal intensity was normalized to 50 pM wildtype IL-4.

Since the Hek293 cell-derived IL-4 F82D N38Q K117N analogue (purified by concanavalin A lectin chromatography) showed impaired biologic activity in HEK-Blue and TF-1 cells, this variant was analysed in both cell lines for its ability to antagonize wildtype IL-4. In HEK-Blue cells, at 200 nM, IL-4 F82D N38Q K117N (purified by concanavalin A lectin chromatography) attenuated wildtype IL-4 activity to a level of about 20% and exhibited a K_i of 135 ± 54 pM. In TF-1 cells the antagonistic efficacy of this variant was much lower, as it attenuated the activity of wildtype IL-4 only to a level of about 50% (K_i -value was not determined) (figure 2.36B/C; table 2.4). Testing of higher concentrations of IL-4 F82D

N38Q K117N in HEK-Blue cells showed that this variant was not completely inactive. At 10 nM this variant exhibited about 30% activity in HEK-Blue cells compared to wildtype IL-4 (figure 2.36D), explaining why IL-4 F82D N38Q K117N could only partially abrogate IL-4 dependent signalling in TF-1 and HEK-Blue cells.

Table 2.4: Inhibitory constants of the glycoengineered IL-4 F82D K117C/N variants *in vitro*. The Ki-values were calculated using the IC50 values of the IL-4 F82D K117C/N variants and the EC50 value of wildtype IL-4 (EC50 IL-4 WT: TF-1: 6.7 ± 1.5 pM; HEK-Blue: 3.6 ± 1.0 pM) obtained from dose-response curves in TF-1 and HEK-Blue cell assays (as detailed under experimental procedures). Data was used from three independent experiments (n=3).

IL-4 variant	Inhibitory constant (Ki) [pM]	
	TF-1	HEK-Blue
IL-4 F82D K117C-GSH (purified by SulfoLink)		16.6 ± 0.17
IL-4 F82D N38Q K117N (purified by ConA)		135.1 ± 54.3
IL-4 R121D Y124D	98.3 ± 21.3	82.4 ± 20.7

2.6 Hyperglycosylated Hek293 cell-derived IL-4 variants display increased proteolytic stability

One of the pharmacokinetic disadvantages of the original IL-4 antagonist Pitrakinra was its short serum half-life, which was estimated to about 3 hours (Longphre and Fuller 2010). Pitrakinra's small size of only 15 kDa and lack of glycosylation were certainly key determinants, which facilitated a rapid systemic clearance of the drug. Increasing the size of Pitrakinra through conjugation of polyethylene glycol (PEG) indeed improved its serum half-life from a few hours to about 5 days, but also decreased its efficacy to act as an IL-4 antagonist, as the very long PEG moiety critically affected binding to IL-4R α (see patent: WO2011106779A1, (Tomkinson 2011)). Similar to PEGylation, (hyper)glycosylated proteins, i.e. proteins with increased eukaryotic complex N-glycosylation, also show an enhanced circulatory life time, are more resistant to proteolysis and have a higher physicochemical stability compared to non-glycosylated forms (reviewed in: (Solá and Griebenow 2010)).

As wildtype IL-4 only has a single N-glycosylation site and O-glycosylation has not been reported for IL-4, we wanted to produce a hyperglycosylated IL-4 variant through engineering of additional N-glycosylation sites and subsequent expression in Hek293 cells. This should produce an IL-4 variant with increased molecular size to lower its rate of renal excretion and should also result in a lower immunogenicity. Furthermore, we tested whether

this hyperglycosylated Hek293 cell-derived IL-4 variant could be combined with our chemical glycosylation to afford an IL-4 antagonist with enhanced pharmacokinetic properties.

2.6.1 Synthesis of hyperglycosylated IL-4 variants in Hek293 cells

Several potential N-glycosylation sites were constructed at different positions in IL-4 by altering the amino acid sequence of IL-4 to comprise the N-glycosylation motif N-X-S/T with X not being proline. As a design principle, the additional sites were chosen to require minimal mutations, ideally positions where a single amino acid substitution against asparagine was sufficient to generate an N-X-S/T motif to minimize sequence alteration. Furthermore, only positions outside the IL-4R α epitope were considered to prevent interference of the introduced N-glycans with binding to IL-4R α , which might limit the antagonist efficacy of the engineered IL-4 glycoconjugates. Thirdly, N-glycosylation sites were introduced only outside of secondary structure elements, hence preferentially in loop regions which are very likely accessible to glycosyltransferases in the endoplasmic reticulum. Obeying these requirements five IL-4 single amino acid variants with the substitutions Q20N, E26N, T28N, A34N and K61N were designed and transiently expressed in Hek293 cells. In SDS-PAGE analysis, all of these IL-4 variants showed a mobility shift, thereby indicating that the engineered N-glycosylation sites had been indeed recognized and glycosylated by Hek293 cells (figure 2.37; data not shown).

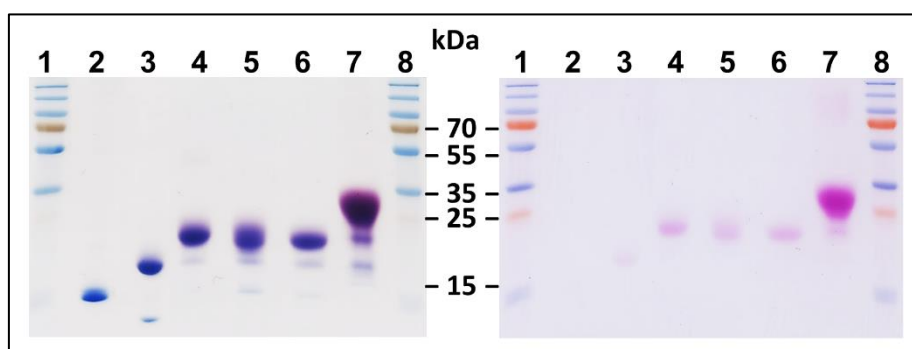


Figure 2.37: SDS-PAGE of purified IL-4 hyperglycosylated variants obtained from Hek293 cells. SDS-PAGE was performed under non-reducing conditions. To visualize the degree of glycosylation the SDS gel was first submitted to periodic acid-Schiff staining (right panel) before Coomassie staining was used for protein detection. 1: size standard; 2: IL-4 F82D N38Q; 3: IL-4 WT; 4: IL-4 F82D Q20N; 5: IL-4 F82D T28N; 6: IL-4 F82DK61N; 7: IL-4 F82D Q20N T28N K61N (ConA purified); 8: size standard.

2.6.2 N-glycan at position 28 disrupts binding to IL-13 R α 1

To assess if the novel N-glycosylation sites did affect the biologic activity/receptor binding, Hek293 cell-derived IL-4 F82D variants comprising one of the following substitutions Q20N, E26N, T28N, A34N or K61N were analysed in cell-based assays, i.e. HEK-Blue- and TF-1 cells. Besides IL-4 variant F82D T28N, all the other IL-4 variants exhibited EC50 values similar to *E. coli*-derived IL-4 F82D (Supplement figure S9.4/S9.5), indicating that the engineered N-glycosylation sites did not interfere with receptor binding. In HEK-Blue cells, only the IL-4 variant F82D T28N showed a considerable loss in activity, which suggests that the N-glycan at position 28 disrupts binding to IL-13R α 1.

Residue Thr28, located in IL-4 loop AB, is part of IL-4 site III that forms a contact interface with the N-terminal fibronectin type III domain in IL-13R α 1, called the D1 domain (figure 2.38).

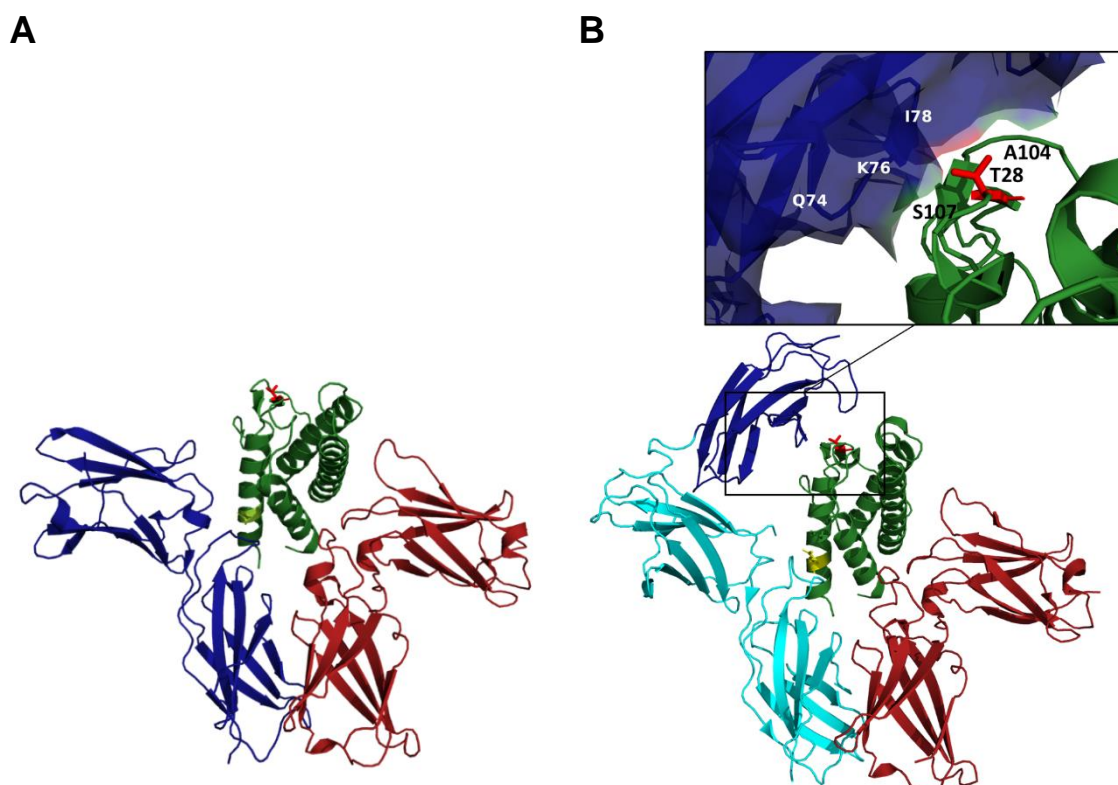


Figure 2.38: Position of residue Thr28 in the IL-4 binding epitope for receptors γ c and IL-13R α 1. A) Cartoon representation showing tertiary IL-4 type I receptor complex with IL-4 residues Thr28 and Arg121 shown as sticks (IL-4: green colour with Thr28 coloured in red and Arg121 coloured in yellow; γ c: blue colour; IL-4R α : red colour). B) Cartoon representation showing tertiary IL-4 type II receptor complex with IL-4 residues Thr28 and Arg121 shown as sticks (IL-4: green colour with Thr28 coloured in red and Arg121 coloured in yellow; IL-13R α 1: D2/D3 domain coloured cyan and D1 domain coloured dark blue; IL-4R α : red colour).

2 Results

Our finding, that introduction of an N-glycan at IL-4 position 28 impairs binding of IL-4 with IL-13R α 1 is particularly surprising, since so far the D1 domain was considered to be only required for interaction of IL-13R α 1 with IL-13, but not necessary for assembly with IL-4, which was thought to only bind to IL-13R α 1 domains D2 and D3 (LaPorte et al. 2008; Arima et al. 2005; Ito et al. 2009).

Since SDS-PAGE analysis showed that the novel N-glycan site T28N was only partially glycosylated, mutation N38Q was introduced additionally in IL-4 F82D T28N (from now on referred to as IL-4 F82D N38Q T28N) to silence IL-4's native N-glycosylation site at position 38. This allowed the preparation of only glycosylated IL-4 F82D N38Q T28N containing a single N-glycan at position 28 by using concanavalin A lectin affinity chromatography (figure 2.39C).

In TF-1 cell assay, at 50 pM, the concanavalin A purified IL-4 variant F82D N38Q T28N only exhibited about 40% activity compared to wildtype IL-4, whereas at this concentration the variant was almost inactive in HEK-Blue cells. To determine the antagonistic efficacy of IL-4 F82D N38Q T28N, dose-dependent competition of this variant with wildtype IL-4 in binding to IL-4 receptor type II was analysed in HEK-Blue cells. At 200 nM, IL-4 variant F82D N38Q T28N attenuated the activity of 50 pM wildtype IL-4 to about 40% (figure 2.39A). Similar to what has been observed for Hek293 cell-derived IL-4 variant F82D N38Q K117N, incubation of HEK-Blue cells with higher concentrations of IL-4 variant F82D N38Q T28N showed that it was not completely inactive, but, at 10 nM, exhibited biologic activity of 35% compared (figure 2.39 B).

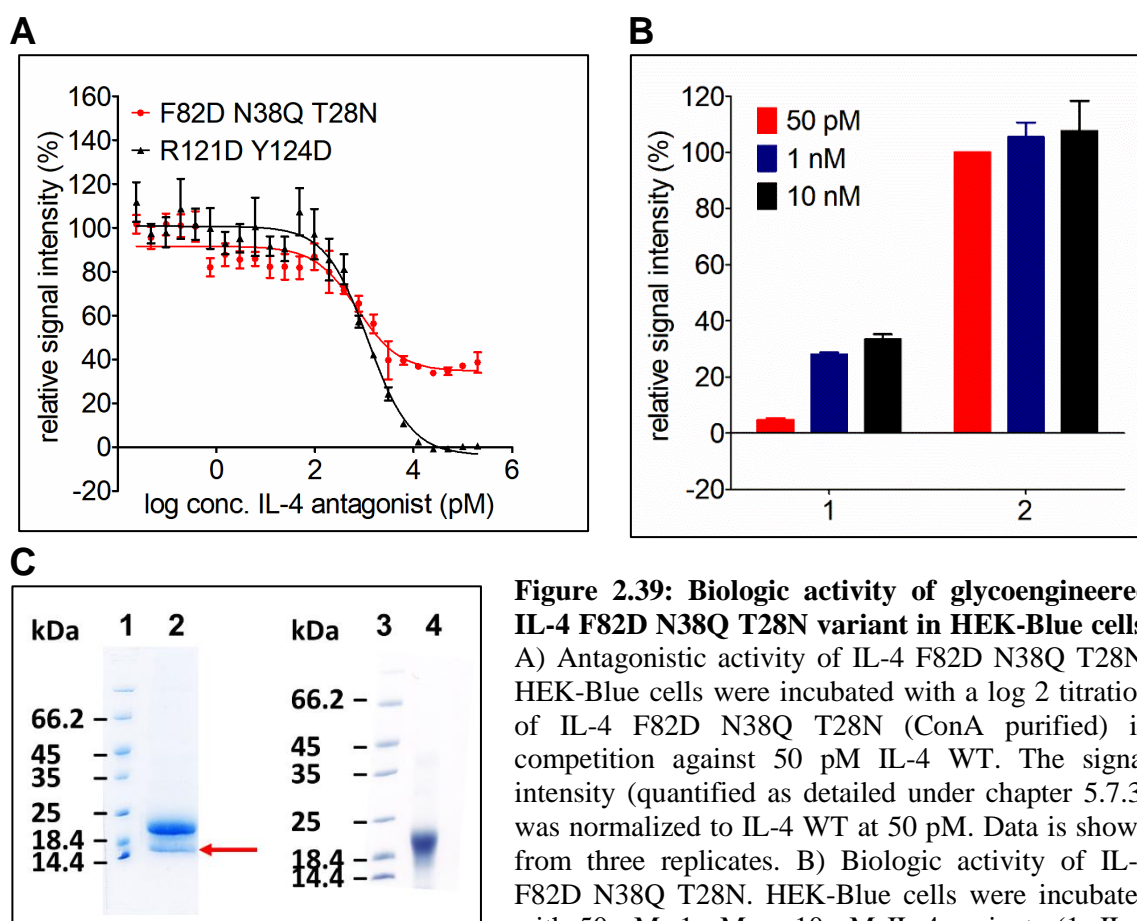


Figure 2.39: Biologic activity of glycoengineered IL-4 F82D N38Q T28N variant in HEK-Blue cells. A) Antagonistic activity of IL-4 F82D N38Q T28N. HEK-Blue cells were incubated with a log 2 titration of IL-4 F82D N38Q T28N (ConA purified) in competition against 50 pM IL-4 WT. The signal intensity (quantified as detailed under chapter 5.7.3) was normalized to IL-4 WT at 50 pM. Data is shown from three replicates. B) Biologic activity of IL-4 F82D N38Q T28N. HEK-Blue cells were incubated with 50 pM, 1 nM or 10 nM IL-4 variants (1: IL-4 F82D N38Q T28N (ConA purified); 2 IL-4 WT) and SEAP induction was normalized to 50 pM wildtype IL-4. C) SDS-PAGE of Hek293 cell-derived IL-4 F82D N38Q T28N (under reducing conditions). 1/3: size standard; 2: IL-4 F82D N38Q T28N (non-glycosylated variant is indicated by red arrow); 4: IL-4 F82D N38Q T28N (ConA purified).

2.6.3 Design of a hyperglycosylated IL-4 antagonistic variant by combining chemical and synthetic glycoengineering

Next, we designed an IL-4 multi-variant carrying three additional N-glycans to afford a hyperglycosylated IL-4 protein with a significant increased molecular size. The three mutations Q20N, T28N and K61N were chosen, because the single amino acid variants showed improved expression yield compared to wildtype IL-4, whereas other mutations tested, e.g. E26N decreased the protein yield. Besides positively affecting the expression yield, the introduction of an additional N-glycan at position 28 (T28N) was shown to partially disrupt binding to the IL-13R α 1 receptor, which hence will benefit our designed IL-4 antagonist. The IL-4 variant F82D Q20N T28N K61N could be expressed in Hek293 cells in similar yield as wildtype IL-4. In addition to immobilized metal affinity

2 Results

chromatography, IL-4 F82D variant Q20N T28N K61N was submitted to concanavalin A lectin chromatography to remove the non-glycosylated protein species (figure 2.40).

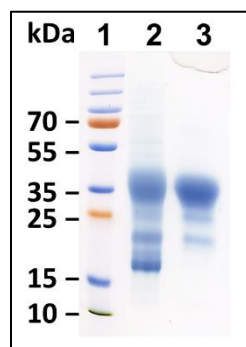


Figure 2.40: Purification of N-glycosylated Hek293 cell-derived IL-4 F82D variant Q20NT28NK61N using ConA affinity chromatography. 1: size standard; IL-4 F82D variant Q20NT28NK61N before (2) and after (3) purification by ConA affinity chromatography.

SDS-PAGE analysis revealed an apparent molecular weight at about 35 kDa for IL-4 F82D Q20N T28N K61N (figure 2.37), which is about a twofold increase in molecular weight compared to *E. coli*-derived wildtype IL-4 and Pitrakinra.

Since an engineered N-glycosylation site at position 121 was not used by Hek293 cells, an IL-4 variant IL-4 F82D Q20N T28N K61N with Arg121 mutated to cysteine was expressed in Hek293 cells to generate a hyperglycosylated IL-4 protein that can be converted into an antagonist by chemical glycosylation.

As already outlined above chemical glycosylation of Hek293 cell-derived IL-4 protein containing an engineered cysteine was shown to be limited to the refolding procedure and refolding of IL-4 variant F82D Q20N T28N K61N R121C was performed as described for Hek293 cell-derived IL-4 F82D R121C (chapter 2.4.3). In SPR analysis IL-4 variant F82D Q20N T28N K61N R121C derived from refolding with thiol-glucose showed a K_D of about 218 ± 28 pM for the IL-4R α ECD respectively. The ten times lower affinity compared to the *E. coli*-derived IL-4 antagonist F82D R121C-Glc (K_D about 20 pM) is likely caused by the significantly increased molecular size due to the additional N-glycans, which affects the association rate thereby decreasing the binding affinity (k_{on} : $1.12 \pm 0.4[M^{-1}s^{-1}] \times 10^6$ / k_{off} : $2.37 \pm 0.5[s^{-1}] \times 10^{-4}$). However, due to introduction of the F82D mutation, which reduces the dissociation rate of IL-4, the binding affinity is not significantly different from wildtype IL-4 (K_D : 183 ± 42) and Pitrakinra (K_D : 163 ± 39 pM) ($p > 0.05$). In competition with wildtype IL-4 in a TF-1 cell assay, the glycosylated IL-4 variant F82D Q20N T28N K61N

R121C-Glc attenuated IL-4 dependent response to background level and exhibited a K_i of about 184 ± 55 pM, which is agreement with its K_D value (figure 2.41).

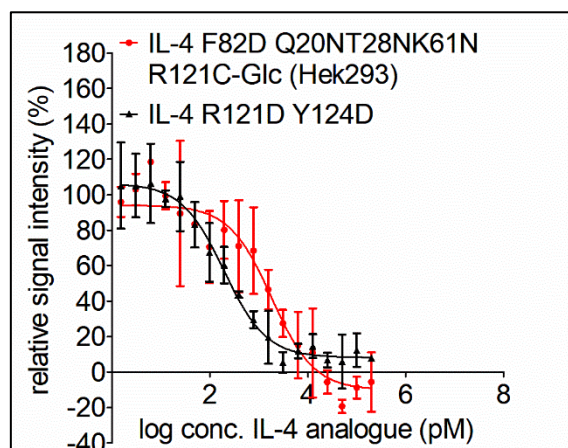


Figure 2.41: Dose response curves of glycoengineered IL-4 variant F82D Q20N T28N K61N R121C-Glc in TF-1 cells. Cells were incubated with a log 2 titration of Hek293 cell-derived IL-4 F82D Q20N T28N K61N R121C-Glc (ConA purified) in competition against 50 pM wildtype IL-4 (*E.coli*). The signal intensity was normalized to wildtype IL-4 at 50 pM.

2.6.4 Hyperglycosylated Hek293 cell-derived IL-4 shows increased proteolytic stability

Glycosylation can confer stability against proteolytic degradation by masking protease cleavage sites in a protein (Ueda et al. 2009; Carter et al. 2004). We therefore analysed if introduction of additional complex N-glycans improves the proteolytic stability of IL-4 *in vitro*.

IL-4 variants derived from different expression systems, i.e. *E. coli*, Hek293 cells and baker's yeast (*P. pastoris*), varying in glycan content and glycan size, were adjusted to a concentration of about 30 μ M and incubated at 37 °C with 10 μ g of bovine trypsin, which was used as a model protease. Protein samples were taken at different time points and submitted to SDS-PAGE. After Coomassie staining of the SDS-gels, residual non-protolysed IL-4 protein in each sample was quantified using Bio-Rad's Image Lab™ software. A regression analysis of the data was performed to determine the "proteolytic" half-life of each variant. Therefore the data was fitted to a one-phase decay model using Graphpad's Prism software.

Initial experiments showed that the mutation F82D did not alter the proteolytic sensitivity compared to wildtype IL-4. *E. coli*-derived IL-4 F82D, which like PitraKinra is not glycosylated due to its prokaryotic origin was the most susceptible to tryptic hydrolysis and

2 Results

showed a half-life of about 1 h (figure 2.42; table 2.5). In contrast, IL-4 F82D protein obtained from expression in Hek293 cells, which carries a single complex N-glycan at IL-4's natural glycosylation site Asn38 exhibited a half-life of about 5 h, showing that the presence of a single complex N-glycan moiety drastically improves proteolytic stability of recombinant IL-4. To investigate, whether the enhanced proteolytic stability observed for Hek293 cell-derived IL-4 is indeed due to complex eukaryotic N-glycosylation, the IL-4 variant N38Q, lacking all glycosylation was produced in Hek293 cells. This non-glycosylated IL-4 analogue showed a half-life of about 2.5 h and thus seems to be more proteolytically stable than *E. coli*-derived IL-4 F82D. This might be due to additional post translational modifications of Hek293 cell-derived IL-4 that do not occur in *E. coli*. For instance N-terminal acetylation, which is assumed to increase protein stability, is a common post translational modification in eukaryotes but is rare in prokaryotes (reviewed in: (Drazic et al. 2016)). In addition, IL-4 variants were recombinantly expressed in Hek293 cells in form of hexahistidine fusion proteins. The hexahistidine tag might also lower the susceptibility of the Hek293 cell-derived protein for trypsin. Furthermore, mass spectrometry analysis of *E. coli*-derived IL-4 protein detected small amounts of mono-oxygenated variants, possibly derived from oxidation of the N-terminal methionine or cysteines. Oxidation of amino acid side chains is known to cause structural damage to proteins and loss of stability. Together, these factors may contribute to the slightly lower proteolytic resistance of *E. coli*-derived IL-4.

Table 2.5: Comparison of proteolytic stability of differentially glycosylated IL-4 variants derived from eukaryotic expression systems. Tryptic degradation of IL-4 variants over time was analysed using SDS-PAGE as detailed under method section (chapter 5.7.2). Half-life \pm standard deviation are given calculated from two independent experiments (n=2).

IL-4 variant	Amount of N-glycans	Half-life [h]
F82D (<i>E.coli</i>)	0	0.9 \pm 0.05
F82D N38Q (Hek293)	0	2.5 \pm 0,1
F82D (Hek293)	1	4.7 \pm 1.7
F82D Q20N (Hek293)	2	12.1 \pm 1.0
F82D Q20N-T28N-K61N (Hek293)	4	30.1 \pm 1.5
WT (<i>P. pastoris</i>)	1	2.4 \pm 0,1
WT (Hek293)	1	3.6 \pm 0,7

However, Hek293 cell-derived IL-4 variants harbouring two (Q20N and the natural site at Asn38) or four N-glycans (Q20N, T28N, K61N and the natural site Asn38) showed a

significantly prolonged half-life (twofold and sixfold respectively) compared to IL-4 F82D (either derived from *E. coli* or Hek293 cells), clearly indicating that (*in vitro*) proteolytic stability of IL-4 can be drastically increased by hyperglycosylation using Hek293 cells as expression systems.

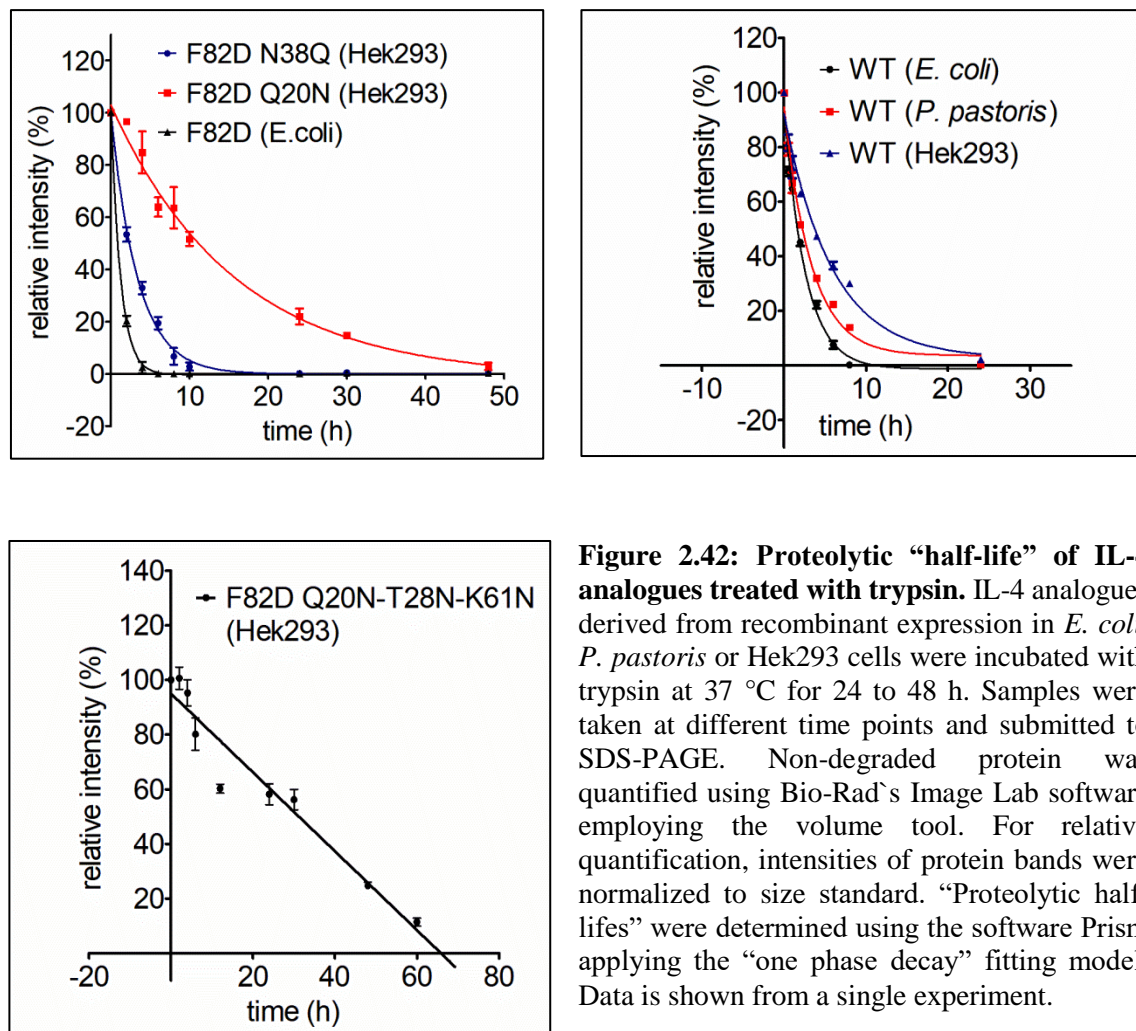


Figure 2.42: Proteolytic “half-life” of IL-4 analogues treated with trypsin. IL-4 analogues derived from recombinant expression in *E. coli*, *P. pastoris* or Hek293 cells were incubated with trypsin at 37 °C for 24 to 48 h. Samples were taken at different time points and submitted to SDS-PAGE. Non-degraded protein was quantified using Bio-Rad’s Image Lab software employing the volume tool. For relative quantification, intensities of protein bands were normalized to size standard. “Proteolytic half-lives” were determined using the software Prism applying the “one phase decay” fitting model. Data is shown from a single experiment.

It is important to note that the sheer size of the N-glycan moiety is not the determining factor of proteolytic stability. Glycoproteins derived from yeast carry large, oligomannose N-glycans, while those from mammalian cells contain N-glycans of hybrid or complex type, which can contain terminal, negatively charged sialic acid residues. In SDS-PAGE wildtype IL-4 derived from expression in baker’s yeast (*P. pastoris*) showed an apparent molecular weight of about 35 kDa, which upon deglycosylation with PNGase F could be reduced to about 15 kDa (figure 2.43). Thus, about 60% of the molecular weight of the yeast-derived IL-4 results from carbohydrates. In contrast wildtype IL-4 expressed in Hek293 cells with a size of about 18 kDa carries a much smaller N-glycan with a size of about 2-3 kDa, thus has a carbohydrate content of only 15%. Surprisingly, during incubation with trypsin, yeast-derived IL-4 protein exhibited a slightly lower proteolytic stability (half-life 2.4 h) than

2 Results

Hek293 cell-derived IL-4 protein (half-life 3.6 h) (figure 2.42). Hence the much larger glycan moiety did not confer increased stability.

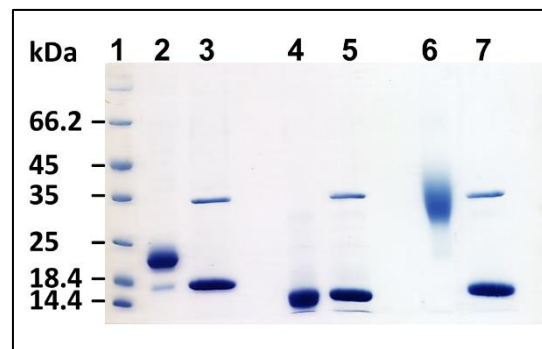


Figure 2.43: IL-4 glycoprotein derived from *E. coli*, yeast and Hek293 cells. To determine the glycan-content of each IL-4 variant, wildtype IL-4 protein derived from recombinant expression in *E. coli*, *P. pastoris* or Hek293 cells were deglycosylated using PNGase F. SDS-PAGE was performed under reducing conditions. 1: size standard; 2: wildtype IL-4 (Hek293); 3: wildtype IL-4 (Hek293) treated with PNGase F; 4: wildtype IL-4 (*E. coli*); 5: wildtype IL-4 (*E. coli*) treated with PNGase F; 6: wildtype IL-4 (*P. pastoris*); 7: wildtype IL-4 (*P. pastoris*) treated with PNGase F.

3. Discussion

3.1 Site-specific glycoengineering to establish blockage of receptor binding in IL-4

Pitrakinra exerts its antagonistic effect through two mutations, i.e. arginine 121 and tyrosine 124 both being replaced by aspartate, that induce an electrostatic mismatch in the binding epitopes for the receptors γc and IL-13R α 1. As a result, Pitrakinra still binds to IL-4R α with wildtype-like affinity but is incapable to activate either the type I or the type II receptor. Pitrakinra was tested for application in allergic asthma until clinical phase II where it failed to meet the endpoint criteria, although positive effects, e.g. fewer number of allergen induced exacerbations could be observed (Wenzel et al. 2007). A major pharmacological disadvantage of Pitrakinra strongly limiting its performance is Pitrakinra's rather short serum half-life of about 3 hours (Longphre and Fuller 2010), due to its small size and lack of glycosylation. In a pharmacokinetics/pharmacodynamics study, Pitrakinra was rapidly absorbed into the blood after application either through subcutaneous injection or inhalation, but serum levels also declined quickly within 12 hours (Burmeister Getz et al. 2009). The short serum half-life would have required frequent application of Pitrakinra, which again might cause negative side effects and trigger immunogenicity against the drug. To overcome rapid clearance of Pitrakinra by renal filtration, the site-specific coupling of a 40 kDa polyethylene glycol (PEG) moiety to IL-4 position 38 was tested. However, while Pitrakinra's serum half-life was strongly increased (half-life time estimated to 5 days), the modification negatively affected the binding affinity of PEGylated Pitrakinra to IL-4R α and hence significantly impaired its inhibitory efficacy (see patent: WO2011106779A1, (Tomkinson 2011)). Furthermore, the therapeutic application of PEG is limited by the susceptibility of PEG to oxidative degradation, the resulting products potentially causing unwanted negative side effects (Ulbricht et al. 2014; McGary 1960). In addition, PEG shows a poor metabolic degradability leading to accumulation in the liver and in some, albeit rare cases, anti-PEG antibodies have been detected (reviewed in: (Zhang et al. 2014)). Hence, while being frequently used in pharmaceuticals to extend serum half-life of biologics, PEGylation certainly is not an ideal modification.

Recently, the monoclonal antibody Dupilumab has been approved for treatment of atopic dermatitis and is currently being investigated for application in asthma therapy (Wenzel et al. 2016; Blauvelt et al. 2017). Since Dupilumab mechanistically resembles the antagonistic

action of Pitrakinra by neutralizing the IL-4R α receptor, this clearly suggests that simultaneous blockage of IL-4/IL-13 activity at the IL-4 receptor IL-4R α presents a successful strategy for the treatment of atopic diseases (reviewed in: (Vatrella et al. 2014)). This motivated us to design novel IL-4 based antagonists more effective than Pitrakinra. In this study, instead of introducing an electrostatic mismatch as in Pitrakinra, a steric hindrance-based approach was employed by introducing bulky molecules into IL-4 binding sites for receptors γ c and IL-13R α 1. In contrast to previous studies, which employed unnatural compounds for modification like PEG or N-ethylmaleimide (Duppatla et al. 2014), we introduced carbohydrate molecules into IL-4 binding epitopes for γ c and IL-13R α 1. Glycoengineering, i.e. manipulation of protein glycosylation, is an emerging strategy in pharma-research employed to optimize pharmacokinetic profiles of protein drugs. Since glycosylation of proteins is a naturally occurring post translational modification in eukaryotes, glycoengineering represents a natural alternative to e.g. PEGylation. Thus, protein glycosylation has been shown to improve most of the pharmacological parameters necessary for optimization of therapeutic efficacy, e.g. physicochemical and metabolic stability (Fernandes and Gregoriadis 1996; Runkel et al. 1998; Ueda et al. 2009), serum half-life (Fernandes and Gregoriadis 1997; Egrie et al. 2003), and immunogenicity (reviewed in: (Solá and Griebenow 2010)). The pharmacological benefit of glycoengineering is highlighted for instance by erythropoietin (EPO) that becomes inactive *in vivo* upon deglycosylation (Tsuda et al. 1990; Wasley et al. 1991). In contrast, a glycoengineered version of erythropoietin called Darbepoietin Alfa, which is used for treatment of anaemia, shows a threefold longer serum half-life due to two additional N-glycosylation sites and thus an increased efficacy (Egrie et al. 2003). A similar effect was reported for a hyperglycosylated interferon α (IFN- α) variant, which comprises four additional N-glycosylation sites and hence exhibits a 25-fold prolonged serum half-life (Ceaglio et al. 2010).

The site-directed conjugation of glycan molecules into IL-4 binding sites therefore offers a novel strategy of implementing IL-4 antagonism while simultaneously improving the pharmacological parameters of the antagonist. In this study, two different approaches were tested for site-specific introduction of glycan molecules: 1) introducing complex N-glycans using a eukaryotic expression system and 2) employing chemical conjugation for introduction of synthetic glycans.

3.1.1 Site-specific introduction of complex N-glycans in IL-4 using Hek293 cells

One of the fastest growing fields in the pharmaceutical industry is the market for therapeutic glycoproteins produced in eukaryotic cell lines. Species-specific variations in glycan architecture and composition render conventional expression systems like yeast, plants or insect cells less suitable for production of therapeutic proteins, since glycan patterns are significantly different from humans (reviewed in: (Lalonde and Durocher 2017; Ghaderi et al. 2012)). For instance, yeast and insect cells, predominantly synthesize polymannosylated N-glycans instead of sialylated mammalian type complex N-glycans (see figure 3.1 for different N-glycan patterns). Since mannose residues are recognized as foreign by e.g. macrophages (see review: (East and Isacke 2002)), hypermannosylated glycans can potentially elicit an immune responses.

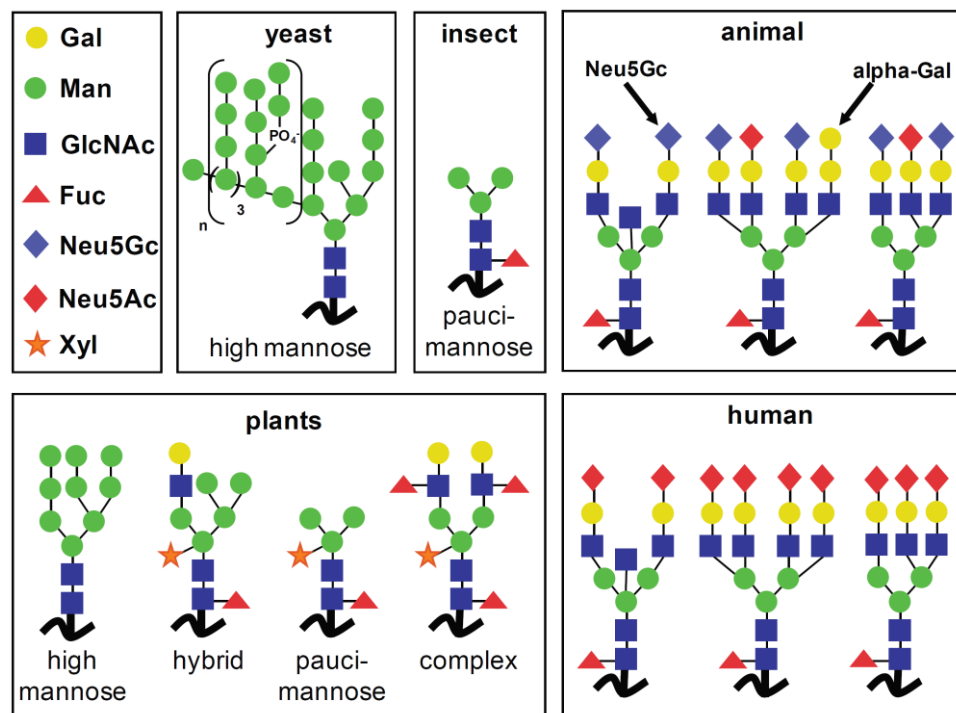


Figure 3.1: Species-specific variations of eukaryotic N-glycan patterns. Protein glycosylation takes place in the endoplasmic reticulum (ER) and the Golgi complex. The basic biosynthesis pathways are highly conserved in eukaryotes and result in the formation of the common Man₃GlcNAc₂ core structure. However, species-specific differences in further glycan processing lead to the high structural diversity of glycan patterns observed between different eukaryotic species. For example, yeast and insect cells mainly express high-mannose glycan structures lacking terminal sialic acid residues, whereas plants are capable of synthesizing complex type glycans that can contain non-human, highly immunogenic xylose moieties. By contrast, mammalian cell lines mainly express sialylated multiantennary complex type N-glycans. Non-human mammalian cell lines can express immunogenic terminal Gala₁₋₃Gal (alpha-Gal) and N-glycolylneuraminic acid (Neu5Gc), whereas the predominant distal carbohydrate residues found on human glycoproteins is N-acetylneuraminic acid (Neu5Ac) (Adopted with permission of Ghaderi et al. (2012) Production platforms for biotherapeutic glycoproteins. Occurrence, impact, and challenges of non-human sialylation. *Biotechnol Genet Eng Rev.* 28:147-75.)

Currently, only recombinant expression in mammalian cell lines provides glycoproteins with human-like glycan pattern. However, while the core architecture of all types of mammalian glycans is highly conserved, the terminal carbohydrate moieties can vary between different mammalian species. Non-human mammalian cell lines, e.g. chinese hamster ovary (CHO) cells, can produce two terminal carbohydrate residues absent in humans, namely alpha 1-3 galactose and N-glycolylneuraminic acid (Neu5Gc), which were shown to be immunogenic and elicit an antibody response in humans (Galili et al. 1984; Galili et al. 1988; Higashi et al. 1977; Muchmore et al. 1998; Padler-Karavani et al. 2008; Kannicht et al. 2013) (reviewed in: (Ghaderi et al. 2012)). Thus, even though the CHO cell line is the prevalent expression host used for recombinant production of therapeutic glycoproteins (see review: (Walsh 2014)), it certainly is not an ideal production platform.

For recombinant expression of biosynthetically glycosylated IL-4, we chose the human embryonic kidney (Hek) 293 cell line, since Hek293 cells provide a human-like N-glycan pattern free of immunogenic carbohydrate moieties (Kannicht et al. 2013)(see review: (Lalonde and Durocher 2017)).

Eukaryotic N-linked glycosylation generally occurs at the Asn-X-Ser/Thr motif, with X being any amino acid except proline (see review: (Aebi 2013)). For site-specific introduction of additional N-glycans, novel Asn-X-Ser/Thr motifs were recombinantly introduced at selected positions in IL-4 binding epitopes for γ c and IL-13R α 1. These IL-4 variants were transiently expressed in Hek293 cells. Unfortunately, subsequent SDS-PAGE analyses revealed that not every engineered N-glycosylation site was glycosylated. Thus, the engineered N-glycosylation motif Asn121-Glu122-Ser123, was not glycosylated. If an N-glycosylation site is recognized/used by the glycosyltransferases in the ER depends on several factors. Thus, the amino acid at the X-position can have profound effect on the glycosylation efficiency. When X is proline, glycosylation does not occur at all (Bause 1983), but also Trp, Asp, or Glu can strongly reduce the glycosylation efficiency (Shakin-Eshleman et al. 1996). Therefore, substitution of Glu122 in the engineered Asn121-Glu122-Ser123 motif against e.g. methionine might have a positive effect on glycosylation of Asn121 and therefore should be tested in follow-up studies. Furthermore, N-glycosylation motifs within secondary structure elements are also only rarely glycosylated, since they are less accessible (Mononen and Karjalainen 1984; Lam et al. 2013). Thus, the engineered N-glycosylation site Asn121-Glu122-Ser123 might not have been recognized by the glycosyltransferases in the ER, as amino acids 121 to 123 are part of the forth helix in IL-4.

A third factor that was shown to notably affect protein N-glycosylation are the culture conditions employed for glycoprotein expression. For instance, small differences in pH and temperature can significantly influence N-glycosylation site-occupancy (Gawlitzeck et al. 2009). Additionally, N-glycan patterns were also shown to be affected by cell culture conditions (Cabrera et al. 2005), e.g. lower oxygen concentrations were correlated with a decrease in galactosylation (Kunkel et al. 2000).

In conclusion, using expression in Hek293 cells as a strategy to site-specifically introduce N-glycans in IL-4 is limited/less feasible, since it is not applicable to all positions in IL-4 and because glycosylation efficiency is difficult to control. Thus, although engineered N-glycosylation sites Asn117-Ala118-Thr119 or Asn28-Val29-Thr30 were glycosylated by Hek293 cells, glycosylation occurred only partially, i.e. the protein was obtained as a mixture of glycosylated and non-glycosylated species. This is detrimental, since non-modified IL-4 exhibits agonistic activity. Subsequent concanavalin A lectin affinity chromatography allowed the isolation of only glycosylated IL-4 protein. However, this purification step was accompanied by a considerable loss of also glycosylated IL-4 protein, since concanavalin A does only bind distinct glycan structures (reviewed in: (Varki et al. 2009)). Most importantly, it was not possible to introduce a eukaryotic N-glycan at position 121, which, however, was required to generate an IL-4 antagonist inhibiting both type I and type II receptor signalling. Hence, design of a glycoengineered Pitracinra analogue was only possible by chemical coupling of glycan molecules.

3.1.2 Cysteine labelling for site-directed chemical introduction of glycans in IL-4

A wide range of chemical coupling strategies exist for modifying proteins rather randomly, e.g. labelling of primary amines or carboxyl groups. However, when regioselectivity is required, the task becomes more complicated, as there are relatively few methods that allow for site-directed conjugation of chemical moieties to a protein. The range of possible coupling strategies is further limited when the protein is expected to be biologically active, since then labelling reactions have to be performed under rather physiological conditions to maintain the protein architecture and function. Therefore, a number of requirements had to be met to successfully glycosylate IL-4. In particular for the intended application of chemical glycosylation to introduce steric hindrance in IL-4 for disrupting binding to γc and IL-13R α 1, a method was required that ensures full modification, since partially modified IL-4 variants would exhibit residual agonistic activity (Duppatla et al. 2014). Moreover, when employing complex and thus costly glycans for conjugation, a high conversion rate is

economically favoured to minimize the amounts of glycan educt required for the reaction. Additionally, glycoconjugates should be stable *in vivo*, as well as possess minimal immunogenicity.

We only found two methods to meet these requirements. The term “click chemistry”, first defined by Kolb and colleagues, refers to a group of reactions that are fast and irreversible with high product yields and which are biocompatible (reviewed in: (Kolb et al. 2001)). The classic click reaction is the copper-catalyzed azide-alkyne cycloaddition (CuAAC), which since its discovery in 2002, has been widely applied for modification of proteins (Rostovtsev et al. 2002; Tornøe et al. 2002). For site-specific bioconjugation at the single amino acid level, azide- or alkyne-carrying unnatural amino acids (UAA) have to be introduced into the protein, which then are subsequently modified with alkynyl- or azide-containing reagents. This approach is attractive, because azide- and alkyne- groups are highly specific towards each other and the resulting triazole conjugates are chemically highly stable. However, CuAAC has several drawbacks limiting its application: Firstly, for the reaction to be fast and efficient it requires a metal catalyst, i.e. copper since otherwise high temperatures (~ 100 °C) would be necessary for coupling to occur (Michael 1893; Rostovtsev et al. 2002). Unfortunately, the instability of Cu(I) facilitates a rapid oxidation to inactive Cu(II) under physiological conditions. For Cu(I) regeneration a reducing agent is required, typically sodium ascorbate (NaAsc). Copper-mediated formation of reactive oxygen species (ROS) is a major problem that limits the use of the CuAAC reaction for modification of biomolecules since ROS cause structural damage of proteins through oxidation of amino acid side chains or cleavage of peptide bonds (Li et al. 2016). To avoid copper-induced cytotoxic effects *in vivo*, a metal-free variant has been developed termed “strain-promoted azide-alkyne cycloaddition”, which however uses more bulky cyclooctyne reagents for modification of azide tags at a lower coupling rate compared to CuAAC (Agard et al. 2004). A further drawback of CuAAC, particularly for large-scale applications are the high costs associated with the reagents required for incorporation of azide or alkyne-carrying unnatural amino acids into the protein. This is even more relevant when confronted with a low protein yield resulting from inefficient metabolic incorporation of unnatural amino acids, which still remains a main difficulty of UAA application (reviewed in: (Wals and Ovaa 2014)).

With respect to the application relevant to this thesis, i.e. modification of IL-4 recombinantly expressed in *E. coli*, it should also be considered that azide groups can be reduced to amines, e.g. during bacterial expression (reducing cytoplasm) and by reducing agents (Baker et al.

1989; Cartwright et al. 1976; Staros et al. 1978; López et al. 2014), such as DTT which is also employed during the refolding procedure of IL-4 containing inclusion bodies.

As aforementioned, CuAAC reactions require a reducing agent, most commonly sodium ascorbate to generate the Cu(I) active catalyst *in situ*. For proteins containing structurally important cysteine-bridges, such as IL-4, this can be a problem, since ascorbate also cleaves protein disulphides in a side-reaction, potentially rendering the protein inactive (Turner et al. 2014; Giustarini et al. 2008). Moreover, although CuAAC already has been applied for conjugation of polysaccharides, e.g. for preparation of hydrogels (Elchinger et al. 2011), copper-mediated oxidative damaging of polysaccharides has been reported (Rahkila et al. 2018; Lallana et al. 2009; Uchida and Kawakishi 1986; Lallana et al. 2011). It has been proposed that hydroxyl radicals, formed under CuAAC conditions catalyse the cleavage of glycosidic bonds, resulting in the degradation of polysaccharides (reviewed in: (Lallana et al. 2011)). Altogether these drawbacks render the CuAAC strategy less suitable for conjugation of glycan molecules to IL-4.

Besides click chemistry, another well-established approach for site-directed protein modification is cysteine labelling. The thiol group in the side chain of cysteine is a natural chemical handle with considerable nucleophilicity that allows for targeted modification. Since IL-4 contains no unpaired cysteines, the introduction of an additional cysteine residue at a selected position in IL-4 is expected to provide great specificity and, therefore, represents a suitable strategy for site-specific modification of IL-4. A variety of thiol-reactive reagents are available for conjugation, such as maleimides, iodoacetamides, methanethiosulfonates or thiol-containing probes (reviewed in: (Spicer and Davis 2014)). Reaction occurs fast and thiol-reactive compounds usually do not show non-specific coupling to other polar groups present in proteins. Furthermore, owing to its small size, cysteine residues can also be introduced at structurally important sites with minimal risk to introduce significant perturbation of the protein architecture. Compared to CuAAC, which requires protein expression in the presence of unnatural amino acids and a corresponding tRNA/tRNA synthetase pair, this strategy does not need special reagents for recombinant protein expression.

Nevertheless, introducing an unpaired cysteine residue into a protein can also be problematic. For instance, the engineered cysteine can perturb correct disulphide formation of naturally occurring cysteines, thereby causing misfolding and loss of protein activity. Furthermore, due to its high reactivity thiol-groups are susceptible to unwanted side-

reactions and thus might require a protecting group, such as glutathione to prevent unwanted modification. This makes subsequent removal of the protecting group necessary to allow for site-specific labelling. However, cysteine labelling has been successfully employed for site-specific modification of IL-4 in the past (Giustarini et al. 2008; Duppatla et al. 2012; Duppatla et al. 2014). Duppatla and colleagues have developed a protocol, which allows the recombinant production of biologically active IL-4 cysteine variants containing a free thiol-group (Duppatla et al. 2012; Duppatla et al. 2014). Therefore, we decided to employ IL-4 cysteine variants for the site-directed chemical introduction of glycan molecules.

3.1.3 Chemical glycosylation of IL-4 cysteine variants – Refolding strategy has the potential for large-scale application

In this work, three strategies have been developed for site-specific chemical coupling of glycan molecules to a recombinantly introduced free thiol-group in IL-4. The first strategy employed the conjugation of an amine-functionalized carbohydrate via the heterobifunctional crosslinker SMCC, containing a thiol-reactive maleimide group and an amine-reactive NHS-ester. This approach appeared attractive for several reasons: 1) No catalyst is needed, since thiols and maleimide react rapidly under physiologic conditions and full conversion is readily achieved 2) formation of a stable and inert glycoconjugate 3) the possibility of conjugating amine containing glycans, which have been isolated from natural sources e.g. cleavage via the endoglycosidase PNGase-F. Using the monosaccharide glucosamine as a model glycan, we successfully established this strategy for preparation of a site-specifically modified IL-4 glycoconjugate. However, various problems hampered the practicability of this strategy. Firstly, a two-step reaction was necessary in order to prevent random labelling of IL-4's amino residues by non-specific reaction with the SMCC NHS-ester and to achieve specific modification of the engineered cysteine residue. Unfortunately, the first reaction, i.e. preparation of the glucosamine-SMCC intermediate, was found to be very inefficient by showing a low conversion efficiency of only about 5%, thus meaning a substantial loss of non-reacted glycan starting material. This inefficient coupling renders this strategy less feasible when more complex (and hence costly) glycans are chosen for glycoengineering. Another concern was the potential risk of increased immunogenicity induced by the rather large linker moiety.

A second, linker-free glycan-coupling procedure was established by using a selenenylsulphide-mediated glycoconjugation reaction (Glyco-SeS). In this synthesis scheme, the thiol-group in the protein is activated first through reaction with a

phenylselenylating agent, upon which coupling to a thiol-glycan can directly proceed, thereby yielding a mixed disulphide-linked glycoconjugate.

Although disulphide bonds are chemically less stable compared to the amide and thioether bonds present in the SMCC-mediated glycan-protein conjugate, disulphide linkages pose a lower risk of immunogenicity, as they occur naturally *in vivo*. In fact, Gamblin and colleagues even demonstrated the disulphide linkage to biologically resemble the N-glycosidic bond, since disulphide-linked glycoconjugates could be processed by glucosyltransferases and thus allowed enzymatic carbohydrate extension (Gamblin et al. 2004). Furthermore, the relatively short disulphide bond of only 2.1 Å enables minimal flexibility and rotational freedom between glycan and protein. Thus, the disulphide bond prevents the glycan moiety from moving out of the binding interface and evading steric hindrance, which is more likely for the longer SMCC-linker with a length of 8.3 Å. That the SMCC-linker actually exhibits higher flexibility was corroborated by the observation that IL-4 variant F82D R121C conjugated to glucosamine via the SMCC-linker showed a fivefold lower affinity for receptor IL-4R α in surface plasmon resonance (SPR) binding analysis and accordingly also a reduced (3fold) inhibitory efficacy in cell-based experiments compared to the disulphide-linked IL-4 F82D R121C glycoconjugates. This suggests that the SMCC-linker exhibits sufficient rotational flexibility to move into IL-4's binding interface for the IL-4R α receptor and sterically hinder IL-4/IL-4R α complex formation, thereby reducing the antagonistic efficacy.

A disadvantage of the Glyco-SeS reaction is that modification only occurs partially, leaving about 20% of IL-4 non-modified. Therefore, an additional purification step was required to separate the antagonistic glycoconjugate from non-modified protein, which exhibited residual agonistic activity. However, since non-modified protein, containing a free thiol-group, bound efficiently to iodoacetyl-activated agarose resin, complete removal of residual IL-4 activity was possible in a single purification step.

A major drawback of the SMCC-linker-based strategy, as well as the Glyco-SeS method is that both coupling schemes require an enzymatic deprotection of the engineered cysteine residue before chemical coupling can occur. Thus, IL-4 cysteine variants, produced by refolding after expression in *E. coli*, were recovered in form of mixed disulphides, i.e. the engineered cysteine residue was conjugated to a glutathione moiety. Previous attempts to remove the glutathione protecting group by chemical reduction also lead to non-specific cleavage of IL-4's native cystine bonds, resulting in complete protein denaturation and precipitation (Duppatla et al. 2012). In contrast, an enzymatic approach (developed by

Duppatla and colleagues, (Duppatla et al. 2012; Duppatla et al. 2014)) employing glutaredoxin-1, glutathione, glutathione reductase and NADPH (see chapter 2.4.2.1) allows specific removal of the glutathionyl residue, releasing the IL-4 cysteine variant with a free thiol-group. However, the underlying complex kinetics of the enzymatic deglutathionylation reaction requires careful optimization of the reaction conditions to avoid chemical reduction of native disulphides in IL-4 and hence renders scale-up of this procedure difficult. Furthermore, this enzymatic removal cannot be applied to all positions in IL-4, since in this study an IL-4 variant containing an engineered cysteine at position 117 was shown to be not susceptible to enzymatic deprotection, possibly due to electrostatic repulsion derived from the proximal charged amino acid side chains. Therefore, the SMCC-based approach, as well as Glyco-SeS strategy could not be applied for glycosylation of Cys117.

However, by integrating the chemical glycosylation step directly into the refolding procedure of IL-4 cysteine variants, we were able to develop a fast and highly efficient chemical glycosylation strategy that does neither require enzymatic deglutathionylation nor thiol-activation by the phenylselenylating reagent. Compared to the other strategies presented in this study, this scheme enabled efficient synthesis of chemically glycosylated IL-4 cysteine variants in much higher yield and also allowed complete, 100% modification of IL-4 protein, thus decreasing the number of purification steps. Furthermore, in contrast to the SMCC-based and Glyco-SeS strategy, the refolding approach was successfully applied to all engineered IL-4 cysteine residues (Cys38, Cys117, Cys121) analysed in this study. Most importantly, this strategy was not limited to single-site glycoconjugation only, but also allowed synthesis of IL-4 double cysteine mutants (F82D N38C R121C), containing two disulphide-linked glycan moieties. Together these advantages render this approach highly suitable for large-scale production.

3.2 Glycoengineering yields effective IL-4 antagonists

3.2.1 Glycoengineering of position 121 generates potent type I and type II receptor antagonists more effective than Pitrakinra

For the design of an IL-4 antagonist inhibiting both IL-4 and IL-13 downstream signalling, we attempted to modify a position in IL-4 required for assembly of both type I and type II receptor. In a previous study, Duppatla and colleagues chemically introduced bulky molecules at several positions in IL-4's binding epitope for γc and IL-13R $\alpha 1$ to induce steric hindrance (Duppatla et al. 2014). They found that in contrast to the previous double mutation

R121D Y124D, site-specific modification of a single IL-4 residue, i.e. Arg121 is already sufficient to fully disrupt binding to γc and IL-13R α 1 (Duppattla et al. 2014). Hence, introduction of a glycan molecule at position 121 was expected to generate an effective IL-4 antagonist abrogating type I and II receptor formation and inhibiting IL-4/IL-13 signalling.

An initial attempt to introduce a eukaryotic complex N-glycan at position 121 by using protein expression in Hek293 cells was not feasible (as already discussed in 3.1.1). Hence, to allow site-directed chemical conjugation of a carbohydrate moiety Arg121 was mutated to cysteine. In SPR-binding studies, IL-4 F82D R121C variants containing disulphide-conjugated glucose moieties showed a tenfold increase in affinity for IL-4R α , compared to Pitracinra. This can be attributed to the mutation F82D, which was additionally introduced to enhance the efficacy of the IL-4 antagonists, since substitution of Phe82 against aspartate has been previously shown to significantly enhance the binding affinity of IL-4 for receptor IL-4R α (Kraich et al. 2006). As already outlined in 3.1.3, the IL-4 variant F82D R121C conjugated to glucosamine via the SMCC-linker showed a fivefold lower affinity for receptor IL-4R α compared to the disulphide-linked glycoconjugates, which is possibly due to the SMCC-linker moving into IL-4's binding epitope for IL-4R α , sterically hindering the IL-4/ IL-4R α complex formation.

The antagonistic efficacy of the IL-4 F82D R121C analogues was tested in cell-based experiments. Regardless of their route of production, none of the chemically glycosylated IL-4 F82D R121C variants exhibited residual IL-4 activity via the IL-4 type I or type II receptor. Thereby, a relatively small monosaccharide moiety, i.e. glucose, was already sufficient to fully abrogate binding to the IL-4 receptors γc and IL-13R α 1, required for IL-4 receptor activation and downstream signalling. Since the disulphide-linked IL-4 glycoconjugates showed a five times higher inhibitory efficacy compared to Pitracinra, our glycoengineered IL-4 F82D R121C analogues present highly effective IL-4 type I and type II receptor antagonists, more potent than Pitracinra.

3.2.2 Design of IL-4 receptor type II specific antagonists

While IL-4R α and IL-13R α 1 receptors are expressed on most cell types, the γc receptor is primarily found on cells of hematopoietic origin, like T-cells (Graber et al. 1998; Wang et al. 2004; Waal Malefyt et al. 1995), which is why the type I receptor is considered to have a more immunoregulatory function. In contrast studies on knock-out mice deficient in IL-13R α 1 have indicated a critical role for the type II receptor in mediating inflammatory

effector processes, like increased mucus production, fibrosis or enhanced airway resistance (Munitz et al. 2008; Ramalingam et al. 2008). Thus, it might be useful to generate a selective IL-4 antagonist, which suppresses inflammatory processes by specifically blocking the type II receptor but which is still capable to activate the type I receptor, mediating γ c-dependent Th2-cell differentiation. Such a selective IL-4 antagonist might possess enhanced utility in the treatment of certain diseases. In particular, IL-4's central role in directing T-helper (Th) cell differentiation towards the Th2-phenotype, suggests that it may be of benefit in the treatment of autoimmune diseases characterized by an imbalance of Th-cells, such as multiple sclerosis and type I diabetes (reviewed in: (Röcken et al. 1996)). The potential of IL-4 in treating of multiple sclerosis has been shown in mice suffering from experimental autoimmune encephalomyelitis (EAE), which is an animal model for multiple sclerosis. Thus, EAE, which is mediated by autoreactive Th1-cells, was shown to be down-regulated after administration of IL-4 (Racke et al. 1994; Furlan et al. 2001). It was proposed, that IL-4 helped to control inflammation associated with EAE through redirecting the immune system towards a Th2-response, especially via alternative activation of M2 macrophages, that are important for tissue repair (Casella et al. 2016; Ponomarev et al. 2007). Alternative activation of macrophages by IL-4 was also shown to be primarily mediated by type I receptor signalling and hence could be addressed by a type II receptor specific IL-4 antagonist (Jiménez-García et al. 2015; Sheikh et al. 2015).

3.2.2.1 Antagonistic effect of glycoengineered IL-4 F82D K117C depends on the architecture of the conjugated glycan

IL-4's binding epitope for IL-13R α 1 and γ c largely overlaps with Arg121 and Tyr124 being the main binding determinants. However, mutational studies revealed differences in the contribution of surrounding residues to the binding affinity (reviewed in: (Mueller et al. 2002)). Hence, the introduction of glycans at more peripheral positions in the binding interface II can potentially generate an IL-4 antagonistic variant specifically blocking the IL-4R α /IL-13R α 1 receptor. One such residue located in the periphery of the binding site II is lysine 117 in IL-4 helix D. Cell-based experiments measuring IL-4 dependent growth suppression of renal Caki-1 cells, which only express the IL-4 type II receptor, indicated Lys117 to be involved in binding of IL-4 to IL-13R α 1 (Schnarr et al. 1997). Thus, whereas amino acid replacement by glutamine did not show any effect, substitution by negatively charged aspartic acid yielded a detectable loss of biologic activity. In contrast, replacement of Lys117 by alanine and glutamine did not affect γ c-dependent induction of T-cell

proliferation (Kruse et al. 1993; Letzelter et al. 1998). In line with these results, calculations of the buried surface area (BSA) performed by Duppatla and colleagues showed different accessibilities of IL-4 residues during complex formation with γc and IL-13R α 1. The BSA analysis revealed Lys117 to be buried to a large extent (%BSA = 72%) upon complex formation with IL-13R α 1, but with the γc receptor, Lys117 only shared little contact (%BSA = 3%) (Duppatla et al. 2014). Hence, position 117 was regarded as a good candidate for the introduction of a glycan moiety and design of a selective IL-4 type II receptor antagonist.

To allow site-directed chemical introduction of a glycan moiety at IL-4 position 117, an IL-4 variant with Lys117 substituted for cysteine was recombinantly expressed in *E. coli*. Mass spectrometry analysis confirmed that refolding in the presence of thiol-glycans allowed the preparation of IL-4 F82D K117C as a disulphide-linked glycoconjugate. Unfortunately, modification was incomplete, as non-conjugated protein containing a free thiol-group was observed. Since the amount of non-glycosylated protein was insignificant ($\leq 5\%$) in the glucose modified K117C variant but accounted for 50% of the K117C analogue conjugated to the bigger glucose tetraacetate moiety, the coupling of thio-glycans to Cys117 seems to be affected by structural constraints. Since non-modified IL-4 exhibits agonistic activity, an additional purification step employing iodoacetyl activated agarose resin was necessary, which allowed the isolation of only glycosylated protein. However, further optimization of the refolding conditions for this variant, e.g. using higher concentration of thiol-glycans, might allow to increase the yield of fully glycosylated protein, making this extra purification step dispensable.

Biosynthetic introduction of a complex N-glycan at position 117 was feasible, as an IL-4 variant containing an engineered N-glycosylation site at position 117, i.e. Asn117N-Ala118-Thr119, was shown to be glycosylated in Hek293 cells. However, glycosylation only occurred partially, since 50% of IL-4 F82D K117N was not modified. In order to remove non-glycosylated protein, concanavalin A affinity chromatography was employed, which allowed the isolation of only the glycosylated species.

Due to mutation F82D, glycoconjugated IL-4 F82D K117C variants exhibited a significantly (about threefold) higher binding affinity for the IL-4R α receptor in SPR binding analysis compared to Pitrakinra. The Hek293 cell-derived IL-4 variant, containing a complex N-glycan at position 117, showed a slightly lower binding affinity for IL-4R α with a K_D value comparable to Pitrakinra. This lower affinity can be ascribed to the increased size of IL-4

F82D K117N due to the additional 2 kDa complex N-glycan (effect of complex N-glycans on receptor binding will be discussed later in more detail, see 3.3).

The antagonistic efficacy of the glycoengineered IL-4 F82D K117C/N analogues was tested in cell-based experiments. Chemically glycosylated IL-4 F82D K117C showed reduced type II receptor activity, whereby conjugation of glucose tetraacetate to position 117 had a stronger effect than the smaller glucose moiety. In contrast, modification with the branched tripeptide glutathione strongly disrupted interaction with IL-13R α 1, causing a nearly complete loss of biologic activity in type II receptor-dependent HEK-Blue cells, which lack the common γ chain receptor. However, this variant still showed considerable activity in TF-1 cells, which carry both IL-4 receptors, demonstrating that introduction of a glutathione moiety at position 117 did not, or only slightly affect γ c-dependent signalling. This variant also acted as a potent inhibitor of wildtype IL-4 in HEK-Blue cells. Thus, as we had anticipated, chemical modification at position 117 yielded a partial agonist, selectively inhibiting type II receptor activity. However, the antagonistic effect of this variant on type II receptor activation is dependent on the molecular architecture of the conjugated moiety, as with increasing size of the conjugated compound (glucose < glucose-tetraacetate < glutathione) a gradual decrease of type II receptor activity could be observed. This became even more apparent, as the Hek293 cell-derived variant K117N did not only show strongly reduced activity in HEK-Blue cells but also partially reduced activity in the TF-1 cell line, indicating that introduction of a complex 2 kDa N-glycan at position 117 does not only disrupt interaction of IL-4 with IL-13R α 1 but also with the γ c receptor.

Based on these data we postulate that conjugation of a glycan residue with similar architecture/diameter as glutathione, such as the trisaccharide maltotriose, might possibly yield the same antagonistic effect as observed for the glutathionylated IL-4 variant F82D K117C.

3.2.2.2 Introduction of a complex N-glycan at position 28 attenuates binding to IL-13R α 1

In addition to position 117, we identified another site in IL-4, which allows the generation of a selective IL-4 type II receptor antagonist. Screening of Hek293 cell-derived IL-4 variants containing additional N-glycan sites revealed that introduction of an N-glycan at position 28 resulted in impaired binding of IL-4 to IL-13R α 1, while retaining high-affinity interaction with IL-4R α . Threonine 28 is located in the centre of the IL-4 binding site III,

comprising the residues Thr28, Asn105, Gln106, Ser107, and Thr108, that form a contact interface with the D1-domain of IL-13R α 1 (figure 3.2).

Similar to other type I cytokine receptors, like gp130 (Xu et al. 2010; Boulanger et al. 2003), granulocyte-macrophage colony-stimulating factor (GM-CSF) (Lopez et al. 2010; Hansen et al. 2008) (reviewed in: (Lopez et al. 2010) and IL-5R α (Patino et al. 2011), the IL-13R α 1 receptor contains, in addition to the canonical cytokine binding homology region (CHR) formed by the D2D3 module, a third N-terminal FNIII domain, termed D1 (LaPorte et al. 2008). The three FNIII domains adopt a wrench-like architecture, where the D1 domain forms an antiparallel beta-sheet with the CD loop of IL-4 and IL-13. Our findings, that introduction of an N-glycan at IL-4 position 28 impairs binding of IL-4 with IL-13R α 1 is particularly surprising, since so far the D1 domain was considered to be only critical for interaction of IL-13R α 1 with IL-13, but not IL-4 (Arima et al. 2005; LaPorte et al. 2008; Ito et al. 2009). Thus, Arima and colleagues demonstrated in a reporter gene assay, that deletion of the D1 domain completely abolished binding of IL-13 to IL-13R α 1, while it still allowed type II receptor activation by IL-4 (Arima et al. 2005). Accordingly, a truncated IL-13R α 1 ectodomain, only consisting of the D2D3 module did not show detectable binding to IL-13 in gel filtration analysis, whereas it still formed a ternary complex with IL-4/IL-4R α (LaPorte et al. 2008).

In contrast to these previous findings, our results now suggest, that the IL-13R α 1 D1 domain is directly involved in binding of IL-4. However, since previous studies showed that IL-4 can still bind to IL-13R α 1-D1 deletion mutants, our observations suggest a lock-and-key based mechanism for ligand-receptor interaction rather than the D1 domain contributing to the overall binding affinity of IL-4 for IL-13R α 1. Thus, similar to what has been proposed for the IL-5/IL-5R α assembly (Patino et al. 2011), the wrench-like architecture of IL-13R α 1 is possibly preformed.

For design of a specific IL-13R α 1 antagonist, introducing a glycan at site 28 in addition to position 117 might result in a synergistic effect, yielding a superior, more effective type II receptor antagonist. However, further experiments are required, to characterize the type of glycans, regarding size and architecture, required to achieve optimal inhibitory efficacy.

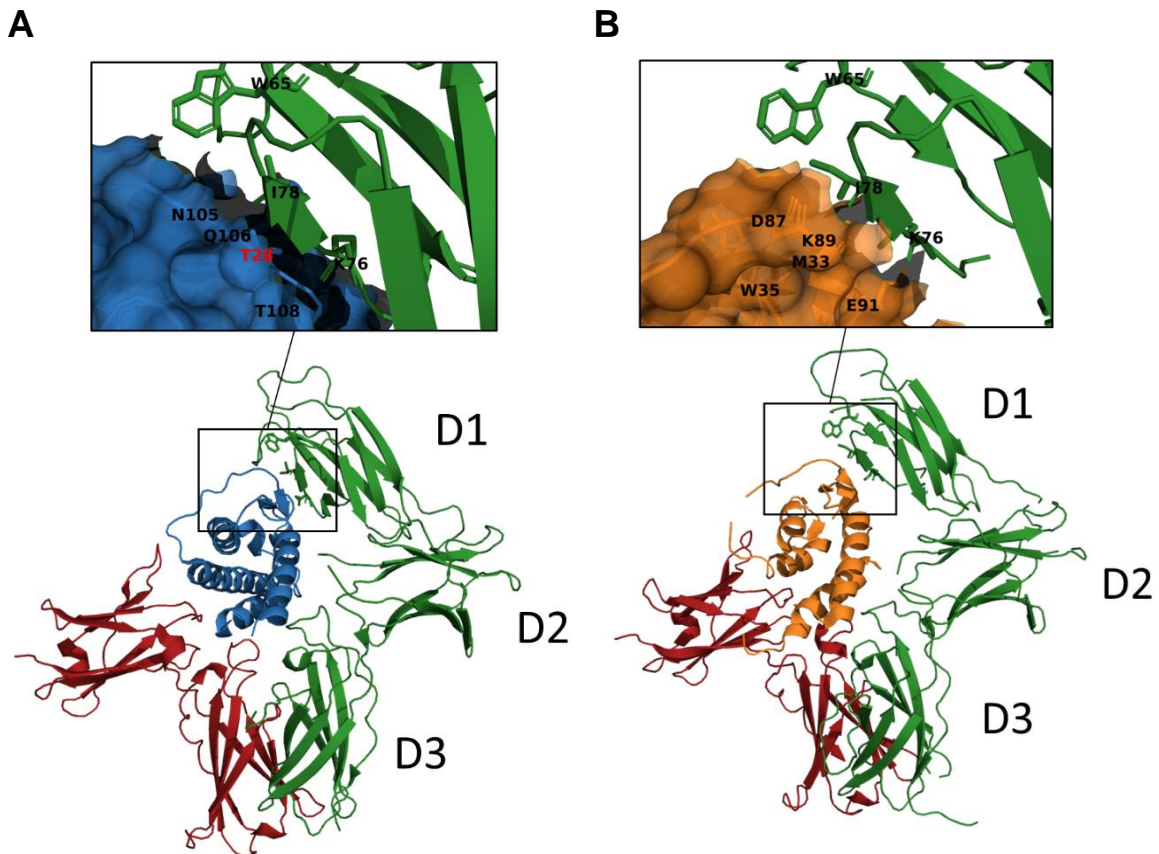


Figure 3.2: Wrench-like architecture of IL-13R α 1 in the type II receptor complex. The three FNIII domains of IL-13R α 1 (D1, D2, and D3) bind to IL-4 (A) and IL-13 (B) with a wrench-like architecture (red: IL-4R α , blue: IL-4, orange: IL-13, green: IL-13R α 1). IL-4 residue T28 is highlighted in red.

3.3 Combination of biosynthetic and chemical glycoengineering generates a highly effective IL-4/IL-13 antagonist with increased stability

As already discussed, only chemical glycosylation allowed the introduction of a glycan moiety at position 121, yielding an antagonistic IL-4 variant inhibiting both type I and type II receptor activation. Unfortunately, rather simple carbohydrate structures are currently synthetically available for chemical glycosylation, as the synthesis of complex, human-like N-glycans is technically not feasible yet (at least not in quantitative yields) (see review: (Krasnova and Wong 2016)). However, to retain the desired effect of enhanced pharmacological parameters, larger and more complex N-glycans are required for chemical glycosylation to achieve e.g. an increase in protein size and solubility. Therefore, a novel approach combining chemical and biosynthetic glycoengineering was used in this study to design an antagonistic IL-4 F82D R121C variant containing additional complex N-glycans.

This strategy employs production in a eukaryotic expression system to provide complex N-glycosylation, thereby improving the pharmacokinetic parameters of IL-4, and subsequent site-directed chemical glycosylation to introduce the “antagonistic” carbohydrate residue, mediating the steric hindrance effect.

Three new N-glycosylation sites, i.e. N-X-S/T motifs, were introduced at IL-4 positions 20, 28 and 61. Since introduction of an N-glycan at position 28 was shown to disrupt binding of IL-4 to IL-13R α 1, an additional N-glycan at position 28 together with the chemically introduced carbohydrate at Cys121 will act synergistically to increase blockage of type II receptor and thus enhance the overall inhibitory efficacy of the IL-4 antagonist.

With those additional sites, IL-4 variant F82D Q20N T28N K61N R121C could be produced in Hek293 cells yielding IL-4 protein containing four complex N-glycans (one native at N38 and three engineered) and a cysteine residue at position 121. Subsequent refolding in the presence of thiol-glucose resulted in an hyperglycosylated IL-4 antagonist, carrying a disulphide bonded glucose residue at position 121, with about twofold molecular size compared to the *E. coli*-derived Pitrakinra. *In vitro* SPR binding experiments revealed, that affinity for receptor IL-4R α was significantly reduced (10fold) compared to only chemically glycosylated *E. coli*-derived antagonistic IL-4 F82D R121C variants lacking N-linked glycans. However, the affinity and inhibitory efficacy in cell-based assays were not different from Pitrakinra.

Reduced receptor interaction and lower biologic activity *in vitro* have also been observed for other glycoengineered proteins, like erythropoietin (reviewed in: (Powell and Gurk-Turner 2002)) or FSH (follicle stimulating hormone) (Perlman et al. 2003). Lower receptor interaction is likely caused by an increase in hydrodynamic radius derived from the additional N-glycans. Negatively charged sialic acid residues can additionally reduce receptor binding through electrostatic repulsion (Egrie and Browne 2001). However, in the case of erythropoietin and FSH the loss of activity *in vitro* did not translate to a lower *in vivo* potency, since higher carbohydrate content was shown to significantly increase therapeutic efficacy due to a longer serum half-life (reviewed in: (Powell and Gurk-Turner 2002)) (Perlman et al. 2003). Therefore, it can be assumed that the glycoengineered IL-4 antagonists designed in this study also exhibit improved *in vivo* potency compared to the non-glycosylated *E. coli*-derived Pitrakinra.

This hypothesis is corroborated by our findings, that hyperglycosylated Hek293 cell-derived IL-4 has a significantly higher proteolytic stability than IL-4 produced in *E. coli*. Since increased N-linked glycosylation was shown to lead to enhanced proteolytic stabilization of

proteins (Loh and Gainer 1980; Aquino et al. 1980; Raju and Scallan 2007), we determined the proteolytic resistance of several IL-4 variants differing in glycosylation pattern. *In vitro* proteolysis stability tests employing trypsin as a model protease revealed that hyperglycosylated Hek293 cell-derived IL-4 variant containing four complex N-glycans exhibits a more than 30-fold higher resistance towards proteolytic degradation than *E. coli*-derived non-glycosylated IL-4 protein. It is important to note that sheer size of the N-glycan moiety thereby is not the determining factor of proteolytic stability, since wildtype IL-4 produced in yeast was less stable than Hek293 cell-derived wildtype IL-4, even though the yeast protein contained an N-glycan of about eight to ten times the size of the complex N-glycan attached by Hek293 cells. The higher proteolytic stability of Hek293 cell-derived IL-4 is possibly due to negatively charged terminal sialic acid residues, which are absent in yeast glycans but have been found to decorate Hek293 cell-derived glycoproteins (Wang et al. 2017; Croset et al. 2012). It has been proposed, that sialylation mediates higher proteolytic stability through a shielding effect, which interferes with the access of proteases to their protein target sites (see review: (Gregoriadis et al. 2000)).

Although physiologically IL-4 is not a substrate of trypsin, as trypsin is primarily found in the digestive system, the same apparent structural parameters that influence resistance to trypsin could similarly modulate the resistance to proteases relevant for degradation of IL-4 *in vivo*, such as matrix metalloproteinases (MMPs). Additionally, it must be considered that we employed trypsin in concentrations much higher than those under physiological conditions. Therefore, it is likely that the proteolytic stability of hyperglycosylated IL-4 *in vivo* might be significantly higher than observed in our experiments.

In summary, these data suggest that such glycoengineered IL-4 antagonists produced by combination of chemical and biosynthetic glycoengineering will possibly exhibit improved pharmacokinetic parameters *in vivo* compared to Pitrakinra and might present valuable alternatives to classical IL-4 inhibitors, such as the neutralizing anti-IL-4R α antibody Dupilumab.

3.4 Future perspective – Design of IL-4 antagonists with tailored glycosylation pattern

Cellular expression of glycoproteins represents a significant obstacle for the biopharmaceutical industry since the produced glycoproteins consist of a heterogenous mixture of different glycoforms, differing in glycan architecture and composition, as well as

site occupancy, which are hardly separable (see review: (Zacchi and Schulz 2016)). This is problematic, as small differences in N-glycan pattern and composition can have serious consequences for the therapeutic efficacy of glycoproteins. Thus, certain carbohydrate moieties can facilitate rapid lectin-mediated clearance or increase immunogenicity, thereby reducing the drug's serum half-life and efficacy. Two well-known lectin receptors are strongly involved in selective glycoprotein endocytosis: The asialoglycoprotein receptor (ASGPR) is a C-type lectin, which is only expressed by hepatocytes in the liver. Its major function is the internalization and subsequent degradation of glycoproteins containing terminal galactose or *N*-acetyl galactosamine residues (Stockert et al. 1982) (reviewed in: (Spiess 1990)). Another C-type lectin receptor important for glycoprotein turnover is the mannose receptor (CD206), primarily found on immune cells like macrophages and dendritic cells. This receptor specifically binds and internalizes glycoproteins with accessible mannose, *N*-acetylglucosamine and fucose residues (Largent et al. 1984; Stahl et al. 1980) (reviewed in: (East and Isacke 2002)). In addition to its importance for glycoprotein clearance, the mannose receptor, together with other so-called pattern recognition receptors, is also involved in innate sensing of pathogens (Ezekowitz et al. 1991; Paveley et al. 2011) (reviewed in: (East and Isacke 2002)). The innate immune system has evolved to identify microbial pathogens based on specific, accessible carbohydrates structures, such as the bacterial cell wall constituent peptidoglycan or mannans and chitin derived from fungi and parasitic worms (Nadesalingam et al. 2005) (Reese et al. 2007) (reviewed in: (Bueter et al. 2013)). One of these mechanisms is the lectin pathway that comprises several lectin receptors, which upon ligand binding activate the complement system and facilitate pathogen clearance (reviewed in: (Fujita 2002)). For instance, the mannose-binding lectin (MBL) binds glycans with mannose, fucose and *N*-acetyl glucosamine, similar to the mannose receptor, but does not recognize sialic acid, which typically represents the terminal carbohydrate residue in mammalian N-glycans (Haurum et al. 1993). Sialic acids are negatively charged and highly hydrophilic acidic α -keto sugars that affect both mass and charge of proteins. The first evidence of sialylation to be important for serum half-life was made through the observation that the loss of sialic acid residues resulted in rapid lectin-mediated clearance of glycoproteins from the blood (Rosa et al. 1984; Morell et al. 1971). Further studies demonstrated that sialic acids additionally confer increased resistance against proteases (Aquino et al. 1980; Fernandes and Gregoriadis 1997). Therefore, sialylation appears to be a key parameter in modulating the *in vivo* serum half-life and therapeutic efficacy of glycoproteins.

Depending on the glycan pattern, protein glycosylation can also be used for controlled delivery of therapeutics to their respective target sites. For instance, terminal mannose/galactose modifications have been successfully employed for lectin-mediated delivery of therapeutics to their site of action, such as mannose-terminated β -glucocerebrosidase (Cerezyme, Genzyme) for macrophage-targeted enzyme replacement therapy for Gaucher disease (Doebber et al. 1982)(reviewed in: (Deegan and Cox 2012)), or galactose-decorated chemotherapeutic agents for treatment of hepatocellular tumours (Zhang et al. 2012; Xu et al. 2009). Furthermore, glycoengineering of the Fc region of antibodies has shown to improve their therapeutic efficacy (reviewed in: (Reusch and Tejada 2015)). This was highlighted for instance by the therapeutic antibody Obinutuzumab/Gazyva (Roche), which was produced in an engineered CHO cell line that expresses proteins with reduced fucosylation (Mossner et al. 2010). Afucosylation of the antibody's Fc region significantly enhanced the antibody's ability to activate natural killer cells and to mediate cellular cytotoxicity (Golay et al. 2013; Bologna et al. 2011).

Hence, due to the critical influence of glycan architecture on pharmacokinetic parameters of proteins, the controlled biosynthesis of only distinct glycan patterns in order to achieve optimized therapeutic efficacy have garnered significant interest. Substantial efforts are being made to manipulate the cellular glycosylation machinery of eukaryotic expression hosts, e.g. through genetic engineering (Yang et al. 2015; Piirainen et al. 2016)(reviewed in: (Khan et al. 2017)). However, so far heterogeneity could only be reduced, but eukaryotic expression of proteins with completely homogenous and human-like glycan-patterns has not been accomplished yet. Thus, on a long-term perspective, the ultimate goal might be to produce glycoengineered IL-4 antagonists by employing a purely chemical approach, making expression in eukaryotic expression hosts needless and allowing the production of an IL-4 glycoconjugate with a chemically highly defined but complex human-like glycosylation pattern. In a proof-of-principle experiment, we successfully demonstrated, that multi-site glycoconjugation of IL-4 via thiol chemistry is indeed possible for simple carbohydrate molecules and only requires more complex glycan compounds for production. Although chemical synthesis of complex glycans in quantitative yields is not feasible yet, recent advances in carbohydrate chemistry suggest that automated synthesis of humanized complex glycans will be possible in the future (reviewed in: (Hsu et al. 2011)). Alternatively, chemo-enzymatic strategies, employing controlled enzymatic elongation of attached glycan moieties could be employed, which was shown to be applicable also to disulphide-linked glycoconjugates (Gamblin et al. 2004).

4. Materials

4.1 Software

Software	Company/Platform
ApE	by M. Wayne Davis
Expasy ProtParam	expasy.org
Expasy SIM – Alignment	expasy.org
Expasy-Translate	expasy.org
ImageLab	<i>Bio-Rad</i> Laboratories
Lightcycler®	Roche
<i>msConvertGUI</i>	proteowizard.sourceforge.net
mMass version 5.5.0	mmass.org
MassLynx Software	Waters
Prism	GraphPad
PyMOL	Schrödinger, LLC

4.2 Laboratory Equipment

Device	Company
ÄKTAprime (low pressure chrom. System)	GE Healthcare
APEX II	Bruker Daltonics
BioLogic DuoFlow™ (HPLC system)	Bio-Rad
C200 (mammalian cells incubator)	Labotec
ChemiDoc™ MP Imaging System	Bio-Rad
Dark Reader® Transilluminator (DNA gel)	Clare Chemical
Labcycler (PCR)	Sensoquest
Lightcycler™ 96 (qPCR)	Roche
Mini-PROTEAN® Tetra Cell system	Bio-Rad
<i>Micromass</i> Quattro Premier™	Waters
Multitron Standard (bacteria incubator)	IN-FORS HT
Multisan Ascent Plate reader	ThermoFisher Scientific
Nanodrop 2000c Spectrophotometer	ThermoFisher Scientific
ProteOn™ XPR 36	Bio-Rad
Q Exactive™	ThermoFisher Scientific

Sonoplus ultrasonic homogenizer Bandelin

4.3 Consumables

<u>Product</u>	<u>Company</u>
Cell culture flasks	Greiner bio-one
Cell culture Erlenmeyer Flasks	Corning
dialysis tubes, cutoff 3.5 kDa, visking	Carl-Roth
Protran® Nitrocellulose Membrane, 0.45 µm	Whatman
ProteOn™ GLC Biosensor	BioRad
96 well cell culture plate flat bottom	Greiner bio-one
Vivaspin Ultrafiltration tubes	Sartorius Stedim Biotech

4.4 Chromatography Columns

<u>Product</u>	<u>Company</u>
C4 column (Jupiter C4, 5 µm, 250 × 4.6 mm, 300 Å)	Phenomenex
C4 column (Jupiter C4, 10 µm, 250 × 10 mm, 300 Å)	Phenomenex
C18 column (µRPC C2/C18 ST 4.6/100)	GE Healthcare
Disposable PD 10 Desalting Column	GE Healthcare
HiTrap Con A 4B	GE Healthcare
HiTrap™ excel column	GE Healthcare
HiTrap™ CM Fast Flow	GE Healthcare

4.5 Reagents

If not stated otherwise, reagents were purchased in highest quality from Sigma-Aldrich, Carl-Roth, AppliChem and ThermoFisher Scientific.

<u>Product</u>	<u>Company</u>
ABsolute QPCR SYBR Green Mix	ThermoFisher Scientific
CoA biotin	NEB
NADH tetrasodium salt	Carl-Roth
GelGreen™ Nucleic Acid Gel Stain	Biotium
Glutathione (ox./red.)	Carl-Roth
Glucosamine hydrochloride	Calbiochem
Kifunensine	Cayman Chemical

LB-medium	Melford
MassRuler DNA Ladder Mix	ThermoFisher Scientific
Methyl-PEG24-Maleimide	ThermoFisher Scientific
PageRuler Plus Prestained protein marker	ThermoFisher Scientific
Phenylselenenylbromide	Sigma-Aldrich
Polyethylenimin (linear, 25.000 kDa)	Polysciences Inc.
Protease inhibitor cocktail set III	Calbiochem
Resazurin sodium salt	AlfaAesar
SulfoLink™ Coupling Resin	ThermoFisher Scientific
SMCC	Apollo Scientific
1-Thio-β-D-glucose sodium salt	Alfa-Aesar
1-Thio-β-D-glucose tetraacetate	Alfa-Aesar
Unstained protein marker	ThermoFisher Scientific
WesternBright™ Chemilumineszenz Substrat	Biozym

4.6 Kits

<u>Kit</u>	<u>Company</u>
GeneJET Plasmid Miniprep Kit	Fermentas
Hi Yield® Small DNA Fragments Extraction Kit	Südlabor
Plasmid Plus Midi Kit	Qiagen
Perfect Pure RNA Cultured Cell Kit	5Prime
Penta·His HRP Conjugate kit	5prime
Plasmid Plus Midi Kit	Qiagen
Phosphatase Substrate Kit	ThermoFisher Scientific
RevertAid First Strand cDNA Synthesis Kit	ThermoFisher Scientific

4.7 Enzymes

<u>Enzyme</u>	<u>Company</u>
FastAP	Fermentas
FastDigest™ Restriction enzymes	ThermoFisher Scientific
Glutathione reductase (baker`s yeast)	Sigma-Aldrich
Phusion™ High-Fidelity DNA-Polymerase	ThermoFisher Scientific
PNGaseF	Promega

4 Materials

Sequencing grade trypsin	Promega
SFP-Synthase	NEB
T4 DNA Ligase	Fermentas
Endo-H	NEB

4.8 Cell lines

4.8.1 Bacterial strains

Name	Company/genotype
NovaBlue™	Novagen/ <i>endA1 hsdR17</i> ($r_{K12}^- m_{K12}^+$) <i>supE44 thi-1 recA1 gyrA96 relA1 lac F'[proA⁺B⁺ lacI^qZΔM15::Tn10]</i> (Tet ^R)
BLR(DE3)	Novagen/ <i>F⁻ ompT hsdS_B</i> ($r_B^- m_B^-$) <i>gal dcm</i> (DE3) Δ(<i>srl-recA</i>)306::Tn10 (Tet ^R)
BL21 Star(DE3)	Novagen/ <i>F⁻ompT hsdSB</i> ($r_B^- m_B^-$) <i>gal dcm rne131</i> (DE3)

4.8.2 Mammalian cell lines

Name	Company/Description
FreeStyle™ 293-F	ThermoFisher Scientific/human embryonic kidney (Hek) 293 cell line; adapted to growth in high-density, serum free suspension; used in this work for transient overexpression of IL- 4 protein;
Expi293F™	ThermoFisher Scientific/human embryonic kidney (Hek) 293 cell line; adapted to growth in high-density, serum free suspension; used in this work for transient overexpression of IL- 4 protein; has a higher production yield than Freestyle cells
HEK-Blue™ IL-4/IL-13	Invivogen/human embryonic kidney (Hek) 293 cell line; adherent growth; stably transfected with plasmids encoding hSTAT6 gene and STAT6-inducible SEAP reporter gene; used in this work to evaluate bioactivity of IL-4 variants;
TF-1	human myeloid leukemic cell line; suspension culture; growth dependent on various cytokines (GM-CSF, IL-3, IL-4); used in this work to evaluate bioactivity of IL-4 variants;

4.9 Vectors

Name	Company/Description
pHLsec (throm)	mammalian expression vector; Amp ^R , Chicken β -Actin-promotor, optimized secretion signal sequence, C-terminal His6-tag; (optional with a thrombin cleavage site) (Aricescu et al. 2006)
pQKA	Qiagen/ E.coli-expression vector; pQE80L derivative; Kan ^R instead of Amp ^R , T5 /lac promoter
pET28b	Novagen/ <i>E.coli</i> -expression vector; T7/lac-promotor, Kan ^R , N- and C-terminal His6 -tag

4.10 Mutagenesis oligonucleotides

The oligonucleotides used in this thesis were purchased from Sigma-Aldrich and are depicted in a 5' to 3' orientation. Mutational sites are underlined.

Name	Sequence
R121D Y124D_s	GACGATCATGG <u>AC</u> GAGAAAGATTC
R121D Y124D_as	GAAT <u>C</u> TTTCTC <u>GTCC</u> CATGATCGTC
F82D_s	CAGCTGATCCGAG <u>AC</u> CCTGAAACGG
F82D_as	CGTTTCAGG <u>TCT</u> CGGATCAGCTG

Introduction of cysteines

N38C_s	CTGCCTCCAAGT <u>GC</u> CAACTGAGAAG
N38C_as	CTTCTCAGTTGT <u>GCA</u> CTTGGAGGCAG
K117C_s	GGAAAGGCTAT <u>GC</u> ACGATCATGAGAG
K117C_as	CTCTCATGATCGT <u>GCA</u> TAGCCTTTCC
R121C_s	GGCTAAAGACGATCATGT <u>TGT</u> GAGAAATATTCAAAGTG
R121C_as	CACTTTGAATATTTCTC <u>ACAC</u> CATGATCGTCTTTAGCC
Q20C_s	GCCTCACAGAGT <u>GCA</u> AAGACTCTGTGCACCG
Q20C_as	CGGTGCACAGAGTCTT <u>GCA</u> CTCTGTGAGGC
T28C_s	GCACCGAGTTGT <u>TGCG</u> TAAACAGAC
T28C_as	GTCTGTTAC <u>GCA</u> CAACTCGGTGC
K61C_s	CCACCATGAGT <u>TGCG</u> ACTCGCTGC
K61C_as	GCAGCGAGTGTC <u>GCA</u> CTCATGGTGG

Manipulation of Glycosylation sites

Q20N_s GCCTCACAGAGAACAAAGACTCTGTGCACCG
 Q20N_as CGGTGCACAGAGTCTTGTTCTCTGTGAGGC
 E26N_s CTCTGTGCACCAACTTGACCGTAAC
 E26N_as GTTACGGTCAAGTTGGTGCACAGAG
 T28N_s GCACCGAGTTGAACGTAACAGAC
 T28N_as GTCTGTTACGTTCAACTCGGTGC
 A34N_s CAGACATCTTTAAATGCCTCCAAGAAC
 A34N_as GTTCTTGGAGGCATTTAAAGATGTCTG
 K61N_s CCACCATGAGAAACGACACTCGCTGC
 K61N_as GCAGCGAGTGTCGTTCTCATGGTGG
 L96N_s CCTGGCGGGCAACAAATTCCTGTCC
 L96N_as GGACAGGAATTGTTGCCCCGCCAGG
 K117N_T118A_
 I119T_s GGAAAGGCTAAACGCGACCCATGAGAGAGAAATATTC
 K117N_T118A_
 I119T_as GAATATTTCTCTCTCATGGTCGCGTTTAGCCTTTCC
 R121N_K123S_s CTAAAGACGATCATGAACGGAGAGCTATTCAAAGTGTTCC
 R121N_K123S_as GAACACTTTGAATAGCTTCTCGTTCATGATCGTCTTAG
 R121N_E122A_
 K123_s CTAAAGACGATCATGAACGCCAGCTATTCAAAGTGTTCC
 R121N_E122A_
 K123_as GAACACTTTGAATAGCTGGCGTTTCATGATCGTCTTTAG
 N38Q_s CTGCCTCCAAGCAGACAACTGAGAAG
 N38Q_as CTTCTCAGTTGTCTGCTTGGAGGCAG

5. Methods

5.1 Molecular methods

5.1.1 Polymerase chain reaction

For site-directed insertion of mutations into the IL-4 coding sequence, a two-step polymerase chain reaction (PCR) (table 5.1) was employed. For this purpose, complementary oligonucleotides were designed, that carry the desired nucleotide exchange flanked by 9-15 bps complementary to the coding sequence. In the first step, two PCR products are synthesized that overlap at the site of the mutation. In two separate reactions, either the 3`end or 5`end mutagenic oligonucleotide is combined with a 5` or 3`end flanking oligonucleotide that is located outside the IL-4 gene and contains restriction sites for subsequent cloning. Next, in a single reaction both overlapping PCR products serve as a template, which is amplified using only the flanking oligonucleotides. The resulting product carries the IL-4 sequence with the desired mutation and restriction sites at the 3` and 5`end.

Table 5.1 Pipetting protocol for PCR reaction. In the first step, two overlapping PCR products A and B are synthesized. For the final reaction, PCR products A and B are diluted 1:100 and 1 μ L of each is applied to serve as a template. This time only flanking oligonucleotides are used for synthesis of the final product.

component	First step	Second step
DNA template	10 ng plasmid DNA	1 μ L of product A and B (1:100)
dNTP (2.5 mM)	10 μ L	10 μ L
Oligo forward (10 μ M)	2 μ L	2 μ L
Oligo reverse (10 μ M)	2 μ L	2 μ L
5x Phusion HF buffer	1x	1x
Phusion polymerase (2 U/ μ L)	1 μ L	1 μ L
water	ad 50 μ L	ad 50 μ L

PCR amplification is performed on a Labcycler using the thermocycling conditions stated in table 5.2.

Table 5.2: Thermocycler conditions. For amplification, the DNA is denatured at 95 °C, followed by annealing of oligonucleotides. Hybridization temperatures vary from 55 to 60 °C depending on the oligonucleotide sequence. Then, a DNA extension step is performed at 72 °C. These steps are repeated for 35 cycles.

step	temperature	time
1. initial denaturation	95 °C	3 min
2. denaturation	95 °C	30 sec
3. annealing	55 – 60 °C	30 sec
4. extension	72 °C	45 sec
Step 2-4: 35 cycles		
Final extension	72 °C	5 min

5.1.2 Restriction-digest and ligation

For directional cloning of the synthesized PCR product into the desired vector, both vector and PCR-product were treated with the same pair of FastDigest™ restriction enzymes to yield complementary sticky ends (table 5.3). The reaction is performed at 37 °C for 20 min. Subsequently, the linearized vector is incubated with alkaline phosphatase (FastAP), which catalyses the release of 5'- and 3'-phosphate groups from the vector DNA and thus prevents vector re-ligation. After 20 min, the FastAP enzyme is inactivated by incubation at 95 °C for 5 min. Finally, the samples were submitted to agarose gel electrophoresis (2.1.3) and the DNA-fragments corresponding to the linearized vector and PCR-product were purified using the “Hi Yield® PCR Clean-up/Gel Extraction Kit”.

Table 5.3: Restriction digest. The final PCR product and the desired expression vector are digested with the same endonucleases.

component	PCR product	vector
DNA	40 µL PCR product	4 µg
endonuclease A (10 U/µL)	3 µL	4 µL
endonuclease B (10 U/µL)	3 µL	4 µL
Fast digest buffer (10x)	1x	1x
alkaline phosphatase FastAP (1 U/µL)	-	1 µL
Water	ad 70 µL	ad 80 µL

Subsequently, ligation is performed (table 5.4) using a molar ratio of insert to vector of 3:1. The concentration of purified vector and PCR-product is quantified photometrically at 260 nm. The amount of PCR-product (insert) required for 100 ng of vector DNA is calculated using the following equation:

$$ng (insert) = \frac{kb (insert)}{kb (vector)} \cdot ng (vector) \cdot 3$$

Table 5.4: Ligation of vector and insert.

component	Final concentration
vector	100 ng
insert	variable
10xbuffer	1x
Ligase (5 U/ μ L)	1 μ L
water	ad 20 μ L

Afterwards, 10 μ L of ligation reaction were transformed into chemical competent NovaBlue™ *E. coli* cells (5.1.4.2).

5.1.3 DNA agarose gel electrophoresis

TAE-buffer: 40 mM TRIS, 20 mM sodium acetate, 1 mM EDTA, pH 8.5

6x DNA-loading dye: 0.25% (w/v) bromphenol blue, 0.025% (w/v) Xylene-CyanolFF, 30% (v/v) glycerine

For analysis of PCR products and restriction digests 1% (w/v) TAE gels were used. By adding the fluorescent dye GelGreen™ (0.05 μ L/mL gel) to the gel, the DNA can be photometrically detected at 500 nm using a dark reader. If required, DNA probes were mixed with 6x loading dye. For size reference a mass ruler DNA ladder mix was used. Gel electrophoresis was carried out in TAE-buffer using a voltage of 100 V for 40 min.

5.1.4 Preparation of plasmid DNA

5.1.4.1 Generation of chemically competent *E. coli* cells

TfbI-buffer: 30 mM potassium acetate, 100 mM RbCl, 10 mM CaCl₂, 50 mM MnCl₂, 15% (v/v) glycerine; adjust to pH 5.8 with 0.1 M acetic acid

TfbII-buffer: 10 mM MOPS, 75 mM CaCl₂, 10 mM RbCl, 15% (v/v) glycerine; adjust to pH 6.5 with 0.1 M sodium hydroxide

For generation of chemically competent *E. coli* cells, 50 mL of LB media is inoculated with 1 mL of overnight culture at 37 °C and shaking (130 rpm, Multitron Standard, IN-FORS HT). For selection, the appropriate antibiotic is added to the culture. When an optical density (OD₆₀₀) of about 0.4 is reached, cells are cooled on ice for 15 min and subsequently

centrifuged (4500xg, 4 °C, 5 min). The cell-pellet is resuspended in 20 mL of TbfI buffer and the suspension is incubated for 5 min on ice. After another centrifugation step, the cell-pellet is resuspended in 4 mL of TfbII buffer and incubated for 15 min on ice. Finally, aliquots are frozen in liquid nitrogen and stored at -80 °C.

5.1.4.2 DNA transformation into chemically competent *E. coli* cells

Chemically competent bacteria are thawed on ice. To about 100 µL of bacteria, about 10 ng of plasmid DNA are added and the suspension is incubated for 10 min on ice. DNA is introduced into bacterial cells by a heat-shock for 90 sec at 42 °C. Cells are cooled down on ice for 3 min. Then cells are resuspended in 300 µL SOC-medium and incubated at 37 °C for 30 min (130 rpm, Multitron Standard, IN-FORS HT). To obtain single colonies, bacteria are grown overnight on LB-agar plates with the appropriate selection antibiotic at 37 °C.

5.1.4.3 Plasmid DNA preparation

For small-scale preparation of up to 20 µg of plasmid DNA, “GeneJET Plasmid Miniprep Kit” was used. DNA was isolated from 3-5 mL of overnight culture according to the manufacturer’s instructions. For a higher DNA yield, 50-100 mL of overnight culture were prepared. For preparation of endotoxin free plasmid DNA, which is required for transfection of eukaryotic cell lines, the “Plasmid Plus Midi Kit” was applied. The DNA concentration was quantified photometrically at 260 nm using a NanoDrop 2000c UV-Vis spectrophotometer.

5.1.4.4 Sequencing

To validate the correct insertion of the desired DNA fragment into a vector, the purified plasmid DNA was send to the LGC company for sequencing. For sequence-analysis ApE software and Protparam online tools were employed.

5.1.5 Gene expression analysis using qPCR

5.1.5.1 RNA isolation and first strand cDNA synthesis

Quantitative real-time polymerase chain reaction (qPCR) is a technique based on conventional PCR reaction that allows gene expression analysis. In this method, isolated total messenger RNA is first transcribed into complementary DNA (cDNA) employing the reverse transcriptase.

In this study total mRNA was isolated from cultured cells using the “Perfect Pure RNA Cultured Cell Kit” according to the manufacturer’s instructions. Briefly, about 20 million cultured cells are centrifuged and the cell-pellet is treated with lysis buffer. Cell lysates are applied to the purification column and centrifuged. To remove genomic DNA, DNase is applied to the column for 15 min, followed by extensive washing and finally RNA elution. Prior to cDNA synthesis, RNA quality is examined by native agarose gel electrophoresis (2.1.3). The appearance of sharp 18S and 28S ribosomal RNA-bands is considered as evidence for intact RNA.

For conversion of mRNA into complementary DNA, a reverse transcription is performed using the “RevertAid First Strand cDNA Synthesis Kit” according to the manufacturer’s instructions. The PCR product can be directly used in qPCR reactions.

5.1.5.2 Quantitative Real-Time PCR

Quantitative Real-Time (q)PCR allows quantification of transcript levels in a sample using fluorescent probes. SYBR-Green is a fluorescent dye which incorporates into newly synthesized DNA molecules and thereby allows to monitor DNA amplification in each qPCR cycle photometrically.

PCR-reactions were performed on a LightcyclerTM 96. Readily available specific qPCR oligonucleotides for γ c, IL-13R α 1 and IL-4R α and the house-keeping genes Actin and GAPDH were purchased from Sigma-Aldrich (Supplement Table S9.5). For absolute quantification of individual transcript levels, DNA standards were prepared using the generated cDNA as a template (table 5.5). The PCR product was purified using the “Hi Yield® Small DNA Fragments Extraction Kit” and subsequently the DNA concentration was determined photometrically at 260 nm. For analysis, serial dilutions of the standard DNA samples were made in DEPC water containing 0.01 ng/ μ L tRNA to prevent binding of the DNA to the tube wall. Finally, for each transcript to be analysed, a qPCR reaction was prepared with first strand cDNA as a template (table 5.5). Additionally, qPCR reactions were prepared with standard DNA (10 fg/ μ L, 1 fg/ μ L, 0.1 fg/ μ L and 0.01 fg/ μ L) as a template and a negative control containing water instead of a template DNA.

Table 5.5: Pipetting protocol for qPCR.

component	Standard generation	qPCR reaction
ABsolute QPCR SYBR Green Mix (2x)	40 μ L	10 μ L
cDNA	8 μ L (diluted 1:50)	2 μ L (diluted 1:500)
qPCR primer mix (0.75 μ M/primer)	32 μ L	8 μ L

Standard probes and qPCR reactions were performed using the cycling conditions stated in table 5.6.

Table 5.6: Thermocycler conditions for qPCR.

step	temperature	time
1. Initial denaturation	95 °C	15 min
2. denaturation	95 °C	15 sec
3. annealing	58 °C	30 sec
4. extension	72 °C	30 sec
Step 2-4: 45 cycles		
5. Fluorescence quantification	79 °C	20 sec

The obtained data was analysed with the software LightcyclerTM 1.01. Thereby the amount of SYBR green incorporated by one fg of a particular transcript is determined using the generated standard curves. Absolute transcript levels are then calculated using the following equation:

$$\text{absolute transcript level} = \frac{910 \text{ molecules/fg}}{\text{transcript length (kbp)}} * \text{SYBR Green (fg)}$$

The equation is based on the consideration, that a DNA base pair (bp) has an average molecular weight of 650 daltons (1Da = 1,66054e-24 g), hence a DNA molecule with a length of 1000 bp has a weight of 0,0011 fg. Thus, one fg of 1000 bp-DNA molecules contains about 910 copies. The absolute copy number was normalized to 10.000 molecules of house-keeping genes GAPDH and actin.

5.2 Protein analysis methods

5.2.1 Polyacrylamide gel analysis

5.2.1.1 SDS-PAGE

Rotiphorese Gel 40 (29:1):	40% (v/v) acrylamide/bisacrylamide (29:1)
4x Upper TRIS-buffer:	0.5 M TRIS-HCl pH 6.8, 0.4% (w/v) SDS
4x Lower TRIS-buffer:	1.5 M TRIS-HCl pH 8.8, 0.4% (w/v) SDS
SDS-running buffer:	25 mM TRIS, 0.19 M glycine, 0.15% (w/v) SDS
6x protein-loading dye:	375 mM TRIS-HCl pH 6.8, 9% (w/v) SDS, 60% (v/v) glycerine (87%), 0.015% (w/v) bromophenol blue; for reducing conditions add 12% (v/v) β -mercaptoethanol

SDS (sodium dodecyl sulfate)-polyacrylamide gel electrophoresis (SDS-PAGE) allows the separation of proteins according to their molecular weight. First, solubilized protein samples were mixed with a 6 x loading dye containing SDS, followed by heating for 5 min at 95 °C. “Reducing” loading dye additionally contains β -mercaptoethanol, which reduces disulphide bonds and thereby facilitates protein denaturation.

SDS-PAGE was carried out using the Mini-PROTEAN® Tetra Cell system. An electric field is applied at 280-300 V for approximately 40 min. In this work 12% and 15% (v/v) SDS-gels were used (table 5.7).

Table 5.7: Preparation of SDS stacking and resolving gels.

components	Stacking-gel [mL]	Resolving-gel (12%) [mL]	Resolving-gel (15%) [mL]
Rotiphorese 29:1	0.5	3.0	3.75
4x upper buffer	1.25	-	
4x lower buffer	-	2.5	2.5
87% glycerine	-	2.0	2.0
water	3.2	2.5	1.75
TEMED	0.018	0.020	0.020
40% APS	0.018	0.020	0.020

5.2.1.2 Coomassie staining

Coomassie-solution: 10% (v/v) acidic acid, 40% (v/v) ethanol, 50% (v/v) water, 0.12% (w/v) Brilliant Blue R250, 0.12% (w/v) Brilliant Blue G250

Destaining buffer: 30% (v/v) ethanol, 6% (v/v) acidic acid, 64% (v/v) water

Fixing solution: 30% (v/v) methanol, 6% glycerine (v/v)

Under acidic conditions, coomassie dye binds primarily to basic amino acids, e.g. arginine, lysine and histidine of a protein and therefore visualizes proteins in a SDS-gel. The SDS-gel is incubated in Coomassie solution for a minimum of 30 min. Then the gel is soaked in a destaining buffer until unbound dye is completely removed. Finally, the gel is incubated in fixing solution and dried between cellophane films.

5.2.1.3 Silver staining

In case, that staining with Coomassie does not reveal protein-bands or samples containing less than 1 μg of protein are loaded, a silver staining is performed (table 5.8).

Table 5.8: Protocol for silver staining. All wash steps are carried out in water.

step	solution	incubation
1	30 mL 50% (v/v) acetone, 0.75 mL 50% (w/v) TCA, 12.5 μL 37%(w/v) formaldehyde	5 min, washing
2	30 mL water	5 min, washing
3	30 mL 50% (v/v) acetone	5 min
4	30 mL water, 50 μL 10% (w/v) $\text{Na}_2\text{S}_2\text{O}_3$	1 min, washing
5	30 mL water, 0.4 mL 20% (w/v) AgNO_3 , 0.3 mL 37% (w/v) formaldehyde	8 min, washing
6	30 mL water, 0.6 g (w/v) Na_2CO_3 , 12.5 μL 37% (w/v) formaldehyde, 25 μL 10% (w/v) $\text{Na}_2\text{S}_2\text{O}_3$	Incubation until protein-bands are visible
7	1% (v/v) acetic acid	15 min

For fixation, the gel gets soaked in 30% methanol with 6% glycerine and put between cellophane films for drying.

5.2.1.4 Periodic Acid Schiff (PAS) staining of glycosylated proteins

Solution A:	1.0% (v/v) periodic acid in 3% acetic acid
Solution B:	0.1% (w/v) sodium (metabi)sulfite in 10 mM HCl
Solution C:	50% (v/v) ethanol.
Solution D:	0.5% (w/v) sodium metabisulfite in 10 mM HCl
Fixing solution:	30% (v/v) methanol, 6% glycerine (v/v)

Periodic acid converts vicinal hydroxyl groups of sugars to aldehydes. Subsequent treatment with Schiff's reagent (a mixture of pararosaniline and sodium bisulfite) results in reaction of the glycan-aldehydes with the amino-groups of the Schiff reagent, which yields a magenta coloration.

The SDS-gel is first incubated in solution C for 30 min. Then the gel is washed in water for at least 10 min to remove the ethanol. The gel is treated with solution A for 30 min, followed by extensive washing in water. Subsequently, the gel is treated twice with solution B for 10 min, before the gel is soaked in Schiff's reagent for 1 h in the dark. Again, the gel is incubated in solution B for 1 h in the dark, followed by several treatments with solution D for a minimum of 2 h to ensure sufficient coloration. The gel is soaked in fixing solution and dried between cellophane films

5.2.2 Western Blot

5.2.2.1 Electrophoretic blotting on membrane

Blotting-buffer:	24 mM TRIS, 200 mM glycine, 20% (v/v) methanol
TBS-buffer:	10 mM TRIS-HCl pH 7.5, 150 mM NaCl
TBST/T-Puffer:	20 mM TRIS-HCl pH 7.5, 500 mM NaCl, 0.05% (v/v) Tween20, 0.2% (v/v) Triton X-100
Blocking-buffer (5prime):	0.5% (w/v) blocking reagent are solubilized in heated 1x blocking reagent buffer (10x); after the solution has reached room temperature, 0.1% (v/v) Tween20 is added
Antibody-solution:	Penta-His HRP Conjugate (5prime) 1:2000 dilution in blocking-buffer
ECL solution:	1:1 mix of Detection reagent 1 and 2 (Pierce™ ECL Western Blotting Substrate; ThermoFisher Scientific)

For detection of proteins via western blot, proteins are electrophoretically transferred to a nitrocellulose membrane (Protran 0.45 µm) after SDS-PAGE. The nitrocellulose membrane

is directly applied to the gel and is then placed between blotting papers and sponges. This “sandwich” is then mounted into the blotting system, whereby the membrane faces the anode to facilitate the transfer of the negatively charged proteins from the gel to the membrane. The chamber is filled with blotting buffer and an electric field is applied at a voltage of 80 V for 1 h.

5.2.2.2 Detection of proteins containing a polyhistidine tag

For detection of proteins that carry a polyhistidine-tag immunoblotting was performed employing the “Penta·His HRP Conjugate kit” according to the manufacturer`s instructions. Briefly, the membrane is shortly incubated in TBS-buffer followed by treatment with blocking buffer for 1 h to minimize non-specific binding. After washing in TBST/T and finally in TBS the membrane is incubated with the antibody solution for 1 h. Since the anti-his antibody is conjugated to a horseradish peroxidase (HRP), there is no need for treatment with a secondary antibody. Then the membrane is again washed in TBST/T and in TBS. Finally, a 1:1 mixture of WesternBright™ ECL (enzyme-linked chemiluminescence) reagents A and B was applied to the gel for a few minutes before chemiluminescence was analysed using the ChemicDoc System.

5.2.3 Deglycosylation of proteins using endoglycosidase

Reaction buffer (PNGase F): 50 mM TRIS-HCl pH 7.6, 1 mM CaCl₂

Reaction buffer (EndoHf): 50 mM sodium acetate pH 6.0

Endoglycosidases allow the enzymatic release of oligosaccharides from glycoproteins and thereby facilitate the analysis of glycoproteins in SDS-PAGE or mass spectrometry analysis due to the resulting decrease in protein heterogeneity.

For treatment with PNGase F, IL-4 protein was prepared in the appropriate reaction buffer and adjusted to a concentration of 60 μM (about 1 μg/μL). To 12 μL of protein 1 μL of 5% SDS and 1 μL of 1 M DTT is added. To denature the protein, the sample is heated at 95 °C for 5 min. When the solution is cooled down to 21 °C, 2 μL of 10% NP-40 is added. To start the reaction, 20 U of PNGaseF is added and the solution is incubated at 37 °C for 2 h.

For treatment with EndoHf IL-4 protein is prepared in the appropriate reaction buffer and adjusted to a concentration of 5 μM (about 0.1 μg/μL). To 12 μL of protein about 150 U of Endo Hf is added and the solution is incubated at 37 °C for 2 h.

5.2.4 Spectrophotometric determination of protein concentration

To quantify the concentration of a solubilized protein, the UV absorbance in the range of 250 – 320 nm is measured. The concentration is calculated based on the Beer-Lambert law:

$$c = \frac{A_{280} - A_{320}}{\varepsilon_{280} \cdot b}$$

c: concentration in [mol/L]

A₂₈₀: absorbance at 280 nm

A₃₂₀: absorbance at 320 nm

ε: theoretical molar extinction coefficient of the protein at 280 nm in [L·mol⁻¹·cm⁻¹]

b: pathlength in [cm]

A theoretical extinction coefficient of a protein at 280 nm can be calculated from its amino acid sequence, as absorbance at 280 nm is mainly due to the aromatic tryptophan, tyrosine and phenylalanine residues. Background absorbance is measured at 320 nm to determine the contribution of light scattering.

5.2.5 Mass spectrometry

5.2.5.1 ESI-MS analysis of proteins

Electrospray ionisation mass spectrometry (ESI-MS) analysis to determine the molecular weight of proteins was done by Dr. Werner Schmitz (Lehrstuhl für Biochemie und Molekularbiologie, Uni Würzburg). Mass spectra were acquired either with an APEX II Fourier transform ion cyclotron resonance mass spectrometer (Bruker Daltonics) or with a Q Exactive™ Hybrid Quadrupole-Orbitrap™ mass spectrometer (Thermo Scientific). Freeze-dried protein samples were dissolved in methanol/water/acetic acid (49.5/49.5/1) and adjusted to a concentration of about 2 μM. Samples were directly injected into the system and ions were detected in positive mode. Deconvolution of the mass spectra acquired with the APEX II was performed using the Bruker Xmas software. The mass spectra obtained with the Q Exactive in form of Xcalibur .Raw files first were converted into the .mzml format using the software msConvertGUI. For generation of the deconvoluted MS-spectra the .mzml files were then analysed using the software mMass.

5.2.5.2 ESI-MS analysis of SMCC and SMCC-GlcN conjugate

ESI-MS analysis of low-molecular weight compounds, i.e. SMCC and SMCC-glucosamine conjugate, was done by Dr. Markus Krischke (Lehrstuhl für Pharmazeutische Biologie),

employing ultra performance liquid chromatography-tandem mass spectrometry (UPLC-MS-MS). For chromatographic separation, a C18 column (Acquity UPLC BEH, 1.7 μm , 2.1 \times 50 mm with a 5 \times 2.1 mm guard column; Waters; Milford, MA, USA) was employed. Solvent A was 0.1% formic acid, solvent B was acetonitrile. Elution was performed using a linear gradient from 3% to 100 % acetonitrile at a flow rate of 0.25 mL/min in 7 min at a column temperature of 40°C. For ion detection, a full scan experiment was performed from m/z 50 to 1500 m/z in the negative electrospray mode on a Waters Micromass Quattro Premier™ triple quadrupole mass spectrometer. The obtained data was processed using MassLynx Software.

5.3 Recombinant protein expression in *E. coli*

For protein expression in *E. coli*, 10 ng plasmid DNA is transformed into chemical competent *E. coli* cells (5.1.4.2), which are then grown on LB-agar plates with the appropriate antibiotic. A single colony is picked and used for the preparation of a suspension culture, which is cultivated overnight. For expression, 800 mL LB-medium in a 2 L chicane flask are inoculated with 16 mL of “overnight” culture at 37 °C and shaking (130 rpm, Multitron Standard, IN-FORS HT). At an optical density (OD_{600}) of 0.6, the protein expression is induced by adding 1 mM Isopropyl- β -D-thiogalactopyranoside (IPTG) to the expression culture. After 3-4 h cells are harvested by centrifugation (6000 \times g, 4 °C, 30 min). Pelleted cells are resuspended in PBS, pooled, centrifuged (3750 \times g, 4 °C, 20 min) and stored at -20 °C.

5.3.1 Protein extraction of soluble proteins containing a polyhistidine tag

Extraction/binding buffer: 20 mM TRIS, 500 mM NaCl, 10 mM imidazole, pH 8.0

About 3 g (wet weight) of pelleted cells are resuspended in 150 mL extraction buffer, which is also the binding buffer for the subsequent immobilized metal ion affinity chromatography (IMAC). For cell disruption, the cell suspension is placed in an ice bath and sonicated (amplitude 60%, 30 sec/30 sec interval, 15 min, Sonopuls Ultraschall Homogenisator). Afterwards, cell debris are removed by centrifugation (25000 \times g, 20 min, 4 °C) and the supernatant is harvested and stored at 4 °C until further use.

5.3.2 Expression of aggregated protein in form of inclusion bodies

5.3.2.1 Protein extraction from inclusion bodies

STE-buffer: 375 mM sucrose, 1 mM EDTA, 10 mM TRIS-HCl pH 8.0, 1 mM DTT

solubilization buffer: 8 M GuHCl, 100 mM TRIS pH 8.0, 1 mM DTT

About 5 g (wet weight) of pelleted cells are resuspended in 200 mL STE-buffer. For cell disruption, the cell suspension is placed in an ice bath and sonicated (amplitude 60%, 20 sec/20 sec interval, 20 min, Sonopuls Ultraschall Homogenisator). The suspension is centrifuged (21600xg, 4 °C, 30 min) and the supernatant is discarded. The cell-pellet is again resuspended in 200 mL STE-buffer and sonicated once more, followed by centrifugation. Two more times the cell-pellet is solubilized in 200 mL STE-buffer and centrifuged (29400xg, 4 °C, 20 min). The supernatant is discarded and the wet weight of the isolated inclusion bodies is determined. For solubilization the inclusion bodies are first taken up in 7.5 x (w/v) 100 mM TRIS, pH 8.0, before 15 x (w/v) solubilization buffer is added. The suspension is kept at 21 °C for 2 h under mild stirring.

5.3.2.2 Oxidative refolding employing a glutathione redox-couple

Refolding buffer: 1 M arginine, 5 mM EDTA, 50 mM TRIS-HCl pH 8.0, 5 mM ox. glutathione, 2 mM red. glutathione

Dialysis buffer: 25 mM ammonium acetate pH 5.0

The protein-guanidine hydrochloride solution is centrifuged (23708xg, 4 °C, 20 min) to remove insoluble precipitate. The clarified light brown solution is added dropwise to 25 volumes ice-cold refolding buffer under mild stirring to prevent the protein from aggregation. The final protein concentration in the refolding buffer is about 50 µg/mL. The refolding solution is kept at 4 °C for three days. Then the refolding mixture is dialyzed twice against 10 volumes 25 mM ammonium acetate pH 5.0, which is the binding buffer for the following cation exchange chromatography. To remove precipitate the solution is centrifuged (12000xg, 4 °C, 30 min) and the supernatant is additionally filtered through a fluted filter. To prevent the reformation of precipitate, the solution should be applied to cation exchange chromatography (5.6.1) on the same day.

5.4 Expression in Hek293 cells

For expression of natively N-glycosylated protein, the Hek (human embryonal kidney) 293-derived cell lines Freestyle™ 293F and Expi293F™ were employed. These cells are adapted to high-density suspension culture and grow without serum, which facilitates purification of the target proteins from the supernatant. The two cell lines differ in that the Expi293™ expression system allows a higher protein expression yield, compared to the Freestyle™ 293F cells.

5.4.1 Culture conditions of Freestyle™ 293F/Expi293F™ cells

Growth and expression medium of Freestyle™ 293F:

Freestyle™ 293-expression medium + 1% P/S

Growth and expression medium of Expi293F™:

Expi293™-expression medium + 1% P/S

Cells are maintained in a humidified atmosphere (65%) of 8% CO₂ and shaking at 100 rpm (KS 260 basic, IKA) in a 37 °C incubator. Every 4 days, when Freestyle™ 293F and Expi293F™ cells reach a density of about 1-3x10⁶ cells/mL and 3-5x10⁶ cells/mL respectively, cells are seeded at about 0.3x10⁶ cells/mL in 40 mL of fresh medium in a sterile 125 mL polycarbonate Erlenmeyer flask.

5.4.2 Transient protein expression in Hek293 cells

Binding buffer: 50 mM sodium phosphate pH 8.3, 300 mM NaCl, 10mM imidazole

For transient expression, the plasmid encoding the target gene has to be introduced into the host cells. Polyethylenimine (PEI) is a cationic polymer, which binds DNA and forms positively charged particles that attach to anionic cell surfaces. The DNA-PEI molecules are readily endocytosed by the cells and the DNA is released into the cytoplasm.

For transfection of 1 mL cell culture, solution A is prepared to contain 1 µg DNA in 35 µL Opti-MEM I (GIBCO) and solution B is prepared with 2 µg PEI (25 kDa linear, Polyscience) in 35 µL Opti-MEM I. Both solutions are mixed by inversion and incubated for 25 min at 21 °C. Subsequently, the solution is added dropwise to the expression culture while swirling. For expression in Freestyle™ 293F cells are seeded at 0.75x10⁶ cells/mL, whereas for expression in Expi293F™ cells, cells are adjusted to 2.5x10⁶ cells/mL in the appropriate flask. For synthesis of Endo-H sensitive glycol-proteins, expression was performed in the

presence of 5 μ M kifunensine. After 5 days, the cells are removed by centrifugation (5400 g, 4 °C, 15 min) and the protein containing supernatant is harvested and stored at 4 °C until further use.

5.5 Chemical glycoengineering of IL-4 cysteine variants

5.5.1 Enzymatic deglutathionylation of engineered cysteine residues

PE7 buffer: 0.1 M potassium phosphate pH 7.0, 2 mM EDTA

Non-conjugated IL-4 protein containing an unpaired cysteine residue with a free thiol-group can be prepared by enzymatic deprotection of glutathionylated IL-4 cysteine variants employing the so-called glutaredoxin-system, consisting of the enzymes glutaredoxin and glutathione reductase (reviewed in: (Fernandes and Holmgren 2004)). The *E. coli* enzyme glutaredoxin-1 thereby catalyzes the reduction of glutathione mixed disulphides in the presence of glutathione.

Freeze-dried IL-4 protein is first solubilized in water to prevent precipitation and is then mixed with 0.2 M PE7 buffer, to yield 0.1 M PE7 buffer. Then the components of the glutathione system are added to give the final concentrations stated in table 5.9.

Table 5.9: Enzymatic deglutathionylation of an IL-4 cysteine variant.

component	concentration
IL-4 protein	50 μ M
NADPH	0.2 mM
Glutathione (reduced)	0.5 mM
Glutathione reductase (205 U/mg)	6 μ g/mL
Glutaredoxin	0.33 μ g/mL

The reaction is started by adding glutaredoxin-1. To monitor the reaction progress in SDS-PAGE, samples are taken at different time points during the reaction and incubated with a 100-fold molar excess of maleimide-PEG (molecular weight 2.3 kDa). Since at pH 7.0 maleimides are highly thiol-specific, only IL-4 protein containing free-sulfhydryls reacts with maleimide-PEG, which results in an apparent mass increase (2 kDa/PEG-polymer) that is detectable in SDS-PAGE.

The reaction is stopped by adding TFA to a final concentration of 0.1% (v/v) and the reaction mixture is submitted to reverse phase HPLC (5.6.3).

5.5.2 Coupling to amine-containing glycan via the bifunctional crosslinker SMCC

5.5.2.1 Preparation of SMCC-glucosamine intermediate

Reaction buffer: 100 mM sodium phosphate pH 8.0, 2 mM EDTA

The crosslinker SMCC (succinimidyl 4-(N-maleimido-methyl)-cyclohexane-1-carboxylate) is dissolved in acetonitrile at a concentration of 100 mM. A 400 mM glucosamine solution is prepared in 100 mM sodium phosphate pH 8.0, 4 mM EDTA. Both solutions are mixed 1:1 (v/v) to yield a molar ratio for SMCC:glucosamine of 1:4. The mixture is incubated at 21 °C for 2 h. The reaction is stopped by adding TFA to a final concentration of 0.1% (v/v) followed by purification via reverse phase HPLC (5.6.3).

5.5.2.2 Conjugation of SMCC-glucosamine to IL-4

Reaction buffer: 100 mM sodium phosphate pH 6.5

IL-4 protein containing an unpaired cysteine residue is dissolved in reaction buffer at a concentration of about 70 μ M. The glucosamine-SMCC conjugate is dissolved in acetonitrile to give a 5 mM concentration. Both solutions are mixed in a molar ratio for protein to glucosamine-SMCC of about 1:100. The mixture is incubated at 21 °C for 2 h. The reaction is stopped by adding TFA to a final concentration of 0.1% (v/v) and the reaction mixture is submitted to RP-HPLC (5.6.3).

5.5.3 Coupling of thiol-carbohydrates using phenylselenenylbromide activation

Reaction buffer: 10 mM CHES, 70 mM MES, 2 mM CaCl₂, pH 9.5

IL-4 protein containing an unpaired cysteine residue is dissolved in reaction buffer to a final concentration of 66 μ M (about 1 mg/mL). Phenylselenenyl bromide is dissolved in acetonitrile at a concentration of 100 mM. The reaction is started by adding phenylselenenylbromide solution to the protein in a molar ratio of 40:1. The solution is vortexed for 30 sec and then placed on a shaker for 1 h at 21 °C. Non-reacted phenylselenenylbromide and byproducts are removed by size exclusion chromatography using a PD10 column (5.6.4). Phenylselenenyl-activated IL-4 protein is again adjusted to a 66 μ M concentration in reaction buffer and thiol-glycans are dissolved in water at a 30 mM concentration. Both solutions are mixed to give a molar ratio for protein to thio-glycan of about 1:40 and the solution is incubated for 20 min at 21 °C. To increase the coupling yield, further thiol-carbohydrate solution is added to raise

the final concentration to 6 mM. The mixture is incubated for 20 min at 21 °C before it is applied to RP-HPLC (5.6.3).

5.5.4 Preparation of disulphide-linked IL-4 glycoconjugates via refolding

5.5.4.1 Refolding of *E. coli*-derived IL-4 cysteine variants in the presence of thiol-glycans

Renaturation buffer: 1 M arginine, 5 mM EDTA, 50 mM TRIS-HCl pH 8.0, 1 mM thiol-glycan

Binding buffer: 25 mM ammonium acetate pH 5.0

Extraction of IL-4 cysteine analogues from *E. coli*-derived inclusion bodies is exactly performed as described under 5.3.2.1. After stirring for 2 h the GuHCl-protein solution is centrifuged (23708xg, 4 °C, 20 min) to remove insoluble residues. The clarified, light brown solution is added dropwise to 25 volumes ice-cold renaturation buffer, containing 1 mM thiol-glycan, under mild stirring to prevent the protein from aggregation (if the IL-4 variant contains more than one cysteine, the concentration of the thiol-glycan may have to be adjusted). The final concentration of the protein in the refolding buffer is about 50 µg/mL. The renaturation solution is kept at 4 °C for three days. For subsequent cation exchange chromatography, the renaturation mixture is dialyzed twice against 10 volumes 25 mM ammonium acetate pH 5.0. To remove precipitate the solution is centrifuged (12000xg, 4 °C, 30 min) and the supernatant is additionally filtered through a fluted filter. To prevent the reformation of precipitate, the solution should be applied to cation exchange chromatography (5.6.1) on the same day.

5.5.4.2 Refolding of Hek293 cell-derived IL-4 cysteine variants in the presence of thiol-glycans

Denaturation buffer (final conc.):

5 M GuHCl, 100 mM TRIS HCl 8.0, 1 mM DTT

Renaturation buffer:

1 M arginine, 5 mM EDTA, 50 mM TRIS HCl pH 8.0, 1 mM thiol-glycan

IMAC buffer: 50 mM sodium phosphate pH 8.3, 300 mM NaCl, 10mM imidazole

ConA buffer: 20 mM TRIS, 500 mM NaCl, 1 mM MnCl₂, 1 mM CaCl₂, pH 7.4

Purified Hek293 cell-derived IL-4 cysteine analogues are adjusted to a concentration of 1 mg/mL in denaturation buffer and incubated at 21 °C for 2 h under mild stirring. The solution is added dropwise to 20 volumes ice-cold renaturation buffer, containing 1 mM thiol-glycan,

under mild stirring to prevent the protein from aggregation (if the IL-4 variant contains more than one cysteine, the concentration of the thiol-glycan may have to be adjusted). The final concentration of the protein in the refolding buffer is about 50 µg/mL. The renaturation solution is kept at 4 °C for three days, which is followed by chromatographic purification.

5.6 Chromatographic methods for protein purification

5.6.1 Cation exchange chromatography

Binding buffer: 25 mM ammonium acetate, pH 5.0

Elution buffer: 25 mM ammonium acetate, 1.5 M NaCl, pH 5.0

Employed column:

HiTrap™ CM FF, 5 mL (GE Healthcare)

The protein solution is dialysed twice against 10 volumes of binding buffer. To remove precipitate, the solution is centrifuged (12000xg, 4 °C, 30 min) and additionally filtered using a fluted filter. Subsequently, the clarified protein solution is loaded onto the column. Non-specifically bound contaminants are removed from the column by washing with binding buffer until the UV-signal is back to baseline. For elution of the target protein, a gradient is applied from 0% to 100% (v/v) buffer B for 25 mL (5 column volumes). Protein containing fractions are identified by SDS-PAGE (5.2.1).

5.6.2 Immobilized metal ion affinity chromatography (IMAC)

Glutaredoxin purification:

Binding buffer: 20 mM TRIS, 500 mM NaCl, 10 mM imidazole, pH 8.0

Elution buffer: 20 mM TRIS, 500 mM NaCl, 300 mM Imidazole, pH 8.0

Purification of Hek293 cell-derived IL-4:

Binding buffer: 50 mM sodium phosphate pH 8.3, 300 mM NaCl, 10 mM imidazole

Elution buffer: 50 mM sodium phosphate pH 8.3, 300 mM NaCl, 500 mM imidazole

Employed Ni-NTA column:

HisTrap™ excel column, 5 mL (GE Healthcare)

Protein containing a polyhistidine tag can be purified using immobilized metal-ion affinity chromatography (IMAC). For purification via IMAC, protein containing solutions are dialysed twice against 10 volumes of binding buffer. The binding-buffer already contains low amounts of imidazole to prevent non-specific binding. Prior to column application, the

protein solution is centrifuged (25000xg, 4 °C, 20 min) to remove precipitate. After the protein is applied to the column, weakly bound protein is eluted by washing with binding buffer until the UV-signal is back to base-line. Bound protein is eluted via direct application of 100% (v/v) elution buffer to the column. Protein containing fractions are identified by SDS-PAGE (5.2.1).

5.6.3 Reversed-phase high-pressure liquid chromatography (RP-HPLC)

Binding buffer: 0.1% (v/v) TFA

Elution buffer: 100% acetonitrile

Column for IL-4 purification:

Analytical: C4 column (Jupiter C4, 5 μ m, 250 \times 4.6 mm, 300 Å, Phenomenex)

Preparative: C4 column (Jupiter C4, 10 μ m, 250 \times 10 mm, 300 Å, Phenomenex)

Column for SMCC/SMCC-GlcN purification:

C18 column (μ RPC C2/C18 ST 4.6/100, GE Healthcare)

Reversed-phase high-pressure liquid chromatography (RP-HPLC) separates molecules based on hydrophobicity. Prior to injection, samples are acidified with TFA to a final concentration of 0.1% (v/v). To remove precipitate, the solution is centrifuged (25000xg, 4 °C, 5 min). The solution is applied using 0.1% (v/v) TFA as a mobile phase. After the sample is applied to the column, weakly bound protein is eluted by washing with 0.1% (v/v) TFA until the UV-signal is back to base-line. For elution of bound molecules, a linear gradient from 0% to 100% (v/v) acetonitrile is used (table 5.10). Protein containing fractions are identified by SDS-PAGE (5.2.1). Fractions containing low-molecular weight compounds, i.e. SMCC and SMCC-glucosamine were identified by mass spectrometry analysis (5.2.5.2).

Table 5.10: Running protocol for reverse phase HPLC.

	IL-4 protein (250 × 10 mm C4)		SMCC/GlcN (C18)	
	flowrate (mL/min)	volume (mL)	flowrate (mL/min)	volume (mL)
Loop size		variable		0.5
Injection	variable	variable	0.3	1.0
Isocratic flow polar phase	3.0	20	0.5	4.0
Gradient	3.0	80	0.5	8.0
Isocratic flow organic phase	3.0	20	0.5	4.0
Fraction size		2.0		0.5

5.6.4 Size exclusion chromatography

Buffer: 10 mM CHES, 70 mM MES, 2 mM CaCl₂, pH 9.5

Disposable PD 10 Desalting Column (GE Healthcare)

Size exclusion chromatography separates molecules based on difference in size. In this work disposable PD10 columns were used, which contain sephadex G25 medium with a cutoff value of 5 kDa. Briefly, the column is first equilibrated with buffer. Then up to 2.5 mL of the sample are applied and eluted with buffer using gravity flow. Protein containing fractions are analysed using SDS-PAGE (5.2.1), pooled and frozen at -20 °C until further use.

5.6.5 Lectin affinity chromatography

Binding buffer: 20 mM TRIS, 500 mM NaCl, 1 mM MnCl₂, 1 mM CaCl₂, pH 7.4

Elution buffer: 20 mM TRIS, 500 mM NaCl, 500 mM methyl-d-glucoside, pH 7.4

Concanavalin A column:

HiTrap Con A 4B, 1 mL (GE Healthcare)

In lectin chromatography column resins are employed that contain immobilized lectins that allow isolation and separation of glycoproteins dependent on their glycan architectures.

In this work, a concanavalin A (ConA) column was employed for the purification of glycosylated protein. ConA recognizes α -d-mannopyranosyl and α -d-glucopyranosyl conjugated residues.

The binding buffer contains calcium and manganese ions, which are essential for carbohydrate binding of ConA. The protein sample is adjusted to ConA binding buffer and

is then applied to the column at a flow-rate of 0.1 mL/min. After the protein is applied to the column, non-specifically bound protein is removed by washing with binding buffer until the UV-signal is back to baseline. When the UV-signal is back to the baseline, after washing with binding buffer, the protein is eluted with 100% (v/v) elution buffer. Protein containing fractions are identified by SDS-PAGE (5.2.1).

5.6.6 Sulfhydryl immobilization

Coupling Buffer: 50 mM TRIS, 5 mM EDTA, pH 8.5

The SulfoLink™ resin contains iodoacetyl activated agarose beads, which covalently bind proteins with free sulfhydryl-groups.

The SulfoLink™ resin is equilibrated to coupling buffer and transferred to an empty gravity flow column according to the manufacturer's instructions. For 1 mg of protein about 1 mL of resin is used. The protein sample is adjusted to the coupling buffer and added to the resin. The solution is mixed several times by inverting. Then the column is placed upright and is incubated for 45 min at 21 °C. Finally, unbound protein is eluted using gravity flow. The column is washed with 3 column volumes of coupling buffer. The complete flow-through is collected in 1 mL fractions and protein containing fractions are identified via SDS-PAGE (5.2.1). The used coupling resin is discarded.

5.7 Methods for analysis of pharmacological parameters *in vitro*

5.7.1 Surface Plasmon Resonance (SPR)

Surface plasmon resonance (SPR) allows the label-free detection of protein-protein interactions and quantification of binding kinetics. The ligand is immobilized on the gold-coated surface of a sensor chip, which is essentially a glass prism. The analyte is perfused over the sensor surface and ligand-analyte interactions are monitored over time. The binding of the analyte leads to a mass increase and a change in the refractive index of the gold-coated surface, which is converted into resonance units (RU). One RU thereby equals an increase of 1 pg/mm².

The SPR signals are processed in a sensorgram, which is fitted to a kinetic binding model and thus allows determination of binding parameters.

5.7.1.1 Biotinylation of ybbR-fusion protein

Proteins carrying a C- or N-terminal 11-residue peptide tag called ybbR (DSLEFIASKLA) can be biotinylated using the SFP-synthase together with a CoA (coenzyme A)-conjugated probe. The SFP-synthase covalently transfers the 4-phosphopantetheinyl (Ppant) group of CoA onto the N-terminal serine residue of the ybbR-sequence (Yin et al. 2006; Yin et al. 2005).

For biotin labelling the ybbR-fusion protein is mixed with CoA-conjugated biotin, SFP-synthase, etc. (table 5.11) and incubated for 2 h at 22 °C. Then unbound CoA-biotin is removed via ultrafiltration. The protein is frozen and stored at -80 °C.

Table 5.11: CoA labelling of ybbR tag using SFP-synthase.

component	final concentration
HEPES	50 mM
MgCl ₂	10 mM
ybbR-fusion protein	10 μM
SFP-synthase	0.5 μM
CoA biotin	10 μM

5.7.1.2 SPR experimental set-up

HBST300: 10 mM HEPES, 300 mM NaCl, 3.4 mM EDTA, 0.005% Tween-20, pH 7.4

SPR experiments are performed on a ProteOn™ XPR 36 system. Activation of the ProteOn™ GLC Biosensor surface is achieved via perfusion of an EDC/sulfo-NHS mixture (40 mM 1-ethyl-3-(3-dimethylaminopropyl) carbodiimide, 20 mM N-hydroxysulfosuccinimide) for 360 sec at a flowrate of 30 μL/min. Then the biosensor is perfused with streptavidin solution (10 μg/mL in 10 mM sodium acetate pH 4.0) until an adequate RU is reached. Residual free carboxy residues are blocked by perfusion with 1 M ethanolamine, pH 8.5 (30 μL/min, 300 sec). Immobilization of the biotinylated ligand is performed at a flowrate of 30 μL/min until the required density is reached. For analysis of the association rate (k_{on}) the biosensor is perfused with analyte employing different concentrations in HBST300 buffer at a flowrate of 100 μL/min for 240 sec. The k_{off} rate is determined measuring the dissociation of the analyte, whereby only HBST300 without the analyte is perfused over the sensor at 100 μL/min for 300 sec. For regeneration of the immobilized ligand, the biosensor surface is washed with 1 M NaCl, 0.1% Tween20 pH 5.0

at a flowrate of 100 $\mu\text{L}/\text{min}$ for 240 sec, followed by perfusion with 10 mM glycine pH 2.5 at a flowrate of 100 $\mu\text{L}/\text{min}$ for 19 sec. To determine the binding kinetic constants, a simple 1:1 Langmuir fitting model is applied to the obtained sensorgrams with the parameter settings displayed in table 5.12. The dissociation constant K_D is equal to the quotient $k_{\text{off}}/k_{\text{on}}$.

Table 5.12: parameter setting employed for analysis by simple 1:1 Langmuir-type interaction model.

Parameter	Unit	Scope	Type
Concentration	M	Local	Constant
k_a	1/MS	Grouped	Fitted
k_d	1/s	Grouped	Fitted
K_D	M	Grouped	Calculated
Rmax	RU	Grouped	Fitted
Chi2	RU	Local	Calculated
t0 Dissociation	s	Local	Constant
RI	RU	Local	Constant
Begin Association	s	Grouped	Constant
End Association	s	Grouped	Constant
Begin Dissociation	s	Grouped	Constant
End Dissociation	s	Grouped	Constant

5.7.2 Proteolytic stability assay

Reaction buffer: 50 mM TRIS-HCl pH 7.6, 1mM CaCl₂

IL-4 protein is dissolved in reaction buffer and adjusted to a concentration of 30 – 32 μM . To about 500 μL of protein solution, 10 μg of sequencing grade trypsin is added. At different time points, samples are taken and mixed with 1:5 inhibitor cocktail. Samples are immediately frozen at -20 $^{\circ}\text{C}$ until further use.

A SDS-PAGE (5.2.1) is performed with distinct amounts of sample and marker. Coomassie-stained gels are analysed with ImageLab software using the volume tool. Protein-band intensities are normalized to the protein standard.

5.7.3 Cellular experiments

5.7.3.1 HEK-Blue cell SEAP reporter gene assay

Growth medium: DMEM glutamax (Gibco), 10% heatinactivated FBS, 100 $\mu\text{g}/\text{ml}$ streptomycin, 100 U/ml penicillin, 100 $\mu\text{g}/\text{mL}$ zeocin, 10 $\mu\text{g}/\text{mL}$ blasticidin

Assay medium: growth medium without phenol-red

HEK-Blue™ IL-4/IL-13 cells (Invivogen) are stable Hek293-cell transfectants that carry a secreted alkaline phosphatase (SEAP) reporter gene coupled to an IL-4/IL-13 responsive promoter and thus allow analysis of IL-4 dependent signalling.

HEK-Blue™ IL-4/IL-13 cells are maintained in growth medium in a T75 flask at 37 °C and 5% CO₂ in a humidified atmosphere. When cells reach about 80-90% confluency, they are trypsinized and seeded at a density of 1×10^4 cells/mL in 15 mL of fresh medium. For assays, a serial dilution of IL-4 protein is performed in assay medium in 96-well f-bottom microtiter plates. Per well, 100 µL of assay medium containing IL-4 protein is added and plates are incubated at 37 °C for 1 h to adjust to the temperature. HEK-Blue cells are taken up in assay medium and adjusted to 1×10^5 cells/mL. Per well 100 µL of cells are added. After 20-24 h of incubation at 37 °C the supernatant is harvested and a PNPP (p-nitrophenyl phosphate) assay is performed to quantify SEAP activity. For SEAP quantification, 50 µL of supernatant are mixed with 50 µL of PNPP-solution (1 mg/mL) and the SEAP catalysed hydrolysis of PNPP to p-nitrophenol is measured at 405/630 nm on a microplate reader. For analysis, data is used when the control (50 pM IL-4 WT) has reached a signal intensity of 0.3-0.4 at 405 nm above background level. For quantification signal intensities are normalized to control.

5.7.3.2 TF-1 cell proliferation assay

Growth medium: RMPI-1640 (Gibco), 10% heat-inactivated FBS, 100 µg/ml streptomycin, 100 U/ml penicillin, 8 ng/mL GM-CSF

Assay medium: RPMI-1640 (Gibco), 10% heat-inactivated FBS, 100 µg/ml streptomycin, 100 U/ml penicillin, without phenol red

TF-1 cells are a human erythroleukemic cell line, which show IL-4 dependent growth in the absence of GM-CSF (granulocyte-macrophage colony-stimulating factor) and thus can be used for quantification of IL-4 activity.

TF-1 cells are maintained in growth medium in a 75 cm² flask at 37 °C and 5% CO₂ in a humidified atmosphere. Every 3-4 days cells are seeded at a density of 2×10^4 cells/mL in 15 mL of fresh medium. The day before the assay is started, cells are diluted 1:1 with fresh growth medium. Prior to administration of IL-4, cells are starved. For this, cells are washed twice in 10 mL assay medium (centrifugation 400 g, 5 min) to remove GM-CSF. Then cells are seeded at $3-4 \times 10^5$ cells/mL in assay medium and incubated at 37 °C for 4 h. A serial dilution of IL-4 protein is performed in assay medium in 96-well f-bottom microtiter plates. Per well, 100 µL of assay medium containing IL-4 protein is added and plates are incubated

at 37 °C for 1-2 h to adjust to the temperature. Then 100 μ L of cells are added per well and plates are incubated for 72 h.

The cellular metabolic rate is quantified by adding 10 μ L of resazurin dye solution (0.15 mg/mL in PBS) per well. In the presence of NADH or NADPH, resazurin is reduced to resofurin, which can be quantified at 571 nm. After 4 h of incubation at 37 °C, absorbance is measured at 571/749 nm on a microplate reader. For quantification, signal intensities are normalized to control, which is 50 pM IL-4 WT.

6. Summary

The cytokines interleukin 4 (IL-4) and IL-13 are important mediators in the humoral immune response and play a crucial role in the pathogenesis of chronic inflammatory diseases, such as asthma, allergies, and atopic dermatitis. Hence, IL-4 and IL-13 are key targets for treatment of such atopic diseases.

For cell signalling IL-4 can use two transmembrane receptor assemblies, the type I receptor consisting of receptors IL-4R α and γ c, and type II receptor consisting of receptors IL-4R α and IL-13R α 1. The type II receptor is also the functional receptor of IL-13, receptor sharing being the molecular basis for the partially overlapping effects of IL-4 and IL-13. Since both cytokines require the IL-4R α receptor for signal transduction, this allows the dual inhibition of both IL-4 and IL-13 by specifically blocking the receptor IL-4R α .

This study describes the design and synthesis of novel antagonistic variants of human IL-4. Chemical modification was used to target positions localized in IL-4 binding sites for γ c and IL-13R α 1 but outside of the binding epitope for IL-4R α . In contrast to existing studies, which used synthetic chemical compounds like polyethylene glycol for modification of IL-4, we employed glycan molecules as a natural alternative. Since glycosylation can improve important pharmacological parameters of protein therapeutics, such as immunogenicity and serum half-life, the introduced glycan molecules thus would not only confer a steric hindrance based inhibitory effect but simultaneously might improve the pharmacokinetic profile of the IL-4 antagonist.

For chemical conjugation of glycan molecules, IL-4 variants containing additional cysteine residues were produced employing prokaryotic, as well as eukaryotic expression systems. The thiol-groups of the engineered cysteines thereby allow highly specific modification. Different strategies were developed enabling site-directed coupling of amine- or thiol-functionalized monosaccharides to introduced cysteine residues in IL-4. A linker-based coupling procedure and an approach requiring phenylselenyl bromide activation of IL-4 thiol-groups were hampered by several drawbacks, limiting their feasibility. Surprisingly, a third strategy, which involved refolding of IL-4 cysteine variants in the presence of thiol-glycans, readily allowed synthesis of IL-4 glycoconjugates in form of mixed disulphides in milligram amount. This approach, therefore, has the potential for large-scale synthesis of IL-4 antagonists with highly defined glycosylation. Obtaining a homogenous glycoconjugate with exactly defined glycan pattern would allow using the attached glycan structures for

fine-tuning of pharmacokinetic properties of the IL-4 antagonist, such as absorption and metabolic stability.

The IL-4 glycoconjugates generated in this work proved to be highly effective antagonists inhibiting IL-4 and/or IL-13 dependent responses in cell-based experiments and in *in vitro* binding studies. Glycoengineered IL-4 antagonists thus present valuable alternatives to IL-4 inhibitors used for treatment of atopic diseases such as the neutralizing anti-IL-4R α antibody Dupilumab.

7. Zusammenfassung

Die Zytokine Interleukin-4 (IL-4) und IL-13 sind zentrale Mediatoren in der humoralen Immunantwort und sind wesentlich an der Entstehung chronisch inflammatorischer Erkrankungen, wie Asthma, Allergien und atopischer Dermatitis beteiligt. Daher werden IL-4 und IL-13 als wichtige therapeutische Angriffspunkte für die Behandlung atopischer Erkrankungen betrachtet.

Zur Signaltransduktion aktiviert IL-4 zwei heterodimere Rezeptorkomplexe, den Typ I Rezeptor bestehend aus den Untereinheiten IL-4R α und γ c und den Typ II Rezeptor, der sich aus IL-4R α und IL-13R α 1 zusammensetzt. Der Typ II Rezeptor wird auch von IL-13 zur Signalweiterleitung genutzt, wodurch sich die teilweise überschneidenden Funktionen der beiden Zytokine erklären lassen. Die überlappende Rezeptornutzung erlaubt es durch eine gezielte Blockade des IL-4R α -Rezeptors sowohl IL-4, als auch IL-13 gleichzeitig zu inhibieren.

Ziel dieser Arbeit war die Herstellung neuartiger IL-4 basierter Antagonisten. Dazu wurden ausgewählte Positionen innerhalb der IL-4 Bindestelle für γ c and IL-13R α 1, jedoch außerhalb des Bindeepitops für IL-4R α gezielt chemisch modifiziert. Im Gegensatz zu bereits existierenden Studien, die synthetische Gruppen wie Polyethylenglykol (PEG) zur chemischen Modifizierung von IL-4 nutzten, wurden in dieser Arbeit Glykane als natürliche Alternative zu PEG an IL-4 gekoppelt. Da sich Glykosylierung auf wichtige pharmakologische Eigenschaften proteinbasierter Therapeutika, wie Immunogenität oder Serum Halbwertszeit, positiv auswirken kann, würde der Zucker in dieser Strategie nicht nur den auf sterischer Hinderung basierenden inhibitorischen Effekt vermitteln, sondern könnte gleichzeitig zu einer Optimierung der pharmakologischen Eigenschaften des IL-4 Inhibitors beitragen.

Zur chemischen Zucker-Kopplung wurden zusätzliche Cystein-Reste in IL-4 eingebracht, deren freie Thiol-gruppen eine hochspezifische Modifizierung der IL-4 Mutanten erlauben. Die IL-4 Cystein-Mutanten wurden rekombinant in prokaryotischen und eukaryotischen Expressionssystemen hergestellt. Anschließend wurden verschiedene Strategien entwickelt, die eine ortsspezifische Kopplung Amin- und Thiol-haltiger Zucker an die eingebrachten Cystein-Reste in IL-4 ermöglichen. Eine Linker-basierte Reaktion, sowie ein Kopplungsansatz, der eine Aktivierung der Thiol-Gruppe mittels Bromselenobenzol erforderte, wiesen einige Nachteile auf, die eine erhebliche Einschränkung ihrer technischen Durchführbarkeit zur Folge hatte. Eine dritte Strategie hingegen, die eine Rückfaltung der

IL-4 Cystein-Mutanten in Anwesenheit von Thiol-Glykanen involvierte, erlaubte eine effiziente Herstellung von IL-4 Glykokonjugaten in Form gemischter Disulfide im Milligrammbereich. Dieser Ansatz könnte somit zur Produktion homogen glykosylierter IL-4 Antagonisten im Großmaßstab eingesetzt werden. Die Herstellung homogener Glykokonjugate mit klar definierten Glykosylierungsmuster würde es erlauben über die gekoppelten Glykanstrukturen die pharmakologischen Eigenschaften von IL-4, wie Absorption und metabolische Stabilität, gezielt zu modulieren.

Die hergestellten IL-4 Glykokonjugate erwiesen sich als hochwirksame Antagonisten, die die Aktivität von IL-4 und IL-13 in zellbasierten Experimenten inhibieren konnten. Glykosylierte IL-4 Antagonisten stellen somit eine vergleichbare Alternative zu gängigen IL-4 Inhibitoren dar, die zur Behandlung von atopischen Erkrankungen eingesetzt werden, wie beispielweise der neutralisierende anti-IL-4R α Antikörper Dupilumab.

8. Literature

- Abbas, A. K., Murphy, K. M., and Sher, A. 1996. Functional diversity of helper T lymphocytes. *Nature* 383(6603):787-793. <https://doi.org/10.1038/383787a0>.
- Aebi, M. 2013. N-linked protein glycosylation in the ER. *Biochimica et biophysica acta* 1833(11):2430-2437. <https://doi.org/10.1016/j.bbamcr.2013.04.001>.
- Agard, N. J., Prescher, J. A., and Bertozzi, C. R. 2004. A strain-promoted 3 + 2 azide-alkyne cycloaddition for covalent modification of biomolecules in living systems. *Journal of the American Chemical Society* 126(46):15046-15047. <https://doi.org/10.1021/ja044996f>.
- Andrews, A.-L., Holloway, J. W., Holgate, S. T., and Davies, D. E. 2006. IL-4 Receptor Is an Important Modulator of IL-4 and IL-13 Receptor Binding: Implications for the Development of Therapeutic Targets. *The Journal of Immunology* 176(12):7456-7461. <https://doi.org/10.4049/jimmunol.176.12.7456>.
- Andrews, A.-L., Holloway, J. W., Puddicombe, S. M., Holgate, S. T., and Davies, D. E. 2002. Kinetic analysis of the interleukin-13 receptor complex. *J. Biol. Chem.* 277(48):46073-46078. <https://doi.org/10.1074/jbc.M209560200>.
- Aquino, D., Wong, R., Margolis, R. U., and Margolis, R. K. 1980. Sialic acid residues inhibit proteolytic degradation of dopamine beta-hydroxylase. *FEBS letters* 112(2):195-198.
- Aricescu, A. R., Lu, W., and Jones, E. Y. 2006. A time- and cost-efficient system for high-level protein production in mammalian cells. *Acta crystallographica. Section D, Biological crystallography* 62(Pt 10):1243-1250. <https://doi.org/10.1107/S09074444906029799>.
- Arima, K., Sato, K., Tanaka, G., Kanaji, S., Terada, T., Honjo, E., Kuroki, R., Matsuo, Y., and Izuhara, K. 2005. Characterization of the interaction between interleukin-13 and interleukin-13 receptors. *The Journal of biological chemistry* 280(26):24915-24922. <https://doi.org/10.1074/jbc.M502571200>.
- Armstrong, J. K., Hempel, G., Koling, S., Chan, L. S., Fisher, T., Meiselman, H. J., and Garratty, G. 2007. Antibody against poly(ethylene glycol) adversely affects PEG-asparaginase therapy in acute lymphoblastic leukemia patients. *Cancer* 110(1):103-111. <https://doi.org/10.1002/cncr.22739>.
- Baker, N. D., Griffin, R. J., Irwin, W. J., and Slack, J. A. 1989. The reduction of aryl azides by dithiothreitol: A model for bioreduction of aromatic azido-substituted drugs. *International Journal of Pharmaceutics* 52(3):231-238. [https://doi.org/10.1016/0378-5173\(89\)90225-1](https://doi.org/10.1016/0378-5173(89)90225-1).
- Bause, E. 1983. Structural requirements of N-glycosylation of proteins. Studies with proline peptides as conformational probes. *The Biochemical journal* 209(2):331-336.
- Bazan, J. F. 1990. Structural Design and Molecular Evolution of a Cytokine Receptor Superfamily. *Proceedings of the National Academy of Sciences of the United States of America* 87(18):6934-6938.

- Bernardes, G. J. L., Gamblin, D. P., and Davis, B. G. 2006. The direct formation of glycosyl thiols from reducing sugars allows one-pot protein glycoconjugation. *Angewandte Chemie (International ed. in English)* 45(24):4007-4011. <https://doi.org/10.1002/anie.200600685>.
- Blauvelt, A., Bruin-Weller, M. de, Gooderham, M., Cather, J. C., Weisman, J., Pariser, D., Simpson, E. L., Papp, K. A., Hong, H. C.-H., Rubel, D., Foley, P., Prens, E., Griffiths, C. E. M., Etoh, T., Pinto, P. H., Pujol, R. M., Szepietowski, J. C., Ettlér, K., Kemény, L., Zhu, X., Akinlade, B., Hultsch, T., Mastey, V., Gadkari, A., Eckert, L., Amin, N., Graham, N. M. H., Pirozzi, G., Stahl, N., Yancopoulos, G. D., and Shumel, B. 2017. Long-term management of moderate-to-severe atopic dermatitis with dupilumab and concomitant topical corticosteroids (LIBERTY AD CHRONOS): A 1-year, randomised, double-blinded, placebo-controlled, phase 3 trial. *The Lancet* 389(10086):2287-2303. [https://doi.org/10.1016/S0140-6736\(17\)31191-1](https://doi.org/10.1016/S0140-6736(17)31191-1).
- Bochner, B. S., Klunk, D. A., Sterbinsky, S. A., Coffman, R. L., and Schleimer, R. P. 1995. IL-13 selectively induces vascular cell adhesion molecule-1 expression in human endothelial cells. *J. Immunol.* 154(2):799-803.
- Bologna, L., Gotti, E., Manganini, M., Rambaldi, A., Intermesoli, T., Introna, M., and Golay, J. 2011. Mechanism of action of type II, glycoengineered, anti-CD20 monoclonal antibody GA101 in B-chronic lymphocytic leukemia whole blood assays in comparison with rituximab and alemtuzumab. *Journal of immunology (Baltimore, Md. 1950)* 186(6):3762-3769. <https://doi.org/10.4049/jimmunol.1000303>.
- Borish, L. C., Nelson, H. S., Lanz, M. J., Claussen, L., Whitmore, J. B., Agosti, J. M., and Garrison, L. 1999. Interleukin-4 receptor in moderate atopic asthma. A phase I/II randomized, placebo-controlled trial. *American journal of respiratory and critical care medicine* 160(6):1816-1823. <https://doi.org/10.1164/ajrccm.160.6.9808146>.
- Boulanger, M. J., Chow, D.-c., Brevnova, E. E., and Garcia, K. C. 2003. Hexameric structure and assembly of the interleukin-6/IL-6 alpha-receptor/gp130 complex. *Science (New York, N.Y.)* 300(5628):2101-2104. <https://doi.org/10.1126/science.1083901>.
- Bueter, C. L., Specht, C. A., and Levitz, S. M. 2013. Innate sensing of chitin and chitosan. *PLoS pathogens* 9(1):e1003080. <https://doi.org/10.1371/journal.ppat.1003080>.
- Burmeister Getz, E., Fisher, D. M., and Fuller, R. 2009. Human pharmacokinetics/pharmacodynamics of an interleukin-4 and interleukin-13 dual antagonist in asthma. *Journal of clinical pharmacology* 49(9):1025-1036. <https://doi.org/10.1177/0091270009341183>.
- Cabrera, G., Cremata, J. A., Valdés, R., García, R., González, Y., Montesino, R., Gómez, H., and González, M. 2005. Influence of culture conditions on the N-glycosylation of a monoclonal antibody specific for recombinant hepatitis B surface antigen. *Biotechnology and applied biochemistry* 41(Pt 1):67-76. <https://doi.org/10.1042/BA20040032>.

- Caput, D., Laurent, P., Kaghad, M., Lelias, J. M., Lefort, S., Vita, N., and Ferrara, P. 1996. Cloning and characterization of a specific interleukin (IL)-13 binding protein structurally related to the IL-5 receptor alpha chain. *The Journal of biological chemistry* 271(28):16921-16926.
- Carr, C., Aykent, S., Kimack, N. M., and Levine, A. D. 1991. Disulfide assignments in recombinant mouse and human interleukin 4. *Biochemistry* 30(6):1515-1523.
- Carter, C. R. D., Whitmore, K. M., and Thorpe, R. 2004. The significance of carbohydrates on G-CSF: differential sensitivity of G-CSFs to human neutrophil elastase degradation. *Journal of leukocyte biology* 75(3):515-522. <https://doi.org/10.1189/jlb.0803378>.
- Cartwright, I. L., Hutchinson, D. W., and Armstrong, V. W. 1976. The reaction between thiols and 8-azidoadenosine derivatives. *Nucleic acids research* 3(9):2331-2339.
- Casella, G., Garzetti, L., Gatta, A. T., Finardi, A., Maiorino, C., Ruffini, F., Martino, G., Muzio, L., and Furlan, R. 2016. IL4 induces IL6-producing M2 macrophages associated to inhibition of neuroinflammation in vitro and in vivo. *Journal of neuroinflammation* 13(1):139. <https://doi.org/10.1186/s12974-016-0596-5>.
- Ceaglio, N., Etcheverrigaray, M., Conradt, H. S., Grammel, N., Kratje, R., and Oggero, M. 2010. Highly glycosylated human alpha interferon: An insight into a new therapeutic candidate. *Journal of biotechnology* 146(1-2):74-83. <https://doi.org/10.1016/j.jbiotec.2009.12.020>.
- Chang, V. T., Crispin, M., Aricescu, A. R., Harvey, D. J., Nettleship, J. E., Fennelly, J. A., Yu, C., Boles, K. S., Evans, E. J., Stuart, D. I., Dwek, R. A., Jones, E. Y., Owens, R. J., and Davis, S. J. 2007. Glycoprotein structural genomics: solving the glycosylation problem. *Structure (London, England 1993)* 15(3):267-273. <https://doi.org/10.1016/j.str.2007.01.011>.
- Cheng, Y., and Prusoff, W. H. 1973. Relationship between the inhibition constant (K₁) and the concentration of inhibitor which causes 50 per cent inhibition (I₅₀) of an enzymatic reaction. *Biochemical pharmacology* 22(23):3099-3108.
- Chung, S. I., Horton, J. A., Ramalingam, T. R., White, A. O., Chung, E. J., Hudak, K. E., Scroggins, B. T., Arron, J. R., Wynn, T. A., and Citrin, D. E. 2016. IL-13 is a therapeutic target in radiation lung injury. *Scientific reports* 6:39714. <https://doi.org/10.1038/srep39714>.
- Clutterbuck, E. J., Hirst, E. M., and Sanderson, C. J. 1989. Human interleukin-5 (IL-5) regulates the production of eosinophils in human bone marrow cultures: comparison and interaction with IL-1, IL-3, IL-6, and GM-CSF. *Blood* 73(6):1504-1512.
- Coffman, R. L. 1989. Transforming growth factor beta specifically enhances IgA production by lipopolysaccharide-stimulated murine B lymphocytes. *Journal of Experimental Medicine* 170(3):1039-1044. <https://doi.org/10.1084/jem.170.3.1039>.
- Coffman, R. L., Ohara, J., Bond, M. W., Carty, J., Zlotnik, A., and Paul, W. E. 1986. B cell stimulatory factor-1 enhances the IgE response of lipopolysaccharide-activated B cells. *Journal of immunology (Baltimore, Md. 1950)* 136(12):4538-4541.
- Cook, M. L., and Bochner, B. S. 2010. Update on biological therapeutics for asthma. *The World Allergy Organization journal* 3(6):188-194. <https://doi.org/10.1097/WOX.0b013e3181e5ec5a>.

- Corren, J., Busse, W., Meltzer, E. O., Mansfield, L., Bensch, G., Fahrenholz, J., Wenzel, S. E., Chon, Y., Dunn, M., Weng, H. H., and Lin, S.-L. 2010. A randomized, controlled, phase 2 study of AMG 317, an IL-4R α antagonist, in patients with asthma. *American journal of respiratory and critical care medicine* 181(8):788-796. <https://doi.org/10.1164/rccm.200909-1448OC>.
- Croset, A., Delafosse, L., Gaudry, J.-P., Arod, C., Glez, L., Losberger, C., Begue, D., Krstanovic, A., Robert, F., Vilbois, F., Chevalet, L., and Antonsson, B. 2012. Differences in the glycosylation of recombinant proteins expressed in HEK and CHO cells. *Journal of biotechnology* 161(3):336-348. <https://doi.org/10.1016/j.jbiotec.2012.06.038>.
- Davoine, F., and Lacy, P. 2014. Eosinophil cytokines, chemokines, and growth factors: emerging roles in immunity. *Front. Immunol.* 5:570. <https://doi.org/10.3389/fimmu.2014.00570>.
- Deegan, P. B., and Cox, T. M. 2012. Imiglucerase in the treatment of Gaucher disease: a history and perspective. *Drug design, development and therapy* 6:81-106. <https://doi.org/10.2147/DDDT.S14395>.
- Defrance, T., Carayon, P., Billian, G., Guillemot, J. C., Minty, A., Caput, D., and Ferrara, P. 1994. Interleukin 13 is a B cell stimulating factor. *The Journal of experimental medicine* 179(1):135-143.
- Del Prete, G., Maggi, E., Parronchi, P., Chrétien, I., Tiri, A., Macchia, D., Ricci, M., Banchereau, J., Vries, J. de, and Romagnani, S. 1988. IL-4 is an essential factor for the IgE synthesis induced in vitro by human T cell clones and their supernatants. *Journal of immunology* (Baltimore, Md. 1950) 140(12):4193-4198.
- Doebber, T. W., Wu, M. S., Bugianesi, R. L., Ponpipom, M. M., Furbish, F. S., Barranger, J. A., Brady, R. O., and Shen, T. Y. 1982. Enhanced macrophage uptake of synthetically glycosylated human placental beta-glucocerebrosidase. *The Journal of biological chemistry* 257(5):2193-2199.
- Donaldson, D. D., Whitters, M. J., Fitz, L. J., Neben, T. Y., Finnerty, H., Henderson, S. L., Hara, R. M., Beier, D. R., Turner, K. J., Wood, C. R., and Collins, M. 1998. The Murine IL-13 Receptor α 2: Molecular Cloning, Characterization, and Comparison with Murine IL-13 Receptor α 1. *The Journal of Immunology* 161(5):2317-2324.
- Drazic, A., Myklebust, L. M., Ree, R., and Arnesen, T. 2016. The world of protein acetylation. *Biochimica et biophysica acta* 1864(10):1372-1401. <https://doi.org/10.1016/j.bbapap.2016.06.007>.
- Duppatla, V., Gjorgjevikj, M., Schmitz, W., Hermanns, H. M., Schäfer, C. M., Kottmair, M., Müller, T., and Sebald, W. 2014. IL-4 analogues with site-specific chemical modification at position 121 inhibit IL-4 and IL-13 biological activities. *Bioconjug. Chem.* 25(1):52-62. <https://doi.org/10.1021/bc400307k>.

- Duppatla, V., Gjorgjevikj, M., Schmitz, W., Kottmair, M., Mueller, T. D., and Sebald, W. 2012. Enzymatic deglutathionylation to generate interleukin-4 cysteine muteins with free thiol. *Bioconjug. Chem.* 23(7):1396-1405. <https://doi.org/10.1021/bc2004389>.
- East, L., and Isacke, C. M. 2002. The mannose receptor family. *Biochimica et biophysica acta* 1572(2-3):364-386.
- Egleton, R. D., Mitchell, S. A., Huber, J. D., Janders, J., Stropova, D., Polt, R., Yamamura, H. I., Hruby, V. J., and Davis, T. P. 2000. Improved bioavailability to the brain of glycosylated Met-enkephalin analogs. *Brain research* 881(1):37-46.
- Egrie, J. C., and Browne, J. K. 2001. Development and characterization of novel erythropoiesis stimulating protein (NESP). *British journal of cancer* 84 Suppl 1:3-10. <https://doi.org/10.1054/bjoc.2001.1746>.
- Egrie, J. C., Dwyer, E., Browne, J. K., Hitz, A., and Lykos, M. A. 2003. Darbepoetin alfa has a longer circulating half-life and greater in vivo potency than recombinant human erythropoietin. *Experimental hematology* 31(4):290-299.
- Eisenmesser, E. Z., Horita, D. A., Altieri, A. S., and Byrd, R. A. 2001. Solution structure of interleukin-13 and insights into receptor engagement. *Journal of molecular biology* 310(1):231-241. <https://doi.org/10.1006/jmbi.2001.4765>.
- Elbein, A. D., Tropea, J. E., Mitchell, M., and Kaushal, G. P. 1990. Kifunensine, a potent inhibitor of the glycoprotein processing mannosidase I. *The Journal of biological chemistry* 265(26):15599-15605.
- Elchinger, P.-H., Faugeras, P.-A., Boëns, B., Brouillette, F., Montplaisir, D., Zerrouki, R., and Lucas, R. 2011. Polysaccharides: The “Click” Chemistry Impact. *Polymers* 3(4):1607-1651. <https://doi.org/10.3390/polym3041607>.
- Ezekowitz, R. A., Williams, D. J., Koziel, H., Armstrong, M. Y., Warner, A., Richards, F. F., and Rose, R. M. 1991. Uptake of *Pneumocystis carinii* mediated by the macrophage mannose receptor. *Nature* 351(6322):155-158. <https://doi.org/10.1038/351155a0>.
- Fernandes, A. I., and Gregoriadis, G. 1996. Synthesis, characterization and properties of sialylated catalase. *Biochimica et biophysica acta* 1293(1):90-96.
- Fernandes, A. I., and Gregoriadis, G. 1997. Polysialylated asparaginase: preparation, activity and pharmacokinetics. *Biochimica et biophysica acta* 1341(1):26-34.
- Fernandes, A. P., and Holmgren, A. 2004. Glutaredoxins: glutathione-dependent redox enzymes with functions far beyond a simple thioredoxin backup system. *Antioxidants & redox signaling* 6(1):63-74. <https://doi.org/10.1089/152308604771978354>.
- Fichtner-Feigl, S., Strober, W., Kawakami, K., Puri, R. K., and Kitani, A. 2006. IL-13 signaling through the IL-13 α 2 receptor is involved in induction of TGF- β 1 production and fibrosis. *Nat Med* 12(1):99-106. <https://doi.org/10.1038/nm1332>.

- Fish, S. C., Donaldson, D. D., Goldman, S. J., Williams, C. M. M., and Kasaian, M. T. 2005. IgE Generation and Mast Cell Effector Function in Mice Deficient in IL-4 and IL-13. *The Journal of Immunology* 174(12):7716-7724. <https://doi.org/10.4049/jimmunol.174.12.7716>.
- Fujisawa, T., Joshi, B. H., and Puri, R. K. 2012. IL-13 regulates cancer invasion and metastasis through IL-13R α 2 via ERK/AP-1 pathway in mouse model of human ovarian cancer. *Int. J. Cancer* 131(2):344-356. <https://doi.org/10.1002/ijc.26366>.
- Fujita, T. 2002. Evolution of the lectin-complement pathway and its role in innate immunity. *Nature reviews. Immunology* 2(5):346-353. <https://doi.org/10.1038/nri800>.
- Furlan, R., Poliani, P. L., Marconi, P. C., Bergami, A., Ruffini, F., Adorini, L., Glorioso, J. C., Comi, G., and Martino, G. 2001. Central nervous system gene therapy with interleukin-4 inhibits progression of ongoing relapsing-remitting autoimmune encephalomyelitis in Biozzi AB/H mice. *Gene therapy* 8(1):13-19. <https://doi.org/10.1038/sj.gt.3301357>.
- Galili, U., Rachmilewitz, E. A., Peleg, A., and Flechner, I. 1984. A unique natural human IgG antibody with anti-alpha-galactosyl specificity. *The Journal of experimental medicine* 160(5):1519-1531.
- Galili, U., Shohet, S. B., Kobrin, E., Stults, C. L., and Macher, B. A. 1988. Man, apes, and Old World monkeys differ from other mammals in the expression of alpha-galactosyl epitopes on nucleated cells. *The Journal of biological chemistry* 263(33):17755-17762.
- Gamblin, D. P., Garnier, P., van Kasteren, S., Oldham, N. J., Fairbanks, A. J., and Davis, B. G. 2004. Glyco-SeS: selenenylsulfide-mediated protein glycoconjugation--a new strategy in post-translational modification. *Angewandte Chemie (International ed. in English)* 43(7):828-833. <https://doi.org/10.1002/anie.200352975>.
- Gandhi, N. A., Pirozzi, G., and Graham, N. M. H. 2017. Commonality of the IL-4/IL-13 pathway in atopic diseases. *Expert. Rev. Clin. Immunol.* 13(5):425-437. <https://doi.org/10.1080/1744666X.2017.1298443>.
- Gascan, H., Gauchat, J. F., Roncarolo, M. G., Yssel, H., Spits, H., and Vries, J. E. de. 1991. Human B cell clones can be induced to proliferate and to switch to IgE and IgG4 synthesis by interleukin 4 and a signal provided by activated CD4⁺ T cell clones. *The Journal of experimental medicine* 173(3):747-750.
- Gawlitzek, M., Estacio, M., Fürch, T., and Kiss, R. 2009. Identification of cell culture conditions to control N-glycosylation site-occupancy of recombinant glycoproteins expressed in CHO cells. *Biotechnology and bioengineering* 103(6):1164-1175. <https://doi.org/10.1002/bit.22348>.
- Geisberger, R., Lamers, M., and Achatz, G. 2006. The riddle of the dual expression of IgM and IgD. *Immunology* 118(4):429-437. <https://doi.org/10.1111/j.1365-2567.2006.02386.x>.
- Ghaderi, D., Zhang, M., Hurtado-Ziola, N., and Varki, A. 2012. Production platforms for biotherapeutic glycoproteins. Occurrence, impact, and challenges of non-human sialylation. *Biotechnology and Genetic Engineering Reviews* 28(1):147-176. <https://doi.org/10.5661/bger-28-147>.

- Giustarini, D., Dalle-Donne, I., Colombo, R., Milzani, A., and Rossi, R. 2008. Is ascorbate able to reduce disulfide bridges? A cautionary note. *Nitric oxide biology and chemistry* 19(3):252-258. <https://doi.org/10.1016/j.niox.2008.07.003>.
- Golay, J., Da Roit, F., Bologna, L., Ferrara, C., Leusen, J. H., Rambaldi, A., Klein, C., and Introna, M. 2013. Glycoengineered CD20 antibody obinutuzumab activates neutrophils and mediates phagocytosis through CD16B more efficiently than rituximab. *Blood* 122(20):3482-3491. <https://doi.org/10.1182/blood-2013-05-504043>.
- Graber, P., Gretener, D., Herren, S., Aubry, J. P., Elson, G., Poudrier, J., Lecoanet-Henchoz, S., Alouani, S., Losberger, C., Bonnefoy, J. Y., Kosco-Vilbois, M. H., and Gauchat, J. F. 1998. The distribution of IL-13 receptor alpha1 expression on B cells, T cells and monocytes and its regulation by IL-13 and IL-4. *Eur. J. Immunol.* 28(12):4286-4298.
- Gregoriadis, G., Fernandes, A., Mital, M., and McCormack, B. 2000. Polysialic acids: potential in improving the stability and pharmacokinetics of proteins and other therapeutics. *Cellular and molecular life sciences CMLS* 57(13-14):1964-1969. <https://doi.org/10.1007/PL00000676>.
- Grunewald, S. M., Kunzmann, S., Schnarr, B., Ezernieks, J., Sebald, W., and Duschl, A. 1997. A murine interleukin-4 antagonistic mutant protein completely inhibits interleukin-4-induced cell proliferation, differentiation, and signal transduction. *The Journal of biological chemistry* 272(3):1480-1483.
- Grunewald, S. M., Werthmann, A., Schnarr, B., Klein, C. E., Bröcker, E. B., Mohrs, M., Brombacher, F., Sebald, W., and Duschl, A. 1998. An antagonistic IL-4 mutant prevents type I allergy in the mouse: inhibition of the IL-4/IL-13 receptor system completely abrogates humoral immune response to allergen and development of allergic symptoms in vivo. *Journal of immunology (Baltimore, Md. 1950)* 160(8):4004-4009.
- Hage, T., Sebald, W., and Reinemer, P. 1999. Crystal structure of the interleukin-4/receptor alpha chain complex reveals a mosaic binding interface. *Cell* 97(2):271-281.
- Hansen, G., Hercus, T. R., McClure, B. J., Stomski, F. C., Dottore, M., Powell, J., Ramshaw, H., Woodcock, J. M., Xu, Y., Guthridge, M., McKinstry, W. J., Lopez, A. F., and Parker, M. W. 2008. The structure of the GM-CSF receptor complex reveals a distinct mode of cytokine receptor activation. *Cell* 134(3):496-507. <https://doi.org/10.1016/j.cell.2008.05.053>.
- Haurum, J. S., Thiel, S., Haagsman, H. P., Laursen, S. B., Larsen, B., and Jensenius, J. C. 1993. Studies on the carbohydrate-binding characteristics of human pulmonary surfactant-associated protein A and comparison with two other collectins: mannan-binding protein and conglutinin. *The Biochemical journal* 293 (Pt 3):873-878.
- Hershey, G. K. K. 2003. IL-13 receptors and signaling pathways: an evolving web. *J. Allergy Clin. Immunol.* 111(4):677-90; quiz 691.
- Heufler, C., Koch, F., Stanzl, U., Topar, G., Wysocka, M., Trinchieri, G., Enk, A., Steinman, R. M., Romani, N., and Schuler, G. 1996. Interleukin-12 is produced by dendritic cells and

- mediates T helper 1 development as well as interferon-gamma production by T helper 1 cells. *European journal of immunology* 26(3):659-668. <https://doi.org/10.1002/eji.1830260323>.
- Higashi, H., Naiki, M., Matuo, S., and Ōkouchi, K. 1977. Antigen of "serum sickness" type of heterophile antibodies in human sera: Identification as gangliosides with N-glycolylneuraminic acid. *Biochemical and Biophysical Research Communications* 79(2):388-395. [https://doi.org/10.1016/0006-291X\(77\)90169-3](https://doi.org/10.1016/0006-291X(77)90169-3).
- Hsieh, C. S., Heimberger, A. B., Gold, J. S., O'Garra, A., and Murphy, K. M. 1992. Differential regulation of T helper phenotype development by interleukins 4 and 10 in an alpha beta T-cell-receptor transgenic system. *Proc. Natl. Acad. Sci. U S A* 89(13):6065-6069.
- Hsu, C.-H., Hung, S.-C., Wu, C.-Y., and Wong, C.-H. 2011. Toward automated oligosaccharide synthesis. *Angewandte Chemie (International ed. in English)* 50(50):11872-11923. <https://doi.org/10.1002/anie.201100125>.
- Ito, T., Suzuki, S., Kanaji, S., Shiraishi, H., Ohta, S., Arima, K., Tanaka, G., Tamada, T., Honjo, E., Garcia, K. C., Kuroki, R., and Izuhara, K. 2009. Distinct structural requirements for interleukin-4 (IL-4) and IL-13 binding to the shared IL-13 receptor facilitate cellular tuning of cytokine responsiveness. *The Journal of biological chemistry* 284(36):24289-24296. <https://doi.org/10.1074/jbc.M109.007286>.
- Jiménez-García, L., Herránz, S., Luque, A., and Hortelano, S. 2015. Critical role of p38 MAPK in IL-4-induced alternative activation of peritoneal macrophages. *European journal of immunology* 45(1):273-286. <https://doi.org/10.1002/eji.201444806>.
- Kannicht, C., Ramström, M., Kohla, G., Tiemeyer, M., Casademunt, E., Walter, O., and Sandberg, H. 2013. Characterisation of the post-translational modifications of a novel, human cell line-derived recombinant human factor VIII. *Thrombosis research* 131(1):78-88. <https://doi.org/10.1016/j.thromres.2012.09.011>.
- Kaur, D., Hollins, F., Woodman, L., Yang, W., Monk, P., May, R., Bradding, P., and Brightling, C. E. 2006. Mast cells express IL-13R alpha 1: IL-13 promotes human lung mast cell proliferation and Fc epsilon RI expression. *Allergy* 61(9):1047-1053. <https://doi.org/10.1111/j.1398-9995.2006.01139.x>.
- Khan, A. H., Bayat, H., Rajabibazl, M., Sabri, S., and Rahimpour, A. 2017. Humanizing glycosylation pathways in eukaryotic expression systems. *World journal of microbiology & biotechnology* 33(1):4. <https://doi.org/10.1007/s11274-016-2172-7>.
- Kinet, J. P. 1999. The high-affinity IgE receptor (Fc epsilon RI): from physiology to pathology. *Annual review of immunology* 17:931-972. <https://doi.org/10.1146/annurev.immunol.17.1.931>.
- Kolb, H. C., Finn, M. G., and Sharpless, K. B. 2001. Click Chemistry: Diverse Chemical Function from a Few Good Reactions. *Angewandte Chemie (International ed. in English)* 40(11):2004-2021.
- Korenblat, P., Kerwin, E., Leshchenko, I., Yen, K., Holweg, C. T. J., Anzures-Cabrera, J., Martin, C., Putnam, W. S., Governale, L., Olsson, J., and Matthews, J. G. 2018. Efficacy and safety of

- lebrikizumab in adult patients with mild-to-moderate asthma not receiving inhaled corticosteroids. *Respiratory medicine* 134:143-149. <https://doi.org/10.1016/j.rmed.2017.12.006>.
- Kraich, M. 2008. Strukturelle und funktionelle Untersuchungen der Interaktion zwischen Ligand und Rezeptor im Interleukin-4- und Interleukin-13-System. PhD thesis, 2008.
- Kraich, M., Klein, M., Patiño, E., Harrer, H., Nickel, J., Sebald, W., and Mueller, T. D. 2006. A modular interface of IL-4 allows for scalable affinity without affecting specificity for the IL-4 receptor. *BMC. Biol.* 4:13. <https://doi.org/10.1186/1741-7007-4-13>.
- Krasnova, L., and Wong, C.-H. 2016. Understanding the Chemistry and Biology of Glycosylation with Glycan Synthesis. *Annual review of biochemistry* 85:599-630. <https://doi.org/10.1146/annurev-biochem-060614-034420>.
- Kruse, N., Lehrnbecher, T., and Sebald, W. 1991. Site-directed mutagenesis reveals the importance of disulfide bridges and aromatic residues for structure and proliferative activity of human interleukin-4. *FEBS letters* 286(1-2):58-60.
- Kruse, N., Shen, B. J., Arnold, S., Tony, H. P., Müller, T., and Sebald, W. 1993. Two distinct functional sites of human interleukin 4 are identified by variants impaired in either receptor binding or receptor activation. *EMBO. J.* 12(13):5121-5129.
- Kruse, N., Tony, H. P., and Sebald, W. 1992. Conversion of human interleukin-4 into a high affinity antagonist by a single amino acid replacement. *EMBO. J.* 11(9):3237-3244.
- Kunkel, J. P., Jan, D. C., Butler, M., and Jamieson, J. C. 2000. Comparisons of the glycosylation of a monoclonal antibody produced under nominally identical cell culture conditions in two different bioreactors. *Biotechnology progress* 16(3):462-470. <https://doi.org/10.1021/bp000026u>.
- Ladel, C. H., Szalay, G., Riedel, D., and Kaufmann, S. H. 1997. Interleukin-12 secretion by *Mycobacterium tuberculosis*-infected macrophages. *Infection and immunity* 65(5):1936-1938.
- Lallana, E., Fernandez-Megia, E., and Riguera, R. 2009. Surpassing the use of copper in the click functionalization of polymeric nanostructures: a strain-promoted approach. *Journal of the American Chemical Society* 131(16):5748-5750. <https://doi.org/10.1021/ja8100243>.
- Lallana, E., Riguera, R., and Fernandez-Megia, E. 2011. Reliable and efficient procedures for the conjugation of biomolecules through Huisgen azide-alkyne cycloadditions. *Angewandte Chemie (International ed. in English)* 50(38):8794-8804. <https://doi.org/10.1002/anie.201101019>.
- Lalonde, M.-E., and Durocher, Y. 2017. Therapeutic glycoprotein production in mammalian cells. *Journal of biotechnology* 251:128-140. <https://doi.org/10.1016/j.jbiotec.2017.04.028>.
- Lam, P. V. N., Goldman, R., Karagiannis, K., Narsule, T., Simonyan, V., Soika, V., and Mazumder, R. 2013. Structure-based comparative analysis and prediction of N-linked glycosylation sites in evolutionarily distant eukaryotes. *Genomics, proteomics & bioinformatics* 11(2):96-104. <https://doi.org/10.1016/j.gpb.2012.11.003>.

- LaPorte, S. L., Juo, Z. S., Vaclavikova, J., Colf, L. A., Qi, X., Heller, N. M., Keegan, A. D., and Garcia, K. C. 2008. Molecular and structural basis of cytokine receptor pleiotropy in the interleukin-4/13 system. *Cell* 132(2):259-272. <https://doi.org/10.1016/j.cell.2007.12.030>.
- Lappin, M. B., and Campbell, J. D. 2000. The Th1-Th2 classification of cellular immune responses: concepts, current thinking and applications in haematological malignancy. *Blood reviews* 14(4):228-239. <https://doi.org/10.1054/blre.2000.0136>.
- Largent, B. L., Walton, K. M., Hoppe, C. A., Lee, Y. C., and Schnaar, R. L. 1984. Carbohydrate-specific adhesion of alveolar macrophages to mannose-derivatized surfaces. *The Journal of biological chemistry* 259(3):1764-1769.
- Le, H. V., Ramanathan, L., Labdon, J. E., Mays-Ichinco, C. A., Syto, R., Arai, N., Hoy, P., Takebe, Y., Nagabhushan, T. L., and Trotta, P. P. 1988. Isolation and characterization of multiple variants of recombinant human interleukin 4 expressed in mammalian cells. *The Journal of biological chemistry* 263(22):10817-10823.
- Le Gros, G., Ben-Sasson, S. Z., Seder, R., Finkelman, F. D., and Paul, W. E. 1990. Generation of interleukin 4 (IL-4)-producing cells in vivo and in vitro: IL-2 and IL-4 are required for in vitro generation of IL-4-producing cells. *J. Exp. Med.* 172(3):921-929.
- Lefort, S., Vita, N., Reeb, R., Caput, D., and Ferrara, P. 1995. IL-13 and IL-4 share signal transduction elements as well as receptor components in TF-1 cells. *FEBS letters* 366(2-3):122-126.
- Leonard, W. J. 2001. Cytokines and immunodeficiency diseases. *Nat. Rev. Immunol.* 1(3):200-208. <https://doi.org/10.1038/35105066>.
- Letzelter, F., Wang, Y., and Sebald, W. 1998. The interleukin-4 site-2 epitope determining binding of the common receptor gamma chain. *European journal of biochemistry* 257(1):11-20.
- Li, R., Xie, C., Zhang, Y., Li, B., Donelan, W., Li, S., Han, S., Wang, X., Cui, T., and Tang, D. 2014. Expression of recombinant human IL-4 in *Pichia pastoris* and relationship between its glycosylation and biological activity. *Protein expression and purification* 96:1-7. <https://doi.org/10.1016/j.pep.2014.01.005>.
- Li, S., Cai, H., He, J., Chen, H., Lam, S., Cai, T., Zhu, Z., Bark, S. J., and Cai, C. 2016. Extent of the Oxidative Side Reactions to Peptides and Proteins During the CuAAC Reaction. *Bioconjugate chemistry* 27(10):2315-2322. <https://doi.org/10.1021/acs.bioconjchem.6b00267>.
- Loh, Y. P., and Gainer, H. 1980. Evidence that glycosylation of pro-opiocortin and ACTH influences their proteolysis by trypsin and blood proteases. *Molecular and cellular endocrinology* 20(1):35-44.
- Longphre, M. V., and Fuller, R. W. 2010. Aerovant (recombinant human interleukin-4 variant). Pages 123–126 in: *New Drugs and Targets for Asthma and COPD*. T. Hansel, and P. Barnes, eds. KARGER, Basel.
- Lopez, A. F., Hercus, T. R., Ekert, P., Littler, D. R., Guthridge, M., Thomas, D., Ramshaw, H. S., Stomski, F., Perugini, M., D'Andrea, R., Grimbaldeston, M., and Parker, M. W. 2010.

- Molecular basis of cytokine receptor activation. *IUBMB life* 62(7):509-518.
<https://doi.org/10.1002/iub.350>.
- López, C. J., Fleissner, M. R., Brooks, E. K., and Hubbell, W. L. 2014. Stationary-phase EPR for exploring protein structure, conformation, and dynamics in spin-labeled proteins. *Biochemistry* 53(45):7067-7075. <https://doi.org/10.1021/bi5011128>.
- Lundgren, M., Persson, U., Larsson, P., Magnusson, C., Smith, C. I., Hammarström, L., and Severinson, E. 1989. Interleukin 4 induces synthesis of IgE and IgG4 in human B cells. *European journal of immunology* 19(7):1311-1315. <https://doi.org/10.1002/eji.1830190724>.
- Maggi, E., Parronchi, P., Manetti, R., Simonelli, C., Piccinni, M. P., Ruggi, F. S., Carli, M. de, Ricci, M., and Romagnani, S. 1992. Reciprocal regulatory effects of IFN-gamma and IL-4 on the in vitro development of human Th1 and Th2 clones. *J. Immunol.* 148(7):2142-2147.
- McCormick, S. M., and Heller, N. M. 2015. Commentary: IL-4 and IL-13 receptors and signaling. *Cytokine* 75(1):38-50. <https://doi.org/10.1016/j.cyto.2015.05.023>.
- McGary, C. W. 1960. Degradation of poly(ethylene oxide). *J. Polym. Sci.* 46(147):51-57.
<https://doi.org/10.1002/pol.1960.1204614705>.
- McIntyre, T. M. 1993. Transforming growth factor beta 1 selectivity stimulates immunoglobulin G2b secretion by lipopolysaccharide-activated murine B cells. *Journal of Experimental Medicine* 177(4):1031-1037. <https://doi.org/10.1084/jem.177.4.1031>.
- McKenzie, G. J., Fallon, P. G., Emson, C. L., Grecis, R. K., and McKenzie, A. N. 1999. Simultaneous disruption of interleukin (IL)-4 and IL-13 defines individual roles in T helper cell type 2-mediated responses. *The Journal of experimental medicine* 189(10):1565-1572.
- Michael, A. 1893. Ueber die Einwirkung von Diazobenzolimid auf Acetylendicarbonsäuremethylester. *J. Prakt. Chem.* 48(1):94-95.
<https://doi.org/10.1002/prac.18930480114>.
- Miloux, B., Laurent, P., Bonnin, O., Lupker, J., Caput, D., Vita, N., and Ferrara, P. 1997. Cloning of the human IL-13R α 1 chain and reconstitution with the IL-4R α of a functional IL-4/IL-13 receptor complex. *FEBS letters* 401(2-3):163-166. [https://doi.org/10.1016/S0014-5793\(96\)01462-7](https://doi.org/10.1016/S0014-5793(96)01462-7).
- Mononen, I., and Karjalainen, E. 1984. Structural comparison of protein sequences around potential N-glycosylation sites. *Biochimica et Biophysica Acta (BBA) - Protein Structure and Molecular Enzymology* 788(3):364-367. [https://doi.org/10.1016/0167-4838\(84\)90050-5](https://doi.org/10.1016/0167-4838(84)90050-5).
- Morell, A. G., Gregoriadis, G., Scheinberg, I. H., Hickman, J., and Ashwell, G. 1971. The role of sialic acid in determining the survival of glycoproteins in the circulation. *The Journal of biological chemistry* 246(5):1461-1467.
- Mossner, E., Brunker, P., Moser, S., Puntener, U., Schmidt, C., Herter, S., Grau, R., Gerdes, C., Nopora, A., van Puijenbroek, E., Ferrara, C., Sondermann, P., Jager, C., Strein, P., Fertig, G., Friess, T., Schull, C., Bauer, S., Dal Porto, J., Del Nagro, C., Dabbagh, K., Dyer, M. J. S., Poppema, S., Klein, C., and Umans, P. 2010. Increasing the efficacy of CD20 antibody therapy

- through the engineering of a new type II anti-CD20 antibody with enhanced direct and immune effector cell-mediated B-cell cytotoxicity. *Blood* 115(22):4393-4402.
<https://doi.org/10.1182/blood-2009-06-225979>.
- Mott, H. R., and Campbell, I. D. 1995. Four-helix bundle growth factors and their receptors: protein-protein interactions. *Current Opinion in Structural Biology* 5(1):114-121.
- Moy, F. J., Diblasio, E., Wilhelm, J., and Powers, R. 2001. Solution structure of human IL-13 and implication for receptor binding. *Journal of molecular biology* 310(1):219-230.
<https://doi.org/10.1006/jmbi.2001.4764>.
- Muchmore, E. A., Diaz, S., and Varki, A. 1998. A structural difference between the cell surfaces of humans and the great apes. *American journal of physical anthropology* 107(2):187-198.
[https://doi.org/10.1002/\(SICI\)1096-8644\(199810\)107:2<187:AID-AJPA5>3.0.CO;2-S](https://doi.org/10.1002/(SICI)1096-8644(199810)107:2<187:AID-AJPA5>3.0.CO;2-S).
- Mueller, T. D., Zhang, J.-L., Sebald, W., and Duschl, A. 2002. Structure, binding, and antagonists in the IL-4/IL-13 receptor system. *Biochimica et biophysica acta* 1592(3):237-250.
- Müller, T., Sebald, W., and Oschkinat, H. 1994. Antagonist design through forced electrostatic mismatch. *Nature structural biology* 1(10):674-676.
- Munitz, A., Brandt, E. B., Mingler, M., Finkelman, F. D., and Rothenberg, M. E. 2008. Distinct roles for IL-13 and IL-4 via IL-13 receptor alpha1 and the type II IL-4 receptor in asthma pathogenesis. *Proceedings of the National Academy of Sciences of the United States of America* 105(20):7240-7245. <https://doi.org/10.1073/pnas.0802465105>.
- Nadesalingam, J., Dodds, A. W., Reid, K. B. M., and Palaniyar, N. 2005. Mannose-Binding Lectin Recognizes Peptidoglycan via the N-Acetyl Glucosamine Moiety, and Inhibits Ligand-Induced Proinflammatory Effect and Promotes Chemokine Production by Macrophages. *The Journal of Immunology* 175(3):1785-1794. <https://doi.org/10.4049/jimmunol.175.3.1785>.
- Nakamura, T., Lee, R. K., Nam, S. Y., Podack, E. R., Bottomly, K., and Flavell, R. A. 1997. Roles of IL-4 and IFN-gamma in stabilizing the T helper cell type 1 and 2 phenotype. *J. Immunol.* 158(6):2648-2653.
- Padler-Karavani, V., Yu, H., Cao, H., Chokhawala, H., Karp, F., Varki, N., Chen, X., and Varki, A. 2008. Diversity in specificity, abundance, and composition of anti-Neu5Gc antibodies in normal humans: potential implications for disease. *Glycobiology* 18(10):818-830.
<https://doi.org/10.1093/glycob/cwn072>.
- Panettieri, R. A., Wang, M., Braddock, M., Bowen, K., and Colice, G. 2018. Tralokinumab for the treatment of severe, uncontrolled asthma: the ATMOSPHERE clinical development program. *Immunotherapy* 10(6):473-490. <https://doi.org/10.2217/imt-2017-0191>.
- Park, K.-H., Seo, G.-Y., Jang, Y.-S., and Kim, P.-H. 2012. TGF- β and BAFF derived from CD4+CD25+Foxp3+ T cells mediate mouse IgA isotype switching. *Genes Genom* 34(6):619-625. <https://doi.org/10.1007/s13258-012-0062-4>.
- Parker, D. C. 1993. T cell-dependent B cell activation. *Annual review of immunology* 11:331-360.
<https://doi.org/10.1146/annurev.iy.11.040193.001555>.

- Parronchi, P., Carli, M. de, Manetti, R., Simonelli, C., Sampognaro, S., Piccinni, M. P., Macchia, D., Maggi, E., Del Prete, G., and Romagnani, S. 1992. IL-4 and IFN (alpha and gamma) exert opposite regulatory effects on the development of cytolytic potential by Th1 or Th2 human T cell clones. *J. Immunol.* 149(9):2977-2983.
- Patino, E., Kotzsch, A., Sarembo, S., Nickel, J., Schmitz, W., Sebald, W., and Mueller, T. D. 2011. Structure analysis of the IL-5 ligand-receptor complex reveals a wrench-like architecture for IL-5R α . *Structure (London, England 1993)* 19(12):1864-1875. <https://doi.org/10.1016/j.str.2011.08.015>.
- Paveley, R. A., Aynsley, S. A., Turner, J. D., Bourke, C. D., Jenkins, S. J., Cook, P. C., Martinez-Pomares, L., and Mountford, A. P. 2011. The Mannose Receptor (CD206) is an important pattern recognition receptor (PRR) in the detection of the infective stage of the helminth *Schistosoma mansoni* and modulates IFN γ production. *International journal for parasitology* 41(13-14):1335-1345. <https://doi.org/10.1016/j.ijpara.2011.08.005>.
- Perlman, S., van den Hazel, B., Christiansen, J., Gram-Nielsen, S., Jeppesen, C. B., Andersen, K. V., Halkier, T., Okkels, S., and Schambye, H. T. 2003. Glycosylation of an N-terminal extension prolongs the half-life and increases the in vivo activity of follicle stimulating hormone. *The Journal of clinical endocrinology and metabolism* 88(7):3227-3235. <https://doi.org/10.1210/jc.2002-021201>.
- Piirainen, M. A., Boer, H., Ruijter, J. C. de, and Frey, A. D. 2016. A dual approach for improving homogeneity of a human-type N-glycan structure in *Saccharomyces cerevisiae*. *Glycoconjugate journal* 33(2):189-199. <https://doi.org/10.1007/s10719-016-9656-4>.
- Ponomarev, E. D., Maresz, K., Tan, Y., and Dittel, B. N. 2007. CNS-derived interleukin-4 is essential for the regulation of autoimmune inflammation and induces a state of alternative activation in microglial cells. *The Journal of neuroscience the official journal of the Society for Neuroscience* 27(40):10714-10721. <https://doi.org/10.1523/JNEUROSCI.1922-07.2007>.
- Popovic, B., Breed, J., Rees, D. G., Gardener, M. J., Vinall, L. M. K., Kemp, B., Spooner, J., Keen, J., Minter, R., Uddin, F., Colice, G., Wilkinson, T., Vaughan, T., and May, R. D. 2017. Structural Characterisation Reveals Mechanism of IL-13-Neutralising Monoclonal Antibody Tralokinumab as Inhibition of Binding to IL-13R α 1 and IL-13R α 2. *Journal of molecular biology* 429(2):208-219. <https://doi.org/10.1016/j.jmb.2016.12.005>.
- Powell, J., and Gurk-Turner, C. 2002. Darbepoetin alfa (Aranesp). *Proceedings (Baylor University. Medical Center)* 15(3):332-335.
- Powers, R., Garrett, D. S., March, C. J., Frieden, E. A., Gronenborn, A. M., and Clore, G. M. 1992. Three-dimensional solution structure of human interleukin-4 by multidimensional heteronuclear magnetic resonance spectroscopy. *Science (New York, N.Y.)* 256(5064):1673-1677.
- Powers, R., Garrett, D. S., March, C. J., Frieden, E. A., Gronenborn, A. M., and Clore, G. M. 1993. The high-resolution, three-dimensional solution structure of human interleukin-4 determined by

- multidimensional heteronuclear magnetic resonance spectroscopy. *Biochemistry* 32(26):6744-6762.
- Punnonen, J., Aversa, G., Cocks, B. G., McKenzie, A. N., Menon, S., Zurawski, G., Waal Malefyt, R. de, and Vries, J. E. de. 1993. Interleukin 13 induces interleukin 4-independent IgG4 and IgE synthesis and CD23 expression by human B cells. *Proc. Natl. Acad. Sci. U S A* 90(8):3730-3734.
- Racke, M. K., Bonomo, A., Scott, D. E., Cannella, B., Levine, A., Raine, C. S., Shevach, E. M., and Röcken, M. 1994. Cytokine-induced immune deviation as a therapy for inflammatory autoimmune disease. *The Journal of experimental medicine* 180(5):1961-1966.
- Rahkila, J., Ekholm, F., and Leino, R. 2018. Cu(I) mediated degradation of polysaccharides leads to fragments with narrow polydispersities. *Eur. J. Org. Chem.*
<https://doi.org/10.1002/ejoc.201800033>.
- Raju, T. S., and Scallon, B. 2007. Fc glycans terminated with N-acetylglucosamine residues increase antibody resistance to papain. *Biotechnology progress* 23(4):964-971.
<https://doi.org/10.1021/bp070118k>.
- Ramalingam, T. R., Pesce, J. T., Sheikh, F., Cheever, A. W., Mentink-Kane, M. M., Wilson, M. S., Stevens, S., Valenzuela, D. M., Murphy, A. J., Yancopoulos, G. D., Urban, J. F., Donnelly, R. P., and Wynn, T. A. 2008. Unique functions of the type II interleukin 4 receptor identified in mice lacking the interleukin 13 receptor alpha1 chain. *Nature immunology* 9(1):25-33.
<https://doi.org/10.1038/ni1544>.
- Reese, T. A., Liang, H.-E., Tager, A. M., Luster, A. D., van Rooijen, N., Voehringer, D., and Locksley, R. M. 2007. Chitin induces accumulation in tissue of innate immune cells associated with allergy. *Nature* 447(7140):92-96. <https://doi.org/10.1038/nature05746>.
- Reusch, D., and Tejada, M. L. 2015. Fc glycans of therapeutic antibodies as critical quality attributes. *Glycobiology* 25(12):1325-1334. <https://doi.org/10.1093/glycob/cwv065>.
- Roberts, M. J., and Harris, J. M. 1998. Attachment of degradable poly(ethylene glycol) to proteins has the potential to increase therapeutic efficacy. *Journal of pharmaceutical sciences* 87(11):1440-1445. <https://doi.org/10.1021/js9800634>.
- Röcken, M., Racke, M., and Shevach, E. M. 1996. IL-4-induced immune deviation as antigen-specific therapy for inflammatory autoimmune disease. *Immunology today* 17(5):225-231.
- Rodríguez-Martínez, J. A., Rivera-Rivera, I., Solá, R. J., and Griebenow, K. 2009. Enzymatic activity and thermal stability of PEG-alpha-chymotrypsin conjugates. *Biotechnology letters* 31(6):883-887. <https://doi.org/10.1007/s10529-009-9947-y>.
- Rosa, C., Amr, S., Birken, S., Wehmann, R., and Nisula, B. 1984. Effect of desialylation of human chorionic gonadotropin on its metabolic clearance rate in humans. *The Journal of clinical endocrinology and metabolism* 59(6):1215-1219. <https://doi.org/10.1210/jcem-59-6-1215>.
- Rostovtsev, V. V., Green, L. G., Fokin, V. V., and Sharpless, K. B. 2002. A stepwise Huisgen cycloaddition process: copper(I)-catalyzed regioselective "ligation" of azides and terminal

- alkynes. *Angewandte Chemie (International ed. in English)* 41(14):2596-2599.
[https://doi.org/10.1002/1521-3773\(20020715\)41:14<2596:AID-ANIE2596>3.0.CO;2-4](https://doi.org/10.1002/1521-3773(20020715)41:14<2596:AID-ANIE2596>3.0.CO;2-4).
- Rozwarski, D. A., Gronenborn, A. M., Clore, G. M., Bazan, J. F., Bohm, A., Wlodawer, A., Hatada, M., and Karplus, P. A. 1994. Structural comparisons among the short-chain helical cytokines. *Structure (London, England 1993)* 2(3):159-173.
- Runkel, L., Meier, W., Pepinsky, R. B., Karpusas, M., Whitty, A., Kimball, K., Brickelmaier, M., Muldowney, C., Jones, W., and Goelz, S. E. 1998. Structural and functional differences between glycosylated and non-glycosylated forms of human interferon-beta (IFN-beta). *Pharmaceutical research* 15(4):641-649.
- Sanderson, C. J. 1992. Interleukin-5, eosinophils, and disease. *Blood* 79(12):3101-3109.
- Schleimer, R. P., Sterbinsky, S. A., Kaiser, J., Bickel, C. A., Klunk, D. A., Tomioka, K., Newman, W., Luscinikas, F. W., Gimbrone, M. A., and McIntyre, B. W. 1992. IL-4 induces adherence of human eosinophils and basophils but not neutrophils to endothelium. Association with expression of VCAM-1. *J. Immunol.* 148(4):1086-1092.
- Schnarr, B., Ezernieks, J., Sebald, W., and Duschl, A. 1997. IL-4 receptor complexes containing or lacking the gamma C chain are inhibited by an overlapping set of antagonistic IL-4 mutant proteins. *International Immunology* 9(6):861-868.
- Schroeder, H. W., and Cavacini, L. 2010. Structure and function of immunoglobulins. *The Journal of allergy and clinical immunology* 125(2 Suppl 2):S41-52.
<https://doi.org/10.1016/j.jaci.2009.09.046>.
- Seder, R. A., Gazzinelli, R., Sher, A., and Paul, W. E. 1993. Interleukin 12 acts directly on CD4+ T cells to enhance priming for interferon gamma production and diminishes interleukin 4 inhibition of such priming. *Proceedings of the National Academy of Sciences of the United States of America* 90(21):10188-10192.
- Shakin-Eshleman, S. H., Spitalnik, S. L., and Kasturi, L. 1996. The amino acid at the X position of an Asn-X-Ser sequon is an important determinant of N-linked core-glycosylation efficiency. *The Journal of biological chemistry* 271(11):6363-6366.
- Shanafelt, A. B., Forte, C. P., Kasper, J. J., Sanchez-Pescador, L., Wetzel, M., Gundel, R., and Greve, J. M. 1998. An immune cell-selective interleukin 4 agonist. *Proceedings of the National Academy of Sciences of the United States of America* 95(16):9454-9458.
- Sheikh, F., Dickensheets, H., Pedras-Vasconcelos, J., Ramalingam, T., Helming, L., Gordon, S., and Donnelly, R. P. 2015. The Interleukin-13 Receptor- α 1 Chain Is Essential for Induction of the Alternative Macrophage Activation Pathway by IL-13 but Not IL-4. *Journal of innate immunity* 7(5):494-505. <https://doi.org/10.1159/000376579>.
- Shen, B. J., Hage, T., and Sebald, W. 1996. Global and local determinants for the kinetics of interleukin-4/interleukin-4 receptor alpha chain interaction. A biosensor study employing recombinant interleukin-4-binding protein. *European journal of biochemistry* 240(1):252-261.

- Singh, S. M., and Panda, A. K. 2005. Solubilization and refolding of bacterial inclusion body proteins. *Journal of bioscience and bioengineering* 99(4):303-310.
<https://doi.org/10.1263/jbb.99.303>.
- Slager, R. E., Otulana, B. A., Hawkins, G. A., Yen, Y. P., Peters, S. P., Wenzel, S. E., Meyers, D. A., and Bleecker, E. R. 2012. IL-4 receptor polymorphisms predict reduction in asthma exacerbations during response to an anti-IL-4 receptor α antagonist. *The Journal of allergy and clinical immunology* 130(2):516-22.e4. <https://doi.org/10.1016/j.jaci.2012.03.030>.
- Smith, L. J., Redfield, C., Boyd, J., Lawrence, G. M., Edwards, R. G., Smith, R. A., and Dobson, C. M. 1992. Human interleukin 4. The solution structure of a four-helix bundle protein. *Journal of molecular biology* 224(4):899-904.
- Solá, R. J., and Griebenow, K. 2010. Glycosylation of therapeutic proteins: an effective strategy to optimize efficacy. *BioDrugs*. 24(1):9-21. <https://doi.org/10.2165/11530550-000000000-00000>.
- Sonoda, E. 1989. Transforming growth factor beta induces IgA production and acts additively with interleukin 5 for IgA production. *Journal of Experimental Medicine* 170(4):1415-1420.
<https://doi.org/10.1084/jem.170.4.1415>.
- Sornasse, T., Larenas, P. V., Davis, K. A., Vries, J. E. de, and Yssel, H. 1996. Differentiation and stability of T helper 1 and 2 cells derived from naive human neonatal CD4⁺ T cells, analyzed at the single-cell level. *J. Exp. Med.* 184(2):473-483.
- Spicer, C. D., and Davis, B. G. 2014. Selective chemical protein modification. *Nature communications* 5:4740. <https://doi.org/10.1038/ncomms5740>.
- Spiess, M. 1990. The asialoglycoprotein receptor: a model for endocytic transport receptors. *Biochemistry* 29(43):10009-10018.
- Sprang, S. R., and Fernando Bazan, J. 1993. Cytokine structural taxonomy and mechanisms of receptor engagement. *Current Opinion in Structural Biology* 3(6):815-827.
[https://doi.org/10.1016/0959-440X\(93\)90144-A](https://doi.org/10.1016/0959-440X(93)90144-A).
- Stahl, P., Schlesinger, P. H., Sigardson, E., Rodman, J. S., and Lee, Y. C. 1980. Receptor-mediated pinocytosis of mannose glycoconjugates by macrophages: characterization and evidence for receptor recycling. *Cell* 19(1):207-215.
- Staros, J. V., Bayley, H., Standring, D. N., and Knowles, J. R. 1978. Reduction of aryl azides by thiols: implications for the use of photoaffinity reagents. *Biochemical and Biophysical Research Communications* 80(3):568-572.
- Stavnezer, J., and Schrader, C. E. 2014. IgH chain class switch recombination: mechanism and regulation. *Journal of immunology* (Baltimore, Md. 1950) 193(11):5370-5378.
<https://doi.org/10.4049/jimmunol.1401849>.
- Stockert, R. J., Kressner, M. S., Collins, J. C., Sternlieb, I., and Morell, A. G. 1982. IgA interaction with the asialoglycoprotein receptor. *Proceedings of the National Academy of Sciences of the United States of America* 79(20):6229-6231.

- Stone, K. D., Prussin, C., and Metcalfe, D. D. 2010. IgE, mast cells, basophils, and eosinophils. *J. Allergy. Clin. Immunol.* 125(2 Suppl 2):S73-80. <https://doi.org/10.1016/j.jaci.2009.11.017>.
- Swain, S. L., Weinberg, A. D., English, M., and Huston, G. 1990. IL-4 directs the development of Th2-like helper effectors. *J. Immunol.* 145(11):3796-3806.
- Tams, J. W., Vind, J., and Welinder, K. G. 1999. Adapting protein solubility by glycosylation. N-glycosylation mutants of *Coprinus cinereus* peroxidase in salt and organic solutions. *Biochimica et biophysica acta* 1432(2):214-221.
- Tomkinson, A. 2011. Use of modified il-4 mutien receptor antagonists to treat dermatitis.
- Tony, H. P., Shen, B. J., Reusch, P., and Sebald, W. 1994. Design of human interleukin-4 antagonists inhibiting interleukin-4-dependent and interleukin-13-dependent responses in T-cells and B-cells with high efficiency. *Eur. J. Biochem.* 225(2):659-665.
- Tornøe, C. W., Christensen, C., and Meldal, M. 2002. Peptidotriazoles on solid phase: 1,2,3-triazoles by regiospecific copper(i)-catalyzed 1,3-dipolar cycloadditions of terminal alkynes to azides. *The Journal of organic chemistry* 67(9):3057-3064.
- Tsarbopoulos, A., Pramanik, B. N., Nagabhushan, T. L., and Covey, T. R. 1995. Structural analysis of the CHO-derived interleukin-4 by liquid-chromatography/electrospray ionization mass spectrometry. *J. Mass Spectrom.* 30(12):1752-1763. <https://doi.org/10.1002/jms.1190301217>.
- Tsuda, E., Kawanishi, G., Ueda, M., Masuda, S., and Sasaki, R. 1990. The role of carbohydrate in recombinant human erythropoietin. *European journal of biochemistry* 188(2):405-411.
- Turner, D. M., Tom, C. T. M. B., and Renslo, A. R. 2014. Simple plate-based, parallel synthesis of disulfide fragments using the CuAAC click reaction. *ACS combinatorial science* 16(12):661-664. <https://doi.org/10.1021/co500132q>.
- Uchida, K., and Kawakishi, S. 1986. Oxidative depolymerization of polysaccharides induced by the ascorbic acid-copper ion systems. *Agricultural and Biological Chemistry* 50(10):2579-2583. <https://doi.org/10.1271/bbb1961.50.2579>.
- Ueda, T., Tomita, K., Notsu, Y., Ito, T., Fumoto, M., Takakura, T., Nagatome, H., Takimoto, A., Mihara, S.-I., Togame, H., Kawamoto, K., Iwasaki, T., Asakura, K., Oshima, T., Hanasaki, K., Nishimura, S.-I., and Kondo, H. 2009. Chemoenzymatic synthesis of glycosylated glucagon-like peptide 1: effect of glycosylation on proteolytic resistance and in vivo blood glucose-lowering activity. *Journal of the American Chemical Society* 131(17):6237-6245. <https://doi.org/10.1021/ja900261g>.
- Ulbricht, J., Jordan, R., and Luxenhofer, R. 2014. On the biodegradability of polyethylene glycol, polypeptoids and poly(2-oxazoline)s. *Biomaterials* 35(17):4848-4861. <https://doi.org/10.1016/j.biomaterials.2014.02.029>.
- Ultsch, M., Bevers, J., Nakamura, G., Vandlen, R., Kelley, R. F., Wu, L. C., and Eigenbrot, C. 2013. Structural basis of signaling blockade by anti-IL-13 antibody Lebrikizumab. *Journal of molecular biology* 425(8):1330-1339. <https://doi.org/10.1016/j.jmb.2013.01.024>.

- van Kasteren, S. I., Kramer, H. B., Gamblin, D. P., and Davis, B. G. 2007. Site-selective glycosylation of proteins: creating synthetic glycoproteins. *Nature protocols* 2(12):3185-3194. <https://doi.org/10.1038/nprot.2007.430>.
- Varki, A., Cummings, R. D., Esko, J. D., Freeze, H. H., Stanley, P., Bertozzi, C. R., Hart, G. W., and Etzler, M. E. 2009. *Essentials of Glycobiology*. 2nd ed., Cold Spring Harbor (NY).
- Vatrella, A., Fabozzi, I., Calabrese, C., Maselli, R., and Pelaia, G. 2014. Dupilumab: a novel treatment for asthma. *J. Asthma. Allergy*. 7:123-130. <https://doi.org/10.2147/JAA.S52387>.
- Vieira, L. Q., Hondowicz, B. D., Afonso, L. C., Wysocka, M., Trinchieri, G., and Scott, P. 1994. Infection with *Leishmania major* induces interleukin-12 production in vivo. *Immunology letters* 40(2):157-161.
- Waal Malefyt, R. de, Abrams, J. S., Zurawski, S. M., Lecron, J. C., Mohan-Peterson, S., Sanjanwala, B., Bennett, B., Silver, J., Vries, J. E. de, and Yssel, H. 1995. Differential regulation of IL-13 and IL-4 production by human CD8+ and CD4+ Th0, Th1 and Th2 T cell clones and EBV-transformed B cells. *International Immunology* 7(9):1405-1416.
- Wals, K., and Ovaa, H. 2014. Unnatural amino acid incorporation in *E. coli*: current and future applications in the design of therapeutic proteins. *Frontiers in chemistry* 2:15. <https://doi.org/10.3389/fchem.2014.00015>.
- Walsh, G. 2014. Biopharmaceutical benchmarks 2014. *Nature biotechnology* 32(10):992-1000. <https://doi.org/10.1038/nbt.3040>.
- Walsh, K. P., and Mills, K. H. G. 2013. Dendritic cells and other innate determinants of T helper cell polarisation. *Trends in immunology* 34(11):521-530. <https://doi.org/10.1016/j.it.2013.07.006>.
- Walter, M. R., Cook, W. J., Zhao, B. G., Cameron, R. P., Ealick, S. E., Walter, R. L., Reichert, P., Nagabhushan, T. L., Trotta, P. P., and Bugg, C. E. 1992. Crystal structure of recombinant human interleukin-4. *The Journal of biological chemistry* 267(28):20371-20376.
- Wang, I.-M., Lin, H., Goldman, S. J., and Kobayashi, M. 2004. STAT-1 is activated by IL-4 and IL-13 in multiple cell types. *Molecular immunology* 41(9):873-884. <https://doi.org/10.1016/j.molimm.2004.04.027>.
- Wang, L., Ray, A., Jiang, X., Wang, J.-y., Basu, S., Liu, X., Qian, T., He, R., Dittel, B. N., and Chu, Y. 2015. T regulatory cells and B cells cooperate to form a regulatory loop that maintains gut homeostasis and suppresses dextran sulfate sodium-induced colitis. *Mucosal immunology* 8(6):1297-1312. <https://doi.org/10.1038/mi.2015.20>.
- Wang, W., Soriano, B., and Chen, Q. 2017. Glycan profiling of proteins using lectin binding by Surface Plasmon Resonance. *Analytical biochemistry* 538:53-63. <https://doi.org/10.1016/j.ab.2017.09.014>.
- Wang, X., Lupardus, P., LaPorte, S. L., and Garcia, K. C. 2009. Structural Biology of Shared Cytokine Receptors. *Annu. Rev. Immunol.* 27(1):29-60. <https://doi.org/10.1146/annurev.immunol.24.021605.090616>.

- Wang, Y., Shen, B. J., and Sebald, W. 1997. A mixed-charge pair in human interleukin 4 dominates high-affinity interaction with the receptor alpha chain. *Proceedings of the National Academy of Sciences of the United States of America* 94(5):1657-1662.
- Wasley, L. C., Timony, G., Murtha, P., Stoudemire, J., Dorner, A. J., Caro, J., Krieger, M., and Kaufman, R. J. 1991. The importance of N- and O-linked oligosaccharides for the biosynthesis and in vitro and in vivo biologic activities of erythropoietin. *Blood* 77(12):2624-2632.
- Wenzel, S., Castro, M., Corren, J., Maspero, J., Wang, L., Zhang, B., Pirozzi, G., Sutherland, E. R., Evans, R. R., Joish, V. N., Eckert, L., Graham, N. M. H., Stahl, N., Yancopoulos, G. D., Louis-Tisserand, M., and Teper, A. 2016. Dupilumab efficacy and safety in adults with uncontrolled persistent asthma despite use of medium-to-high-dose inhaled corticosteroids plus a long-acting β 2 agonist: A randomised double-blind placebo-controlled pivotal phase 2b dose-ranging trial. *The Lancet* 388(10039):31-44. [https://doi.org/10.1016/S0140-6736\(16\)30307-5](https://doi.org/10.1016/S0140-6736(16)30307-5).
- Wenzel, S., Wilbraham, D., Fuller, R., Getz, E. B., and Longphre, M. 2007. Effect of an interleukin-4 variant on late phase asthmatic response to allergen challenge in asthmatic patients: results of two phase 2a studies. *Lancet* 370(9596):1422-1431. [https://doi.org/10.1016/S0140-6736\(07\)61600-6](https://doi.org/10.1016/S0140-6736(07)61600-6).
- Wlodawer, A., Wlodaver, A., Pavlovsky, A., and Gustchina, A. 1992. Crystal structure of human recombinant interleukin-4 at 2.25 Å resolution. *FEBS letters* 309(1):59-64.
- Worm, M., and Henz, B. M. 1997. Molecular regulation of human IgE synthesis. *J. Mol. Med.* 75(6):440-447.
- Xia, H. Z., Du, Z., Craig, S., Klisch, G., Noben-Trauth, N., Kochan, J. P., Huff, T. H., Irani, A. M., and Schwartz, L. B. 1997. Effect of recombinant human IL-4 on tryptase, chymase, and Fc epsilon receptor type I expression in recombinant human stem cell factor-dependent fetal liver-derived human mast cells. *J. Immunol.* 159(6):2911-2921.
- Xu, Y., Kershaw, N. J., Luo, C. S., Soo, P., Pocock, M. J., Czabotar, P. E., Hilton, D. J., Nicola, N. A., Garrett, T. P. J., and Zhang, J.-G. 2010. Crystal structure of the entire ectodomain of gp130: insights into the molecular assembly of the tall cytokine receptor complexes. *The Journal of biological chemistry* 285(28):21214-21218. <https://doi.org/10.1074/jbc.C110.129502>.
- Xu, Z., Chen, L., Gu, W., Gao, Y., Lin, L., Zhang, Z., Xi, Y., and Li, Y. 2009. The performance of docetaxel-loaded solid lipid nanoparticles targeted to hepatocellular carcinoma. *Biomaterials* 30(2):226-232. <https://doi.org/10.1016/j.biomaterials.2008.09.014>.
- Yang, Z., Wang, S., Halim, A., Schulz, M. A., Frodin, M., Rahman, S. H., Vester-Christensen, M. B., Behrens, C., Kristensen, C., Vakhrushev, S. Y., Bennett, E. P., Wandall, H. H., and Clausen, H. 2015. Engineered CHO cells for production of diverse, homogeneous glycoproteins. *Nature biotechnology* 33(8):842-844. <https://doi.org/10.1038/nbt.3280>.
- Yin, J., Lin, A. J., Golan, D. E., and Walsh, C. T. 2006. Site-specific protein labeling by Sfp phosphopantetheinyl transferase. *Nature protocols* 1(1):280-285. <https://doi.org/10.1038/nprot.2006.43>.

- Yin, J., Straight, P. D., McLoughlin, S. M., Zhou, Z., Lin, A. J., Golan, D. E., Kelleher, N. L., Kolter, R., and Walsh, C. T. 2005. Genetically encoded short peptide tag for versatile protein labeling by Sfp phosphopantetheinyl transferase. *Proceedings of the National Academy of Sciences of the United States of America* 102(44):15815-15820. <https://doi.org/10.1073/pnas.0507705102>.
- Zacchi, L. F., and Schulz, B. L. 2016. N-glycoprotein macroheterogeneity: biological implications and proteomic characterization. *Glycoconjugate journal* 33(3):359-376. <https://doi.org/10.1007/s10719-015-9641-3>.
- Zalipsky, S. 1995. Chemistry of polyethylene glycol conjugates with biologically active molecules. *Advanced Drug Delivery Reviews* 16(2-3):157-182. [https://doi.org/10.1016/0169-409X\(95\)00023-Z](https://doi.org/10.1016/0169-409X(95)00023-Z).
- Zhang, F., Liu, M.-r., and Wan, H.-t. 2014. Discussion about several potential drawbacks of PEGylated therapeutic proteins. *Biol. Pharm. Bull.* 37(3):335-339.
- Zhang, J.-L., Buehner, M., and Sebald, W. 2002. Functional epitope of common gamma chain for interleukin-4 binding. *European journal of biochemistry* 269(5):1490-1499.
- Zhang, X., Guo, S., Fan, R., Yu, M., Li, F., Zhu, C., and Gan, Y. 2012. Dual-functional liposome for tumor targeting and overcoming multidrug resistance in hepatocellular carcinoma cells. *Biomaterials* 33(29):7103-7114. <https://doi.org/10.1016/j.biomaterials.2012.06.048>.
- Zhu, Z., Homer, R. J., Wang, Z., Chen, Q., Geba, G. P., Wang, J., Zhang, Y., and Elias, J. A. 1999. Pulmonary expression of interleukin-13 causes inflammation, mucus hypersecretion, subepithelial fibrosis, physiologic abnormalities, and eotaxin production. *J. Clin. Invest.* 103(6):779-788. <https://doi.org/10.1172/JCI5909>.
- Zotos, D., Coquet, J. M., Zhang, Y., Light, A., D'Costa, K., Kallies, A., Corcoran, L. M., Godfrey, D. I., Toellner, K.-M., Smyth, M. J., Nutt, S. L., and Tarlinton, D. M. 2010. IL-21 regulates germinal center B cell differentiation and proliferation through a B cell-intrinsic mechanism. *The Journal of experimental medicine* 207(2):365-378. <https://doi.org/10.1084/jem.20091777>.
- Zurawski, S. M., Vega, F., Huyghe, B., and Zurawski, G. 1993. Receptors for interleukin-13 and interleukin-4 are complex and share a novel component that functions in signal transduction. *EMBO. J.* 12(7):2663-2670.

9. Supplement

9.1 Generation of glycoengineered IL-4 analogues

IL-4 sequence:

1 H K C D I T L Q E I I K T L N S L T E **Q₂₀**
 1 CACAAGTGCATATCACCTTACAGGAGATCATCAAACCTTTGAACAGCCTCACAGAG**CAG**

 21 K T L C T **E₂₆** L **T₂₈** V T D I F **A₃₄** A S K **N₃₈** T T
 61 AAGACTCTGTGCACC**GAGTTGACC**GTAACAGACATCTTT**GCT**GCCTCCAAG**AAC**CAACT

 41 E K E T F C R A A T V L R Q F Y S H H E
 121 GAGAAGGAAACCTTCTGCAGGGCTGCGACTGTGCTCCGGCAGTTCTACAGCCACCATGAG

 61 **K₆₁** D T R C L G A T A Q Q F H R H K Q L I
 181 **AAG**GACTCGCTGCCTGGGTGCGACTGCACAGCAGTTCCACAGGCACAAGCAGCTGATC

 81 R **F₈₂** L K R L D R N L W G L A G **L₉₆** N S C P
 241 CG**TT**CCTGAAACGGCTCGACAGGAACCTCTGGGGCCTGGCGGGC**TTGA**ATTCCTGTCTT

 101 V K E A N Q S T L E N F L E R L **K₁₁₇** T I M
 301 GTGAAGGAAGCCAACCAGAGTACGTTGGAAAACCTTCTGGAAAGGCTA**AAGACGAT**CATG

 121 **R₁₂₁** E K Y S K C S S *
 361 **AGAGAGAAA**TATTCAAAGTGTTCGAGCTGA

Cys-variants

N38C: **TGC**
 F82D: **GAC**
 K117C: **TGC**
 R121C: **TGT**

Asp-variants:

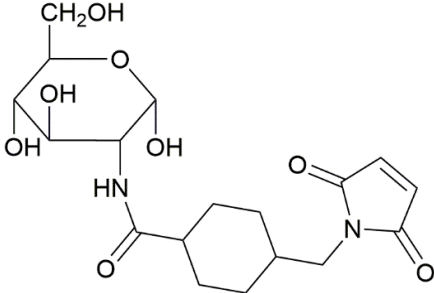
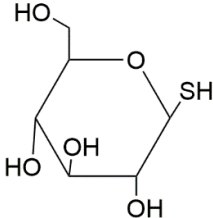
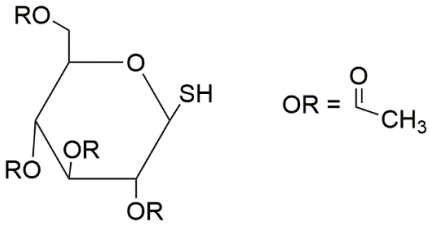
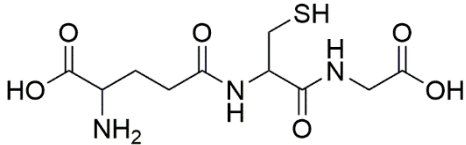
Q20N: **AAC**
 E26N: **AAC**
 T28N: **AAC**
 A34N: **AAT**
 N38Q: **CAG**
 K61N: **AAC**
 F82D: **GAC**
 L96N: **AAC**

K117N T118A I119S:
AAC GCG ACCA

R121N K123S:
AACGAG AGC

Figure S9.1: IL-4 coding sequence. Mutational sites are indicated in red and nucleotide exchanges are displayed in the box.

Table S9.1: Chemical compounds/glycans used for modification of IL-4 cysteine analogues.

Compound	Structure	abbreviation
SMCC-glucosamine		SMCC-GlcN
1-thio glucose		Glc
1-thio glucose tetraacetate		4acGlc
glutathione reduced		GSH

9.2 Analytics of IL-4 glycoconjugates

9.2.1 Mass spectrometry analysis of glycoengineered IL-4 F82D R121C/K117C analogues

Table S9.2: Theoretical and measured molecular weights of IL-4 F82D R121C/K117C glycoconjugates. Theoretical and observed molecular weight in mass spectrometry analysis of glycoengineered IL-4 analogues conjugated to different synthetic glycan moieties. Abbreviations are SMCC-GlcN for SMCC-glucosamine conjugate, Glc for glucose, 4acGlc for glucose tetraacetate, GSH for glutathione and Cys for cysteine.

	theoretical	observed	difference
F82D R121C-SH	15003.07	15003.59	0.52
F82D R121C-Glc	15197.28	15197.61	0.33
F82D R121C-4acGlc	15366.44	15365.65	-0.79
F82D R121C-SMCC-GlcN	15401.43	15401.78	0.35
F82D N38C-R121C-Glc	15380.53	15380.63	0.10
F82D N38C R121C-4acGlc	15718.84	15717.69	-1.15
F82D K117C-GSH	15337.4	15336.68	0.72
F82D K117C-Glc	15225.29	15225.53	-0.24
F82D K117C-4acGlc	15394.45	15393.59	0.86
F82D (Hek293) [§]	16525.54	16525.57	-0.03
F82D R121C-Cys (Hek293) [§]	16591.66	16592.53	-0.87
F82D R121C-Glc (Hek293) [*]	16463.5	16464.25	0.75

[§] protein derived from EndoH digest; ^{*} protein derived from PNGase F digest

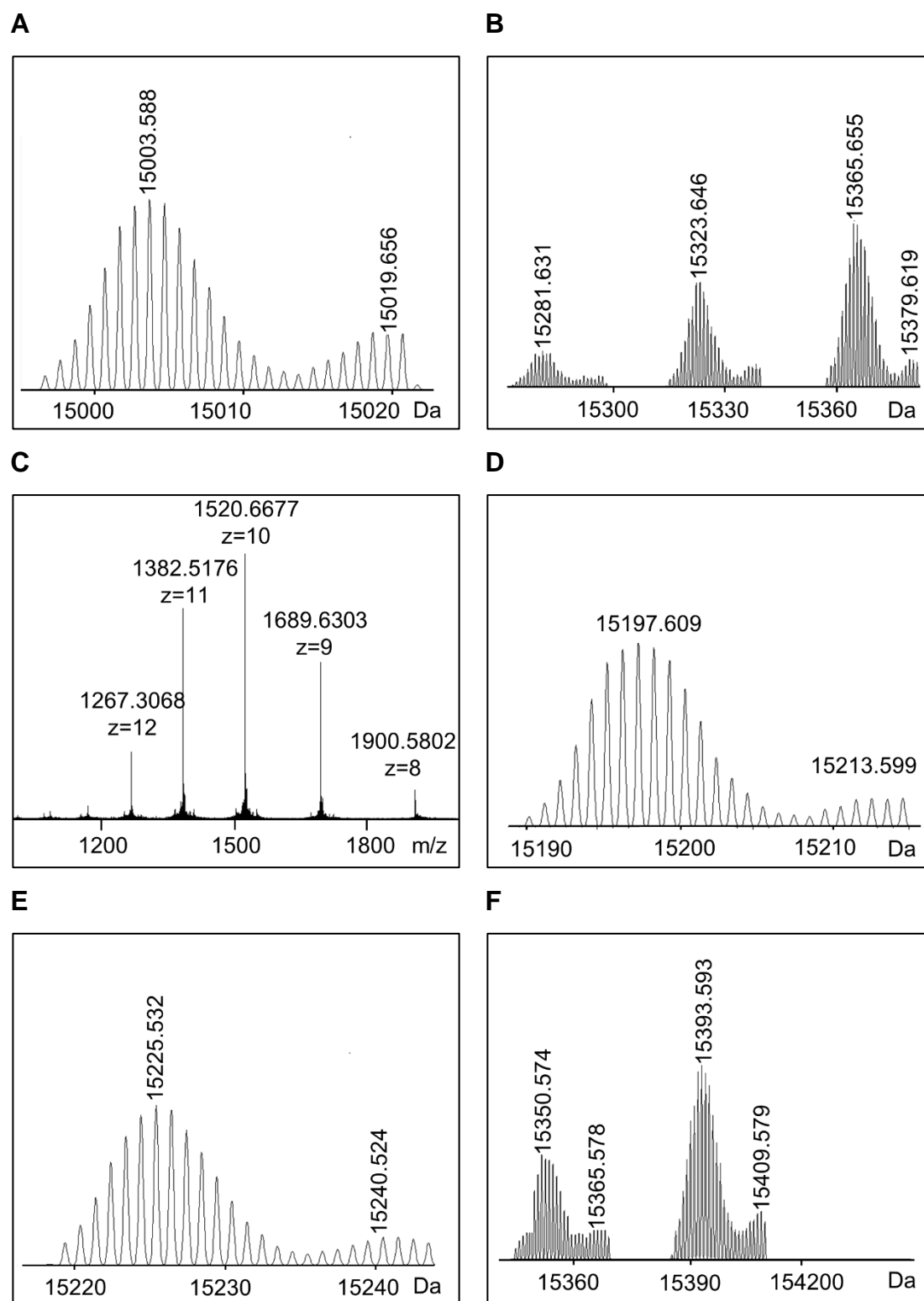


Figure S9.2: Mass spectrometry of IL-4 F82D R121C glycoconjugates. Minor species seen in the spectra with +16 Da represent mono-oxygenated species. Loss of acetate groups (- 42 Da) can be observed for IL-4 analogues conjugated to glucose tetraacetate. A: IL-4 F82D R121C-SH (enzymatically reduced); B: IL-4 F82D R121C-4acGlc; C:IL-4 F82D R121C-Glc (averaged combined spectra); D: IL-4 F82D R121C-Glc (deconvoluted); E: IL-4 F82D K117C-Glc (purified via SulfoLink); F: IL-4 F82D K117C-4acGlc (purified via SulfoLink).

9.2.2 Biologic activity in cell-based assays

Table S9.3: Biologic activity of glycoengineered IL-4 variants in HEK-Blue and TF-1 cells. Cells were incubated with 50 pM of each variant and signal intensity (quantified as detailed under chapter 5.7.3) was normalized to IL-4 WT. Data is shown from three independent experiments (n=3).

IL-4 variant	biologic activity (%)			
	TF-1 cells		HEK-Blue cells	
	mean	SD	mean	SD
WT	99.15	8.67	100.00	6.07
F82D N38C-Glc	90.80	11.55	102.82	4.60
F82D R121C-GSH	5.79	7.85	-0.87	0.91
F82D R121C-Glc	0.46	5.14	-1.42	0.71
F82D R121C-4ac Glc	0.96	8.31	-0.70	0.77
F82D R121C-SMCC GlcN	0.98	7.95	-0.77	0.71
F82D R121C-Glc (Hek293)	0.59	7.26	-0.86	0.30
F82D Q20NT28NK61NR121C-Glc (Hek293)	1.28	4.99	-0.55	0.57
Pitrakinra	-2.62	9.02	-0.73	0.88
F82D K117C-GSH	47.98	9.67	3.04	0.97
F82D K117C-Glc	88.43	10.32	76.17	8.33
F82D K117C 4ac Glc	72.52	11.30	54.12	4.34
R121E	72.73	12.34	-1.96	0.65
F82D N38Q T28N (Hek293; ConA purified)	40.06	7.02	2.62	0.89
F82D N38Q K117N (Hek293; ConA purified)	6.37	7.02	-0.37	0.88

Table S9.4: Biologic activity of glycoengineered IL-4 variants in HEK-Blue cell-assay. Cells were incubated with 50 pM, 1 nM and 10 nM of each variant and signal intensity (quantified as detailed under chapter 5.7.3) was normalized to IL-4 WT. Data is shown from two independent experiments (n=2).

	50 pM (%)	1 nM (%)	10 nM (%)
F82D N38Q T28N (Hek293; ConA purified)	4.84 ± 0.43	29.05 ± 0.72	34.62 ± 0.14
F82D N38Q K117N (Hek293; ConA purified)	- 0.02 ± 0.68	1.87 ± 1.44	25.37 ± 9.34
IL-4 F82D K117C-GSH	1.09 ± 0.67	5.65 ± 0.55	6.45 ± 0.92
IL-4 F82D K117C-GSH (purified via SulfoLink)	0.77 ± 0.55	3.49 ± 0.32	3.39 ± 0.67
IL-4 WT	100.00 ± 6.31	109.54 ± 5.89	107.54 ± 6.52

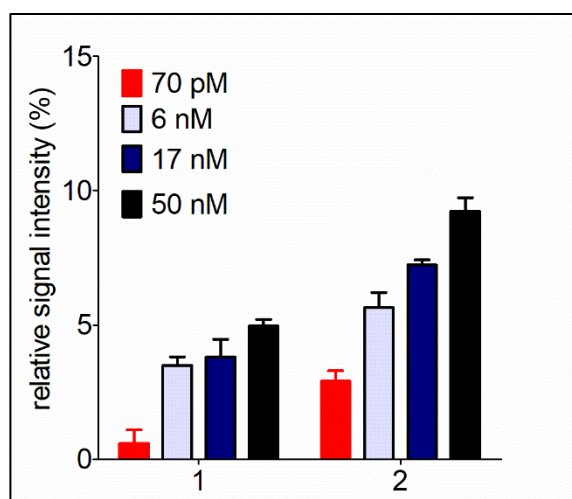


Figure S9.3: Biologic activity of glutathionylated IL-4 F82D K117C variants in HEK-Blue cells. HEK-Blue cells were incubated with 70 pM, 6 nM, 17 nM and 50 nM of fully glutathionylated IL-4 F82D K117C-GSH purified via SulfoLink (1) and partially modified IL-4 F82D K117C-GSH (2). Partially glutathionylated IL-4 F82D K117C-GSH was shown to consist of about 5% non-conjugated IL-4 F82D K117C with a free thiol-group, which probably causes the slightly higher biologic activity.

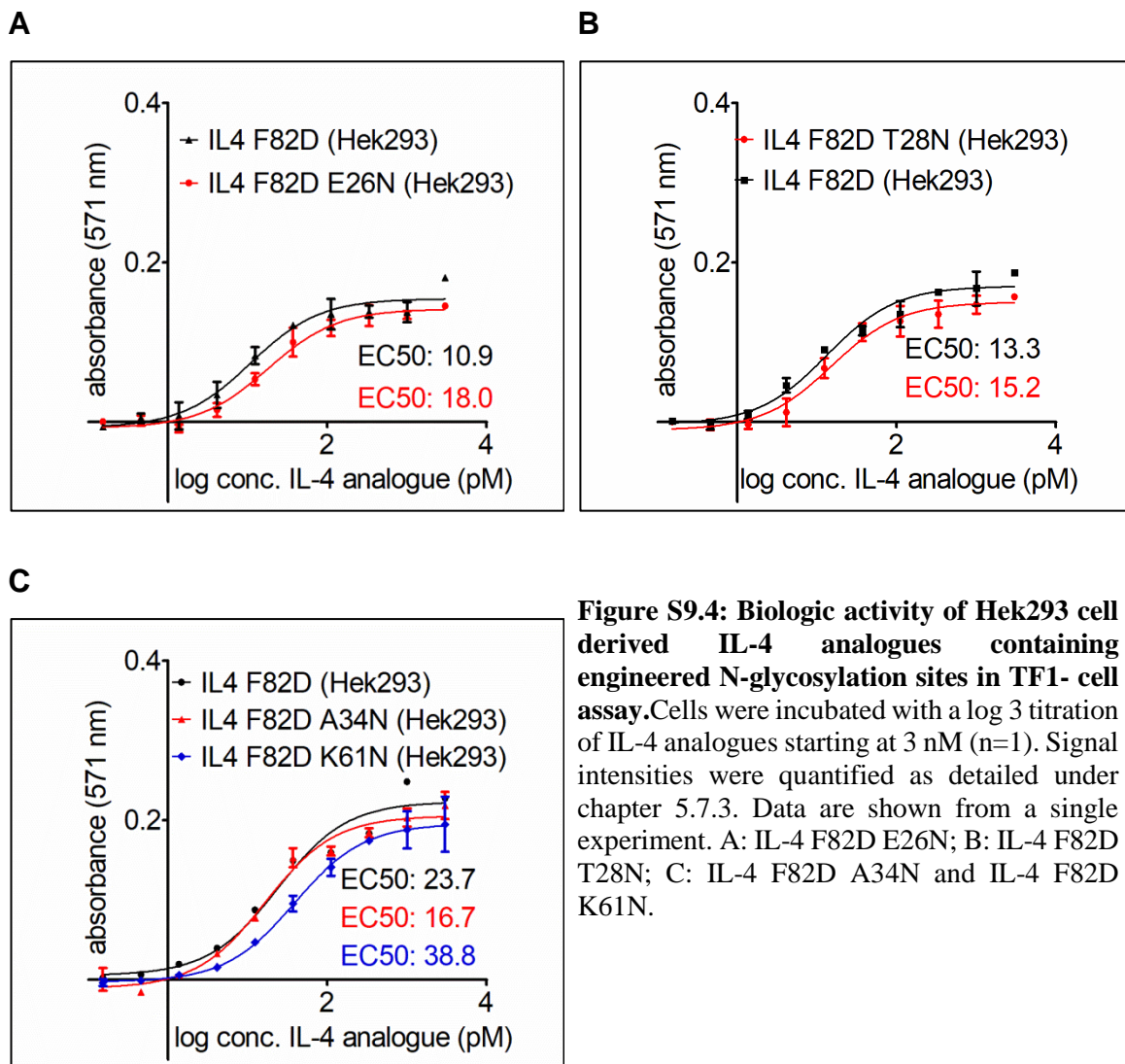


Figure S9.4: Biologic activity of Hek293 cell derived IL-4 analogues containing engineered N-glycosylation sites in TF1- cell assay. Cells were incubated with a log 3 titration of IL-4 analogues starting at 3 nM (n=1). Signal intensities were quantified as detailed under chapter 5.7.3. Data are shown from a single experiment. A: IL-4 F82D E26N; B: IL-4 F82D T28N; C: IL-4 F82D A34N and IL-4 F82D K61N.

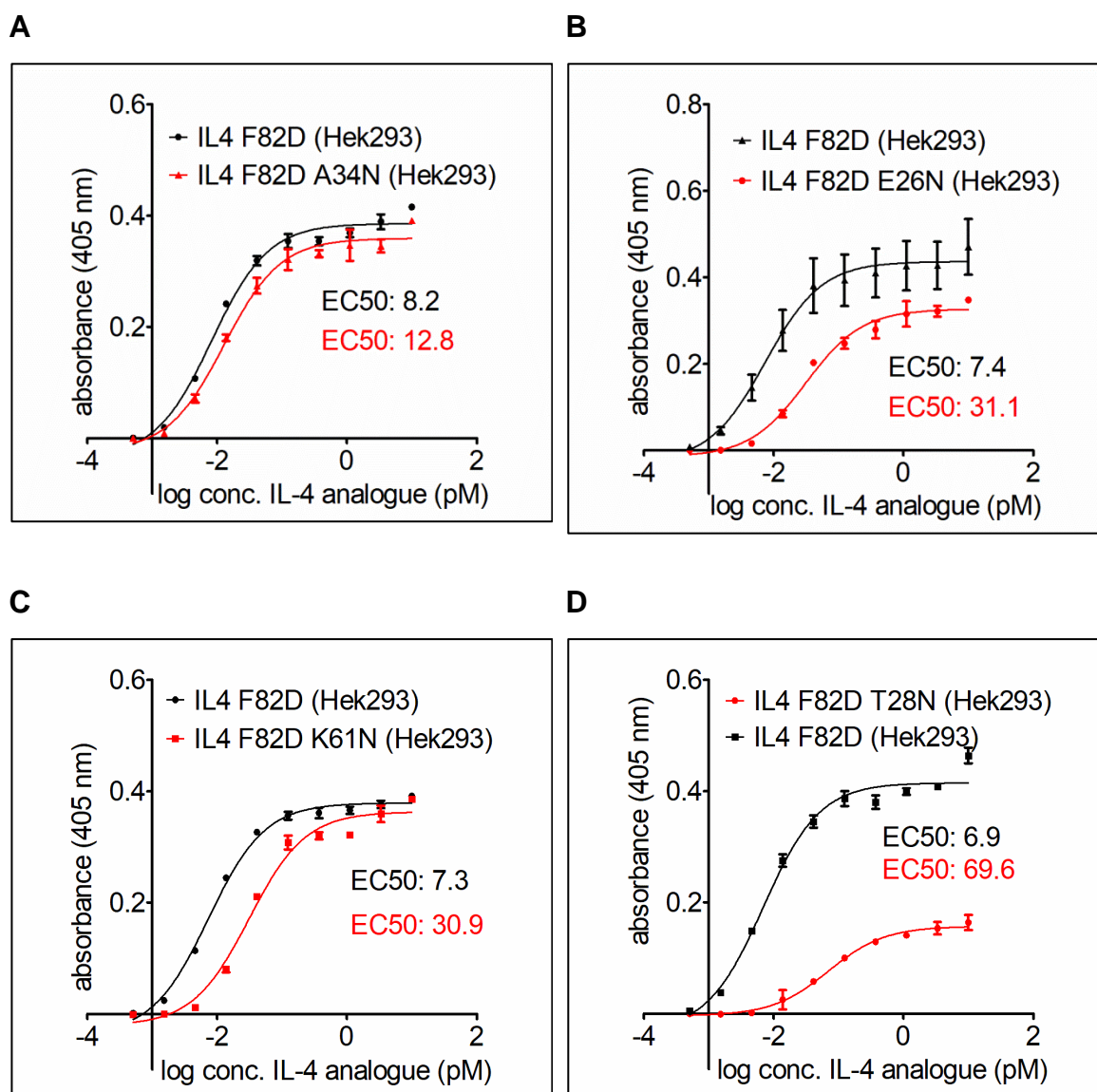


Figure S9.5: Biologic activity of Hek293 cell derived IL-4 analogues containing engineered N-glycosylation sites in HEK-Blue cells. Cells were incubated with a log₃ titration of IL-4 analogues starting at 10 nM (n=1). Signal intensities were quantified as detailed under chapter 5.7.3. A: IL-4 F82D A34N; B: IL-4 F82D E26N; C: IL-4 F82D K61N; D: IL-4 F82D T28N.

9.3 Gene Expression Analysis of IL-4 receptors IL-4R α , γ c (IL2RG) and IL-13R α 1 in TF-1 cells

Table S9.5: Readily available qPCR primers for IL-4R α , IL-13R α 1, γ c and GAPDH were purchased from Sigma Aldrich.

Gene description	Sequence
Actin_s	GAC GAC ATG GAG AAA ATC TG
Actin_as	ATG ATC TGG GTC ATC TTC TC
GAPDH_s	ACA GTT GCC ATG TAG ACC
GAPDH_as	TTT TTG GTT GAG CAC AGG
IL2RG_s	CTC GGA TAA TGA TAA AGT CCA G
IL2RG_as	CAC CAG ATT CTG CAG TTT TAG
IL-4R α _s	TCA GCA TCA CCA AGA TTA AG
IL-4R α _as	AGA GCT TGG TAA GAC AAT TC
IL-13R α 1_s	AAG AAA ATA GCT CCG GAA AC
IL-13R α 1-as	TAG GCT TCT CAC TCT CAT TG

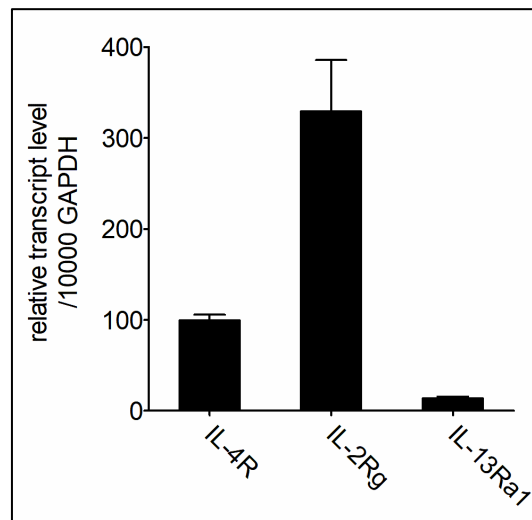


Figure S9.6: Quantitative Real Time PCR of IL-4 receptor transcript levels in TF1 cells. Total mRNA was extracted from 2×10^7 TF-1 cells and transcribed into cDNA (for experimental details see chapter 5.1.5). QPCR reactions were performed on a LightcyclerTM (Roche, Switzerland) using the ABsolute QPCR SYBR Green Capillary Mix (Thermo Scientific, USA). For quantification receptor-gene expression levels were normalized to 10 000 molecules GAPDH.

9.4 Abbreviations

Table S9.6: Abbreviations

Å	angstrom
AgNO ₃	silver nitrate
Amp ^R	ampicillin resistance
BSA	buried surface area
CHES	N-cyclohexyl-2-aminoethanesulfonic acid
CaCl ₂	calcium chloride
CHR	cytokine binding homology region
CoA	coenzyme A
ConA	concanavalin A
CuAAC	copper-catalyzed azide-alkyne cycloaddition
Da	dalton
(c)DNA	(coding) deoxyribonucleic acid
DTT	dithiothreitol
<i>E. coli</i>	<i>Escherichia coli</i>
EC ₅₀	half maximal effective concentration
ECD	ectodomain
EDC	1-ethyl-3-(3-dimethylaminopropyl)carbodiimide
EDTA	ethylenediaminetetraacetic acid
Endo-H	endoglycosidase-H
ER	endoplasmic reticulum
FBS	fetal bovine serum
FEV ₁	forced expiratory pressure in 1 second
FNIII domain	fibronectin type III domain
g	gravitational constant
GlcN	glucosamine
GlcNAc	N-acetylglucosamine
GM-CSF	granulocyte-macrophage colony stimulating factor
grxA	glutaredoxin
GSH	glutathione (reduced)
GSSG	glutathione (oxidized)
GuHCl	guanidine hydrochloride

HCl	hydrochloride
IFN	interferon
Ig	immunoglobulin
IL	interleukin
IMAC	immobilized metal affinity chromatography
IPTG	isopropyl β -D-1-thiogalactopyranoside
JAK	janus kinase
Kan ^R	kanamycin resistance
ka	association rate constant
kd	dissociation rate constant
K _D	dissociation constant
K _i	inhibitory constant
LB(-medium)	lysogeny broth (-medium)
MES	2-(N-morpholino)ethansulfonsäure
MnCl ₂	manganese chloride
MHC	major histocompatibility complex
MOPS	3-(N-morpholino)propanesulfonic acid
MS	mass spectrometry
NaCl	sodium chloride
NaCO ₃	sodium carbonate
Na ₂ S ₂ O ₃	sodium thiosulfate
NAD(P)H	nicotinamide adenine dinucleotide (phosphate)
Hek293 cells	human embryonic kidney cells 293
HEPES	4-(2-hydroxyethyl)-1-piperazineethanesulfonic acid
His6-tag	hexahistidine-tag
HRP	horseradish peroxidase
IB	Inclusion body
IC ₅₀	half-maximal inhibitory concentration
Neu5Ac	N-acetylneuraminic acid
Neu5Gc	N-glycolylneuraminic acid
NHS	N-hydroxysuccinimide
PAGE	polyacrylamide gel electrophoresis
(q)PCR	(quantitative) polymerase chain reaction
(MA-) PEG	(maleimide-) polyethylene glycol

PEI	polyethylenimine
<i>P. pastoris</i>	<i>Pichia pastoris</i>
PNGaseF	peptide-N-glykosidase F
pnpp	p-nitrophenyl phosphate
ROS	reactive oxygen species
RP-HPLC	reverse phase-high pressure liquid chromatography
RT	room temperature
RU	resonance unit (SPR)
RbCl	rubidium chloride
rpm	rounds per minute
SDS	sodium dodecyl sulfate
SEAP	secreted alkaline phosphatase
SMCC	succinimidyl 4-(N-maleimidomethyl) cyclohexane-1-carboxylate
SPR	surface plasmon resonance
STAT	signal transducer and activator of transcription
TCA	trichloroacetic acid
TFA	trifluoroacetic acid
TGF	transforming growth factor
Th-cell	T-helper cell
TRIS	tris(hydroxymethyl)aminomethane
(t)RNA	(transfer) ribonucleic acid
UAA	unnatural amino acid
UPLC	ultra performance liquid chromatography
UV	ultraviolet
VCAM1	vascular cell adhesion molecule-1
WT	wildtype
w/v	weight per volume

9.5 Acknowledgements

9.6 Curriculum Vitae

9.7 Affidavit

I hereby confirm that my thesis entitled “Design of novel IL-4 antagonists employing site-specific chemical and biosynthetic glycosylation” is the result of my own work. I did not receive any help or support from commercial consultants. All sources and / or materials applied are listed and specified in the thesis.

Furthermore, I confirm that this thesis has not yet been submitted as part of another examination process neither in identical nor in similar form.

Place, Date

Signature

Eidesstattliche Erklärung

Hiermit erkläre ich an Eides statt, die Dissertation „Herstellung neuer IL-4 basierter Antagonisten durch zielgerichtete chemische und biosynthetische Glykosylierung“ eigenständig, d.h. insbesondere selbständig und ohne Hilfe eines kommerziellen Promotionsberaters, angefertigt und keine anderen als die von mir angegebenen Quellen und Hilfsmittel verwendet zu haben.

Ich erkläre außerdem, dass die Dissertation weder in gleicher noch in ähnlicher Form bereits in einem anderen Prüfungsverfahren vorgelegen hat.

Ort, Datum

Unterschrift